UNIWERSYTET ŚLĄSKI W KATOWICACH

WYDZIAŁ NAUK PRZYRODNICZYCH

INSTYTUT NAUK O ZIEMI

mgr Małgorzata Wendorff-Belon

Środowisko sedymentacji osadów oligocenu w sub-basenach środkowej Paratetydy: analiza biomarkerów w wybranych profilach Karpat zewnętrznych i basenu transylwańskiego

ROZPRAWA DOKTORSKA

Promotor:

Prof. dr hab. Leszek Marynowski

Promotor pomocniczy:

Dr hab. inż. Irena Matyasik, prof. INiG-PIB

Sosnowiec, 2026 rok

Składam serdeczne podziękowania:

Promotorowi prof. dr hab. Leszkowi Marynowskiemu za możliwość realizacji pracy i przede wszystkim za otwartość, wrażliwość, wsparcie, wiarę we mnie oraz wszelką pomoc udzieloną na każdym etapie pracy.

Promotor pomocniczej dr hab. Irenie Matyasik, prof. INiG-PIB za wsparcie merytoryczne w tematyce naftowej i pomoc w trakcie finalizacji pracy.

Dr. hab. Mariuszowi Rospondkowi, prof. UJ za wprowadzenie mnie w świat geochemii organicznej i biomarkerów oraz możliwość zanurzenia się w oligoceńskim oceanie Paratetydy.

Pani dr Ewie Malacie za niezawodne, szczere i fachowe wsparcie merytoryczne i edytorskie oraz za wykonanie analizy zespołów otwornic.

Dyrekcji Instytutu Nafty i Gazu - Państwowego Instytutu Badawczego za umożliwienie mi realizacji pracy oraz życzliwość na etapie jej finalizacji.

Moim Przyjaciółkom i Przyjaciołom, Współpracownikom z INiG-PIB, UJ i UŚ, dzięki którym udało mi się osiągnąć ten cel.

Mojemu najukochańszemu Mężowi Marcinowi, moim synkom Tytusowi i Juliuszowi, Mojej wspaniałej Rodzinie, za bycie zawsze ze mną, za siłę, oparcie i inspirację.

Pracę dedykuję Klaudiuszowi.

Spis treści

Publikacje wchodzące w skład rozprawy

Publikacja 1

Wendorff, M., Rospondek, M., Kluska, B., Marynowski, L., 2017. Organic matter maturity and hydrocarbon potential of the Lower Oligocene Menilite facies in the Eastern Flysch Carpathians (Tarcău and Vrancea Nappes), Romania. Applied Geochemistry 78, 295–310. http://dx.doi.org/10.1016/j.apgeochem.2017.01.009; 100 pkt MNiSW, Journal IF 3,4

Publikacja 2

Wendorff-Belon, M., Rospondek, M., Marynowski, L., 2021. Early Oligocene environment of the central Paratethys revealed by biomarkers and pyrite framboids from the Tarcău and Vrancea nappes (Eastern Outer Carpathians, Romania). Marine and Petroleum Geology 128, 105037. https://doi.org/10.1016/j.marpetgeo.2021.105037; 140 pkt MNiSW, Journal IF 3,6

Publikacja 3

Wendorff-Belon, M., Loręc, R., Wierzbicki, A., Rospondek, M., Marynowski, L., 2025. Oligocene environmental changes in the Central Paratethys: geochemical and palynofacial record from the north-western Transylvanian Basin (Romania). Palaeogeography, Palaeoclimatology, Palaeoecology 676, 113124. https://doi.org/10.1016/j.palaeo.2025.113124; 100 pkt MNiSW, Journal IF 2,7

Pozostałe publikacje

Marynowski, L., Bucha, M., Smolarek, J., Wendorff, M., Simoneit, B.R.T., 2018. Occurrence and significance of mono-, di- and anhydrosaccharide biomolecules in Mesozoic and Cenozoic lignites and fossil wood. Organic Geochemistry 116, 13–22.

Kasina, M., Wendorff-Belon, M., Kowalski, P.R., Michalik, M. 2019. Characterization of incineration residues from wastewater treatment plant in Polish city: a future waste based source of valuable elements? Journal of Material Cycles and Waste Management 21, 885–896. doi: https://doi.org/10.1007/s10163-019-00845-1

Wójcik-Tabol, P., Wendorff-Belon, M., Kosakowski, P., Zakrzewski, A., Marynowski, L., 2022. Paleoenvironment, organic matter maturity and hydrocarbon potential of the menilite shales (Silesian unit, Polish Outer Carpathians) – organic and inorganic geochemical proxies. Marine and Petroleum Geology 142, 105767. https://doi.org/10.1016/j.marpetgeo.2022.105767

Dąbek-Głowacka J., Wójcik-Tabol P., Nowak G.J., Wendorff-Belon M., Marynowski L., 2023. Łupki antrakozjowe niecki śródsudeckiej w świetle wskaźników geochemii organicznej – wstępne wyniki analizy bituminów. Przegląd Geologiczny 71, 269–273. doi: http://dx.doi.org/10.7306/2023.23

Kasina, M., Telk, A., Wendorff-Belon, M., 2024. Comprehensive characterization and environmental implications of industrial and hazardous incineration ashes: insights into chemistry, mineralogy, elements' fractionation and leaching potential. Scientific Reports 14, 29010. doi: https://doi.org/10.1038/s41598-024-80782-8

Matyasik, I., Wendorff-Belon, M., 2024. Poszukiwania naturalnego wodoru – ewenement geologiczny czy potencjał poszukiwawczy. Wiadomości Naftowe i Gazownicze 24, 4–8.

Wendorff-Belon, M., Janiga, M., Bieleń, W., 2025. Znaczniki chemiczne stosowane w monitoringu podziemnych składowisk CO_2 – przegląd i metody oznaczania. Nafta-Gaz 10, 650–658. doi: 10.18668/NG.2025.10.02

Hebda, K., Janiga, M., Wendorff-Belon, M., 2026. Zawartości radonu i wodoru w powietrzu glebowym potencjalnych struktur typu *fairy circle* z rejonu Lubelszczyzny. Nafta-Gaz 1, 7–16. doi: 10.18668/NG.2026.01.01

Streszczenie w języku angielskim

At the Eocene/Oligocene transition, the progressive collision of Africa with Eurasia, Apulia, and the Arabian plate led to the final disappearance of the Tethys Ocean and the isolation of the marginal Paratethys Basin. Under conditions of a cooling climate and eustatic changes, the Paratethys was divided into smaller basins temporarily isolated from each other and from the global ocean. As a result of long-term water stratification and oxygen depletion, the deposition of rocks rich in organic matter (OM) occurred, represented primarily by shales, mudstones, and cherts of the Menilite facies. These rocks are widely considered source rocks for hydrocarbon deposits extending from the Vienna Basin through the Carpathians, the Black Sea, and the Caspian Sea regions, as far as Kazakhstan.

This work constitutes a comprehensive geochemical and petrographic study, the primary objective of which is to determine the sedimentary environmental conditions prevailing during the Oligocene in the Central Paratethys basins, namely the Tarcău and Vrancea basins and the Transylvanian Basin (TB). In these regions, previous molecular studies were very limited (Romanian Eastern Carpathians) or had not been conducted at all (TB). Using a variety of research methods, including gas chromatography-mass spectrometry, Rock-Eval pyrolysis, vitrinite reflectance and pyrite framboid measurements, and palynofacies analysis, an attempt was made to determine the mechanisms leading to the burial of significant amounts of organic carbon. Furthermore, the source of OM was determined, as well as the thermal maturity of OM and the hydrocarbon potential of the studied rocks were evaluated. Three Oligocene rock successions were selected for the study: two located within the Tarcău and Vrancea nappes belonging to the Romanian sector of the Outer Carpathians, and a third situated in the north-western part of the TB in northern Romania.

Geochemical and petrographic studies of the rocks from the Vrancea and Tarcău nappes revealed variations in the degree of OM transformation between the analysed tectonic units. A higher degree of thermal maturity, corresponding to the onset of the oil window, was found in the Tărcuţa profile within the Tarcău Nappe, as indicated by vitrinite reflectance values, the T_{max} parameter (from Rock-Eval pyrolysis), and biomarker-based indices. Rocks from the Vrancea Nappe contain thermally immature OM. They are characterized by good to very good hydrocarbon potential, inferred from high total organic carbon content and high hydrogen index values.

In the TB, the presence of OM with a low stage of thermal maturity was established, evidenced by the presence of diasterenes and hopenes, products of early diagenesis, as well as

low vitrinite reflectance values, low T_{max} parameters, and biomarker indices. Lower Oligocene rocks exhibit very good hydrocarbon potential.

During the Early Oligocene in the Vrancea Basin, intensive bioproductivity of phytoplankton (diatoms and dinoflagellates) predominated, supported by the influx of nutrients from the land, as evidenced by the presence of terrestrial plant biomarkers (mainly gymnosperms). The presence of isorenieratane, its aryl derivatives, and Me,*i*-Bu-maleimides derived from green sulfur bacteria, combined with the predominance of small pyrite framboids, suggest at least periodic development of euxinic conditions reaching into the photic zone. This phenomenon was accompanied by a decrease in surface water salinity, which favored water column stratification and the burial of significant amounts of OM.

In the Tarcău Basin, OM of bacterial and cyanobacterial origin was deposited, with a simultaneous absence of compounds derived from higher plants, indicating open basin conditions and less intensive planktonic production. Anoxia/euxinia developed in the deeper parts of the water column, and the chemocline was located deeper, moving at least periodically above the sediment-water interface but remaining below the photic zone.

The results of biomarker and palynofacies analyses document the dynamic evolution of the sedimentary environment in the NW part of the TB. During the Early Oligocene, deep-water conditions prevailed with a clear dominance of OM of marine origin. Strong water stratification and the development of anoxia, or even euxinia periodically reaching the photic zone, occurred in the basin, confirmed by the presence of isorenieratane derivatives and a high proportion of small pyrite framboids. At the transition between the Early and Late Oligocene, progressive basin shallowing was recorded, correlated with the thrusting of the Pienides and the associated compressional episode in this part of the TB. An increased supply of terrestrial material is marked by a rich assemblage of higher plant biomarkers and numerous fragments of cuticles and wood. Oxidizing conditions prevailed in the water column. However, in the uppermost part of the profile within intervals richer in OM, recurrences of anoxic episodes and eutrophication were recorded, likely related to nutrient influx from the land and a decrease in water salinity.

In summary, the research presented in this dissertation allowed for the reconstruction of the evolution of the sedimentary environment in the NW TB and the Tarcău and Vrancea basins, highlighting the influence of tectonics and euxinia on organic carbon accumulation processes. The obtained biomarker data constitute valuable material for hydrocarbon prospection in the Carpathian region.

Streszczenie w języku polskim

Na przełomie eocenu i oligocenu postępująca kolizja Afryki z Eurazją, Apulią i płytą arabską doprowadziła do ostatecznego zaniku Oceanu Tetydy i wyodrębnienia się marginalnego basenu Paratetydy. W warunkach ochładzającego się klimatu i zmian eustatycznych Paratetyda uległa podziałowi na pomniejsze baseny czasowo izolowane od siebie i od oceanu światowego. W wyniku długotrwałej stratyfikacji wód oraz zubożenia w tlen, nastąpiła depozycja skał bogatych w materię organiczną (MO), reprezentowanych głównie przez iłowce, mułowce i rogowce facji menilitowej. Skały te uważane są powszechnie za skały macierzyste dla złóż węglowodorów od basenu wiedeńskiego przez Karpaty, Morze Czarne, Morze Kaspijskie, aż po Kazachstan.

Praca stanowi kompleksowe studium geochemiczne i petrograficzne, którego głównym celem jest określenie warunków środowiska sedymentacji panujących w oligocenie w basenach środkowej Paratetydy, tj. w basenach Tarcău, Vrancea oraz basenie transylwańskim (TB), gdzie dotychczasowe badania molekularne były bardzo ograniczone (rumuńska część Karpat wschodnich) lub w ogóle nie były prowadzone (TB). Przy użyciu różnorodnych metod badawczych (chromatografia gazowa sprzężona ze spektrometrią mas, analiza Rock-Eval, analiza refleksyjności witrynitu, pomiary framboidów pirytowych, czy analiza palinofacjalna) podjęto próbę określenia mechanizmów prowadzących do pogrzebania znacznych ilości węgla organicznego, określono źródło MO oraz oceniono dojrzałość termiczną MO i potencjał węglowodorowy badanych skał. Do badań wybrano trzy oligoceńskie sukcesje skalne, dwie z nich zlokalizowane w obrębie płaszczowin Tarcău i Vrancea, należących do rumuńskiego sektora Karpat zewnętrznych, a trzecia znajdująca się w północno-zachodniej części TB w północnej Rumunii.

Badania geochemiczne i petrograficzne skał z płaszczowiny Vrancea i Tarcău wykazały zróżnicowanie w stopniu przeobrażenia MO pomiędzy analizowanymi jednostkami tektonicznymi. Wyższy stopień dojrzałości termicznej, odpowiadający wejściu w początkową fazę okna ropnego, stwierdzono w profilu Tărcuţa w obrębie płaszczowiny Tarcău, na co wskazują wartości refleksyjności witrynitu, parametru T_{max} (z pirolizy Rock-Eval) oraz wskaźników opartych na biomarkerach. Skały z płaszczowiny Vrancea zawierają MO niedojrzałą termicznie. Charakteryzują się one bardzo dobrym potencjałem węglowodorowym, co wywnioskowano na podstawie wysokiej zawartości całkowitego węgla organicznego oraz wysokich wartości wskaźnika wodorowego HI.

W TB stwierdzono obecność MO o niskim stopniu zaawansowania dojrzałości termicznej, o czym świadczy obecność diasterenów i hopenów, będących produktem wczesnej diagenezy, niskie wartości refleksyjności witrynitu, a także parametru T_{max} i wskaźniki biomarkerowe. Skały dolnego oligocenu wykazują bardzo dobry do dobrego potencjał węglowodorowy.

We wczesnym oligocenie w basenie Vrancea dominowała intensywna bioproduktywność fitoplanktonu (okrzemek i bruzdnic) wspierana dopływem nutrientów z lądu, o czym świadczy obecność biomarkerów roślin lądowych (głównie nagozalążkowych). Obecność izorenieratanu i jego arylowych pochodnych oraz Me,*i*-Bu-malemidów, pochodzących od zielonych bakterii siarkowych, oraz przewaga drobnych framboidów pirytowych sugerują przynajmniej okresowy rozwój warunków euksynicznych, sięgających strefy fotycznej. Zjawisku temu towarzyszył spadek zasolenia wód powierzchniowych, co sprzyjało stratyfikacji kolumny wody i pogrzebaniu znacznych ilości MO. W basenie Tarcău deponowana była MO pochodzenia bakteryjnego i cyjanobakteryjnego przy jednoczesnym braku związków pochodzących od roślin wyższych, co świadczy o warunkach otwartego basenu i mniej intensywnej produkcji planktonicznej. Anoksja/euksynia rozwinęła się w głębszych partiach kolumny wody, a chemoklina zlokalizowana byłą głębiej, przemieszczając się co najmniej okresowo powyżej granicy woda-osad, lecz poniżej strefy fotycznej.

Wyniki analizy biomarkerów oraz palinofacjalnej dokumentują dynamiczną ewolucję środowiska sedymentacji NW części TB. We wczesnym oligocenie panowały warunki głębokowodne z wyraźną dominacją MO pochodzenia morskiego. W basenie dochodziło do silnej stratyfikacji wód i rozwoju anoksji, a nawet euksynii, okresowo obejmującej strefę fotyczną, co potwierdzono obecnością izorenieratanu i wysokim udziałem drobnych framboidów pirytowych. Na przełomie wczesnego i późnego oligocenu odnotowano postępujące wypłycanie basenu, skorelowane z nasuwaniem się Pienidów i towarzyszącym mu epizodem kompresyjnym tej części TB. Wzmożona dostawa materiału lądowego zaznacza się w postaci bogatego zespołu biomarkerów roślin wyższych oraz licznych fragmentów kutikul i drewna. W kolumnie wody panowały warunki utleniające. Jednak w najwyższej części profilu w interwałach bogatszych w MO, odnotowano nawroty epizodów beztlenowych i eutrofizacji, prawdopodobnie związanych z dopływem nutrientów z lądu i spadkiem zasolenia wód.

Podsumowując, badania przedstawione w rozprawie pozwoliły na stworzenie rekonstrukcji ewolucji środowiska sedymentacji NW TB oraz basenów Tarcău i Vrancea, podkreślając wpływ tektoniki i zjawiska euksynii na procesy akumulacji węgla organicznego. Uzyskane dane biomarkerowe stanowią cenny materiał dla prospekcji węglowodorów w rejonie karpackim.

1. Wstęp

Na przełomie eocenu i oligocenu (~33,9 mln lat temu; Cohen et al., 2013) postępująca kolizja Afryki z Eurazją, Apulią i płytą arabską doprowadziła do ostatecznego zaniku Oceanu Tetydy i wyodrębnienia się z północnej części Morza Śródziemnego marginalnego basenu Paratetydy (Baldi, 1980; Rusu, 1988). Głównym czynnikiem wpływającym na ewolucję paleogeograficzną Paratetydy był powstający i rozwijający się w tym czasie łańcuch alpidów, rozciągający się od Pirenejów na zachodzie po Mały Kaukaz i Kopet-Dag na wschodzie. Wraz z intensywną tektoniką, postępujące na początku oligocenu ochłodzenie klimatu (Zachos et al., 2001) i zmiany eustatyczne (eustatic sea-level drop) doprowadziły do podziału Paratetydy na pomniejsze baseny czasowo izolowane od siebie i od oceanu światowego (np. Rögl, 1998). Basen Paratetydy dzieli się klasycznie na aktywny tektonicznie region z pomniejszymi basenami Paratetydy zachodniej, obejmującej alpejski basen przedgórski oraz Paratetydy środkowej, obejmującej liczne baseny od dzisiejszej Austrii po Rumunię, m.in. karpacki basen fliszowy, basen transylwański i węgierski basen paleogeński (Ryc. 1). Region stabilny tektoniczne, obejmujący baseny Morza Czarnego i Kaspijskiego, zwany jest Paratetydą wschodnią i stanowi powierzchniowo największą część Paratetydy (Ryc. 1) (Popov et al. 2004; Kováč et al. 2017; Sant et al. 2017).

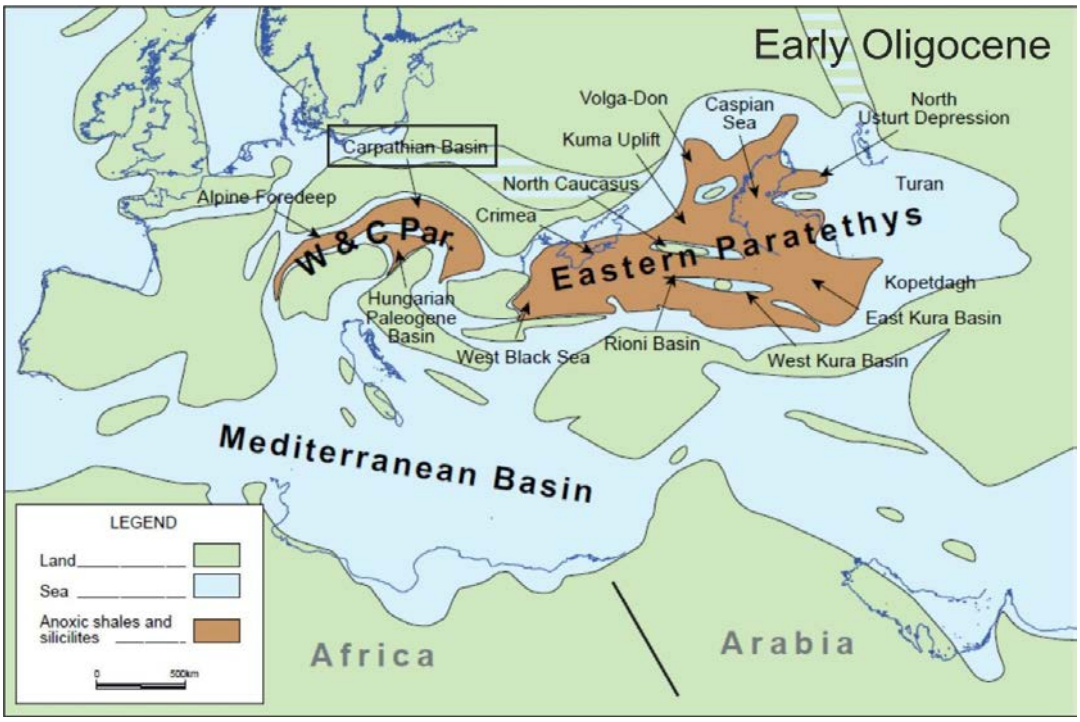

Ryc. 1. Paleogeografia Paratetydy we wczesnym oligocenie z wyróżnieniem (w kolorze brązowym) obszarów występowania facji bogatych w materię organiczną (tutaj jako „anoxic shales and silicites") (za Popov et al., 2004).

Powtarzająca się izolacja poszczególnych basenów doprowadziła do ewolucji organizmów endemicznych, reprezentowanych przez mięczaki (np. Baldi, 1986; Popov et al., 1993; Popov & Studencka, 2015), ryby (np. Kotlarczyk et al, 2006; Bieńkowska-Wasiluk et al., 2024) czy nannoflorę wapienną (np. Melinte, 2005). Pierwotnie koncept Paratetydy, jako ogromnego marginalnego morza ograniczał się do neogenu (Laskarev, 1924), jednak w latach 80-tych rozszerzony został o paleogen (Baldi, 1980; Rusu, 1988). Około 3 miliony lat temu nastąpił ostateczny zanik wielu z tych basenów i obecnie istnieją tylko pozostałości kiedyś rozległego morza. Są to: Morze Czarne, Morze Kaspijskie i Jezioro Aralskie (np. Palcu & Krijgsman, 2023). W oligocenie w wyniku wspomnianej izolacji, nastały warunki długotrwałej stratyfikacji wód oraz zubożenia w tlen (np. Köster et al., 1998b), sprzyjających osadzaniu się na szeroką skalę skał bogatych w materię organiczną (MO). Skały te, reprezentowane głównie przez iłowce, mułowce i rogowce, z rejonu Paratetydy zachodniej (alpejskiego basenu przedgórskiego) znane są jako formacja Schöneck (np. Schulz et al., 2005), natomiast z obszaru Paratetydy środkowej jako warstwy menilitowe z basenu karpackiego (np. Świdziński, 1947), Tard Clay z węgierskiego basenu paleogeńskiego (np. Bechtel et al., 2012) czy Ileanda z basenu transylwańskiego (Hofmann, 1879). W Paratetydzie wschodniej (rejon Morza Czarnego i Kaspijskiego) sedymentacja kontynuowała się po wczesny miocen, a jej odzwierciedleniem są nieraz miąższe (dochodzące do 2 km) sekwencje łupków bitumicznych formacji Maikop (np. Popov et al., 2008; Georgiev, 2012). W obrębie obszaru Paratetydy, skały głównie oligocenu i w mniejszym stopniu miocenu, odegrały kluczową rolę jako skały macierzyste w procesie generowania węglowodorów, szczególnie w jej środkowej i wschodniej części (np. Sachsenhofer et al.; 2018). Pochodzące z tego okresu facje ciemnych, nieraz zsilifikowanych łupków i rogowców występujące w obrębie warstw menilitowych, ze względu na dużą zawartość MO i powinowactwo do większości rop karpackich (np. ten Haven et al., 1993; Bessereau et al., 1997; Kotarba et al., 2007; Kosakowski et al., 2009; 2018), są szczególnie interesującym materiałem badawczym dla geologów i geochemików zajmujących się poszukiwaniami naftowymi. Od lat dziewięćdziesiątych XX wieku były one wielokrotnie badane w zakresie molekularnej geochemii organicznej, zwłaszcza na obszarze polskiej części Karpat zewnętrznych (np. ten Haven et al., 1993; Köster et al., 1995, 1998a, b; Kruge et al., 1996; Rospondek et al., 1997; Kotarba, 2007; Dziadzio & Matyasik, 2021; Wójcik-Tabol et al., 2022; Zakrzewski et al., 2024) i w mniejszym stopniu części ukraińskiej (Kotarba et al. 2005, 2007; Więcław et al., 2012; Rauball et al., 2019). W literaturze przedmiotu, w ujętych w pracy lokalizacjach, znajdujących się na obszarze rumuńskiej części Karpat wschodnich, badania MO

na poziomie molekularnym ograniczają się do pojedynczych prac (Sachsenhofer et al., 2015), zaś w rejonie basenu transylwańskiego przedstawione badania mają charakter pionierski.

Ze względu na szerokie rozprzestrzenienie geograficzne, diachroniczność sedymentacji oraz ogromne zróżnicowanie litofacjalne i geochemiczne, geneza skał oligocenu/miocenu z obszaru Paratetydy pozostawia szerokie pole do interpretacji paleośrodowiskowych. MO zawarta w skałach stanowi unikalne źródło informacji na temat środowiska depozycji panującego w basenie i pierwotnych producentów sedymentacyjnej MO, a także warunków i stopnia jej diagenezy. Biomarkery wchodzące w skład MO, analizowane w ramach niniejszej pracy, są niezwykle czułym narzędziem stosowanym w rekonstrukcjach paleośrodowisk, zwłaszcza w przypadku skał o ubogiej faunie lub jej braku. Biomarkery to związki organiczne pochodzące od organizmów żywych o niezmienionej bądź zmienionej w niewielkim stopniu (zachowane są cechy diagnostyczne pozwalające przyporządkować je do związku, z którego powstały) strukturze w stosunku do związku syntetyzowanego przez ich biologicznego prekursora. Prócz interpretacji środowiskowych, służyć mogą także do oceny stopnia dojrzałości MO w kontekście poszukiwań złóż węglowodorów, czy do korelacji skała źródłowa/ropa naftowa i ropa naftowa/ropa naftowa (Peters et al., 2005).

2. Cele pracy

Głównym celem pracy jest określenie warunków środowiska sedymentacji panujących w oligocenie w basenach środkowej Paratetydy, tj. w basenach Tarcău i Vrancea, należących do karpackiego basenu fliszowego oraz w basenie transylwańskim, w kontekście zdarzeń globalnych, tj. nakładającego się na siebie ochłodzenia klimatu (Aubry, 1992) i reorganizacji tektonicznej obszaru tetydzkiego, tj. izolacji Paratetydy od oceanu światowego (np. Palcu & Krijgsman, 2023), przy użyciu różnorodnych metod geochemicznych i petrograficznych, skupionych głównie na analizie MO zawartej w badanych skałach. W pracy podjęto próbę określenia mechanizmów prowadzących do powstania specyficznych warunków paleośrodowiskowych, a w konsekwencji do pogrzebania gigantycznych ilości MO w skałach oligocenu. Dodatkowo, starano się określić źródło MO na podstawie biomarkerów występujących w skałach, ze wsparciem analizy otwornic i palinofacji.

Drugim istotnym celem pracy jest określenie dojrzałości termicznej i potencjału węglowodorowego MO badanych skał z wykorzystaniem wskaźników biomarkerowych i tych otrzymanych przy zastosowaniu niezależnych metod, jak piroliza Rock-Eval i refleksyjność witrynitu.

3. Przedmiot badań i metody

Na potrzeby pracy doktorskiej materiał badawczy pobrany został z dwóch obszarów: północno-wschodniej części Karpat wschodnich (rumuńskich) oraz z północno-wschodniej części wyżyny transylwańskiej (zwanej dalej w kontekście geologicznym jako basen transylwański) (Ryc. 2). W przypadku Karpat wschodnich, opróbowano dwa kilkusetmetrowe (nieciągłe) odsłonięcia skał oligoceńskich wychodzące wzdłuż potoków zlokalizowanych w obrębie płaszczowiny Tarcău (profil Tărcuţa od nazwy strumienia) i sąsiadującej z nią płaszczowiny Vrancea (profil Nechit od nazwy rzeki). W przypadku basenu transylwańskiego pobrano próby z wychodni skał oligoceńskich wzdłuż potoku Fântânele (trzy sekcje profilu), zlokalizowanego w miejscowości o tej samej nazwie. Profile są szczegółowo omówione w publikacjach wchodzących w skład rozprawy. Analizom poddano kilkadziesiąt próbek skalnych, reprezentujących zróżnicowane litologie, tj. iłowce, mułowce, rogowce, margle bitumiczne i laminowane wapienie kokkolitowe wieku oligoceńskiego (potwierdzonego wynikami analiz zespołów otwornicowych wykonanych przez dr Ewę Malatę z ING UJ). Skały z Karpat wschodnich należą do ogniwa dolnych menilitów (Lower Menilite Member, dolny rupel) oraz do ogniwa margli bitumicznych (Bituminous Marls Member, górny rupel), natomiast utwory z basenu transylwańskiego reprezentowane są przez odpowiednik formacji menilitowej, lokalnie zwany formacją Ileanda (górny rupel) oraz następujące po niej skały należące do formacji Vima (górny rupel/szat).

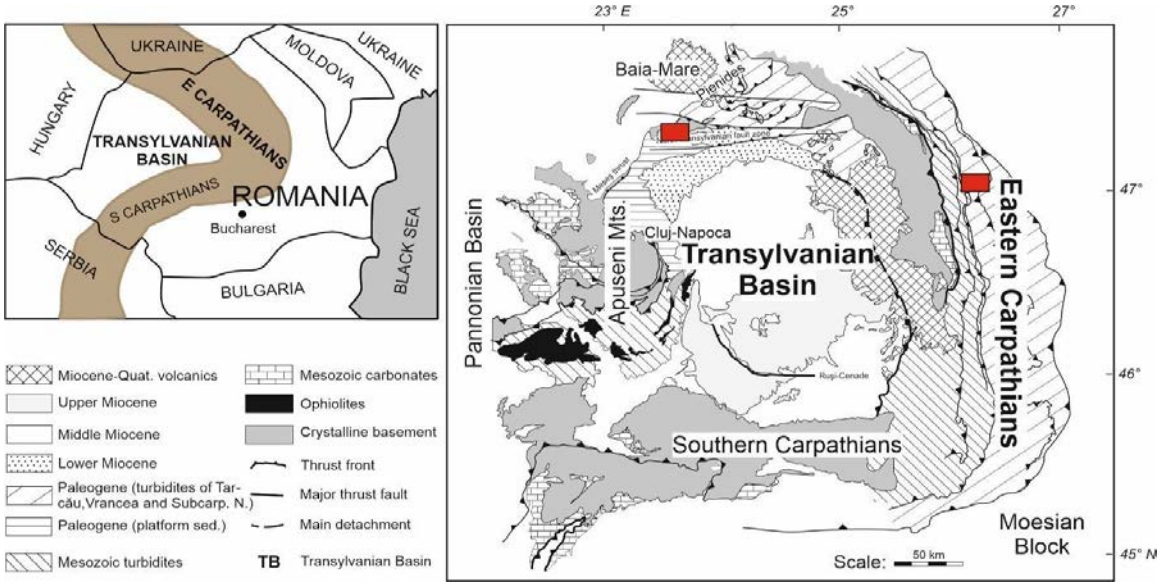

Ryc. 2. Obszar badań (zaznaczony w postaci czerwonych prostokątów) na tle mapy geologicznej Rumunii. Prostokąt po lewej – basen transylwański, profil Fântânele; prostokąt po prawej - Karpaty wschodnie, płaszczowiny Tarcău i Vrancea, profile Nechit i Tărcuţa (mapa za Krezsek & Bally, 2006; zmodyfikowane).

Metody badawcze zastosowane w celu realizacji założeń pracy to przede wszystkim badania laboratoryjne nakierowane na identyfikację składu molekularnego MO zawartej w ekstrahowalnej materii organicznej w skałach, zakończone analizą chromatografii gazowej sprzężonej ze spektrometrią mas (GC-MS). Efektem końcowym takich analiz jest identyfikacja i interpretacja związków organicznych, a zwłaszcza biomarkerów, wchodzących w skład frakcji alifatycznych i aromatycznych. Dodatkowo, dla wybranych próbek z płaszczowin Tarcău i Vrancea, wykonano derywatyzację (*N*-(*tert*-butylodimetylosililo)-*N*-metylotrifluoroacetamidem - MTBSTFA) frakcji polarnych w celu umożliwienia identyfikacji metodą GC-MS związków z grupy maleimidów. Na Ryc. 3 przedstawiono standardowy tok badań MO, którym poddano wybrane próbki skalne.

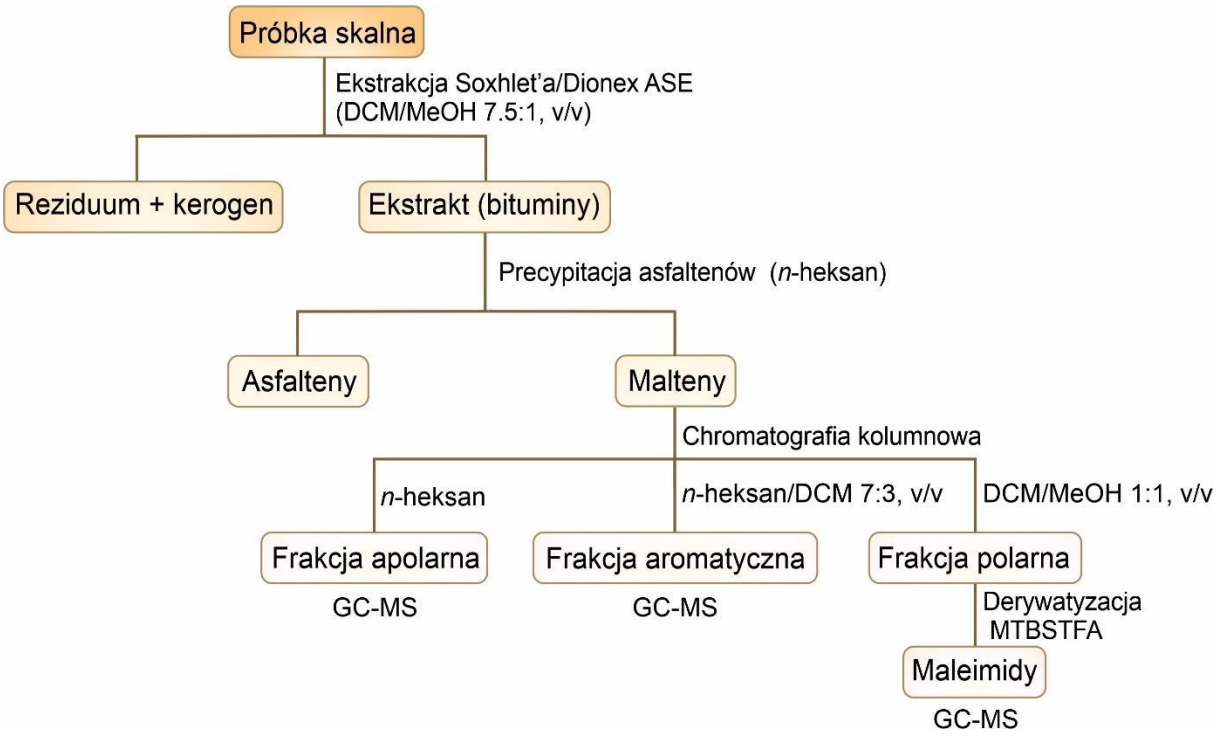

Ryc. 3. Schemat metod analizy materii organicznej zawartej w skałach oligoceńskich wykonanych w ramach realizacji rozprawy. DCM - dichlorometan; MeOH - metanol; v/v - stosunek objętościowy; GC-MS - chromatografia gazowa sprzężona ze spektrometrią mas.

Z metod badań geochemicznych wykonano także analizę zawartości całkowitego węgla organicznego (total organic carbon – TOC) i siarki całkowitej (total sulfur - TS) oraz pirolizę Rock-Eval, natomiast z metod optycznych pomiary refleksyjności witrynitu (R_o), pomiary średnic framboidów pirytowych oraz analizę palinofacjalną. W Tabeli 1 zestawiono podstawowe informacje o obszarze badań, zastosowanych metodach i ilościach próbek

poddanych danej metodzie. Przy każdej metodzie skrótowo opisano jakiego typu informacje można uzyskać dzięki jej zastosowaniu.

Tabela 1. Obszar badań i metodyka badawcza zastosowana w rozprawie doktorskiej.

Obszar badań	**Lokalizacja geograficzna**	**Interwał**	**Metody/ilość prób poddanych analizie**							**Publikacja**
			Analiza zespołów otwornic	*Refleksyjność witrynitu*	*Analiza rozkładu średnic framboidów pirytowych*	*Analiza palinofacji*	*Analiza elementarna (TOC i TS)*	*Wskaźniki biomarkerowe (GC-MS)*	*Piroliza Rock-Eval*	
			Wiek	Dojrzałość termiczna MO	Warunki redoks	Pierwotni producenci MO, środowisko depozycyjne, warunki redoks	Produktywność, warunki redoks	Pierwotni producenci MO, produktywność, warunki redoks, zasolenie, dojrzałość termiczna MO	Zawartość TOC, dojrzałość termiczna MO, potencjał węglowodorowy	
Wschodnie Karpaty zewnętrzne Płaszczowiny Tarcău i Vrancea (należące do Mołdawidów zewnętrznych)	Okolice miejscowości Piatra Neamţ, odsłonięcia wzdłuż potoków Nechit i Tărcuţa (Ryc. 2)	Dolny oligocen (rupel) ogniwo dolnych menilitów i margli bitumicznych	+/14	+/15	+/21	-	+/36	+/40	+/28	Wendorff et al. (2017) Wendorff-Belon et al. (2021)
Basen transylwański	Okolice miejscowości Targu Lapuş, odsłonięcie wzdłuż potoku Fântânele (Ryc. 2)	Dolny i górny oligocen (rupel/szat) Formacja Ileanda i Vima	+/12	+/7	+/13	+/13	+/18	+/18	+/18	Wendorff-Belon et al. (2025)

4. Wyniki badań i dyskusja

4.1. Dojrzałość termiczna materii organicznej i potencjał węglowodorowy oligoceńskich skał z płaszczowin Tarcău i Vrancea oraz z basenu transylwańskiego

Na podstawie:

Wendorff, M., Rospondek, M., Kluska, B., Marynowski, L., 2017. Organic matter maturity and hydrocarbon potential of the Lower Oligocene Menilite facies in the Eastern Flysch Carpathians (Tarcău and Vrancea Nappes), Romania. Applied Geochemistry 78, 295–310.

oraz

Wendorff-Belon, M., Loręc, R., Wierzbicki, A., Rospondek, M., Marynowski, L., 2025. Oligocene environmental changes in the Central Paratethys: geochemical and palynofacial record from the north-western Transylvanian Basin (Romania). Palaeogeography, Palaeoclimatology, Palaeoecology 676, 113124.

Przeprowadzono kompleksową analizę geochemiczną (parametry z pirolizy Rock-Eval i biomarkerowe) oraz petrograficzną (refleksyjność witrynitu) MO zawartej w skałach z Karpat wschodnich pochodzących z profili Tărcuţa (płaszczowina Tarcău) i Nechit (płaszczowina Vrancea), oraz w skałach z profilu Fântânele z basenu transylwańskiego, pod kątem określenia stopnia dojrzałości termicznej, a także oceny potencjału węglowodorowego badanych skał.

MO z pierwszego obszaru, tj. Karpat wschodnich, wykazuje zróżnicowany stopień dojrzałości termicznej w zależności od płaszczowiny, z której pochodzi. Próbki z profilu Tărcuţa w płaszczowinie Tarcău zawierają MO niedojrzałą do znajdującej się w początkowej fazie generacji węglowodorów (tzw. fazie okna ropnego), na co wskazują wartości refleksyjności witrynitu (R_o = ~0,51%) oraz parametrów z pirolizy Rock-Eval (T_{max} = ~430°C i production index PI = $S_1/(S_1+S_2)$ = ~0,27; Ryc. 4 A), a także obecność szczelin zaimpregnowanych bituminami w pojedynczych próbkach z sąsiadującego odsłonięcia w potoku Goşman (nie będących przedmiotem rozprawy). W skałach z profilu Nechit, MO jest niedojrzała termicznie, co potwierdzają wyniki wszystkich wymienionych analiz, tj. R_o = ~0.38%, T_{max} = ~425 °C, PI = ~0,08. Wskaźniki dojrzałości oparte na biomarkerach, zwłaszcza stosunek epimerów steranu C_{29} 20S/(20S+20R), epimerów hopanu C_{31} αβ 22S/(22S+22R) i izomerów strukturalnych hopanu C_{30} βα/(βα+αβ), podkreślają owe zróżnicowanie. Większość próbek z profilu Tărcuţa zawiera MO o dojrzałości osiągającej wejście w tzw. okno ropne (Ryc. 4B i C), w przeciwieństwie do niedojrzałej MO z profilu Nechit. Biomarkery stanowią więc

najczulsze narzędzie do oceny stopnia dojrzałości termicznej MO w przypadku badanych skał, lecz mają ograniczenie w związku z faktem osiągnięcia stanu równowagi (np. w odniesieniu do grupy hopanów).

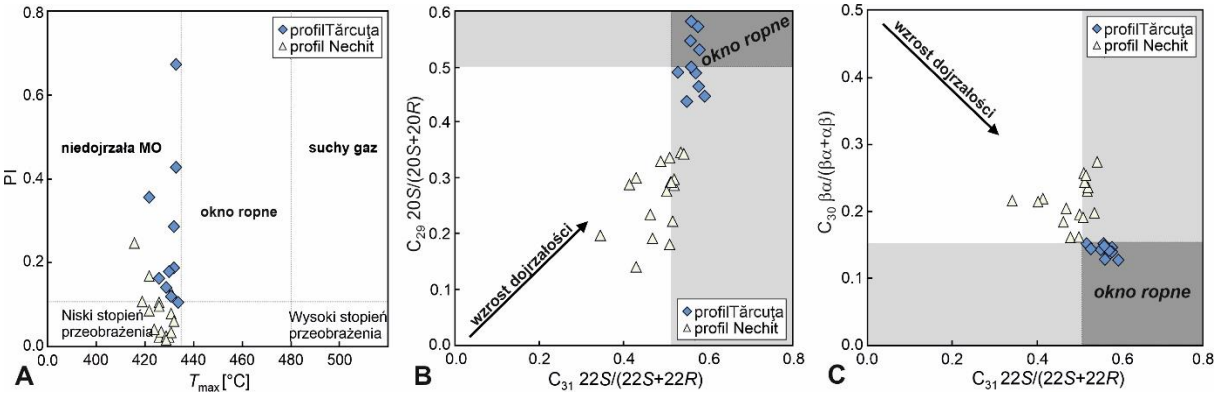

Ryc. 4. Wykresy korelacyjne przedstawiające różny poziom zaawansowania dojrzałości termicznej MO dla próbek z płaszczowiny Tarcău i Vrancea. A – parametry z pirolizy Rock-Eval, B i C – parametry oparte na biomarkerach.

Różny stopień zaawansowania dojrzałości termicznej pomiędzy badanymi lokalizacjami, wynikać może z położenia płaszczowiny Tarcău w bardziej wewnętrznej strefie orogenu karpackiego, w porównaniu do płaszczowiny Vrancea, a tym samym z różnym czasem pogrążenia, który z kolei zależy od intensywności późniejszych procesów erozyjnych i ekshumacyjnych. Analogiczny trend wzrastającej dojrzałości w kierunku orogenu jest opisany w polskiej części Karpat zewnętrznych, gdzie MO z płaszczowiny skolskiej jest niedojrzała (T_{max} = ~420°C), wzrastając do zaawansowanego stadium okna ropnego w płaszczowinie śląskiej (T_{max} = ~450°C) (np. Köster et al., 1998a; Kotarba et al., 2007).

Skały z profilu Nechit wykazują w większości dobry do bardzo dobrego potencjał węglowodorowy, o czym świadczy wysoka zawartość TOC średnio na poziomie 3,64% wag. Suma węglowodorów wolnych wyrażonych wartością parametru S_1 otrzymanego w wyniku pirolizy Rock-Eval i węglowodorów wygenerowanych w wyniku krakingu kerogenu (S_2) w tym samym procesie, zwana potencjałem węglowodorowym (S_1+S_2) wynosząca średnio 15,68 mg HC/g skały, również wskazuje na dobry do bardzo dobrego potencjał skał oligoceńskich z profilu Nechit. Potencjał ten jednak nie został zrealizowany w badanym rejonie, o czym świadczą wysokie wartości wskaźnika wodorowego (HI = 213-595 mg HC/g TOC). Z kolei skały z profilu Tărcuţa charakteryzują się umiarkowanym do dobrego potencjałem węglowodorowym (TOC ~1,89% wag. i suma S_1 i S_2 ~6,07 mg HC/g skały). Podsumowując, badane skały wykazują wysoki potencjał macierzystości, choć należy zaznaczyć, że powyższe wnioski ograniczają się do poziomów skał bogatych w MO.

Prawdopodobnie część węglowodorów została wygenerowana w skałach z profilu Tărcuţa, o czym świadczy obecność szczelin zaimpregnowanych bituminami oraz wartości parametru S_1 osiągające nawet 4,17 mg HC/g skały (dla próbki skrzemionkowanego łupka z ogniwa dolnych menilitów) oraz stosunku zawartości ekstrahowalnej MO do TOC (do 259 mg EOM/g TOC dla czarnego łupka menilitowego).

Na drugim z badanych obszarów, tj. w basenie transylwańskim, skały z profilu Fântânele zawierają MO o niskim stopniu dojrzałości termicznej, co przejawia się w obecności związków nienasyconych, jak diastereny i 4-metylodiastereny, stanowiące efekt wczesnej diagenezy ich biologicznych prekursorów (steroli i 4-metylosteroli) (de Leeuw et al., 1989; Peters et al., 2005). Pomierzone refleksyjności witrynitu na poziomie 0,42% oraz wartości T_{max} = ~422°C, potwierdzają niedojrzałość termiczną badanej MO. Próbki z formacji Ileanda zawierają w przewadze kerogen typu II (ropotwórczy), w skałach formacji Vima wzrasta domieszka kerogenu typu III (gazotwórczego) (Ryc. 5 A). Formacje wykazują zróżnicowanie pod kątem potencjału generacyjnego węglowodorów (Ryc. 5 B), co wynika ze zróżnicowanej zawartości MO, wyrażonej w TOC dochodzącym do 5,88% wag. (średnio 3,06% wag.) dla próbek z formacji Ileanda i do 2,30% wag. (średnio 1,11% wag.) dla formacji Vima. Ciemne, laminowane skrzemionkowane skały (typowe łupki menilitowe), o wysokiej zawartości TOC i jednocześnie wysokich wartościach parametru S_1+S_2 (~15,16 mg HC/g skały), scharakteryzować można jako skały o bardzo dobrym potencjale węglowodorowym. Skały z formacji Vima wykazują głównie średni do słabego potencjał węglowodorowy (S_1+S_2 =~2,18 mg HC/g skały) (Ryc. 5 B).

Pomimo wysokiego potencjału węglowodorowego, skały formacji Ileanda nie są perspektywiczne dla eksploracji złóż węglowodorów w tym rejonie basenu transylwańskiego, co potwierdzają inni autorzy, wskazując na niedostateczną dojrzałość MO w skałach z formacji Ileanda (Popescu, 1995; De Broucker et al., 1998). Związane jest to z niewystarczającą głębokością pogrążenia skał oligocenu odpowiadającą początkowi etapu generowania węglowodorów. Gröger et al. (2008), na podstawie badań trakowych cyrkonu, wykluczył istotny wzrost strumienia cieplnego wynikający z nacisku osadów od paleogenu do wczesnego miocenu w północnej części basenu transylwańskiego.

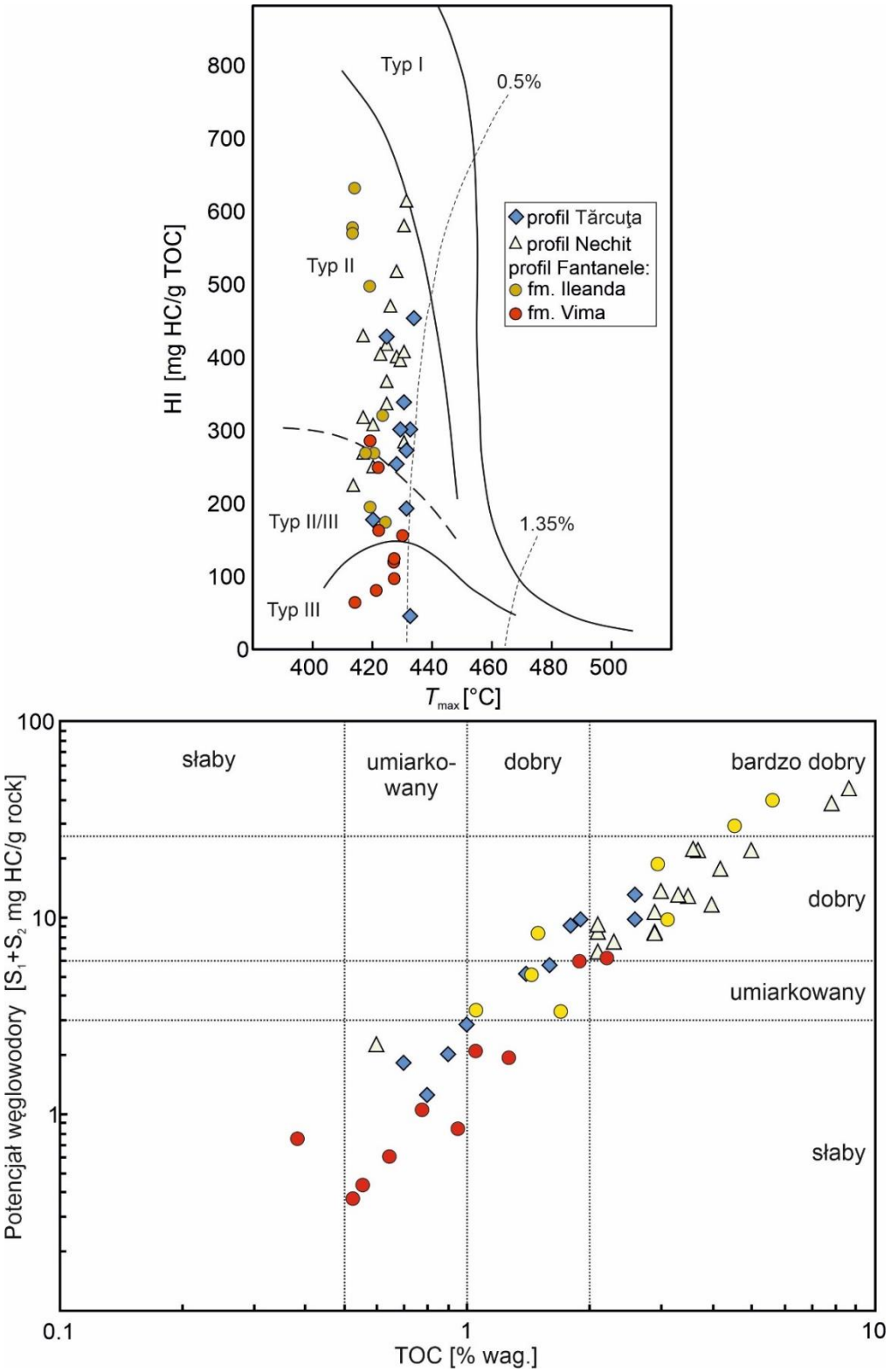

Ryc. 5. Diagramy korelacyjne oparte na parametrach z pirolizy Rock-Eval. U góry – diagram van Krevelena przedstawiający typy kerogenu w skałach ze wszystkich lokalizacji; u dołu – diagram przedstawiający potencjał węglowodorowy badanych skał.

4.2. Paleośrodowisko sedymentacji osadów oligocenu w basenach Tarcău i Vrancea

Na podstawie:
Wendorff-Belon, M., Rospondek, M., Marynowski, L., 2021. Early Oligocene environment of the central Paratethys revealed by biomarkers and pyrite framboids from the Tarcău and Vrancea nappes (Eastern Outer Carpathians, Romania). Marine and Petroleum Geology 128, 105037.

Badane skały facji menilitowej zawierają MO o zróżnicowanym składzie molekularnym w zależności od litologii. W skałach skrzemionkowanych zauważalna jest przewaga hopanoidów (związków pochodzenia bakteryjnego) oraz średniołańcuchowych *n*-alkanów, głównie pochodzenia algowego, natomiast w łupkach marglistych i mułowcach zaznacza się przewaga długołańcuchowych nieparzystowęglowych *n*-alkanów (*n*-C_{27}, *n*-C_{29}, *n*-C_{31}), pochodzących z wosków epikutykularnych roślin lądowych (np. Eglinton & Hamilton, 1967; Rieley et al., 1991). Pomiędzy badanymi lokalizacjami również zaobserwowano znaczną odmienność w składzie badanej MO. Bogatszy zestaw biomarkerów w skałach z profilu Nechit kontrastuje z bardziej ujednoliconym i uboższym składem MO w próbkach z profilu Tărcuţa. Charakterystyczna dystrybucja *n*-alkanów o przewadze krótko- i średniołańcuchowych cząsteczek, przewaga cyklicznych izoprenoidów (steranów i hopanów) nad *n*-alkanami, wskazują na niewielki wpływ dojrzałości termicznej czy biodegradacji na pierwotny skład MO. Dla opisywanego w rozdziale 4.1. i pracy nr 1 stopnia dojrzałości termicznej (profil Nechit - T_{max} = ~425°C i R_o = ~0,38%; profil Tărcuţa - T_{max} = ~431°C i R_o = ~0,51%), większość biomarkerów powinna wykazywać stabilność, nie ulegając znaczącej degradacji termicznej (np. Peters et al., 2005). Zachowany rozkład związków organicznych powinien więc odzwierciedlać uwarunkowania facjalne oraz pierwotne warunki panujące w basenach Vrancea i Tarcău na etapie wczesnej diagenezy.

4.2.1. Źródło MO

W basenie Vrancea we wczesnym oligocenie dominowały organizmy biosylifikujące, reprezentowane przez okrzemki i bruzdnice, co potwierdza obecność odpowiednio – wysoko rozgałęzionych izoprenoidów w formie alkanów (HBI) i tiofenów (HBIT), oraz trójaromatycznych dinosteroidów (A-ring methyl triaromatic steroids) (dystrybucja związków na Ryc. 6 w pracy nr 2). Identyfikacja HBI zarówno w łupkach menilitowych z polskiej części

Karpat zewnętrznych (Rospondek et al., 1997; Köster et al., 1998b; Sachsenhofer et al., 2015; Wójcik-Tabol et al., 2022; Zakrzewski et al., 2024), a także w marglach bitumicznych oraz dolnych i górnych łupkach dysodylowych (datowanych na późny rupel/szat aż po akwitan, np. Tăbără et al., 2015; Sachsenhofer et al., 2015) w rumuńskim sektorze Karpat zewnętrznych, wskazuje na niezwykle istotny wkład okrzemek w deponowaną MO w oligocenie aż po wczesny miocen. Istotna przewaga steranów nad hopanami, wyrażona niskimi wartościami stosunku 17α H/S (Ryc. 6), i przeważnie wysokie wartości TOC (osiągające 8,62% wag. dla ogniwa dolnych menilitów i 10,82% wag. dla ogniwa margli bitumicznych) odzwierciedlają intensywną bioproduktywność w tej części basenu Vrancea. Obecność biomarkerów pochodzących od roślin żywicujących (np. simonellit, reten, tetrahydroreten - na Ryc. 8 w pracy nr 2) oraz oleananu, charakterystycznego dla roślin okrytonasiennych, w profilu Nechit wskazuje na stałą dostawę terygenicznej MO do basenu Vrancea we wczesnym oligocenie. Znaczący wkład biomasy prokariotycznej, został udokumentowany we wszystkich badanych próbkach na podstawie obecności znacznych ilości hopanoidów (Ryc. 5 w pracy nr 2). Dodatkowo w dziesięciu próbkach z profilu Nechit zidentyfikowano arylowe izoprenoidy, które współwystępują z izorenieratanem i Me,*i*-Bu maleimidami w kilku z tych próbek, świadcząc o epizodycznej, wzmożonej działalności zielonych bakterii siarkowych (*Chlorobiaceae*) w basenie Vrancea w rupelu (Ryc. 8 w pracy nr 2). *Chlorobiaceae* to fotoautotroficzne, ściśle beztlenowe bakterie, wykorzystujące zredukowane formy siarki (H_2S, siarka elementarna) jako źródła elektronów. Produkują wyspecjalizowane pigmenty, jak bakteriochlorofile *c*, *d* i *e* oraz karotenoidy, np. izorenieraten (Summons i Powell, 1987; Koopmans et al., 1996a), których produkty diagenezy, jak Me,*i*-Bu maleimidy, izorenieratan i arylowe izoprenoidy, świadczą nie tylko o działalności tych bakterii, ale także o istnieniu euksynii sięgającej do strefy fotycznej (np. Grice et al., 1996; Koopmans et al., 1996a; Schwark & Frimmel, 2004; Naeher et al., 2013). Dominacja hopanów nad steranami (17α H/S osiągająca 9,48 dla próbki TAR 4; Ryc. 6) i korelująca z monometylowymi C_{15} i C_{17} alkanami w próbkach z profilu Tărcuţa, szczególnie w skrzemionkowanych łupkach i rogowcach, wskazuje na intensywną działalność prokariotów, a dokładniej cyjanobakterii. Obecność cyjanobakterii operujących w kolumnie wody w czasie depozycji łupków menilitowych z obszaru polskich Karpat zewnętrznych (płaszczowina skolska i dukielska) udokumentowana została na podstawie składu izotopowego węgla C_{31}-C_{35} homohopanów (Köster et al., 1998b). Jedynie w próbce wapienia tylawskiego z profilu Tărcuţa zidentyfikowano związek C_{25} HBI, co idzie w parze z jego genezą związaną z intensywnymi zakwitami kokkolitoforów i okrzemek w prawdopodobnie izolowanym anoksycznym basenie (np. Haczewski, 1989). Brak HBI w

pozostałych próbkach niekoniecznie musi świadczyć o nieobecności okrzemek w basenie Tarcău we wczesnym oligocenie. Można to tłumaczyć aktywnością okrzemek, które nie syntezują związków prekursorskich dla HBI lub degradacją tych związków w natlenionej strefie kolumny wody. Udział substancji pochodzenia lądowego był znikomy, na co wskazują wartości wskaźnika TAR <1 (terrigenous vs aquatic *n*-alkanes ratio; Bourbonniere & Meyers, 1996) dla większości próbek (Tabela 1, w pracy nr 2), jak również brak biomarkerów pochodzących od roślin wyższych, prócz oleananu w dwóch próbkach margli bitumicznych.

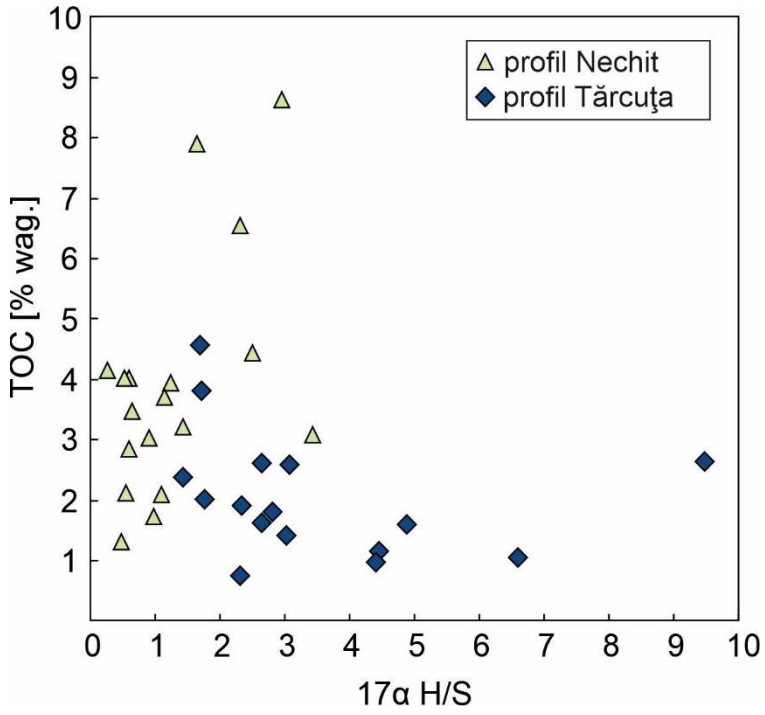

Ryc. 6. Wykres zależności TOC od stosunku 17α hopanów do steranów (17α H/S) dla badanych próbek z profilu Nechit (płaszczowina Vrancea) i profilu Tărcuţa (płaszczowina Tarcău).

4.2.2. Paleozasolenie

Depozycja we wczesnym oligocenie w basenie Vrancea, zwłaszcza dolnej części ogniwa dolnych menilitów i najwyższej margli bitumicznych, zachodziła w warunkach obniżonego zasolenia, co stwierdzono na podstawie stosunku 2-metylo-2-(trimetylotridecylo)chromanów (MTTCI), sięgającego 0,9 i podwyższonych wartości stosunku pristanu do fytanu (Pr/Ph) (Schwark et al., 1998; Peters et al., 2005, Wang et al., 2011). Spadek zasolenia wód w tej części basenu został zanotowany także przez Filipek (2020) na podstawie obecności *Botryococcus* sp. (zielonych alg tworzących maty w wodach słodkich po brakiczne) w składzie palinofacjalnym skał z tego samego profilu. Mechanizmem odpowiedzialnym za spadek zasolenia mogła być

wzmożona dostawa wód z lądu do przynajmniej czasowo izolowanego basenu, o czym świadczy obecność biomarkerów charakterystycznych dla roślin lądowych w składzie molekularnym ze wszystkich badanych próbek z profilu Nechit. Spadek zasolenia wód na początku rupelu, tj. w górnej części NP21 (standardowego poziomu nannoplanktonu wapiennego wg. Martini, 1971) jest zjawiskiem szeroko opisywanym w wielu rejonach Paratetydy (np. jako tzw. Solenovian Event w Paratetydzie wschodniej; np. Rusu, 1999; Sachsenhofer et al., 2018), jednak zachodził on wcześniej, niż depozycja osadów ogniwa dolnych menilitów i margli bitumicznych (NP23-24). Nie wyklucza to jednak zaistnienia podobnych warunków lokalnie, co związane może być ze zróżnicowaniem środowiska sedymentacji (płytkowodne, bliższe linii brzegowej vs. otwarty basen, duża odległość od lądu) zarówno w obrębie całej Paratetydy jak i w obrębie poszczególnych basenów.

4.2.3. Warunki redoks

Analiza średnic framboidów pirytowych jest jedną z metod wykorzystywanych w interpretacjach paleośrodowiskowych, a konkretnie warunków redoks panujących w basenach sedymentacyjnych (np. Zatoń et al., 2008). Pozwala na rozróżnienie pomiędzy warunkami euksynicznymi (pozbawionymi tlenu, z obecnością siarkowodoru), dysoksycznymi (ubogimi w tlen) i anoksycznymi (beztlenowymi, bez siarkowodoru) (np. Wignall & Newton, 1998). Wilkin et al. (1996) rozróżniają dwa typy framboidów: syngenetyczne (średnica <6 μm), o ujednoliconych rozmiarach, które tworzą się w toni wodnej, opadając po osiągnięciu krytycznej średnicy około 5-6 μm, oraz framboidy diagenetyczne (> 6 μm średnicy), powstające w osadzie pod tlenową lub dysoksyczną warstwą wody. Framboidy syngenetyczne nie przyrastają po akumulacji na dnie basenu, mogą jedynie zwiększać się poprzez wtórny wzrost pirytu euhedralnego (lecz wówczas nie są brane pod uwagę przy pomiarach). Identyfikacja typu framboidów opiera się na analizie średnich wartości ich średnic oraz odchylenia standardowego (Zatoń et al., 2008).

W skałach z profilu Nechit zaobserwowano dominację drobnych framboidów pirytowych (<5 μm), stanowiących do 92,1% populacji w czarnych skrzemionkowanych łupkach ogniwa dolnych menilitów (Ryc. 3 i Tabela 2 w pracy nr 2). Taki rozkład wielkości średnic pirytów wskazuje na ich powstawanie w środowisku euksynicznym w kolumnie wody (np. Wilkin et al., 1996; Bond & Wignall, 2010; Dustira et al., 2013). Brak bioturbacji oraz obecność otwornic bentonicznych (*Bulimina*, *Chilostomella*) typowych dla środowisk dysoksycznych, a nawet anoksycznych, w próbkach z profilu Nechit dodatkowo wskazują na warunki niedoboru tlenu

przy dnie. Podobny wniosek można wysnuć na podstawie obecności związków HBIT w większości badanych próbek z profilu Nechit (Tabela 1 w pracy nr 2), świadczących o wzmożonej działalności bakterii redukujących siarczany w środowisku beztlenowym. Związki te mają skłonność do zachowania się w zapisie geologicznym dzięki włączaniu w swoją strukturę siarki na etapie wczesnej diagenezy w osadzie (Kohnen et al., 1990), bądź jeszcze w euksynicznej strefie kolumny wody (Hebting et al., 2006).

Jednak wskaźniki oparte na biomarkerach, tj. stosunek Pr/Ph zwykle > 1 oraz niskie wartości indeksu homohopanowego C_{35} HHI, sugerują obecność warunków dysoksycznych-oksycznych (np. Didyk et al., 1978) w basenie Vrancea, zwłaszcza w czasie depozycji ogniwa margli bitumicznych (Tabela 1 w pracy nr 2). Rozbieżność ta może wynikać ze zróżnicowania warunków natlenienia w kolumnie wody – powierzchniowe warstwy mogły być bardziej natlenione, i w nich mogło dochodzić do utlenienia związków prekursorkich dla pristanu, fitanu czy hopanoidów, podczas gdy głębsze partie charakteryzowały się niedoborem tlenu i rozwojem warunków anoksycznych/euksynicznych.

W wybranych skałach z profilu Nechit dodatkowo stwierdzono 2-metylo-3-*iso*-butylo-maleimidy (Me,*i*-Bu-malemidy) (Ryc. 9 w pracy nr 2), związki będące efektem diagenezy izorenieratenu, podobnie jak arylowe izoprenoidy (Ryc. 8 w pracy nr 2), choć te mogą mieć alternatywne źródło w postaci karotenoidów (np. Koopmans et al., 1996b). Jednakże współwystępowanie wskazanych biomarkerów i identyfikacja izorenieratanu w kilku próbkach z profilu Nechit może wskazywać na epizodyczną działalność *Chlorobiaceae* w badanej części basenu Vrancea i w związku z tym na okresowe warunki euksynii w strefie fotycznej kolumny wody, a więc warunki sprzyjające pogrzebaniu znacznych ilości MO (TOC sięgające 8,62% wag. dla ogniwa dolnych menilitów i 10,82% wag. dla ogniwa margli bitumicznych). Euksynia w strefie fotycznej mogła być wywołana dopływem bogatej w składniki odżywcze wody słodkiej do izolowanego basenu, udokumentowanego obecnością biomarkerów roślin lądowych i spadkiem zasolenia, wyrażonym wysokimi wartościami MTTCI. To z kolei prowadzić mogło do wzmożonej produkcji pierwotnej i w konsekwencji do eutrofizacji.

W większości skał z profilu Tărcuţa również zaznacza się wyraźna przewaga drobnych framboidów pirytowych (do 92,3%; Tabela 2 w pracy nr 2), co może wskazywać na okresowe rozwinięcie się warunków euksynicznych w kolumnie wody. Niskie wartości stosunku dibenzotiofenu do fenantrenu (DBT/P; Hughes et al., 1995), brak C_{25} HBIT i obecność pirytu sugerują efektywne wiązanie siarki przez żelazo, a tym samym jej ograniczoną dostępność do reakcji z MO. Brak biomarkerów pochodzących od *Chlorobiaceae* sugeruje, iż euksynia nie sięgnęła strefy fotycznej bądź trwała niedostatecznie długo, by pozostawić zapis w składzie

molekularnym MO (np. Huang et al., 2000). Jednak zważywszy na inne wskaźniki, tj. ogromną ilość drobnych framboidów, powszechną laminację osadów, czy obecność otwornic bentonicznych typu *Bulimina* czy *Chillostomella*, wnioskować można, że anoksja/euksynia rozwinęła się w głębszych partiach kolumny wody. Framboidy pirytowe powstawały w pobliżu chemokliny zlokalizowanej głębiej i przemieszczającej się co najmniej okresowo powyżej granicy woda-osad, lecz poniżej strefy fotycznej. Warto jednak zauważyć, że obecność wymienionych otwornic może być związana bardziej ze środowiskami o wzmożonej bioproduktywności, niż z warunkami deficytu tlenowego (Rathburn & Corliss, 1994).

Wskaźniki biomarkerowe (Pr/Ph, C_{35} HHI) sugerują dysoksyczne warunki w trakcie depozycji ogniwa dolnych menilitów, fluktuujące w kierunku warunków utleniających w czasie depozycji ogniwa margli bitumicznych (Tabela 1 i Ryc. 3 w pracy nr 2), podobnie jak w przypadku próbek z profilu Nechit. Wczesna diageneza prekursorów pochodzących od organizmów fotoautotroficznych prawdopodobnie rozpoczynała się w górnej, natlenionej części kolumny wody, gdzie mogła być dodatkowo modyfikowana przez fotodegradację (Rontani et al., 1991; 2011), ograniczającą ich reaktywność względem zredukowanej siarki. Alternatywnym wytłumaczeniem tych rozbieżności może być okresowe natlenienie wód dennych związanych z lokalnym upwellingiem. Zjawisko to było proponowane przez różnych autorów (np. Veto, 1987; Koltun, 1992; Soták, 2010), jako główny mechanizm prowadzący do anoksji i wysokiej produktywności w Paratetydzie środkowej we wczesnym oligocenie. Kotlarczyk & Uchman (2012) wykazali jednak, że w basenie skolskim, interpretowanym jako przedłużenie basenu Tarcău, anoksja związana z upwellingiem rozwinęła się dopiero w późnym rupelu i szacie (NP24–NP25), czyli po sedymentacji margli bitumicznych. W przypadku basenu Vrancea, położonego prawdopodobnie w marginalnej części Paratetydy środkowej, możliwe było występowanie upwellingu przybrzeżnego połączonego z dopływem składników odżywczych z lądu i podwyższoną produktywnością (wyrażoną wysokimi wartościami TOC i HI oraz niskim stosunkiem 17α H/S). Zjawisko to jest powszechnie obserwowane we współczesnych środowiskach szelfowych (np. u wybrzeży Peru) i znane również z innych basenów paleozoicznych (np. formacja Phosphoria; Maughan, 1993). Natlenienie wód mogło być związane także z epizodycznym napływem słonych, natlenionych wód głębinowych – podobnie jak we współczesnym Morzu Bałtyckim (np. Mohrholz et al., 2006; 2015), gdzie co kilka dekad dochodzi do mieszania bardziej zasolonych i natlenionych wód z Morza Północnego z anoksycznymi wodami dennymi głębi gotlandzkiej (Franck et al., 1987; Mohrholz et al., 2015).

4.2.4. Środowisko sedymentacyjne i bioproduktywność

Opisane różnice w składzie molekularnym MO charakteryzujące skały z profilu Nechit i Tărcuţa odzwierciedlają odmienne pierwotne warunki środowiskowe kontrolowane przez produktywność biologiczną, związaną z kolei z różnym położeniem basenów Vrancea i Tarcău we wczesnym oligocenie. Pierwotna produkcja była wyraźnie wyższa w domenie Vrancea, niż w Tarcău, co potwierdzają wysokie wartości TOC i HI oraz niskie wartości stosunku 17α H/S. Z kolei obecność biomarkerów roślin wyższych może być związana z bliskością basenu Vrancea do lądu, gdzie dostępność składników odżywczych sprzyjała wzmożonemu rozwojowi fitoplanktonu (Ryc. 15 w pracy nr 2). Wysokie wartości MTTCI wskazują na epizodyczny dopływ wód słodkich i spadek zasolenia, szczególnie podczas sedymentacji ogniwa margli bitumicznych. W tym czasie zjawisko stratyfikacji gęstościowej (związanej z zasoleniem) nałożyć się mogło na zwiększoną bioproduktywność, co sugerowano również dla zachodniej Paratetydy pod koniec wczesnego oligocenu, w trakcie depozycji odpowiedników margli dynowskich (NP23; Schulz et al., 2005). Prezentowana interpretacja środowiska depozycji we wczesnym oligocenie w badanej części basenu Vrancea stoi w zgodzie z tą proponowaną przez innych autorów. Miclăuş et al. (2009) wskazuje na warunki płytkowodne do umiarkowanej głębokości z intensywną dostawą materiału lądowego i wysoką energią transportu, opierając swoją interpretację na obecności piaskowców z kopułowym warstwowaniem przekątnym (podobnie u Filipek, 2020) oraz dobrze zachowanej skamieniałości płastugi (flat fish) w marglach bitumicznych (Baciu & Chanet, 2002). Zespoły dinocyst zidentyfikowane w marglach bitumicznych z sąsiadującego odsłonięcia (w korycie rzeki Tazlau), charakterystyczne dla środowiska przybrzeżnego o wodach bogatych w nutrienty, wspierają tę interpretację (Sachsenhofer et al., 2015). Dostawa materiału terygenicznego, udokumentowanego obecnością biomarkerów roślin wyższych, a także obecnością fragmentów kutikul w zespołach palinofacjalnych opisanych przez Filipek (2020) w profilu Nechit, uzasadniają scenariusz przynajmniej częściowo wynurzonego wybrzuszenia przedgórskiego (forebulge) z rozwiniętym systemem delt w sąsiedztwie basenu Vrancea we wczesnym oligocenie, postulowany przez Miclăuş et al. (2009) na podstawie analizy proweniencji materiału detrytycznego w arenitach kwarcowych z ogniwa dolnych menilitów, a także obecności klastów pochodzących spoza basenu Vrancea w zlepieńcach poligenicznych opisywanych w pracy Amadori et al. (2012).

Próbki z profilu Tărcuţa, charakteryzujące się wysokimi wartościami stosunku 17α H/S, niskimi wartościami wskaźnika TAR, brakiem biomarkerów roślin wyższych oraz generalnie

niższymi wartościami TOC i HI, mogą z kolei odzwierciedlać depozycję w środowisku otwartego basenu z mniej intensywną produkcją organizmów syntetyzujących sterole we wczesnym oligocenie (Ryc. 15 w pracy nr 2). Warunki głębokowodne w trakcie depozycji osadów dolnego oligocenu w tym samym rejonie zostały również zasugerowane przez Tăbărę (2017), który na podstawie badań palinofacjalnych stwierdził, że ogniwa dolnych menilitów i margli bitumicznych zostały zdeponowane w dystalnym, suboksyczno-anoksycznym basenie. Środowisko hemi-pelagiczne dla margli bitumicznych zaproponowane zostało przez Amadori et al. (2012).

4.3. Paleośrodowisko sedymentacji osadów oligocenu w północno-wschodniej części basenu transylwańskiego

Na podstawie:
Wendorff-Belon, M., Loręc, R., Wierzbicki, A., Rospondek, M., Marynowski, L., 2025. Oligocene environmental changes in the Central Paratethys: geochemical and palynofacial record from the north-western Transylvanian Basin (Romania). Palaeogeography, Palaeoclimatology, Palaeoecology 676, 113124.

Złożony i bardzo dobrze zachowany skład palinofacjalny i molekularny (MO niedojrzała, odniesienie w rozdziale 4.1.) w skałach formacji Ileanda i Vima z profilu Fântânele umożliwił kompleksową interpretację pierwotnego źródła MO i warunków panujących w NW części basenu transylwańskiego w oligocenie (późny rupel po szat). Dodatkowo wykonano analizę rozkładu średnic framboidów pirytowych w celu uszczegółowienia rekonstrukcji warunków redoks panujących w basenie (np. Zatoń et al., 2008; Gallego-Torres et al., 2015).

4.3.1. Źródło MO

W badanej sukcesji skalnej zaznacza się generalny trend zmiany składu MO od przewagi substancji pochodzenia morskiego w późnym rupelu, po wzrost udziału substancji pochodzącej od roślin wyższych w szacie. Wskazują na to m.in. dane pirolizy Rock-Eval (Ryc. 5). Wysokie wartości HI w ciemnym, laminowanym interwale łupkowym (F3–F11) formacji Ileanda wskazują na dominację kerogenu typu II (morskiego) pochodzenia algowego/mikrobiologicznego, natomiast w skałach z formacji Vima zaznacza się przewaga kerogenu typu III oraz II/III, pochodzącego od roślin wyższych (Espitalié et al., 1984).

Wskaźniki biomarkerowe, jak TAR <1 i niski stosunek C_{29}/C_{27} steranów, w większości próbek z formacji Ileanda (Tabela 4 w pracy nr 3) wspierają tę interpretację. Dodatkową przesłanką wskazującą na obecność kerogenu typu II w skałach formacji Ileanda, może być dominujący udział (do 80%) amorficznej substancji organicznej (AOM) o charakterystycznej granularnej teksturze, wykazującej punktową („patchy") fluorescencję, interpretowanej jako produkt degradacji bakteryjnej biomasy pochodzenia algowego (Pacton et al., 2011; Tăbără et al., 2015). W skałach z formacji Vima zauważalny jest wzrost udziału detrytusu roślinnego (do 40%; Ryc. 8), reprezentowany głównie przez fragmenty kutikuli i drewna, wzrost wskaźnika TAR oraz stosunku C_{29}/C_{27} steranów. Dodatkowo w najwyższej części profilu zidentyfikowano biomarkery żywic roślin iglastych, jak 14-metylo-16,17-bisnorabieta-8,11,13-trien i dehydroabietan, a także związki pochodzące od roślin kwitnących, jak monoaromatyczny 27,28-bisnoroleana-13,15,17-trien, des-A-oleanan, diaromatyczny des-A-24,27-dinoroleana-5,7,9,11,13-pentaen, czy monoaromatyczne 27,28-bisnorursana-13,15,17-trien i 27,28-bisnorlupana-13,15,17-trien. Obecność tych związków koreluje z wysokimi wartościami wskaźnika $CPI_{23\text{-}32}$, sięgającymi 3,16 (Carbon Preference Index; Tabela 2 w pracy nr 3), Ab/triMTTC (suma związków pochodzących od kwasu abietynowego w stosunku do 3MeMTTC, opis w Tabeli 4 w pracy nr 3) oraz stosunku oleanenów do $C_{30}\alpha\beta$ hopanu [O/(O + H)]. Podobnie bogaty zestaw biomarkerów roślin wyższych opisano w formacji Tard Clay z węgierskiego basenu paleogeńskiego (Bechtel et al., 2012).

Na podstawie analizy biomarkerów możliwe było uszczegółowienie składu fitoplanktonu aktywnego w trakcie sedymentacji badanej sekwencji osadowej. Identyfikacja związków HBI w formie alkanów i tiofenów w zdecydowanej większości próbek wskazuje na istotny wkład okrzemek w zdeponowaną MO. Aktywność bruzdnic była najintensywniejsza w trakcie szatu, na co wskazują 4-metylodiastereny i cysty bruzdnic, notowane w największej ilości w najwyższej części profilu (górna część formacji Vima). Obecność *Pelagophyceae* w górnym rupelu i pod koniec szatu stwierdzić można na podstawie C_{30} steranu (24-*n*-propylocholestanu) w próbkach z formacji Ileanda i górnej części formacji Vima. Hopanoidy obecne choć w małych ilościach w stosunku do steranów (wysokie wartości wskaźnika $\Sigma S/\Sigma H$), zwłaszcza w ciemnych laminowanych łupkach formacji Ileanda, wskazują na wkład MO pochodzenia bakteryjnego.

4.3.2. Paleozasolenie

Spadek zasolenia w kolumnie wody powyżej chemokliny, z warunków normalnego zasolenia w późnym rupelu po warunki brakiczne w szacie, zanotowano na podstawie wskaźników MTTCI i Pr/Ph (Ryc. 11B w pracy nr 3). Wysłodzenie wód może być związane z wypłycaniem NW części basenu transylwańskiego w szacie (np. Huismans et al., 1997; Krezsek & Bally, 2006), na który wskazuje zmiana składu palinofacjalnego (Ryc. 8) oraz biomarkerowego w badanym profilu. Wzrost udziału fragmentów roślinnych w składzie palinofacjalnym, dobry stan zachowania palinomorfów świadczący o krótkim transporcie, a także bogaty zestaw biomarkerów pochodzących od roślin wyższych (zarówno kwitnących jak i iglastych), sugerują intensywną dostawę materiału lądowego i środowisko o wyższej energii (Bordenave, 1993). Dostawa wód z lądu wiąże się ze spadkiem zasolenia i wzrostem dopływu nutrientów (fosforanów, azotanów) do basenu, a to w konsekwencji prowadzi do wzmożonej aktywności fitoplanktonu, odzwierciedlonej w badanych skałach, zwłaszcza w interwałach formacji Vima złożonych z ciemnych mułowców, znaczącym wkładem 4-metylodiasterenów, C_{25} HBIT i dinocyst. Epizod spadku zasolenia wód, poprzedzający pojawienie się gatunków endemicznych w Paratetydzie środkowej udokumentowany został na podstawie identyfikacji endemicznej nannoflory wapiennej *Braarudosphaera bigelowii* (Krhovský et al., 1992; Melinte-Dobrinescu & Brustur, 2008) oraz wyraźnego bio-horizontu wyróżnionego na podstawie obecności ślimaka "*Cardium*" *lipoldi* i małży *Janschinella garetzkii* w profilu Fântânele w formacji Bizuşa, tj. poniżej formacji Ileanda, w dolnej części NP23 (Rusu, 1988; Rusu et al., 1996; Melinte-Dobrinescu & Brustur, 2008).

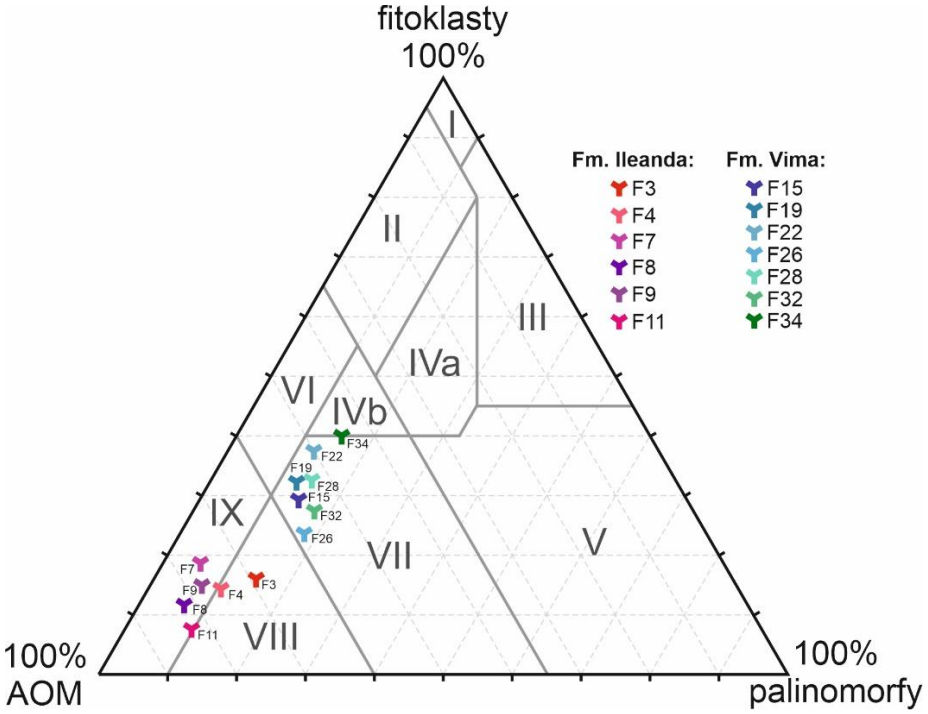

Ryc. 8. Diagram trójskładnikowy: amorficznej materia organiczna (AOM) – palinomorfy – fitoklasty (wg. Tyson, 1989), ilustrujący zmiany środowisk sedymentacyjnych formacji (Fm.) Ileanda i Vima. Pola palinofacji: I – silnie proksymalny szelf lub basen; II – marginalny basen dysoksyczny-anoksyczny; III – heterolityczny szelf oksyczny („szelf proksymalny"); IV – przejście od szelfu do basenu; V – szelf oksyczny z dominacją mułu („szelf dystalny"); VI – proksymalny szelf suboksyczny-anoksyczny; VII – dystalny „szelf" dysoksyczny-anoksyczny; VIII – dystalny szelf dysoksyczny-anoksyczny; IX – dystalny basen suboksyczny-anoksyczny.

4.3.3. Warunki redoks

W profilu Fântânele wyróżniono interwały charakteryzujące się wysoką zawartością TOC, tj. kilkunastometrowy interwał ciemnych łupków formacji Ileanda z TOC dochodzącym do 5,9 % wag., oraz dwie wkładki ciemnych mułowców w wyższej partii formacji Vima z TOC na poziomie ok. 1,98-2,30% wag., co sugeruje restrykcyjne warunki Eh strefy przydennej lub wzmożoną produktywność w trakcie depozycji tych skał. Skały z dolnej części formacji Vima wykazują TOC nieprzekraczający 1,10 % wag., co może być związane zarówno z natlenieniem kolumny wody, spadkiem bioproduktywności, ale także z silnym rozcieńczeniem MO w skałach o genezie turbidytowej. Wskaźnik biomarkerowy Pr/Ph <1 (0,48-0,88, jedna próbka 1,13; Tabela 4 w pracy nr 3) dla interwałów o wysokim TOC, sugeruje rozwinięcie się warunków anoksycznych w strefie przydennej (np. Peters et al., 2005). Z kolei obecność HBIT, których geneza wiąże się z inkorporacją siarki produkowanej przez mikroorganizmy redukujące siarczany w strukturę związku HBI na etapie wczesnej diagenezy (np. Sinninghe Damsté et al., 1989) czy jeszcze w kolumnie wody (Hebting et al., 2006), sugeruje euksynię

co najmniej przy dnie lub sięgającą wyżej w kolumnie wody. Analiza średnic framboidów pirytowych potwierdza dane biomarkerowe. Bardzo wysoki udział drobnych framboidów o średnicy nieprzekraczającej 5 µm, dochodzący do 96%, wskazuje na anoksyczne/euksyniczne warunki w kolumnie wody (Ryc. 11C w pracy nr 3). W większości skał formacji Ileanda zanotowano obecność arylowych izoprenoidów z największą koncentracją dla próbki wapienia tylawskiego, a w przypadku dwóch próbek niewielkie ilości izorenieratanu, świadczące niepodważalnie o okresowym rozwinięciu się euksynii w strefie fotycznej. Zjawisko to wiąże się z pogrzebaniem ogromnych zasobów MO, co na tak szeroką skalę współcześnie obserwowane jest np. w Morzu Czarnym, gdzie poziom toksycznych wód wysyconych siarkowodorem sięga 150-200 m i stan taki trwa od holocenu (np. Sinnighe Damsté et al., 1993).

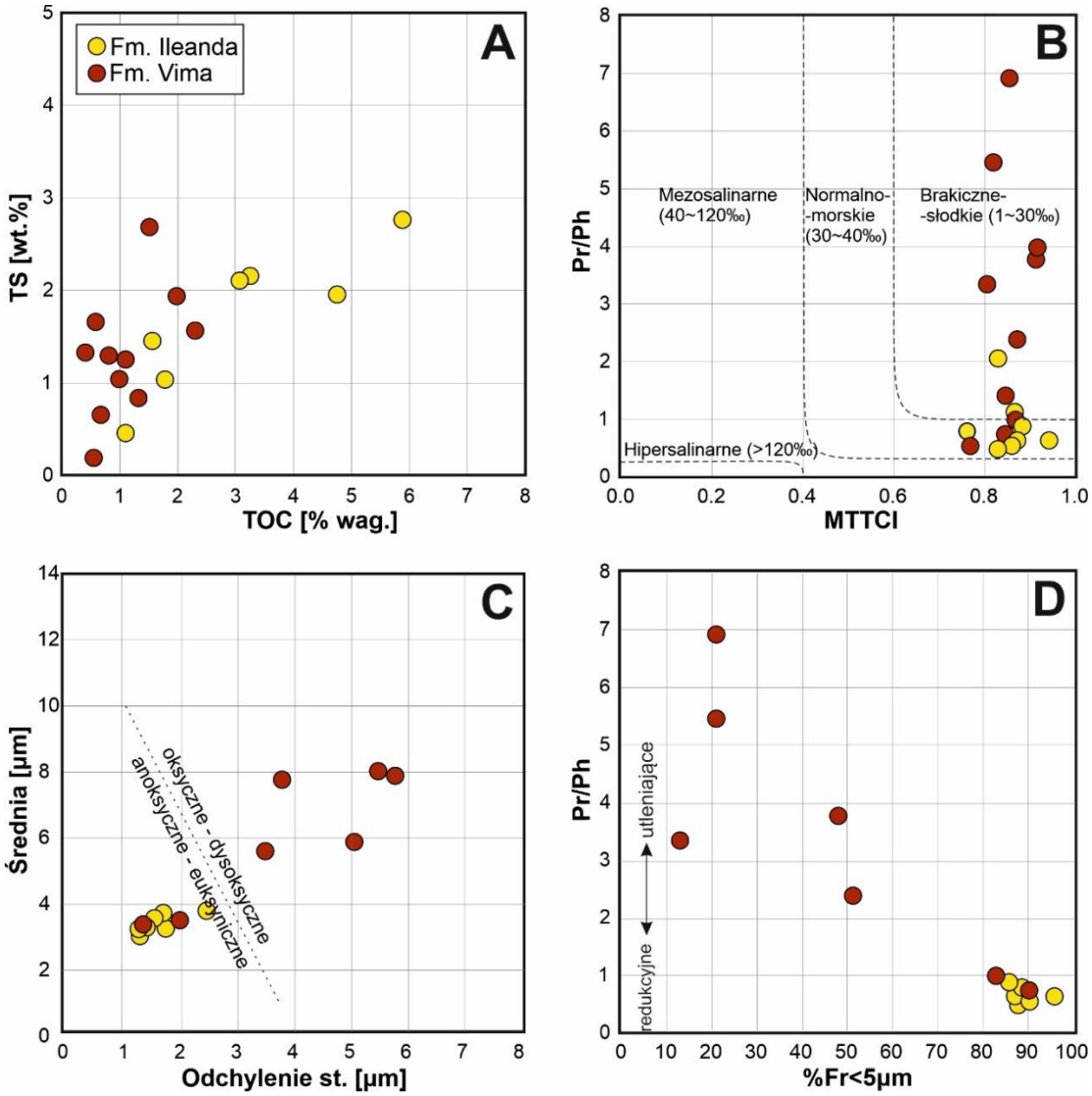

Ryc. 9. **(A)** Diagram zmienności całkowitej zawartości siarki (TS) względem całkowitej zawartości węgla organicznego (TOC), opracowany na podstawie Wignall (1994). **(B)** Wykres korelacyjny stosunku prystanu do fitanu (Pr/Ph) względem wskaźnika metylotrimetyltridecylchromanu (MTTCI), z zaznaczonymi granicami pól zasolenia według Wang et al. (2011). **(C)** Wykres statystyczny rozkładu wielkości framboidów pirytowych:

średnia średnica framboidów (Średnia) w funkcji odchylenia standardowego (Odchylenie st.). **(D)** Zależność Pr/Ph względem udziału drobnych framboidów (%Fr < 5 μm), wskazująca na warunki anoksyczne/euksyniczne dla formacji Ileanda oraz bardziej oksyczne dla formacji Vima.

Diametralna zmiana, manifestująca się spadkiem zawartości TOC (0,67-1,51% wag.), mniejszym udziałem drobnych framboidów i pojawieniem się framboidów o zróżnicowanych średnicach dochodzących do 56 μm, a także wyższymi wartościami Pr/Ph (2,05-6,92) zanotowana została w dolnej części formacji Vima (Ryc. 9A, C, D), co wskazuje na warunki tlenowe w kolumnie wody pod koniec rupelu. W trakcie szatu nastąpiły epizody beztlenowe zarówno na dnie basenu, jak i w kolumnie wody, o czym świadczą Pr/Ph<1, 88-95% udział drobnych framboidów oraz wysokie relatywne wartości C_{25} HBIT w stosunku do sąsiadującego *n*-C_{23} alkanu (C_{25}HBIT/*n*-C_{23}; Ryc. 10 w pracy nr 3), charakteryzujące interwały ciemnych mułowców. Najwyższe koncentracje arylowych izoprenoidów dla tych skał sugerują epizodyczny rozwój warunków euksynicznych w strefie fotycznej, aczkolwiek aby uzyskać pewność co do pochodzenia tych związków od *Chlorobiaceae*, należałoby potwierdzić ich skład izotopowy węgla (Koopmans et al., 1996). Brak izorenieratanu w próbkach z formacji Vima może być związany ze zwiększeniem głębokości zalegania chemokliny, spowodowanym wzmożonym mieszaniem się warstw wody lub zmniejszoną penetracją światła, będącą konsekwencją wysokiej mętności oraz intensywnej produkcji biologicznej w wodach szelfowych, gdzie dominuje sedymentacja o charakterze turbidytowym (analogia do holoceńskich osadów szelfowych Morza Czarnego; Huang et al., 2000). Jednocześnie wysoki stosunek ΣS/ΣH, niskie wartości TAR, a także wysokie wartości C_{25}HBIT/*n*-C_{23} wskazywać mogą na intensywny rozwój fitoplanktonu odpowiedzialnego za rozwój warunków deficytu tlenowego, umożliwiającego pogrzebanie znacznych ilości MO w osadzie (TOC do 2,30% wag.).

4.3.4. Podsumowanie paleośrodowiska sedymentacji w NW basenie transylwańskim

Zarówno cechy litologiczne (laminowane, ciemne łapki typu menilitowego), jak i skład palinofacji i biomarkerów w skałach formacji Ileanda wskazują na warunki głębokiego basenu panujące w późnym rupelu (NP23-24), co związane może być z N-S ekstensją tej części basenu transylwańskiego (Huismans, et al., 1997). W tym czasie rozwinęły się specyficzne warunki paleośrodowiska, sprzyjające pogrzebaniu MO, jak intensywna bioproduktywność (wysoki TOC, HI, stosunek ΣS/ΣH, obecność HBI, niski TAR), stratyfikacja kolumny wody, tj. obecność anoksji (niski Pr/Ph, dominacja drobnych framboidów pirytowych, obecność HBIT

i HBI tiolanów), przynajmniej okresowo sięgającej do strefy fotycznej (arylowe izoprenoidy i izorenieratan).

Na przełomie rupelu i szatu (dolna część formacji Vima, NP24) panowały warunki otwartego morza o normalnym zasoleniu, i dobrym natlenieniu kolumny wody z anoksją w wodach przydennych. Potwierdzają to wysokie wartości stosunku Pr/Ph, framboidy pirytowe o zróżnicowanych średnicach oraz brak izorenieratanu i śladowe ilości arylowych izoprenoidów. W tym czasie w Paratetydzie utrzymywały się warunki otwartego morza, co znajduje odzwierciedlenie w obecności wapienia jasielskiego (dolny szat) w formacji Vima, interpretowanego jako efekt kosmopolitycznych zakwitów nannoflory wapiennej (Melinte-Dobrinescu & Brustur, 2008), powiązanej prawdopodobnie z odtworzeniem komunikacji Paratetydy z Morzem Śródziemnym i Morzem Północnym poprzez Korytarz Słoweński i Górny Rów Renu (Baldi, 1984; Kováč et al., 2016).

Górna części formacji Vima, charakteryzująca się obecnością licznych biomarkerów roślin wyższych, czy fragmentów kutikul i drewna, stanowi zapis przejścia ku środowisku płytszego basenu, związanego z zapoczątkowanym w późnym oligocenie nasuwaniem się Pienidów i towarzyszącemu mu epizodowi kompresyjnemu NW basenu transylwańskiego (Huismans et al., 1997; Krėzsek & Bally, 2006; Popescu, 2021). Następowała okresowa eutrofizacja (bardzo wysoki stosunek ΣS/ΣH, wysoka zawartość biomarkerów pochodzących od okrzemek i bruzdnic), rozwój stratyfikacji związanej ze spadkiem zasolenia (wysoki MTTCI) oraz powstawanie warunków euksynicznych w strefie fotycznej w czasie sedymentacji interwałów ciemnych mułowców. Aktywność tektoniczna zbiegła się prawdopodobnie z późno-oligoceńskim ociepleniem klimatu (Zachos et al., 2001), co potwierdzają dane nannoflorystyczne (Melinte-Dobrinescu & Brustur, 2008; Kallanxhi et al., 2018) i zespoły otwornicowe (Székely & Filipescu, 2016), wskazujące na adaptację do cieplejszych wód powierzchniowych. Obserwacje te powiązano ze wzmożonym dopływem wód z Morza Śródziemnego i Oceanu Indyjskiego oraz osłabieniem dopływu chłodniejszych wód po zamknięciu Rowu Górnego Renu (Martini, 1990; Gebhardt, 2003). Podobne wnioski dotyczące ocieplania klimatu od borealnego w interwale NP24 po cieplejszy klimat w zonie NP25 wysnuł Rusu (1996) na podstawie analizy mięczaków.

5. Podsumowanie i wnioski

Na podstawie przeprowadzonych badań geochemicznych, palinofacjalnych i petrograficznych oligoceńskich skał z wybranych profili Karpat zewnętrznych (płaszczowiny

Tarcău i Vrancea) oraz NW części basenu transylwańskiego, dokonano rekonstrukcji paleośrodowiska sedymentacji w domenie środkowej Paratetydy oraz oceny dojrzałości termicznej i potencjału węglowodorowego badanej MO. Pomimo cech wspólnych analizowanych profili, jak obecność miąższych pakietów skrzemionkowanych skał wzbogaconych w MO, charakterystyka geochemiczna skał wskazuje na niezwykle zróżnicowane warunki panujące w każdej z badanych części basenów.

Stopień dojrzałości termicznej MO jest zróżnicowany pomiędzy analizowanymi jednostkami tektonicznymi. Najbardziej zaawansowaną dojrzałość termiczną wykazuje MO z profilu Tărcuţa (płaszczowina Tarcău), wchodząc częściowo w tzw. okno ropne (średnia refleksyjność witrynitu 0,51% i T_{max} =~430°C). Próbki z profilu Nechit (płaszczowina Vrancea) zawierają głównie niedojrzałą MO osiągającą ok. 0,4% w skali refleksyjności witrynitu i wykazującą średnio T_{max} ok. 425° C. Najbardziej niedojrzała jest MO pochodząca z profilu Fântânele, gdzie refleksyjność witrynitu wynosi średnio 0,42%, a T_{max} 422°C. Zróżnicowanie dojrzałości MO odzwierciedla odmienne warunki tektoniczne i historię pogrążenia poszczególnych płaszczowin. Wyższe wartości refleksyjności witrynitu i T_{max} w jednostce Tarcău wiążą się z jej położeniem w bardziej wewnętrznej strefie orogenu karpackiego. Skały z profilu Nechit charakteryzują się głównie bardzo dobrym potencjałem generacyjnym, natomiast skały z profilu Tărcuţa umiarkowanym do dobrego.

Skały z NW basenu transylwańskiego nie osiągnęły dojrzałości termicznej umożliwiającej generację węglowodorów, co potwierdzają wskaźniki biomarkerowe, pirolityczne oraz wartości refleksyjności witrynitu. Formacja Ileanda charakteryzuje się dobrym do bardzo dobrego potencjałem węglowodorowym, natomiast formacja Vima słabym do średniego.

MO w skałach z płaszczowiny Vrancea pochodzi głównie od organizmów planktonicznych (okrzemki, bruzdnice) oraz bakterii fotosyntetyzujących, przy niewielkim udziale związków pochodzących od roślin wyższych. W skałach z płaszczowiny Tarcău przewaga biomarkerów pochodzenia bakteryjnego i cyjanobakteryjnego oraz brak biomarkerów roślin wyższych, wskazują na depozycję w warunkach otwartego, głębszego basenu o ograniczonym dopływie materii terygenicznej.

W profilu Fântânele na podstawie analizy biomarkerów oraz palinofacji zaobserwowano wyraźny trend zmian składu MO, od dominacji substancji algowej w formacji Ileanda po wzrost udziału materiału roślinnego w formacji Vima, udokumentowanego obecnością licznych związków pochodzących od roślin kwitnących i żywicujących oraz fragmentów kutikul i

drewna. Zmiana ta odzwierciedla postępujące wypłycanie basenu oraz zwiększoną dostawę materiału lądowego w późnym oligocenie.

Wyniki analiz biomarkerowych oraz rozkładu framboidów pirytowych wskazują na rozwój warunków euksynicznych, epizodycznie sięgających strefy fotycznej, zarówno w basenie Vrancea, jak i transylwańskim we wczesnym oligocenie. Świadczą o tym obecność drobnych framboidów pirytowych, arylowych izoprenoidów i izorenieratanu. Jednocześnie zaobserwowano spadek zasolenia wód w obu analizowanych basenach, co interpretowane jest jako rezultat powszechnie opisywanej izolacji Paratetydy od oceanu światowego (pierwsze wydarzenie spadku zasolenia wód – tzw. Solenovian Event na przełomie eocenu i oligocenu) i zwiększonego dopływu wód słodkich z lądu. Zjawisku temu towarzyszył wzrost bioproduktywności, udokumentowany wysokimi wartościami TOC, HI oraz związków pochodzących od fitoplanktonu.

W późnym oligocenie, reprezentowanym przez formację Vima, w NW basenie transylwańskim następowały okresowe epizody eutrofizacji i deficytu tlenowego, którym towarzyszyło pogrzebanie znacznych ilości MO. Epizody te mogły być związane z wypłycaniem basenu i spadkiem zasolenia wód, będących efektem intensywnej przebudowy tektonicznej wynikającej z nasuwania się Pienidów.

Wyniki badań dostarczają istotnych informacji o ewolucji paleośrodowisk środkowej Paratetydy w oligocenie, wskazując na istotną rolę izolacji basenów, bioproduktywności oraz zjawiska euksynii w strefie fotycznej, w procesach sedymentacyjnych. Model topograficznie ograniczonego, przynajmniej okresowo izolowanego basenu o intensywnej aktywności tektonicznej, prowadzącej do zróżnicowanej morfologii dna morskiego, zaproponowany dla karpackiego basenu fliszowego w oligocenie (np. Miclăuș et al., 2009; Jankowski & Probulski, 2011; Guerrera et al., 2012), wydaje się dobrze uzasadniać rozwój pomniejszych basenów różniących się pod względem produktywności, zasolenia czy struktury kolumny wody. Aby jednak zweryfikować taki scenariusz, konieczne wydają się dalsze kompleksowe badania geochemiczne, palinofacjalne i sedymentologiczne równowiekowych skał zlokalizowanych w poprzek osi poszczególnych basenów.

Uzyskane dane biomarkerowe stanowią cenny materiał porównawczy dla innych równowiekowych basenów sedymentacyjnych, a także mogą być wykorzystane w prospekcji węglowodorów, zwłaszcza w zakresie korelacji skał macierzystych z potencjalnymi złożami ropy naftowej rejonu karpackiego.

6. Bibliografia

Amadori, M.L., Belayouni, H., Guerrera, F., Martín-Martín, M., Martín-Rojas, I., Miclăuş, C., Raffaelli, G., 2012. New data on the Vrancea Nappe (Moldavidian Basin, Outer Carpathian Domain, Romania): Paleogeographic and geodynamic reconstructions. International Journal of Earth Sciences 101, 1599–1623.

Aubry, M.-P., 1992, Late Paleogene calcareous nannoplankton evolution: A tale of climatic deterioration, In: Prothero, D., Berggren, W.A., (Eds.), The Eocene-Oligocene climatic and biotic changes: Princeton, New Jersey, Princeton University Press, 272–309.

Baciu, D.S., Chanet, B., 2002. Les Poissons plats fossiles (Teleostei: pleuronectiformes) de l'Oligocene de Piatra Neamt (Roumanie). ORYCTOS 4, 17–38.

Baldi, T., 1980. The early history of the Paratethys. Földt. Közl., Bulletin of Hungarian Geological Society 110, 456– 472.

Baldi, T., 1984. The terminal Eocene and Early Oligocene events in Hungary and the separation of an anoxic, cold Paratethys. Eclogae Geologicae Helvetiae 77, 1–27.

Baldi, T., 1986. Mid-Tertiary stratigraphy and palaeogeographic evolution of Hungary. Akadémiai Kiadó, Budapest, 1–20.Balla, Z., 1987. Tertiary paleomagnetic data for the Carpatho-Pannonian region in the light of Miocene rotation kinematics. Tectonophysics 139, 67–98.

Bechtel, A., Hámor-Vidó, M., Gratzer, R., Sachsenhofer, R.F., Püttmann, W., 2012. Facies evolution and stratigraphic correlation in the early Oligocene Tard Clay of Hungary as revealed by maceral, biomarker and stable isotope composition. Marine and Petroleum Geology 35, 55–74.

Bessereau, G., Roure, F., Kotarba, M., Kuśmierek, J., Strzetelski, W., 1997. Structure and hydrocarbon habitat of the Polish Carpathians. In: Ziegler, P.A., Horvfith, F. (Eds.), Peri-Tethys Mémoir 2 – Structure and prospects of Alpine Basins and Forelands. Mémoires du Muséum National d'Histoire Naturelle, Paris, 343–373.

Bieńkowska-Wasiluk, M., Granica, M., Kovalchuk, O., 2024. A new extinct shad from Poland in the light of clupeiform diversity and distribution within the Paratethys during the Oligocene. Acta Geologica Polonica 74, e23. doi: 10.24425/agp.2024.151753,

Bojanowski, M.J., Ciurej, A., Haczewski, G., Jokubauskas, P., Schouten, S., Tyszka, J., Bijl, P.K., 2018. The Central Paratethys during Oligocene as an ancient counterpart of the present-day Black Sea: Unique records from the coccolith limestones. Marine Geology 403, 301–328. doi:10.1016/j.margeo.2018.06.011.

Bond, D.P.G., Wignall, P.B., 2010. Pyrite framboid study of marine Permian–Triassic boundary sections: a complex anoxic event and its relationship to contemporaneous mass extinction. Geological Society of America Bulletin 122, 1265–1279.

Bordenave, M.L., 1993, Applied Petroleum Geochemistry. Editions Technip, Paris. 524 p.

Bourbonniere, R.A., Meyers, P.A., 1996. Sedimentary geolipid records of historical changes in the watersheds and productivities of Lakes Ontario and Erie. Limnology and Oceanography 41, 352–359.

Cohen, K.M., Finney, S.C., Gibbard, P.L., Fan, J.-X., 2013; updated. The ICS International Chronostratigraphic Chart. Episodes 36, 199–204.

De Broucker, G., Mellin, A., Duindam, P., 1998. Tectono-Stratigraphic evolution of the Transylvanian Basin, pre-salt sequence, Romania. In: Dinu, C., Mocanu, V. (Eds.), Geological and Hydrocarbon Potential of the Romanian Areas, Bucharest Geosciences Forum 1, 36–70.

de Leeuw, J.W., Cox, H.C., van Graas, G., van de Meer, F.W., Peakman, T.M., Baas, J.M.A., van de Graaf, B., 1989. Limited double-bond isomerization and selective hydrogenation of sterenes during early diagenesis. Geochimica et Cosmochimica Acta 53, 903–909.

Didyk, B.M., Simoneit, B.R.T. Brassell, S.C., Eglinton, G., 1978. Organic geochemical indicators of paleoenvironmental conditions of sedimentation. Nature 272, 216–222.

Dustira, A.M., Wignall, P.B., Joachimski, M., Blomeier, D., Hartkopf-Fröder, C., Bond, D. P.G., 2013. Gradual onset of anoxia across the Permian–Triassic boundary in Svalbard, Norway. Palaeogeography, Palaeoclimatology, Palaeoecology 374, 303–313.

Dziadzio, P.S., Matyasik, I., 2006. Reconstruction of petroleum systems based on integrated geochemical and geological investigations: selected examples from the Middle Outer Carpathians in Poland. In: Golonka, J., Picha, F.J. (Eds.), The Carpathians and their foreland: Geology and hydrocarbon resources. American Association of Petroleum Geologists Memoir 84, Tulsa, Oklahoma, 377–378.

Dziadzio, P. S., Z. Borys, S. Kuk, E. Masowski, J. Probulski, M. Pietrusiak, A. Górka, J. Moryc, A. Baszkiewicz, P. Karnkowski, P.H. Karnkowski, Pietrusiak, M., 2006. Hydrocarbon resources of the Polish Outer Carpathians—Reservoir parameters, trap types, and selected hydrocarbon fields: A stratigraphic review. In: Golonka, J., Picha, F.J. (Eds.), The Carpathians and their foreland: Geology and hydrocarbon resources. American Association of Petroleum Geologists Memoir 84, Tulsa, Oklahoma, 259–291.

Dziadzio, P.S., Matyasik, I., 2021. Sedimentological and geochemical characterisation of the Lower Oligocene Menilite shales from the Magura, Dukla, and Silesian nappes, Polish Outer Carpathians-A new concept. Marine and Petroleum Geology 132, 105247.

Eglinton, G., Hamilton, R.J., 1967. Leaf epicuticular waxes. Science 156, 1322–1335.

Espitalié, J., Senga Makadi, K., Trichet, J., 1984. Role of the mineral matrix during kerogen pyrolysis. Organic Geochemistry 6, 365–382. https://doi.org/10.1016/0146-6380(84)90059-7.

Filipek, A., 2020. Palynofacies analysis, sedimentology and hydrocarbon potential of the Menilite Beds (Oligocene) in the Slovakian and Romanian Outer Carpathians. Geological Quarterly 64, 589–610. doi: http://dx.doi.org/10.7306/gq.1541.

Franck, H., Matthaus, W., Sammler, R., 1987. Major inflows of saline water into the Baltic Sea during the present century. Gerlands Beitrage zur Geophysik 96, 517–531.

Gallego-Torres, D., Reolid, M., Nieto-Moreno, V., Martínez-Casado, F.J., 2015. Pyrite framboid size distribution as a record for relative variations in sedimentation rate: An example

on the Toarcian Oceanic Anoxic Event in Southiberian Palaeomargin. Sedimentary Geology 330, 59-73. https://doi.org/10.1016/j.sedgeo.2015.09.013.

Gebhardt, H., 2003. Palaeobiogeography of Late Oligocene to Early Miocene Central European Ostracoda and Foraminifera: progressive isolation of the Mainz Basin, northern Upper Rhine Graben and Hanau Basin/Wetterau. Palaeogeography, Palaeoclimatology, Palaeoecology 201, 343–354.

Georgiev, G., 2012. Geology and hydrocarbon systems in the Western Black sea. Turkish Journal of Earth Sciences 21, 723–754.

Grice, K., Gibbson, R., Atkinson, J.E., Schwark, L., Eckardt, C.B., Maxwell, J.R., 1996. Maleimides (1H-pyrrole-2,5-diones) as molecular indicators of anoxygenic photosynthesis in ancient water column. Geochimica et Cosmochimica Acta 60, 3913–3924.

Gröger, H.R., Fügenschuh, B., Tischler, M., Schmid, S.M., Foeken, J.P.T., 2008. Tertiary cooling and exhumation history in the Maramureș area (internal eastern Carpathians, northern Romania): thermochronology and structural data. Geological Society of London Special Publications 298, 169–195. https://doi.org/10.1144/sp298.9 0305-8719/08/ $15.00.

Guerrera, F., Martín-Martín, M., Martín-Pérez, J.A., Martín-Rojas, I., Miclăuş, C., Serrano, F., 2012. Tectonic control on the sedimentary record of the central Moldavidian Basin (Eastern Carpathians, Romania). Geologica Carpathica 63, 463–479.

Haczewski, G., 1989. Coccolith limestone horizons in the Menilite-Krosno series (Oligocene, Carpathians)–identification, correlation and origin. Annales Societatis Geologorum Poloniae 59, 435–523. (in Polish with English Summary).

Hebting, Y., Schaeffer, P., Behrens, A., Adam, P., Schmitt, G., Schneckenburger, P., Bernasconi, S.M., Albrecht, P., 2006. Biomarker evidence for a major preservation pathway of sedimentary organic carbon. Science 312, 1627–1631.

Hofmann, K., 1879. Bericht über die im östlichen Teile des Szilágyer Comitates wahrend der Sommercampagne 1878 vollführten geologischen Specialaufnahmen. Föld. Közl., IX/5-6, 231–283. Budapest.

Huang, Y., Freeman, K., Wilkin R.T., Arthur, M.A., Jones, A.D., 2000. Black Sea chemocline oscillations during the Holocene: molecular and isotopic studies of marginal sediments. Organic Geochemistry 31, 1525–1531.

Hughes, W.B., Holba, A.G., Dzou, L.I.P., 1995. The ratios of dibenzothiophene to phenanthrene and pristane to phytane as indicators of depositional environment and lithology of petroleum source rocks. Geochemica et Cosmochimica Acta 59, 3581–3598.

Huismans, R.S., Bertotti, G., Ciulavu, D., Sanders, C.A.E., Cloetingh, S., Dinu, C., 1997. Structural evolution of the Transylvanian Basin (Romania): a sedimentary basin in the bend of the Carpathians. Tectonophysics 272, 249–268.

Jankowski, L., Probulski, J., 2011. Tectonic and basinal evolution of the Outer Carpathians based on example of geological structure of the Grabownica, Strachocina and Łodyna hydrocarbon deposits (in Polish with English summary). Geologia 37, 555–583.

Kallanxhi, M-E., Bălc, R., Ćorić, S., Székely, S-F., Filipescu, S., 2018. The Rupelian–Chattian transition in the north-western Transylvanian Basin (Romania) revealed by calcareous nannofossils: implications for biostratigraphy and palaeoenvironmental reconstruction. Geologica Carpathica 69, 264–282. doi: 10.1515/geoca-2018-0016.

Kohnen, M.E.L., Sinninghe Damsté, J.S., Kock-Van Dalen, A.C., ten Haven, H.L., Rullkötter, J., de Leeuw, J.W., 1990. Origin and diagenetic transformations of C_{25} and C_{30} highly branched isoprenoid sulphur compounds: Further evidence for the formation of organically bound sulphur during early diagenesis. Geochimica et Cosmochimica Acta 54, 3053–3063.

Koltun, Y.V., 1992. Organic matter in Oligocene Menilite formation rocks of the Ukrainian Carpathians: palaeoenvironment and geochemical evolution. Organic Geochemistry 18, 423–430.

Koopmans, M.P., Köster, J., van Kaam-Peters, H.M.E., King, F., Schouten, S., Hartgers, W.A., de Leeuw, J.W., Sinninghe Damsté, J.S., 1996a. Diagenetic and catagenetic products of isorenieratene: Molecular indicators for photic zone anoxia. Geochimica et Cosmochimica Acta 60, 4467–4496.

Koopmans, M.P., Schouten, S., Kohnen. M.E.L., Sinninghe Damste, J.S., 1996b. Restricted utility of aryl isoprenoids as indicators for photic zone anoxia. Geochimica et Cosmochimica Acta 60, 4873–4876.

Kosakowski, P., Więcław, D., Kotarba, M.J., 2009. Source rock characteristic of the selected flysch deposits in the transfrontier area of the Polish Outer Carpathians. Kwartalnik AGH, Geologia 35, 155–190. (in Polish with English abstract)

Kosakowski, P., Koltun, Y., Machowski, G., Poprawa, P., Papiernik, B., 2018. The geochemical characteristics of the Oligocene–Lower Miocene Menilite Formation in the Polish and Ukrainian Outer Carpathians: a review. Journal of Petroleum Geology 41, 319–335.

Köster, J., Rospondek, M.J., Zubrzycki, A., Kotarba, M., de Leeuw, J.W., Sinninghe Damsté, J.S., 1995. A molecular organic geochemical study of black shales associated with diatomites from the Oligocene Menilite Shales (Flysch Carpathians, SE Poland): Grimalt, J.O., Dorronsoro C. (Eds.) Organic Geochemistry, Developments and Applications to Energy, Climate, Environment and Human History, A.I.G.O.A., San Sebastian, 87–89.

Köster, J., M. Kotarba, E. Lafargue, and P. Kosakowski, 1998a. Source rock habitat and hydrocarbon potential of Oligocene Menilite Formation (Flysch Carpathians, Southeast Poland): an organic geochemical and isotope approach. Organic Geochemistry 29, 543–558.

Köster, J., M. Rospondek, S. Schouten, M. Kotarba, A. Zubrzycki, J.S., Sinninghe Damsté, 1998b. Biomarker geochemistry of a foreland basin: The Oligocene Menilite Formation in the Flysch Carpathians of Southeast Poland. Organic Geochemistry 29, 649–669.

Kotarba, M.J., Więcław, D., Koltun, Y.V., Lewan, M.D., Marynowski, L., Anddudok, I.V., 2005. Organic geochemical study and genetic correlations between source rocks and hydrocarbons from surface seeps and deep accumulations in the Starunia area, fore-Carpathian region, Ukraine. In: Kotarba, M.J. (Ed.), Polish and Ukrainian Geological Studies (2004–2005) at Starunia – the Area of Discoveries of Woolly Rhinoceroses. Geological Institute and Society of Research on Environmental Changes. "Geosphere", Warszawa-Kraków,125–145.

Kotarba, M.J., Więcław, D., Koltun, Y.V., Marynowski, L., Kuśmierek, J., Dudok, I.V., 2007. Organic geochemical study and genetic correlation of natural gas, oil and Menilite source rocks in the area between San and Stryi rivers (Polish and Ukrainian Carpathians). Organic Geochemistry 38, 1431–1456.

Kotlarczyk, J., Jerzmańska, A., Świdnicka, E., Wiszniowska, T., 2006. A framework of ichtyofaunal ecostrtigraphy of the Oligocene-Early Miocene strata of the Polish Outer Carpathian Basin. Annales Societatis Geologorum Poloniae 76, 1–111.

Kotlarczyk, J., Uchman, A., 2012. Integrated ichnology and ichthyology of the Oligocene Menilite Formation, Skole and Subsilesian nappes, Polish Carpathians: A proxy to oxygenation history. Palaeogeography, Palaeoclimatology, Palaeoecology 331–332, 104–118.

Kováč, M., Plašienka, D., Soták, J., Vojtko, R., Oszczypko, N., Less, G., Ćosović, V., Fügenschuh, B., Králiková, S., 2016. Paleogene palaeogeography and basin evolution of the Western Carpathians, Northern Pannonian domain and adjoining areas. Global and Planetary Change 140, 9–27.

Kováč, M., Márton, E., Oszczypko, N., Vojtko, R., Hók, J., Králiková, S., Plašienka, D., Klučiar, T., Hudáčková, N., Oszczypko-Clowes, M., 2017. Neogene palaeogeography and basin evolution of the Western Carpathians, Northern Pannonian domain and adjoining areas. Global and Planetary Change 155, 133–154. https://doi.org/10.1016/j.gloplacha.2017.07.004.

Krézsek, C., Bally, A.W., 2006. The Transylvanian Basin (Romania) and its relation to the Carpathian Fold and Thrust Belt: Insights in gravitational salt tectonics. Marine and Petroleum Geology 23, 405–442.

Krhovský, J., Adamová, M., Hladíková, J., Maslowská, H., 1992. Paleoenvironmental changes across the Eocene/Oligocene boundary in the Ždánice and Pouzdřany units (Western Carpathians, Czechoslovakia): the long-term trend and orbitally forced changes in calcareous nannofossil assemblages. In: Hamršmíd, B., Young, J. (Eds.), Nannoplankton Research. Proceedings of the Fourth INA Conference, Prague 1991, Vol. II: Tertiary Biostratigraphy and Paleoecology; Quaternary coccoliths. Knihovnička ZPN 14b, 105–187.

Kruge, M.A., Mastalerz, M., Solecki, A., Stankiewicz, B.A., 1996. Organic geochemistry and petrology of oil source rocks, Carpathian Overthrust region, southeastern Poland: Implications for petroleum generation. Organic Geochemistry 24, 897–912.

Laskarev, V., 1924. Sur les equivalents du Sarmatien superieur en Serbie. In: Vujević, P. (Ed.), Receuil de traveaux offert à M. Jovan Cvijic par ses amis et collaborateurs. Drzhavna Shtamparija, Beograd, 73–85.

Martini, E., 1971. Standard Tertiary and Quaternary calcareous nannoplankton zonations. In: Farinacci, A. (Ed.), Proceedings of the II. Planktonic Conference, Rome, 1970. Editura Tecnoscienza 2, 739–785.

Martini, E., 1990. The Rhine graben system, a connection between northern and southern seas in the European Tertiary. Veroff. Übersee-Mus. Bremen A 10, 83–98.

Matyasik, I., 2009, Petroleum system of Silesian and Dukla Units in Jaslo-Krosno-Sanok area. Nafta-Gaz 3, 201–206. (in Polish with English abstract)

Maughan, E.K., 1993. Phosphoria Formation (Permian) and its resource significance in the Western Interior, USA. Global Environment and Resources Conference, Calgary, August 15–19, 1993.

Melinte, M.C., 2005. Oligocene palaeoenvironmental changes in the Romanian Carpathians, revealed by calcareous nannofossils. Studia Geologica Polonica 124, 341–352.

Melinte-Dobrinescu, M., Brustur, T., 2008. Oligocene – lower Miocene events in Romania. Acta Palaeontologica Romaniae 6, 203–215.

Miclăuş, C., Loiacono, F., Puglisi, D., Baciu, D.S., 2009. Eocene-Oligocene sedimentation in the external areas of the Moldavide Basin (Marginal Folds Nappe, Eastern Carpathians, Romania): Sedimentological, paleontological and petrographic approaches. Geologica Carpathica 60, 397–417.

Mohrholz, V., Mohrholz Dutz, J., Gerd Kraus, G., 2006. The impact of exceptionally warm summer inflow events on the environmental conditions in the Bornholm Basin. Journal of Marine Systems 60, 285–301. https://doi.org/10.1016/j.jmarsys.2005.10.002.

Mohrholz, V., Naumann, M., Nausch, G., Krüger, S., Gr¨awe, U., 2015. Fresh oxygen for the Baltic Sea – an exceptional saline inflow after a decade of stagnation. Journal of Marine Systems 148, 152–166. https://doi.org/10.1016/j.jmarsys.2015.03.005.

Naeher, S., Schaeffer, P., Adam, P., Schubert, C.J., 2013. Maleimides in recent sediments — using chlorophyll degradation products for palaeoenvironmental reconstructions. Geochimica et Cosmochimica Acta 119, 248–263.

Pacton, M., Gorin, G.E., Vasconcelos, C., 2011. Amorphous organic matter — experimental data on formation and the role of microbes. Review of Palaeobotany and Palynology 166, 253–267.

Palcu, D.V., Krijgsman, W., 2023. The dire straits of Paratethys: gateways to the anoxic giant of Eurasia. Geological Society, London, Special Publications 523, 111–139. https://doi.org/10.1144/sp523-2021-73.

Peters, K.E., Walters, C.C., Moldowan, J.M., 2005. The Biomarker Guide, vol. 2: Biomarkers and isotopes in petroleum systems and Earth history. Cambridge University Press, Cambridge, 704 p.

Popescu, B.M., 1995. Romania's petroleum systems and their remaining potential. Petroleum Geoscience 1, 337−350.

Popescu, B.M., 2021. Transcarpathian petroleum province in Romania. Geo-Eco-Marina 27, 5−35. doi: 10.5281/zenodo.5801082

Popov, S., Akhmet'ev, M.A., Zaporozhets, N.I., Voronina, A.A., Stolyarov, A.S., 1993. Evolution of the Eastern Paratethys in the Late Eocene-Early Miocene. Stratigraphy and Geological Correlation 6, 572–600.

Popov, S.V., Rögl, F., Rozanov, A.Y., Steininger, F.F., Shcherba, I.G., Kovač, M., 2004. Lithological-paleogeographic maps of Paratethys–10 MAPS Late Eocene to Pliocene. Courier Forschungsinstitut Senckenberg 250, Frankfurt, p. 46.

Popov, S.V., Sychevskaya, E.K., Akhmet'ev, M.A., Zaporozhets, N.I., Golovina, L.A., 2008. Stratigraphy of the Maikop Group and Pteropoda Beds in northern Azerbaijan. Stratigraphy and Geological Correlation 16, 664–677.

Popov, S.V., Studencka, B., 2015. Brackish-water Solenovian mollusks from the Lower Oligocene of the Polish Carpathians. Paleontological Journal 49, 342–355. https://doi.org/10.1134/S0031030115040140.

Rathburn, A.E., Corliss, B.H., 1994. The ecology of living (stained) deep-sea benthic foraminifera from the Sulu Sea. Paleoecology 9, 87–150.

Rauball, J.F., Sachsenhofer, R.F., Bechtel, A., Coric, S., Gratzer, R., 2019. The Oligocene–Miocene Menilite Formation in the Ukrainian Carpathians: a world-class source rock. Journal of Petroleum Geology 42, 393–415. https://doi.org/10.1111/jpg.12743.

Rieley, G., Collier, R.J., Jones, D.M., Eglinton, G., Eakin, P.A., Fallick, A.E., 1991. Sources of sedimentary lipids deduced from stable carbon-isotope analyses of individual compounds. Nature 352, 425–427.

Rögl, F., 1998, Palaeogeographic consideration for Mediterranean and Paratethys seaways (Oligocene to Miocene). Annalen des Naturhistorischen Museum in Wien 99A, 279–310.

Rontani, J. F., Baillet, G., Aubert, C., 1991. Production of acyclic isoprenoid compounds during the photodegradation of chlorophyll a in sea water. Journal of Photochemistry and Photobiology A: Chemistry 59, 369–377.

Rontani, J-F., Belt, S.T., Vaultier, F., Brown, T.A., 2011. Visible light induced photo-oxidation of highly branched isoprenoid (HBI) alkenes: a significant dependence on the number and nature of the double bonds. Organic Geochemistry 42, 812–822.

Rospondek, M.J., Köster, J., Sinninghe Damsté, J.S., 1997. Novel C_{26} highly branched isoprenoid thiophenes and alkane from the Menilite Formation, Outer Carpathians, southeast Poland. Organic Geochemistry 26, 295–304.

Rusu, A., 1988. Oligocene events in Transylvania (Romania) and the first separation of Paratethys. D.S. Institute of Geological Geofiz 72–73 (3), 207– 223.

Rusu, A., 1996. Changes in marine molluscan assemblages from the upper Oligocene–lower Miocene in NW Transylvania. Oligocene–Miocene transition and main geological events in Romania, 28 August–2 September 1996. B. Material of Symposium. Romanian Journal of Paleontology 76 (Suppl. 1), 58–62.

Rusu, A., Popescu, G., Melinte, M., 1996. Oligocene–Miocene transition and main geological events in Romania. Excursion Guide of IGCP Project No.326. Romanian Journal of Stratigraphy 76, 1, 3–47.

Rusu, A., 1999. Rupelian mollusk fauna of Solenovian type found in Eastern Carpathian (Romania). Acta Palaeontologica Romaniae 2, 449-452.

Sachsenhofer, R. F., J. Hentschke, A. Bechtel, Ćorić, S., Gratzer, R., Gross, D., Horsfield, B., Rachetti, A., Soliman, A., 2015. Hydrocarbon potential and depositional environments of Oligo-Miocene rocks in the Eastern Carpathians (Vrancea Nappe, Romania). Marine and Petroleum Geology 68, 269–290.

Sachsenhofer, R.F., Popov, S.V., Ćorić, S., Mayer, J., Misch, D., Morton, M.T., Pupp, M., Rauball, J., Tari, G., 2018. Paratethyan petroleum source rocks: an overview. Journal of Petroleum Geology 41, 219–246.

Sant, K., Palcu, D.V., Mandic, O., Krijgsmann, W., 2017. Changing seas in the Early–Middle Miocene of Central Europe: a Mediterranean approach to Paratethyan stratigraphy. Terra Nova 29, 273–281. https://doi.org/10.1111/ter.12273.

Schulz, H.M., Bechtel, A., Sachsenhofer, R.F., 2005. The birth of the Paratethys during the Early Oligocene: From Tethys to an ancient Black Sea analogue? Global and Planetary Change 49, 163–176.

Schwark, L., Vliex, M., Schaeffer, P., 1998. Geochemical characterization of Malm Zeta laminated carbonates from the Franconian Alb, SW-Germany (II). Organic Geochemistry 29, 1921–1952.

Schwark, L., Frimmel, A., 2004. Chemostratigraphy of the Posidonia Black Shale, SW-Germany: II. Assessment of extent and persistence of photic-zone anoxia using aryl isoprenoid distributions. Chemical Geology 206, 231–248.

Soták, J., 2010. Paleoenvironmental changes across the Eocene-Oligocene boundary: insights from the Central-Carpathian Paleogene Basin. Geologica Carpathica 61, 393–418. doi: 10.2478/v10096-010-0024-1.

Sinninghe Damsté, J.S., van Koert, E.R., Kock-van Dalen, A.C., de Leeuw, J.W., Schneck, P.A., 1989. Characterisation of highly branched isoprenoid thiophenes occurring in sediments and immature crude oils. Organic Geochemistry 14, 555–567.

Sinninghe Damsté, J.S., Hartgers, W.A., Baas, M., de Leeuw, J.W., 1993. Characterization of high-molecular-weight organic matter in marls of the Salt IV Formation of Mulhouse Basin. Organic Geochemistry 20, 1237–1252.

Summons, R.E., Powell, T.G., 1987. Identification of aryl isoprenoids in source rocks and crude oils: biological markers for the green sulphur bacteria. Geochimica et Cosmochimica Acta 51, 557–566.

Székely, S.-F., Filipescu, S., 2015. Taxonomic record of the Oligocene benthic foraminifera from the Vima Formation (Transylvanian Basin, Romania). Acta Palaeontologica Romaniei 11, 25–62.

Székely, S.-F., Filipescu, S., 2016. Biostratigraphy and paleoenvironments of the Late Oligocene in the north-western Transylvanian Basin revealed by the foraminifera assemblages. Palaeogeography, Palaeoclimatology, Palaeoecology 449, 484–509.

Świdziński, H., 1947. Słownik stratygraficzny północnych Karpat fliszowych. Biuletyn Instytutu Geologicznego 124.

Ţabără, D., Pacton, M., Makou, M., Chirila, G., 2015. Palynofacies and geochemical analysis of Oligo-Miocene bituminous rocks from the Moldavidian Domain (Eastern Carpathians, Romania): implications for petroleum exploration. Revue of Paleobotany and Palynology 216, 101–122.

Ţabără, D., 2017. Dinoflagellate cysts stratigraphy and palynofacies of Oligocene sequences in the Northern Eastern Carpathians. Acta Palaeontologica Romaniae 13, 49–63.

Tari, G., Báldi, T., Báldi-Beke, M., 1993. Paleogene netroarc flexural basin beneath the Neogene Pannonian Basin: a geodynamic model. Tectonophysics 226, 433–455.

ten Haven, H.L., Lafargue, E., Kotarba, M., 1993. Oil/oil and oil/source rock correlations in the Carpathian Foredeep and overthrust, south-east Poland. Organic Geochemistry 20, 935–959.

Tyson, R.V., 1989. Late Jurassic palynofacies trends, Piper and Kimmeridge Clay formations, UK onshore and Northern North Sea. In: Batten, D.J., Keen, M.C. (Eds.), North west European Micropalaentology and Palinology, British Micropaleontological Society Series, Ellis Horwood, Chichester, 135–172.

Vetö, I., 1987, An Oligocene sink for organic carbon: upwelling in the Paratethys?: Palaeogeography, Palaeoclimatology, Palaeoecology 60, 143–153.

Wang, L., Song, Z., Yin, Q., George, S.M., 2011. Paleosalinity significance of occurrence and distribution of methyltrimethyltridecyl chromans in the upper Cretaceous Nenjiang Formation, Songliao Basin, China. Organic Geochemistry 42, 1411–1419.

Więcław, D., Kotarba, M.J., Kowalski, A., Koltun Y.V., 2012. Origin and maturity of oils in the Ukrainian Carpathians and their Mesozoic basement. Geological Quarterly 56, 158–168.

Wignall, P. B., 1994, Black Shales: Oxford, Clarendon Press, 127 p.

Wignall, P.B., Newton, R., 1998. Pyrite framboid diameter as a measure of oxygen deficiency in ancient mudrocks. American Journal of Science 298, 537–552.

Wilkin, R.T., Barnes, H.L., Brantley, S.L., 1996. The size distribution of framboidal pyrite in modern sediments: an indicator of redox conditions. Geochimica et Cosmochimica Acta 60, 3897–3912.

Wójcik-Tabol, P., Wendorff-Belon, M., Kosakowski, P., Zakrzewski, A., Marynowski, L., 2022. Paleoenvironment, organic matter maturity and hydrocarbon potential of the menilite shales (Silesian unit, Polish Outer Carpathians) – organic and inorganic geochemical proxies. Marine and Petroleum Geology 142, 105767. https://doi.org/10.1016/j.marpetgeo.2022.105767

Zachos, J., Pagani, M., Sloan, L., Thomas, E., Billups, K., 2001. Trends, rhythms, and aberrations in global climate 65 Ma to present. Science 292, 686–693.

Zakrzewski, A., Waliczek, M., Machowski, G., Ząbek, G., Konon, A., Więcław, D., 2024. When an explosion of life leads to death – hypoxic zones in the Menilite Shales from the Silesian Unit (Polish Outer Carpathians), Marine and Petroleum Geology 168, 107024. https://doi.org/10.1016/j.marpetgeo.2024.107024.

Zatoń, M., Rakociński, M., Marynowski, L., 2008. Pyrite framboids as paleoenvironmental indicators. Przegląd Geologiczny 56, 158–164.

Oświadczenia współautorów o wkładzie w powstawanie pracy

Załącznik nr 9
do pisma okólnego nr 2
Prorektora ds. nauki i finansów
z dnia 19 lutego 2024 r.

Kraków, 5.03.2026
miejscowość, data

Małgorzata Wendorf-Belon
imię i nazwisko kandydata

wendorff-belon@inig.pl
adres e-mail

OŚWIADCZENIE OSOBY UBIEGAJĄCEJ SIĘ O WŁASNYM WKŁADZIE W POWSTAWANIE PRACY

Oświadczam, że w pracy:
Wendorff, Małgorzata, **Rospondek** Mariusz, **Kluska**, Bartosz, **Marynowski**, Leszek, 2017. Organic matter maturity and hydrocarbon potential of the Lower Oligocene Menilite facies in the Eastern Flysch Carpathians (Tarcău and Vrancea Nappes), Romania. Applied Geochemistry 78, 295–310. http://dx.doi.org/10.1016/j.apgeochem.2017.01.009

Mój udział polegał na przygotowaniu koncepcji publikacji, wyborze profili do badań i pobraniu próbek w terenie. Byłam odpowiedzialna za prowadzenie badań laboratoryjnych, analizę wyników badań i ich integrację, przygotowanie i edycję tekstu publikacji oraz wykonanie figur i tabel.

M. Wendorff-Belon
.....
podpis

Kraków, 5.03.2026

Małgorzata Wendorf-Belon

First and last name of co-author of the publication

Instytut Nafty I Gazu – Państwowy Instytut Badawczy
Affiliation

A STATEMENT OF THE APPLICANT'S AUTHOR OF THEIR CONTRIBUTION TO THE WORK

I declare that for the following work:

Wendorff, Małgorzata, **Rospondek** Mariusz, **Kluska,** Bartosz, **Marynowski,** Leszek, 2017. Organic matter maturity and hydrocarbon potential of the Lower Oligocene Menilite facies in the Eastern Flysch Carpathians (Tarcău and Vrancea Nappes), Romania. Applied Geochemistry 78, 295–310. http://dx.doi.org/10.1016/j.apgeochem.2017.01.009

My participation consisted of developing the publication concept, selecting the study profiles, and conducting field sampling. I was responsible for performing the laboratory analyses, interpreting and integrating the research data, drafting and editing the manuscript, and preparing all figures and tables.

M. Wendorff-Belon

.....

Signature of the author of the publication

Załącznik nr 10
do pisma okólnego nr 2
Prorektora ds. nauki i finansów
z dnia 19 lutego 2024 r.

OŚWIADCZENIE

WSPÓŁAUTORA OSOBY UBIEGAJĄEJ SIĘ O WŁASNYM WKŁADZIE W POWSTAWANIE PRACY

Miejsce Kraków, dnia 09.06.2025

Bartosz Kluska
Imię i nazwisko współautora publikacji

Instytut Nauk Geologicznych, Uniwersytet Jagielloński
Afiliacja

OŚWIADCZENIE

Oświadczam, że w pracy:

Małgorzata Wendorff, Mariusz J. Rospondek, Bartosz Kluska, Leszek Marynowski, 2017
Organic matter maturity and hydrocarbon potential of the Lower Oligocene Menilite facies in the Eastern Flysch Carpathians (Tarcău and Vrancea Nappes), Romania
Applied Geochemistry, 78, 295-310
(autorzy, rok wydania, tytuł, czasopismo lub wydawca, tom, strony)

Mój udział polegał na wykonaniu analiz zawartości węgla organicznego (TOC), pomiarów parametrów pirolitycznych (S1, S2, Tmax) oraz analizie statystycznej uzyskanych danych. Ponadto, uczestniczyłem w interpretacji i dyskusji dotyczacej dojrzałości termicznej badanych skał.

opisać szczegółowo swój własny – (a nie osoby ubiegającej się) – udział w powstaniu pracy, (np. mój udział w powstanie tej publikacji polegał na wykonaniu doświadczeń techniką ....., analizie statystycznej wyników eksperymentów zilustrowanych na ryc. ...., przygotowaniu tekstu manuskryptu zamieszczonego w rozdziale....., kierowaniu projektem naukowym obejmującym badania opisane w tej pracy, itp.).*

Bartosz Kluska
.....

Podpis współautora publikacji

A STATEMENT OF THE APPLICANT'S CO-AUTHOR OF THEIR CONTRIBUTION TO THE WORK

Location Krakow, date 09.06.2025

Bartosz Kluska.
First and last name of co-author of the publication

Institute of Geological Sciences, Jagiellonian University
Affiliation

STATEMENT

I declare that for the following work:

Małgorzata Wendorff, Mariusz J. Rospondek, Bartosz Kluska, Leszek Marynowski, 2017
Organic matter maturity and hydrocarbon potential of the Lower Oligocene Menilite facies in the Eastern Flysch Carpathians (Tarcău and Vrancea Nappes), Romania
Applied Geochemistry, 78, 295-310
(authors, year of publication, title, journal or publisher, volume, pages)

My participation consisted of performing analyses of total organic content (TOC) analyses, pirolitic parameter measurements (S1, S2, Tmax) and statistical analysis of the obtained results. Furthermore, I participated in interpretation and discussion regarding thermal maturity of the investigated rocks.

describe in detail your involvement – (and not that of your students, technicians and colleges) – in the creation of the work, (e.g., my participation in the creation of this publication consisted in the performance of Experiments using the ..... technique, statistical analysis of the experimental results illustrated on Fig. ...., preparation of the manuscript text in the chapter....., scientific management project covering the research described in this paper, etc.).*

Bartosz Kluska
.....

Signature of the co-author of the publication

* applies to co-authors

Załącznik nr 10
do pisma okólnego nr 2
Prorektora ds. nauki i finansów
z dnia 19 lutego 2024 r.

OŚWIADCZENIE

WSPÓŁAUTORA OSOBY UBIEGAJĄEJ SIĘ O WŁASNYM WKŁADZIE W POWSTAWANIE PRACY

Sosnowiec, 2.03.2026

Leszek Marynowski
Imię i nazwisko współautora publikacji

Instytut Nauk o Ziemi, Uniwersytet Śląski w Katowicach
Afiliacja

OŚWIADCZENIE

Oświadczam, że w pracy:
Wendorff, Małgorzata, **Rospondek** Mariusz, **Kluska**, Bartosz, **Marynowski**, Leszek, 2017. Organic matter maturity and hydrocarbon potential of the Lower Oligocene Menilite facies in the Eastern Flysch Carpathians (Tarcău and Vrancea Nappes), Romania. Applied Geochemistry 78, 295–310. http://dx.doi.org/10.1016/j.apgeochem.2017.01.009

Mój udział polegał na koordynacji tworzenia ostatecznej wersji artykułu i na wsparciu merytorycznym w trakcie jego pisania. Byłem odpowiedzialny za wykonanie analiz GC-MS frakcji alifatycznych i aromatycznych i wsparcie merytoryczne w pomiarach refleksyjności witrynitu.

.....

Podpis współautora publikacji

A STATEMENT OF THE APPLICANT'S CO-AUTHOR OF THEIR CONTRIBUTION TO THE WORK

Sosnowiec, 1.10.2025

Leszek Marynowski
First and last name of co-author of the publication

Instytut Nauk o Ziemi, Uniwersytet Śląski w Katowicach
Affiliation

STATEMENT

I declare that for the following work:

Wendorff, Małgorzata, **Rospondek**, Mariusz, **Kluska**, Bartosz, **Marynowski**, Leszek, 2017. Organic matter maturity and hydrocarbon potential of the Lower Oligocene Menilite facies in the Eastern Flysch Carpathians (Tarcău and Vrancea Nappes), Romania. Applied Geochemistry 78, 295–310. http://dx.doi.org/10.1016/j.apgeochem.2017.01.009

My participation consisted of coordinating the preparation of the final version of the article and providing substantial support throughout the manuscript preparation process. I was responsible for performing GC-MS analyses of the aliphatic and aromatic fractions and providing support in vitrinite reflectance measurements.

.....

Signature of the co-author of the publication

* applies to co-authors

Załącznik nr 10
do pisma okólnego nr 2
Prorektora ds. nauki i finansów
z dnia 19 lutego 2024 r.

OŚWIADCZENIE

WSPÓŁAUTORA OSOBY UBIEGAJĄEJ SIĘ O WŁASNYM WKŁADZIE W POWSTAWANIE PRACY

Kraków, 1.10.2025

Mariusz Rospondek
Imię i nazwisko współautora publikacji

Instytut Nauk Geologicznych, Uniwersytet Jagielloński
Afiliacja

OŚWIADCZENIE

Oświadczam, że w pracy:
Wendorff, Małgorzata, **Rospondek**, Mariusz, **Kluska**, Bartosz, **Marynowski**, Leszek, 2017. Organic matter maturity and hydrocarbon potential of the Lower Oligocene Menilite facies in the Eastern Flysch Carpathians (Tarcău and Vrancea Nappes), Romania. Applied Geochemistry 78, 295–310. http://dx.doi.org/10.1016/j.apgeochem.2017.01.009

Mój udział polegał na koordynacji tworzenia ostatecznej wersji artykułu i na wsparciu merytorycznym w trakcie jego pisania. Byłem przede wszystkim odpowiedzialny za konsultacje w doborze metodyki i w interpretacji wyników, a także redagowanie rozdziału opisującego geologię obszaru badań, dyskusję wyników i wnioski.

Brak kontaktu ze współautorem

Podpis współautora publikacji

A STATEMENT OF THE APPLICANT'S CO-AUTHOR OF THEIR CONTRIBUTION TO THE WORK

Kraków, 1.10.2025

Mariusz Rospondek
First and last name of co-author of the publication

Instytut Nauk Geologicznych, Uniwersytet Jagielloński
Affiliation

STATEMENT

I declare that for the following work:

Wendorff, Małgorzata, **Rospondek**, Mariusz, **Kluska**, Bartosz, **Marynowski**, Leszek, 2017. Organic matter maturity and hydrocarbon potential of the Lower Oligocene Menilite facies in the Eastern Flysch Carpathians (Tarcău and Vrancea Nappes), Romania. Applied Geochemistry 78, 295–310. http://dx.doi.org/10.1016/j.apgeochem.2017.01.009

My participation consisted of coordinating the preparation of the final version of the article and providing substantial support throughout the manuscript preparation process. My tasks included consulting on the selection of appropriate research methodology, interpreting the results, and editing the sections describing the geology of the study area, the discussion of findings, and the conclusions.

Brak kontaktu ze współautorem

Signature of the co-author of the publication

Załącznik nr 9
do pisma okólnego nr 2
Prorektora ds. nauki i finansów
z dnia 19 lutego 2024 r.

Kraków, 5.03.2026
miejscowość, data

Małgorzata Wendorf-Belon

imię i nazwisko kandydata

wendorff-belon@inig.pl
adres e-mail

OŚWIADCZENIE OSOBY UBIEGAJĄCEJ SIĘ O WŁASNYM WKŁADZIE W POWSTAWANIE PRACY

Oświadczam, że w pracy:
Wendorff-Belon, Małgorzata, **Rospondek,** Mariusz, **Marynowski,** Leszek, 2021. Early Oligocene environment of the Central Paratethys revealed by biomarkers and pyrite framboids from the Tarcău and Vrancea nappes (Eastern Outer Carpathians, Romania). Marine and Petroleum Geology 128, 105037. https://doi.org/10.1016/j.marpetgeo.2021.105037

Mój udział polegał na przygotowaniu koncepcji publikacji i doborze metod badań. Byłam odpowiedzialna za prowadzenie badań laboratoryjnych, analizę i interpretację wyników badań. Zredagowałam tekst artykułu oraz przygotowałam rysunki i tabele.

M. Wendorff-Belon
.....

podpis

Kraków, 5.03.2026

Małgorzata Wendorf-Belon

First and last name of co-author of the publication

Instytut Nafty I Gazu – Państwowy Instytut Badawczy
Affiliation

A STATEMENT OF THE APPLICANT'S AUTHOR OF THEIR CONTRIBUTION TO THE WORK

I declare that for the following work:

Wendorff-Belon, Małgorzata, **Rospondek,** Mariusz, **Marynowski,** Leszek, 2021. Early Oligocene environment of the Central Paratethys revealed by biomarkers and pyrite framboids from the Tarcău and Vrancea nappes (Eastern Outer Carpathians, Romania). Marine and Petroleum Geology 128, 105037. https://doi.org/10.1016/j.marpetgeo.2021.105037

My participation consisted of developing the research concept and selecting the appropriate analytical methods. I was responsible for conducting the laboratory investigations, as well as the analysis and interpretation of the research data. I drafted the manuscript and prepared all figures and tables.

M. Wendorff - Belon

.....

Signature of the author of the publication

Załącznik nr 10
do pisma okólnego nr 2
Prorektora ds. nauki i finansów
z dnia 19 lutego 2024 r.

OŚWIADCZENIE

WSPÓŁAUTORA OSOBY UBIEGAJĄEJ SIĘ O WŁASNYM WKŁADZIE W POWSTAWANIE PRACY

Sosnowiec, 2.03.2026

Leszek Marynowski
Imię i nazwisko współautora publikacji

Instytut Nauk o Ziemi, Uniwersytet Śląski w Katowicach
Afiliacja

OŚWIADCZENIE

Oświadczam, że w pracy:

Wendorff-Belon, Małgorzata, **Rospondek**, Mariusz, **Marynowski**, Leszek, 2021. Early Oligocene environment of the Central Paratethys revealed by biomarkers and pyrite framboids from the Tarcău and Vrancea nappes (Eastern Outer Carpathians, Romania). Marine and Petroleum Geology 128, 105037. https://doi.org/10.1016/j.marpetgeo.2021.105037

Mój udział polegał na pomocy w interpretacji wyników oraz konsultacji w trakcie pisania manuskryptu artykułu. Akceptowałem jego końcową wersję przed przekazaniem do publikacji. Byłem też odpowiedzialny za wykonanie analiz GC-MS oraz wsparcie w pomiarach średnicy framboidów pirytowych.

.....

Podpis współautora publikacji

A STATEMENT OF THE APPLICANT'S CO-AUTHOR OF THEIR CONTRIBUTION TO THE WORK

Sosnowiec, 1.10.2025

Leszek Marynowski
First and last name of co-author of the publication

Instytut Nauk o Ziemi, Uniwersytet Śląski w Katowicach
Affiliation

STATEMENT

I declare that for the following work:

Wendorff-Belon, Małgorzata, **Rospondek**, Mariusz, **Marynowski**, Leszek, 2021. Early Oligocene environment of the Central Paratethys revealed by biomarkers and pyrite framboids from the Tarcău and Vrancea nappes (Eastern Outer Carpathians, Romania). Marine and Petroleum Geology 128, 105037. https://doi.org/10.1016/j.marpetgeo.2021.105037

My contribution involved assisting in the interpretation of the results, consulting during the manuscript writing process, and approving its final version before submission for publication. I was also responsible for conducting GC-MS analyses and supporting the measurement of pyrite framboid diameters.

.....

Signature of the co-author of the publication

* applies to co-authors

Załącznik nr 10
do pisma okólnego nr 2
Prorektora ds. nauki i finansów
z dnia 19 lutego 2024 r.

OŚWIADCZENIE

WSPÓŁAUTORA OSOBY UBIEGAJĄEJ SIĘ O WŁASNYM WKŁADZIE W POWSTAWANIE PRACY

Kraków, 1.10.2025

Mariusz Rospondek
Imię i nazwisko współautora publikacji

Instytut Nauk Geologicznych, Uniwersytet Jagielloński
Afiliacja

OŚWIADCZENIE

Oświadczam, że w pracy:

Wendorff-Belon, Małgorzata, **Rospondek**, Mariusz, **Marynowski**, Leszek, 2021. Early Oligocene environment of the central Paratethys revealed by biomarkers and pyrite framboids from the Tarcău and Vrancea Nappes (Eastern Outer Carpathians, Romania). Marine and Petroleum Geology 128, 105037. https://doi.org/10.1016/j.marpetgeo.2021.105037

Mój udział polegał na poborze części próbek w terenie i pomocy w ich doborze do badań. Wsparłem doktorantkę w kreowaniu metodyki badań, interpretacji wyników oraz we wstępnym sformułowaniu rozdziału dotyczącego wniosków.

Brak kontaktu ze współautorem

Podpis współautora publikacji

A STATEMENT OF THE APPLICANT'S CO-AUTHOR OF THEIR CONTRIBUTION TO THE WORK

Kraków, 1.10.2025

Mariusz Rospondek
First and last name of co-author of the publication

Instytut Nauk Geologicznych, Uniwersytet Jagielloński
Affiliation

STATEMENT

I declare that for the following work:

Wendorff-Belon, Małgorzata, **Rospondek**, Mariusz, **Marynowski**, Leszek, 2021. Early Oligocene environment of the central Paratethys revealed by biomarkers and pyrite framboids from the Tarcău and Vrancea nappes (Eastern Outer Carpathians, Romania). Marine and Petroleum Geology 128, 105037. https://doi.org/10.1016/j.marpetgeo.2021.105037

My participation consisted of collecting and assisting in the field campaigs in Romania. I supported the doctoral candidate in developing the research methodology, interpreting the results, and drafting the preliminary concluding chapter.

Brak kontaktu ze współautorem

Signature of the co-author of the publication

Załącznik nr 9
do pisma okólnego nr 2
Prorektora ds. nauki i finansów
z dnia 19 lutego 2024 r.

Kraków, 5.03.2026
miejscowość, data

Małgorzata Wendorf-Belon

imię i nazwisko kandydata

wendorff-belon@inig.pl
adres e-mail

OŚWIADCZENIE OSOBY UBIEGAJĄCEJ SIĘ O WŁASNYM WKŁADZIE W POWSTAWANIE PRACY

Oświadczam, że w pracy:
Wendorff-Belon, Małgorzata, **Loręc**, Robert, **Wierzbicki,** Adam, **Rospondek,** Mariusz, **Marynowski**, Leszek, 2025. Oligocene environmental changes in the Central Paratethys: geochemical and palynofacial record from the north-western Transylvanian Basin (Romania). Palaeogeography, Palaeoclimatology, Palaeoecology 676, 113124. https://doi.org/10.1016/j.palaeo.2025.113124

Mój udział polegał na poborze próbek w terenie, przygotowaniu koncepcji publikacji i doborze metod badań. Byłam odpowiedzialna za prowadzenie badań laboratoryjnych (dotyczących części biomarkerowej, analizy framboidów pirytowych i refleksyjności witrynitu), analizę, interpretację oraz integrację wyników badań. Zredagowałam tekst artykułu oraz przygotowałam większość rysunków i tabel (z wyłączeniem części dotyczącej analizy palinofacji i zespołów otwornic).

M. Wendorff-Belon
.....

podpis

Kraków, 5.03.2026

Małgorzata Wendorf-Belon

First and last name of co-author of the publication

Instytut Nafty I Gazu – Państwowy Instytut Badawczy
Affiliation

A STATEMENT OF THE APPLICANT'S AUTHOR OF THEIR CONTRIBUTION TO THE WORK

I declare that for the following work:

Wendorff-Belon, Małgorzata, **Loręc,** Robert, **Wierzbicki,** Adam, **Rospondek,** Mariusz, **Marynowski,** Leszek, 2025. Oligocene environmental changes in the Central Paratethys: geochemical and palynofacial record from the north-western Transylvanian Basin (Romania). Palaeogeography, Palaeoclimatology, Palaeoecology 676, 113124. https://doi.org/10.1016/j.palaeo.2025.113124

My participation consisted of field sampling, developing the research concept, and selecting the analytical methods. I was responsible for conducting the laboratory investigations (specifically biomarker analysis, pyrite framboid analysis, and vitrinite reflectance), as well as the analysis, interpretation, and integration of the research data. I drafted the manuscript and prepared the majority of the figures and tables (excluding those related to palynofacies analysis and foraminiferal assemblages).

M. Wendorf-Belon

.....

Signature of the author of the publication

Załącznik nr 10
do pisma okólnego nr 2
Prorektora ds. nauki i finansów
z dnia 19 lutego 2024 r.

OŚWIADCZENIE

WSPÓŁAUTORA OSOBY UBIEGAJĄCEJ SIĘ O WŁASNYM WKŁADZIE W POWSTAWANIE PRACY

Kraków, 30.09.2025

Robert Loręc
Imię i nazwisko współautora publikacji

Instytut Nauk Geologicznych, Uniwersytet Jagielloński
Afiliacja

OŚWIADCZENIE

Oświadczam, że w pracy:

Wendorff-Belon, Małgorzata, **Loręc**, Robert, **Wierzbicki**, Adam, **Rospondek**, Mariusz, **Marynowski**, Leszek, 2025. Oligocene environmental changes in the Central Paratethys: geochemical and palynofacial record from the north-western Transylvanian Basin (Romania). Palaeogeography, Palaeoclimatology, Palaeoecology 676, 113124. https://doi.org/10.1016/j.palaeo.2025.113124

Mój udział polegał na pomocy w trakcie prac terenowych (pobór prób), tworzeniu metodyki badań i wykonaniu części prac laboratoryjnych prowadzących do otrzymania frakcji gotowych do analizy GC-MS. Brałem udział w interpretacji i opisie wyników tych analiz (istotny wkład w opracowanie Figur 2, 3 i 6).

.....

Podpis współautora publikacji

A STATEMENT OF THE APPLICANT'S CO-AUTHOR OF THEIR CONTRIBUTION TO THE WORK

Kraków, 30.09.2025

Robert Loręc
First and last name of co-author of the publication

Instytut Nauk Geologicznych, Uniwersytet Jagielloński
Affiliation

STATEMENT

I declare that for the following work:

Wendorff-Belon, Małgorzata, **Loręc**, Robert, **Wierzbicki**, Adam, **Rospondek**, Mariusz, **Marynowski**, Leszek, 2025. Oligocene environmental changes in the Central Paratethys: geochemical and palynofacial record from the north-western Transylvanian Basin (Romania). Palaeogeography, Palaeoclimatology, Palaeoecology 676, 113124. https://doi.org/10.1016/j.palaeo.2025.113124

My contribution included assisting during fieldwork (sample collection), developing the research methodology, and performing part of the laboratory procedures, leading to the preparation of fractions for GC-MS analysis. I participated in the interpretation and description of the results (substantial contribution in preparation of Figures 2, 3 and 6).

Signature of the co-author of the publication

* applies to co-authors

Załącznik nr 10
do pisma okólnego nr 2
Prorektora ds. nauki i finansów
z dnia 19 lutego 2024 r.

OŚWIADCZENIE

WSPÓŁAUTORA OSOBY UBIEGAJĄEJ SIĘ O WŁASNYM WKŁADZIE W POWSTAWANIE PRACY

Kraków, 30.09.2025

Adam Wierzbicki
Imię i nazwisko współautora publikacji

Instytut Nauk Geologicznych, Uniwersytet Jagielloński
Afiliacja

OŚWIADCZENIE

Oświadczam, że w pracy:

Wendorff-Belon, Małgorzata, **Loręc**, Robert, **Wierzbicki**, Adam, **Rospondek**, Mariusz, **Marynowski**, Leszek, 2025. Oligocene environmental changes in the Central Paratethys: geochemical and palynofacial record from the north-western Transylvanian Basin (Romania). Palaeogeography, Palaeoclimatology, Palaeoecology 676, 113124. https://doi.org/10.1016/j.palaeo.2025.113124

Mój udział polegał na wykonaniu analiz palinofacjalnych, a także na opisie i interpretacji wyników tych analiz (wraz z wykonaniem Figur 4 i 12 podsumowujących wyniki analiz). Pomogłem w przygotowywaniu draftu artykułu i akceptowałem jego ostateczną wersję.

.....

Podpis współautora publikacji

A STATEMENT OF THE APPLICANT'S CO-AUTHOR OF THEIR CONTRIBUTION TO THE WORK

Kraków, 30.09.2025

Adam Wierzbicki
First and last name of co-author of the publication

Instytut Nauk Geologicznych, Uniwersytet Jagielloński
Affiliation

STATEMENT

I declare that for the following work:

Wendorff-Belon, Małgorzata, **Loręc**, Robert, **Wierzbicki**, Adam, **Rospondek**, Mariusz, **Marynowski**, Leszek, 2025. Oligocene environmental changes in the Central Paratethys: geochemical and palynofacial record from the north-western Transylvanian Basin (Romania). Palaeogeography, Palaeoclimatology, Palaeoecology 676, 113124. https://doi.org/10.1016/j.palaeo.2025.113124

My contribution involved conducting palynofacies analyses, as well as describing and interpreting the results (including the preparation of Figures 4 and 11, illustrating the findings). I assisted in drafting the article and approved its final version before submission.

.....

Signature of the co-author of the publication

* applies to co-authors

Załącznik nr 10
do pisma okólnego nr 2
Prorektora ds. nauki i finansów
z dnia 19 lutego 2024 r.

OŚWIADCZENIE

WSPÓŁAUTORA OSOBY UBIEGAJĄEJ SIĘ O WŁASNYM WKŁADZIE W POWSTAWANIE PRACY

Sosnowiec, 2.03.2026

Leszek Marynowski
Imię i nazwisko współautora publikacji

Instytut Nauk o Ziemi, Uniwersytet Śląski w Katowicach
Afiliacja

OŚWIADCZENIE

Oświadczam, że w pracy:

Wendorff-Belon, Małgorzata, **Loręc**, Robert, **Wierzbicki**, Adam, **Rospondek**, Mariusz, **Marynowski**, Leszek, 2025. Oligocene environmental changes in the Central Paratethys: geochemical and palynofacial record from the north-western Transylvanian Basin (Romania). Palaeogeography, Palaeoclimatology, Palaeoecology 676, 113124. https://doi.org/10.1016/j.palaeo.2025.113124

Mój udział polegał na konsultacji w interpretacji wyników, wsparciu merytorycznym w trakcie powstawania manuskryptu, a także akceptowałem jego ostateczną wersję przed przekazaniem do publikacji. Koordynowałem analizy GC-MS, pomiary średnicy pirytów framboidowych oraz wsparłem p. Wendorff-Belon w poprawnym wykonaniu pomiarów refleksyjności witrynitu.

.....

Podpis współautora publikacji

A STATEMENT OF THE APPLICANT'S CO-AUTHOR OF THEIR CONTRIBUTION TO THE WORK

Sosnowiec, 1.10.2025

Leszek Marynowski
First and last name of co-author of the publication

Instytut Nauk o Ziemi, Uniwersytet Śląski w Katowicach
Affiliation

STATEMENT

I declare that for the following work:

Wendorff-Belon, Małgorzata, **Loręc**, Robert, **Wierzbicki**, Adam, **Rospondek**, Mariusz, **Marynowski**, Leszek, 2025. Oligocene environmental changes in the Central Paratethys: geochemical and palynofacial record from the north-western Transylvanian Basin (Romania). Palaeogeography, Palaeoclimatology, Palaeoecology 676, 113124. https://doi.org/10.1016/j.palaeo.2025.113124

My contribution included consulting on the interpretation of results, providing support during the manuscript preparation, and approving its final version before submission for publication. I coordinated the GC-MS analyses, the measurements of pyrite framboid diameters, and supported Ms. Wendorff-Belon in accurately performing vitrinite reflectance measurements.

.....

Signature of the co-author of the publication

* applies to co-authors

Załącznik nr 10
do pisma okólnego nr 2
Prorektora ds. nauki i finansów
z dnia 19 lutego 2024 r.

OŚWIADCZENIE

WSPÓŁAUTORA OSOBY UBIEGAJĄEJ SIĘ O WŁASNYM WKŁADZIE W POWSTAWANIE PRACY

Kraków, 1.10.2025

Mariusz Rospondek
Imię i nazwisko współautora publikacji

Instytut Nauk Geologicznych, Uniwersytet Jagielloński
Afiliacja

OŚWIADCZENIE

Oświadczam, że w pracy:

Wendorff-Belon, Małgorzata, **Loręc**, Robert, **Wierzbicki**, Adam, **Rospondek**, Mariusz, **Marynowski**, Leszek, 2025. Oligocene environmental changes in the Central Paratethys: geochemical and palynofacial record from the north-western Transylvanian Basin (Romania). Palaeogeography, Palaeoclimatology, Palaeoecology 676, 113124. https://doi.org/10.1016/j.palaeo.2025.113124

Mój udział polegał na wsparciu merytorycznym i poborze próbek w terenie. Uczestniczyłem w doborze próbek do badań i wsparłem w kreowaniu metodyki badań. Byłem też odpowiedzialny za naukową koncepcję artykułu.

Brak kontaktu ze współautorem

Podpis współautora publikacji

A STATEMENT OF THE APPLICANT'S CO-AUTHOR OF THEIR CONTRIBUTION TO THE WORK

Kraków, 1.10.2025

Mariusz Rospondek
First and last name of co-author of the publication

Instytut Nauk Geologicznych, Uniwersytet Jagielloński
Affiliation

STATEMENT

I declare that for the following work:

Wendorff-Belon, Małgorzata, **Loręc**, Robert, **Wierzbicki**, Adam, **Rospondek**, Mariusz, **Marynowski**, Leszek, 2025. Oligocene environmental changes in the Central Paratethys: geochemical and palynofacial record from the north-western Transylvanian Basin (Romania). Palaeogeography, Palaeoclimatology, Palaeoecology 676, 113124. https://doi.org/10.1016/j.palaeo.2025.113124

My contribution involved a field sampling and selecting appropriate samples for analysis. I contributed to the development of the research methodology. I was responsible for the scientific concept of the article.

Brak kontaktu ze współautorem

Signature of the co-author of the publication

Publikacja 1

Wendorff, M., Rospondek, M., Kluska, B., Marynowski, L., 2017. Organic matter maturity and hydrocarbon potential of the Lower Oligocene Menilite facies in the Eastern Flysch Carpathians (Tarcău and Vrancea Nappes), Romania. Applied Geochemistry 78, 295–310.

Applied Geochemistry 78 (2017) 295–310

Contents lists available at ScienceDirect

Applied Geochemistry

journal homepage: www.elsevier.com/locate/apgeochem

Organic matter maturity and hydrocarbon potential of the Lower Oligocene Menilite facies in the Eastern Flysch Carpathians (Tarcău and Vrancea Nappes), Romania☆

Małgorzata Wendorff [a, *], Mariusz J. Rospondek [a], Bartosz Kluska [a], Leszek Marynowski [b]

[a] Institute of Geological Sciences, Jagiellonian University, ul. Gronostajowa 3a, 30-387 Krakow, Poland
[b] Faculty of Earth Sciences, University of Silesia, ul. Będzińska 60, 41-200, Sosnowiec, Poland

ARTICLE INFO

Article history:
Received 4 August 2016
Received in revised form
10 January 2017
Accepted 11 January 2017
Available online 12 January 2017

Keywords:
Eastern Flysch Carpathians
Lower Oligocene
Menilite facies
Thermal maturity
Hydrocarbon potential
Biomarker ratios

ABSTRACT

Bulk organic geochemical and molecular composition data have been used to analyse the hydrocarbon potential and organic matter maturity of the Lower Oligocene Menilite facies from two adjacent tectonic units of the Eastern Flysch Carpathians (Tarcău and Vrancea Nappes), Romania due to the importance of these source rocks in hydrocarbon exploration in entire Paratethys realm. The data show strong variability in organic matter quantity and quality. Organic carbon content reaches peak values in the siliceous facies of the Lower Menilite Member (up to 8.6 wt% TOC), which contains type II kerogen. With increasing contribution of flysch sedimentation mixed type II/III kerogen gains importance. The biomarker distribution reveals strong variation in the supplied organic matter common for flysch-influenced sedimentary environments. Terrigenous input is marked by epicuticular wax imprint in *n*-alkane distribution and occurrence of conifer biomarkers, while marine organic matter origin is expressed by the occurrence of short-chain *n*-alkanes and hopanes especially in the siliceous facies. Thus, these source rocks can be classified as oil-prone and subordinately mixed oil/gas-prone. The maturity in the outer tectonic unit (Vrancea) is low (T_{max} ~425 °C, R_o ~0.4%) but increases towards the inner Tarcău Nappe (T_{max} ~430 °C, R_o ~0.5%) reaching onset of hydrocarbon generation. The studied rocks have good petroleum potential, but hydrocarbons were generated only in more mature Tarcău Nappe, where solid bitumen veins were observed. Bitumen impregnation of numerous vitrinite grains possibly suppressed vitrinite reflectance, thus leading to more accurate maturity assessment based on molecular proxies (biomarker maturity indices). The observed difference in maturity levels between the nappes results from the more inner position of the sampled Tarcău Nappe succession within the orogen relative to the Vrancea unit. This is related to different burial histories, as well as variation in subsequent erosion and exhumation levels. The actual hydrocarbon potential in the studied area varies due to local interplay of these critical factors.

1. Introduction

Oligocene-Early Miocene source rocks account for ~12.5% of the world's discovered reserves of hydrocarbons (Klemme and Ulmishek, 1991). The source rocks for a number of these hydrocarbon accumulations are Oligocene organic matter-rich facies deposited throughout the entire Paratethys of which western domain was closed forming fold-thrust belt of the Outer Carpathians. In the entire Carpathians they are represented by the rocks of the Menilite-type facies, a prolific source rock yielding oil and gas accumulations in the Krosno-Gorlice area in the Western Carpathians in Poland as well as in the Eastern Carpathians, e.g. Boryslav-Pokuttya fields in Ukraine (Kotarba et al., 2007) and Ploieşti deposits in Romania (Popescu, 1995). Equivalents of such rocks occurring in the Pannonian Basin are Tard Clay Formation (Bechtel et al., 2012) and in the Western Black Sea Basin, e.g. Ruslar Formation (Sachsenhofer et al., 2009). These facies continue further to the east as Maikop Formation in the Eastern Black Sea Basin

☆ Editorial handling by Prof. M. Kersten.

* Corresponding author.
E-mail addresses: malgorzata.wendorff@uj.edu.pl (M. Wendorff), m.rospondek@uj.edu.pl (M.J. Rospondek), bartosz.kluska@doctoral.uj.edu.pl (B. Kluska), marynows@wnoz.us.edu.pl (L. Marynowski).

http://dx.doi.org/10.1016/j.apgeochem.2017.01.009
0883-2927/

(Lichtschlag et al., 2010) and in the Caspian region (Bechtel et al., 2013, 2014) with their easternmost counterparts occurring in Kazakhstan and Turkmenistan (Gürgey, 2003). The Oligocene sequences are often dominated by organic-rich shales due to interplay of favourable factors such as high organic productivity, development of anoxic conditions, and a relatively low input of terrigenous material (Köster et al., 1995, 1998b; Kruge et al., 1996; Rögl, 1999; Popov et al., 2004; Krézsek and Bally, 2006). Organic matter of the Menilite facies was widely studied including its molecular composition in the Western Carpathians (ten Haven et al., 1993; Kruge et al., 1996; Rospondek et al., 1997; Köster et al., 1995, 1998b; Kotarba and Koltun, 2006; Kotarba et al., 2007; Ślączka et al., 2006), but significantly less in the Romanian Eastern Carpathians (bulk geochemistry: e.g. Belayouni et al., 2009; Amadori et al., 2012; molecular composition: Sachsenhofer et al., 2015). Therefore, for the purpose of this study, samples of the rocks of the Menilite facies, mainly of the most prolific Lower Menilite and Bituminous Marl Members (further in the text collectively abbreviated as the Menilite facies), were collected in the Flysch Carpathians near Piatra Neamţ city along two sections located in the different tectonic units (the Tarcău and Vrancea Nappes) at a distance of ~15 km, in order to assess and compare their thermal maturity and hydrocarbon potential. Maturity was studied by examination of vitrinite reflectance, Rock Eval pyrolysis (T_{max}), TOC determination and application of biomarker parameters. The published study on the molecular composition of the Menilite facies has concerned samples from a single tectonic unit, i.e. Vrancea Nappe and is focused on the Oligocene/Miocene omitting the Lower Menilite Member (Sachsenhofer et al., 2015).

2. Geological setting

The Eastern Carpathians are ~600 km long segment of the Carpathian Orogen (Fig. 1), which is bordered to the west by the Transylvanian Basin and the easternmost part of the Pannonian Basin, to the east by the Moldavian and Scythian platforms, Dobrogea Orogen and to the south and southeast by the Moesian Platform (Fig. 1). The Carpathians are traditionally divided into the inner and outer zones (e.g. Uhlig, 1907). The outer part of the Eastern Carpathians (the Eastern Outer or Eastern Flysch Carpathians) called Moldavid Nappe Complex (Fig. 1B) consists of eastward-verging thin-skinned thrust sheets that rode on top of the subducted East European plate (Krézsek and Bally, 2006). This 'accretionary wedge' overrides the relatively undeformed Eastern European foreland (Săndulescu, 1984; Krézsek and Bally, 2006; Maţenco et al., 2010). Respectively, the Teleajen (or Convolute Flysch), Macla, Audia, Tarcău, Vrancea (or Marginal Folds) and Pericarpathian Nappes are distinguished from the hinterland to the foreland (Fig. 1A and B). These tectonic units (except for the Pericarpathian Nappe) are built up mainly of Cretaceous to Miocene flysch-type sediments containing sequences of sandstones intercalated with shaly, and pelagic organic-rich rocks. The most important of these are represented by the Oligocene-Early Miocene deposits, known as the Menilite facies (or Menilite lithofacies according to Belayouni et al., 2009). The Menilite facies consist of the Lower Menilite, Bituminous Marl, Lower Dysodilic Shale and Upper Dysodilic Shale Members (Fig. 1S (Supporting Materials)). Their deposition is related to the Oligocene-Early Miocene anoxic event, which was probably controlled by climatic factors and advancing isolation of the Paratethys from the Mediterranean realm as a consequence of the progressing collision between African and Eurasian plates (Rögl, 1999). At that time the Tarcău and Vrancea domains represented the central and outer part of the Moldavian sector of the Carpathian Foredeep Basin during the sag stage of the basin evolution (Guerrera et al., 2012). The Tarcău Nappe represents the central foredeep basin filled with turbiditic facies brought by active fluvio-deltaic systems from either sides of the basin, while the Vrancea Nappe corresponds to forebulge depozone with sediments supplied by fluvio-deltaic systems developed on eastern high relief land representing forebulge zone, named Perimoldavian Cordillera (Bădescu, 2005; Miclăuş et al., 2009).

3. Samples and methods

3.1. Samples

The Menilite facies investigated in this study are well developed and exposed in the neighbouring Tarcău and Vrancea Nappes, south of the Piatra Neamţ city (Fig. 1A). Both studied sections are located at a distance of about 15 km measured along the W-E transect perpendicular to the thrust-fold axes (Fig. 2). The sequence consists mainly of siliceous flysch with numerous black shale beds and minor black/bluish cherts of the Lower Menilite Mb. and calciclastic flysch with prevailing laminated bituminous marlstones of the Bituminous Marl Mb. (see: Belayouni et al., 2009; Miclăuş et al., 2009; Amadori et al., 2012; Guerrera et al., 2012) with intercalations of sandstone beds, generally occurring as thickening upward sequences in the sections.

The first succession was sampled by Ardeluţa Village along a ~300 m long outcrop in the Tărcuţa Creek, a southern tributary of the Tarcău River, in the Tarcău Nappe. There, the Oligocene succession consists of Unit A (Podu Secu and Ardeluţa Members), Unit B (Lower Menilite, Bituminous Marl and Lower Dysodilic Shale Mbs), and the Miocene Fusaru Formation including Upper Dysodilic Shale Mb. (log 6 in Guerrera et al., 2012). The sampled section begins about 100 m up from the river mouth (Fig. 2), where siliceous black shales and cherts were collected (TAR 1–9). Beneath the bridge over the Tărcuţa Creek (46°42′39.80″N and 26°11′43.60″E) several (~7) intercalations of the Tylawa Limestone (TAR 10) crop out within distal flysch facies of the Lower Menilite Mb. (Fig. 1S). The identification of the Tylawa Limestone is based on the Early Oligocene foraminifera identified in the overlaying shale (TAR 16) and is consistent with its stratigraphic position recognised by Haczewski (1989). The presence of the Tylawa Limestone has not been recognised so far in the investigated area.

The samples TAR 17–22 represent the Bituminous Marl Mb, though their stratigraphic position was not ascertained by paleontological study. In addition, several Lower Oligocene samples of the limestone and shales were collected from the Goşman Creek (Fig. 2), where the rocks are impregnated with solid bitumen along fissures (46°43′41.79″N and 26°14′52.93″E).

The second section represents a ~500 m long exposure cropping out in the Bistriţa half-window of the Vrancea Nappe (Fig. 2). The samples were collected from two sub-sections along the Nechit River cutting through the anticline with Eocene greenish marls in the hinge. The first sub-section in the Nechit Village (Fig. 2, location 2A; 46°46′13.10″N and 26°24′07.20″E) is located in the river bank scarp by the road bridge over the river, and represents the western limb of the anticline. Here, the samples NECH 8–25 (black shales and mudstones), and ~200 m below, NECH 0–7 (black siliceous shales and cherts) all representing the Lower Menilite Mb. and NECH 100–103 (bluish-grey bedded limestones) representing the Bituminous Marl Mb. were collected. The Bituminous Marl Mb. is equivalent of the Dynów Marl Mb. (or Jawornik Marl Unit in the Dukla Nappe according to Radomski and Ślączka (1985)) in the Western Flysch Carpathians. The second sub-section is located in the eastern limb of the anticline and outcrops in the river bank scarp by the road bridge over the river by western outskirts of the Nechit Village (Fig. 2, location 2B; 46°46′16.67″N and 26°25′22.47″E). There the following samples were collected: NECH

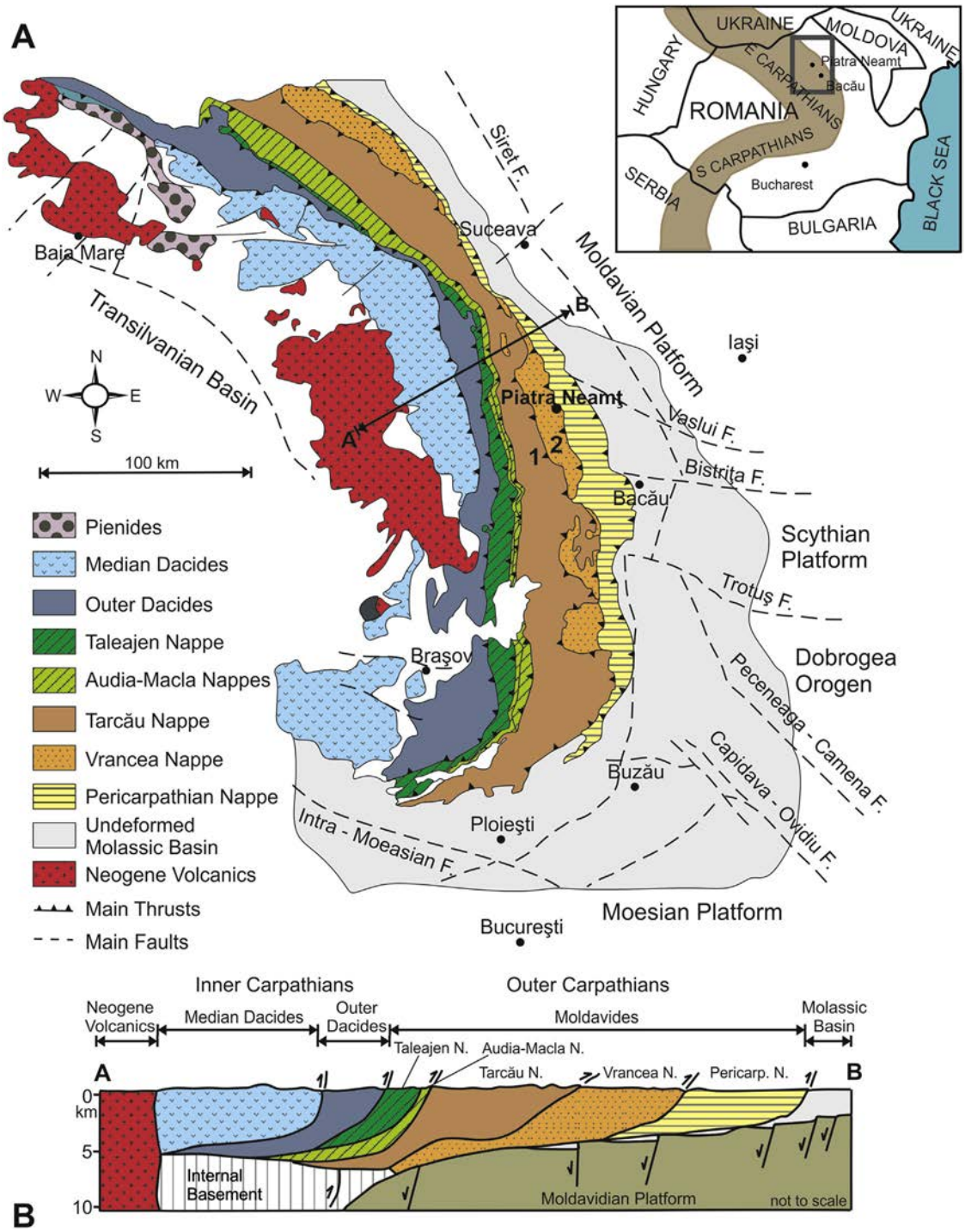

Fig. 1. Geological setting: (A) Geological sketch map of the Eastern Carpathians (modified after Bădescu, 2005) with the locations of the studied Oligocene sections (1 – the Tărcuţa Creek section, 2 – the Nechit River section), (B) Geological cross-section of the Eastern Carpathians (Bădescu, 2005).

200–212 representing the Lower Menilite Mb. including cherts (NECH 200) and siliceous shales (NECH 201–211) and bluish-grey bedded limestones (NECH 212) belonging to the Bituminous Marl Mb. The stratigraphy and lithology of the Nechit River succession has been described in details by Miclăuş et al. (2009). For the purpose of the study 37organic-rich rock samples (16 from the Tarcău Nappe and 21 from the Vrancea Nappe) were selected for organic geochemical analyses. Lithology of the studied samples is given in Tables 1 and 2.

3.2. Vitrinite reflectance

Thirteen polished block samples were analysed for their vitrinite reflectance. Random reflectance was measured with an AXIOPLAN II microscope using 546 nm light and immersion oil of refractive index 1.546 at a total magnification of × 500. The standards used had reflectance (R_o) values of 0.898%.

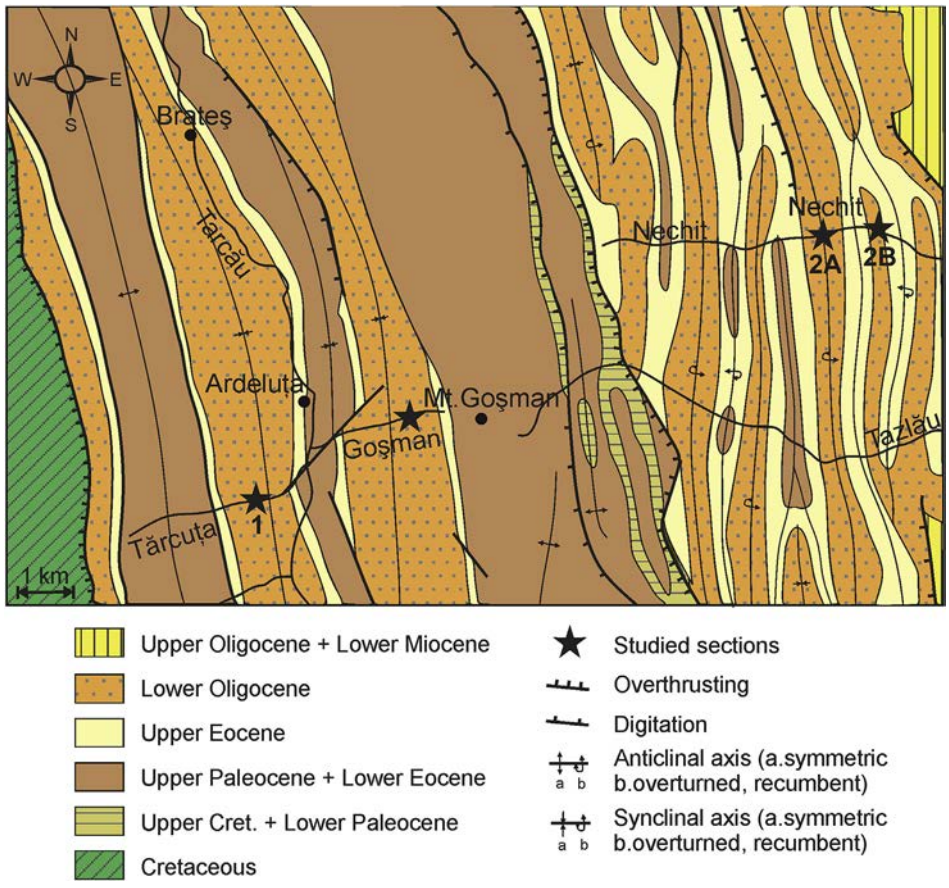

Fig. 2. Detailed geological map of the Tarcău Nappe in the Ardeluța area and the Vrancea Nappe (the Bistrița half-window) in the Nechit area (simplified after Murgeanu and Mirăuță, 1968). 1 – the Tărcuța Creek section, 2A, 2B – the Nechit River sub-sections.

3.3. Total organic carbon and Rock Eval pyrolysis

The Total Organic Carbon (TOC) was determined for 36 samples using an Eltra Elemental Analyser, model CS530. Prior to the TOC analyses, samples were pulverised and treated with 10% HCl at 50 °C until no further decomposition of carbonates was observed.

Rock Eval pyrolysis was carried out on 28 samples using Delsi Rock Eval II Analyser following standard methods described by Espitalié et al. (1985) and Peters (1986). The S_1 and S_2 peaks (mg HC/g rock) were used to calculate the hydrogen index (HI = S_2 x 100/TOC [mg HC/g TOC]) and the production index (PI = S_1/(S_1 + S_2); Espitalié et al., 1977). T_{max} was measured as a maturity indicator.

3.4. Extraction and chromatographic separation

Out of total 37 samples, the representative 29 samples were selected for detailed geochemical analyses. The surfaces of the samples were removed before analyses in aim to minimise the effects of weathering and possible contaminations. The samples were pulverised (~100 g) and Soxhlet-extracted in pre-extracted cellulose thimbles with dichloromethane (DCM) and methanol (MeOH) mixture (7.5: 1 vol) for 48 h. Copper wires were added to the extracts to remove elemental sulphur. The solvents were evaporated in a rotary evaporator close to the dryness and obtained extractable organic matter (EOM) dried over anhydrous sodium sulphate (Na_2SO_4) overnight, then weighted and fractionated into maltenes and asphaltenes by asphaltene precipitation in *n*-hexane. An aliquot of the maltenes (~50–100 mg) was fractionated by column chromatography (CC) using columns (200 × 10 mm, 15 ml bed volume) packed with activated alumina (at 150 °C for 2 h). Prior to chromatography *n*-eicos-1-ene (140 μg), 2-phenylindene (39.8 μg), hexamethylbenzene (40.2 μg) and 2-hexadecylthiophene (27.9 μg) were added to maltenes as internal standards. The separation of apolar, aromatic and polar fractions was achieved with three bed volumes of *n*-hexane, *n*-hexane/DCM (7: 3 vol) and DCM/MeOH (1: 1 vol), respectively.

3.5. Gas chromatography – mass spectrometry

Apolar and aromatic fractions were analysed using gas chromatography – mass spectrometry (GC–MS). GC–MS analyses were performed with an Agilent 7890A chromatograph equipped with an EPC Cool On-Column Inlet and fitted with one of the two fused silica capillary columns of different polarity used in this study, i.e. either HP-5 MS or DB-35 MS (60 m × 0.32 mm, 0.25 μm film thickness). Helium was used as carrier gas. Samples were injected on column at 40 °C. The oven temperature was kept constant for 3 min, increased up to 120 °C at 20 °C per min, subsequently to 300 °C at 3 °C per min and kept at 300 °C for 60 min. The chromatograph was coupled to an Agilent 5975C Network with mass selective detector (MSD). The spectrometer was operated with an ion source temperature set at 200 °C, ionisation energy 70 eV and a cycle time of 1 s in the scan range of *m/z* 50–700. Spectra from the Wiley Registry of Mass Spectral Data (7th ed.) and from literature specified in the appropriate text sections were used for MS data comparison. Quantification of the compounds for calculating molecular parameters was performed by integration of peak areas in

Table 1
Vitrinite reflectance, bulk geochemical data and pyrolysis Rock Eval parameters.

Sample/Lithology	R_o (%)	Bulk geochemical parameters			Rock Eval parameters				
		TOC (wt%)	mg EOM/ g rock	mg EOM/ g TOC	T_{max} (°C)	S_1 (mg HC/g rock)	S_2 (mg HC/g rock)	PI (S_1/S_1+S_2)	HI (mg HC/g TOC)
Tarcău Nappe – Tărcuța Creek Section									
Bituminous Marl Member									
TAR 22/black shale	0.59	1.63	2.79	171	–	–	–	–	–
TAR 21/black shale	–	1.41	–	–	432	1.48	3.70	0.29	265
TAR 20/marly grey shale	–	1.04	–	–	429	0.40	2.47	0.14	247
TAR 19/black shale	–	0.85	0.83	98	433	0.99	0.26	0.67	30
Lower Menilite Member									
TAR 16/marly grey shale	–	0.71	3.14	156	422	0.65	1.18	0.36	165
TAR 15/siliceous black shale	–	1.81	1.72	95	426	1.47	7.64	0.16	422
TAR 14/siliceous black shale	–	1.92	–	–	433	4.17	5.60	0.43	292
TAR 13/marly shale	0.55	1.16	1.32	114	–	–	–	–	–
TAR 11/black shale	–	2.58	3.65	141	431	1.17	8.63	0.12	335
TAR 10/laminated limestone	–	0.98	1.40	143	432	0.38	1.65	0.19	169
TAR 8/black shale	0.43	2.61	6.77	259	434	1.38	11.74	0.11	450
TAR 5/black chert	0.43	2.38	3.78	159	–	–	–	–	–
TAR 3/black shale	0.59	1.59	3.63	227	430	1.02	4.71	0.18	296
TAR 2/laminated grey marl	0.44	4.57	6.53	143	–	–	–	–	–
Vrancea Nappe – Nechit River Section									
Bituminous Marl Member									
NECH 102/marly limestone	–	0.57	0.73	128	419	0.40	1.88	0.18	329
Lower Menilite Member									
NECH 25/black shale	0.39	2.86	1.95	68	422	1.42	7.05	0.17	247
NECH 23/marly black shale	–	2.87	–	–	426	0.23	10.51	0.02	366
NECH 21/marly black shale	–	2.12	1.86	88	431	0.86	5.84	0.13	275
NECH 19A/black shale	0.37	4.01	3.14	78	419	1.25	10.45	0.17	261
NECH 17/marly black shale	–	2.95	–	–	416	2.06	6.29	0.02	213
NECH 15/black shale	0.43	3.47	2.56	74	426	1.34	11.57	0.11	333
NECH 12/siliceous black shale	–	7.90	–	–	427	1.34	37.02	0.25	469
NECH 10/marly black shale	0.36	3.02	3.21	106	426	1.32	12.43	0.10	411
NECH 9/black shale	–	2.29	–	–	422	0.65	6.95	0.09	303
NECH 7/marly shale	–	2.11	–	–	429	0.20	8.35	0.02	396
NECH 5/black shale	0.34	3.22	–	–	430	0.29	12.91	0.02	401
NECH 1/black shale	–	2.18	2.07	99	431	0.71	8.50	0.08	405
NECH 0/black shale	0.35	3.70	3.25	88	431	0.74	21.49	0.03	581
NECH 0D/siliceous black shale	–	8.62	1.63	19	429	0.69	44.98	0.02	522
NECH 200/siliceous black shale	0.43	3.73	–	–	432	0.19	22.18	0.01	595
NECH 204/siliceous black shale	0.41	4.15	3.90	94	424	1.08	16.79	0.06	405
NECH 205/siliceous black shale	–	5.13	–	–	419	0.90	21.30	0.04	415
NECH 211/black shale	0.38	4.45	3.78	85	–	–	–	–	–

the appropriate mass chromatograms or total ion current chromatograms (TIC; e.g. for the pristane/phytane ratio).

4. Results

4.1. Vitrinite reflectance

Vitrinite-type grains, commonly from 20 to 50 μm (Fig. 3), occasionally up to 0.5 mm, occur scarcely in all the analysed samples, in contrast to the frequently observed liptinite/bitumen lenticular laminae. R_o values range between 0.43 and 0.59% (av. 0.51%) and 0.34–0.43% (av. 0.38%) for the samples from the Tarcău and Vrancea Nappes, respectively (Table 1). The histograms of the R_o measured differ between both units. The R_o distribution in the Vrancea Nappe is unimodal with maximum oscillating in the interval of 0.30–0.40%, while the distribution in the Tarcău Nappe rocks is variable with several maxima, i.e. around 0.30–0.40%, 0.60% and about 1.0% (Fig. 4).

4.2. Bulk geochemical data

The samples from the Tarcău Nappe contain from 0.9 to 4.6 wt% TOC with an average of 1.9 wt%. TOC contents for the samples from the Vrancea Nappe are more variable and oscillate between 0.6 and 8.6 wt% (Table 1) with an average of 3.6 wt% and are considerably higher than those for the Tarcău Nappe. The highest TOC values are reached for the siliceous black shales (e.g. NECH 0D and NECH 12) while for the marlstones TOC contents are lower than 1 wt%. In general, TOC and EOM amounts correlate well, except for the black shale sample (NECH 0D) from the Vrancea Nappe and several samples from the Tarcău Nappe which reveal extremely high EOM yields, reaching 6.8 mg EOM/g rock for the TAR 8 sample. The EOM ratios normalised to TOC (mg EOM/g TOC) vary from 95 to 259 mg/g (av. 155 mg/g) for the rocks from the Tarcău Nappe and from 19 to 128 mg/g (84 mg/g) for the samples from the Vrancea Nappe (Table 1).

4.3. Rock Eval pyrolysis

Rock Eval analyses of bulk samples from the Tarcău Nappe revealed hydrogen index (HI) values between 165 and 450 mg HC/g TOC except for the sample TAR 19 with a HI of 30 mg/g. Such low HI value associated with low TOC content may suggest mineral matrix errors effecting the HC yields (Espitalié et al., 1980; Katz, 1983). However, the biomarker distribution indicates the presence of terrigenous organic matter. Most of the samples from the Vrancea Nappe have HI values varying from 213 up to even 595 mg HC/g TOC for the siliceous shale sample NECH 200 (Table 1).

The T_{max} values range from 422 to 434 °C with an average of 430 °C in the inner Tarcău Nappe while for the outer unit from 416

Table 2
Molecular maturity parameters: carbon preference index (CPI, Bray and Evans, 1961), pristane to phytane ratio (Pr/Ph, Didyk et al., 1978), C_{29} sterane epimer ratio (C_{29} 20*S*/(20*S* + 20*R*), Seifert and Moldowan, 1986), trisnorhopane ratio (Ts/(Ts + Tm), Seifert and Moldowan, 1978), C_{30} hopane structural isomer ratio (C_{30} βα/(βα + αβ), Seifert and Moldowan, 1980), C_{31} hopane epimer ratio (C_{31} 22*S*/(22*S* + 22*R*), Seifert and Moldowan, 1980), triaromatic sterane index (TA(I)/TA(I + II), Peters et al., 2005), methylphenantrene index (MPI-1, Radke and Welte, 1983). n.c. - not calculated.

Sample/lithology	CPI	Pr/Ph	C_{29} sterane 20*S*/(20*S* + 20*R*)	Ts/(Ts + Tm)	C_{30} hopane βα/(βα+αβ)	C_{31} hopane 22*S*/(22*S* + 22*R*)	TA(I)/TA(I + II) (%)	MPI-1
Tarcău Nappe – Tărcuța Creek Section								
Bituminous Marl Member								
TAR 22/black shale	1.07	2.32	0.49	0.59	0.14	0.57	12.55	0.50
TAR 19/black shale	1.14	6.18	n.c.	n.c.	n.c.	0.60	n.c.	n.c.
TAR 18/black shale	1.01	2.03	0.44	0.58	0.14	0.55	11.00	0.52
Lower Menilite Member								
TAR 16/marly grey shale	1.11	2.95	0.55	0.55	0.15	0.56	13.18	0.51
TAR 15/siliceous black shale	1.01	1.22	n.c.	n.c.	0.15	0.52	n.c.	n.c.
TAR 13/marly shale	1.01	1.33	0.49	0.46	0.14	0.53	n.c.	0.60
TAR 11/black shale	0.98	1.19	0.57	0.53	0.15	0.58	6.87	0.55
TAR 10/laminated limestone	1.00	1.31	0.58	0.44	0.12	0.56	4.90	0.45
TAR 8/black shale	0.94	1.31	n.c.	0.53	0.14	0.56	6.68	n.c.
TAR 7/black shale	0.98	1.30	0.46	0.54	0.13	0.58	6.80	0.50
TAR 5/black chert	1.08	2.76	n.c.	0.42	0.14	0.57	8.74	0.48
TAR 4/siliceous black shale	1.07	1.57	0.53	0.42	0.12	0.58	7.65	0.45
TAR 3/black shale	1.07	0.80	0.45	0.45	0.13	0.59	3.95	0.50
TAR 2/laminated grey marl	0.93	1.67	0.50	0.52	0.15	0.56	4.36	0.33
Vrancea Nappe – Nechit River Section								
Bituminous Marl Member								
NECH 103/grey shale	1.13	2.16	0.18	0.40	0.16	0.51	6.03	0.35
NECH 102/marly limestone	0.82	1.24	0.33	0.33	0.16	0.49	6.68	n.c.
Lower Menilite Member								
NECH25/black shale	1.15	1.89	0.29	0.22	0.23	0.52	3.99	0.49
NECH 21/marly black shale	1.23	2.31	0.29	0.18	0.26	0.51	4.46	0.46
NECH 19A/black shale	1.17	1.85	0.30	0.21	0.24	0.52	2.93	0.47
NECH 15/black shale	1.23	2.63	0.29	0.21	0.24	0.51	4.55	0.46
NECH 10/marly black shale	1.16	2.86	0.35	0.32	0.20	0.54	6.00	n.c.
NECH 3/black shale	1.28	2.12	0.28	0.29	0.19	0.50	2.84	0.58
NECH 1/black shale	1.15	1.69	0.34	0.21	0.27	0.54	3.87	0.57
NECH 0/black shale	1.54	2.60	0.34	0.27	0.19	0.51	3.07	n.c.
NECH 0A/black shale	0.99	1.55	0.23	0.25	0.18	0.46	5.65	n.c.
NECH 0D/siliceous black shale	1.01	1.59	0.19	0.21	0.20	0.47	8.14	0.50
NECH 202/black shale	1.13	1.84	0.14	0.19	0.23	0.43	9.59	0.44
NECH 204/siliceous black shale	1.11	1.39	0.29	0.16	0.22	0.41	3.73	0.56
NECH 207/grey shale	1.17	1.24	0.30	n.c.	0.22	0.43	5.54	0.43
NECH 211/siliceous black shale	1.39	3.60	0.22	0.10	0.25	0.52	3.49	0.39

to 432 °C with slightly lower average of 425 °C (Table 1). T_{max} values do not show noticeable correlation with lithology and position of the samples in the sections.

The comparison of T_{max} with HI allows defining organic matter evolution pathways, when the S_3 peak is unavailable (Espitalié et al., 1985). Almost all the data points are located in the oil-prone type II kerogen field with varying admixture of type III kerogen (Fig. 5). Prevalence of type II occurs mostly in the black siliceous shales of the Lower Menilite Member from the Vrancea Nappe.

Production index (PI) varies from 0.11 to 0.67 (av. 0.27) for the samples from the Tarcău Nappe section and from 0.01 to 0.25 (av. 0.08) for the Vrancea Nappe section (Table 1).

4.4. Molecular composition and molecular maturity parameters

Total ion currents (TIC) of apolar fractions of selected samples representing each investigated tectonic unit are shown in Fig. 6. Biomarker composition is generally very uniform but distribution varies in the analysed samples from both sections. The dominant hydrocarbon series are *n*-alkanes (Fig. 6), acyclic isoprenoids (Fig. 2S), steranes (Fig. 3S) and hopanes (Fig. 4S). Some characteristic biomarkers reported from Menilite facies like highly branched isoprenoids (Rospondek et al., 1997) or oleananes (Kruge et al., 1996; Köster et al., 1998b; Kotarba et al., 2007) are missing. Maturity molecular parameters based on relevant compounds are presented in Table 2 and discussed further on.

4.4.1. *n*-Alkanes and acyclic isoprenoids

n-Alkanes cover a range of homologues from *n*-C_{13} up to *n*-C_{34} (Fig. 2S) with a few samples containing molecules only to *n*-C_{32} or extending up to *n*-C_{37}. The *n*-alkane series are dominated by short (*n*-C_{13} to *n*-C_{19}) to middle-chain (*n*-C_{20} to *n*-C_{25}) members. A slight odd over even predominance among long chain molecules (*n*-C_{27}, *n*-C_{29}, *n*-C_{31}) can be observed in some extracts from both sections (Fig. 6 and Fig. 2S). The Carbon Preference Index (CPI; according to Bray and Evans, 1961) generally oscillates around 1.0 for the Tarcău Nappe samples (0.93–1.14). The extracts from the Vrancea section reveal more variable CPI values in the range of 0.99–1.54 (av. 1.2), apart from the single sample of the marly limestone (NECH 102) with CPI ~0.82 (Table 2).

The identified acyclic isoprenoids including *nor*-pristane, pristane (Pr) and phytane (Ph) are present in high abundances in all the samples with pristane being one of the most abundant compounds (Fig. 6 and Fig. 2S). Calculated Pr/Ph ratios (according to Didyk et al., 1978) vary broadly from 0.80 up to 6.18 (av. 2.0) for the samples from the Tarcău Nappe and from 1.24 to 3.60 (av. 1.95) for those rocks from the Vrancea Nappe (Table 2).

4.4.2. Steranes

Steranes are present in variable quantities varying in distribution patterns for both analysed sections (Fig. 3S). In the Tarcău

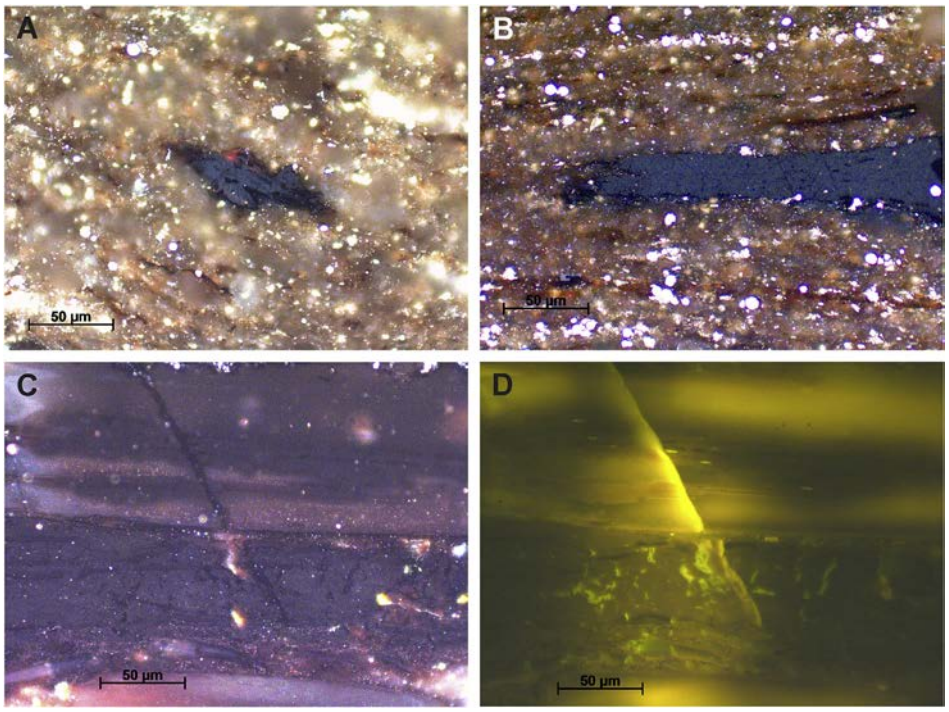

Fig. 3. Photomicrographs of vitrinite-type macerals under reflected white (A, B, C) and fluorescent light (D) using oil immersion. Two upper pictures show representative vitrinite-type grains for (A) the Tarcău Nappe section (sample TAR 2) and (B) the Vrancea Nappe section (sample NECH 0). The same fragment of a large reworked vitrinite grain in reflected white (C) and fluorescent light (D) revealing the most intensive fluorescence in pores and along fissures impregnated with bitumen (sample NECH 19A).

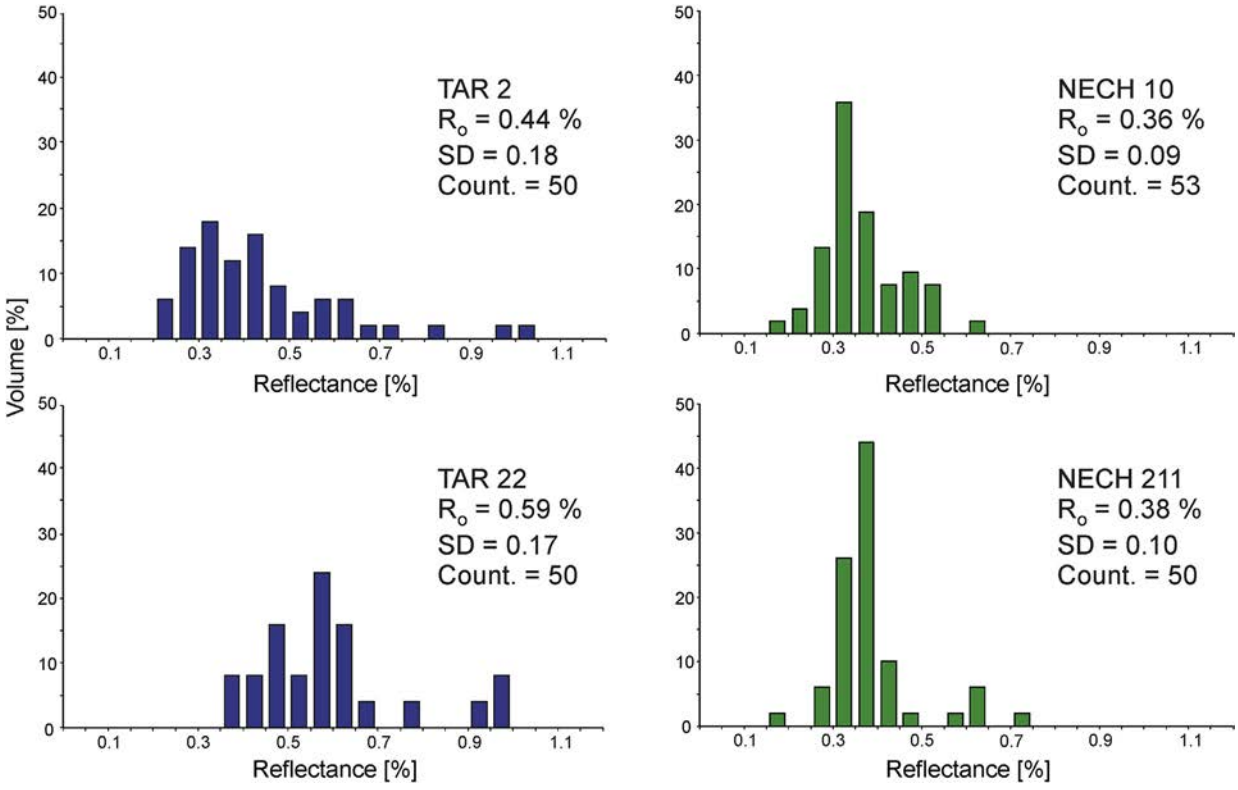

Fig. 4. Histograms showing polymodal distribution of R_o for the Tarcău Nappe (TAR 2 and 22 samples) and monomodal for the Vrancea Nappe (NECH 10 and 211). SD – standard deviation, count. – number of countings.

Nappe samples they are subordinate, while in the Vrancea they are major constituents. Regular steranes occur in the C_{27}–C_{30} range in all the samples from the Tarcău Nappe, with C_{29} or C_{27} members dominating. Both 5α(H),14α(H),17α(H) and 5α(H),14β(H),17β(H)

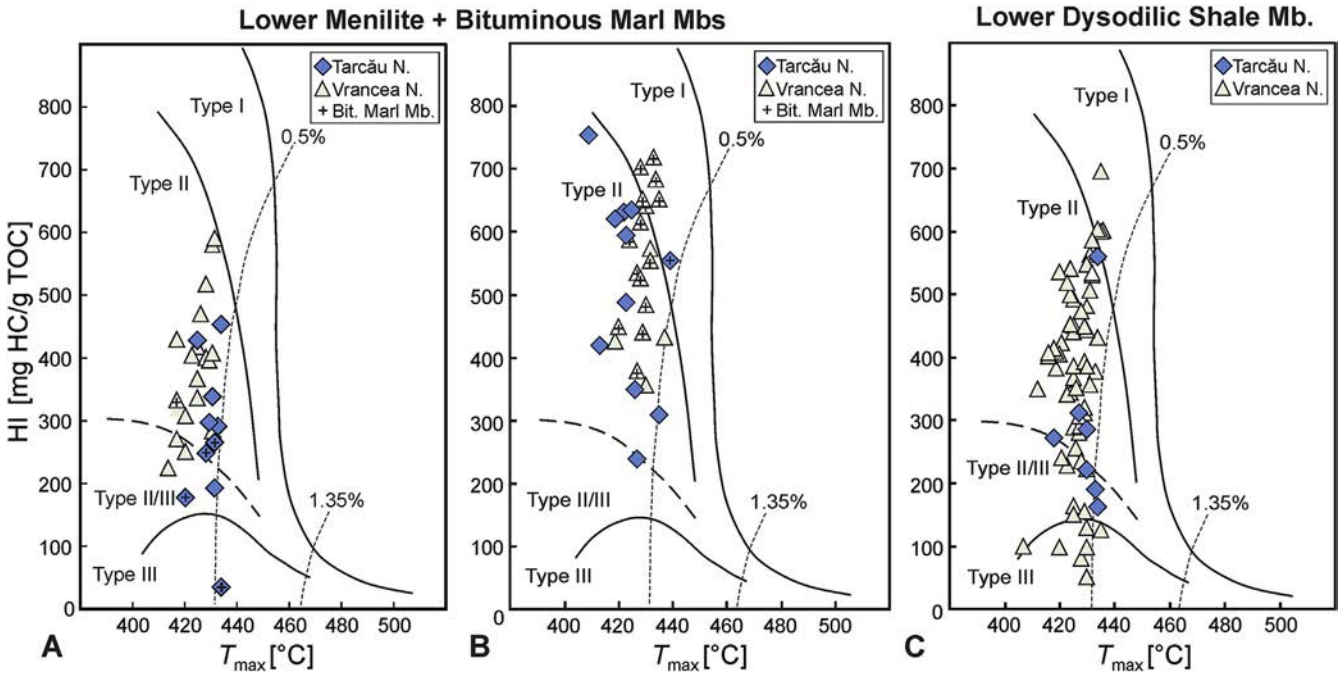

Fig. 5. Plot of hydrogen index (HI) vs. T_{max} (according to Espitalié et al., 1985) outlining kerogen types for the analysed samples (A) and those available in literature for the Lower Menilite and Bituminous Marl Mbs (B) and the Lower Dysodilic Shale Mb. (C) from the Tarcău and Vrancea Nappes (for Tarcău from Belayouni et al., 2009; for Vrancea from Amadori et al., 2012 and Sachsenhofer et al., 2015).

configurations – noted ααα and αββ respectively - occur in comparable amounts, except for C_{27} with more abundant ααα isomers. The C_{28} steranes are the less abundant and their molecules with thermally more stable αββ configuration become important constituents. In the samples from the Vrancea section steranes in ααα-20*R* configuration prevail over ααα-20*S* epimers. The αββ isomers are present in small amounts (Fig. 3S) or are below the detection limit.

Ratios of epimers *sinister* to *rectus* 20*S*/(20*S* + 20*R*) (Seifert and Moldowan, 1986) calculated for the C_{29} ααα steranes fall in the range from 0.44 to 0.58 (av. 0.51) for the Tarcău Nappe samples and between 0.14 and 0.35 (av. 0.27) for those from the Vrancea Nappe (Table 2). Results for the samples revealing ratios higher than 0.55, i.e. above the thermal equilibrium level, should be treated with caution since these were obtained for rocks with very low concentrations of steranes. In addition 4-methylsteranes were detected in small amounts in samples from both sections.

Apart from the regular steranes almost all the samples contain significant concentrations of diasteranes in C_{27}–C_{29} range with both 13α(H),17β(H) and 13β(H),17α(H) configurations, except for the C_{29} diasterane with only βα configuration present (Fig. 3S; C_{29} βα diasterane elutes as a shoulder of the C_{27} ααα-20*R* sterane peak). The most prominent are C_{27} βα and C_{28} βα isomers, with both 20*S* and 20*R* epimers occurring in comparable concentrations.

Triaromatic steranes are predominant constituents of almost all analysed aromatic fractions from both sections. Triaromatic Sterane Index: TA(I)/TA(I + II) (Peters et al., 2005), where TA(I) is a sum of C_{20} and C_{21} triaromatic steroids and TA(II) is a sum of C_{26} to C_{28} (20*S* + 20*R*) members, reveals highly variable values ranging from 4.0 to 13.2% (av. 7.9%) for the Tarcău Nappe samples (Table 2). The rocks from the Vrancea Nappe have values oscillating from 2.8 to 9.6% (av. 5.0%). The variation shows that it is less reliable maturity indicator than parameters based on aliphatic steranes.

4.4.3. Hopanes

Hopanoids are important constituents of the apolar fractions of the investigated rocks in both sections, sometimes they are more abundant than *n*-alkanes (Fig. 6). Their distribution pattern is characterised by the occurrence of C_{29} to C_{35} and occasionally C_{36} homologues, predominantly with 17α(H),21β(H) configuration (Fig. 4S). The most abundant is 17α(H),21β(H) C_{30} and next 17α(H),21β(H) C_{29} hopane.

Trisnorhopanes (Ts – 18α(H)-22,29,30-trisnorneohopane and Tm – 17α(H)-22,29,30-trisnorhopane) were recognised in all the samples. Ts/(Ts + Tm) ratio (Seifert and Moldowan, 1978) ranges from 0.42 to 0.59 with an average of 0.50 for the Tarcău Nappe rocks (Table 2) The predominance of the thermally stable Ts over Tm characterises majority of the analysed rocks from this section. The samples from the Vrancea Nappe reveal values significantly lower and highly variable in the range of 0.10–0.40 (av. 0.24), indicating the predominance of the Tm.

The calculated ratio of 17β((H),21α(H)-C_{30} hopane (moretane) to 17α(H),21β(H) configuration, i.e. βα/(βα + αβ) C_{30} hopane ratio (Seifert and Moldowan, 1980), fall within different ranges for each section. Lower values obtained for the samples from the Tarcău Nappe oscillate around 0.12–0.15 (av. 0.14), while the Vrancea Nappe samples reveal higher ratios ranging from 0.16 to 0.27 (av. 0.22) (Table 2).

Ratios of epimers 22*S*/(22*S* + 22*R*) (Seifert and Moldowan, 1980) obtained for the C_{31} homologue fall in the range of 0.52–0.60 (av. 0.57) for the Tarcău Nappe samples indicating the prevalence of the thermally stable isomer. The samples from the Vrancea Nappe section reveal lower 22*S*/(22*S* + 22*R*) C_{31} hopane ratios ranging from 0.41 to 0.54 (av. 0.49) (Table 2).

Benzohopanes being the products of diagenetic hopane transformation are represented by series of C_{32} to C_{35} homologues (Hussler et al., 1984; Schaeffer et al., 1995) in most of the studied samples from both sections.

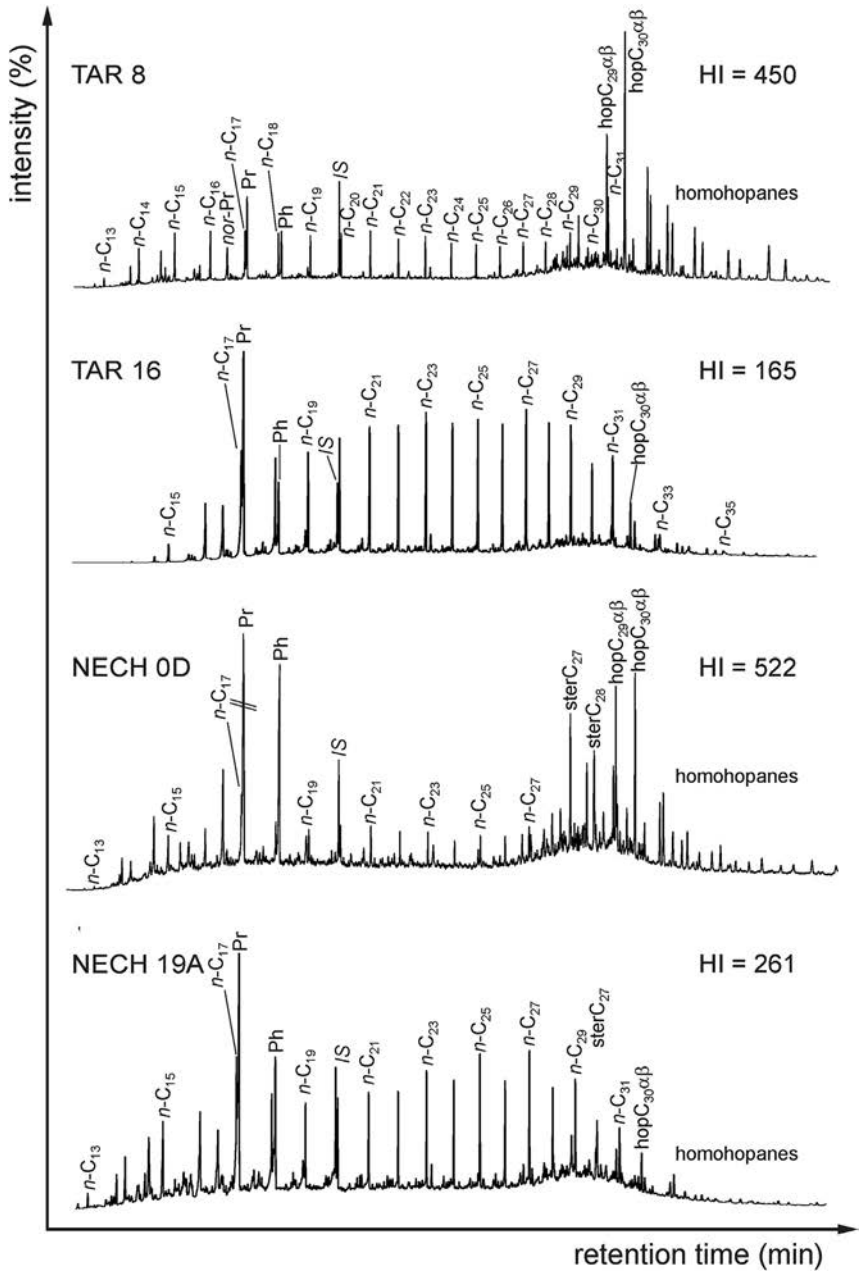

Fig. 6. Variation in the distribution of biomarkers in apolar fractions between the Tarcău (TAR 8 and 16) and Vrancea (NECH 0D and 19A) Nappes; IS – internal standard (*n*-eicos-1-ene). Total ion current (TIC) chromatograms, column HP-5 MS.

4.4.4. Aromatic vascular plant biomarkes, naphthalenes and phenanthrenes

Aromatic biomarkers of vascular plant origin, as cadalene (sesquiterpenoid), 1,2,3,4-tetrahydroretene, simonellite and retene (diterpenoids) (Philp, 1985; van Aarssen et al., 2000; Otto and Simoneit, 2001) are present in significant abundances in almost all the aromatic fractions from the Vrancea Nappe. Their relative concentrations vary from sample to sample, but cadalene and tetrahydroretene usually predominate over the others. Several samples from the Tarcău Nappe contain only trace amounts of cadalene or retene.

A series of methylated 2-methyl-2-(trimethyltridecyl)chromans (MTTCs) were identified (Sinninghe Damsté et al., 1987) in most of the samples exclusively in the Vrancea Nappe (Fig. 7). Trimethyl MTTCs predominate over mono- and dimethyl derivatives. Monoaryl diagenetic products of isorenieratene occur in few samples of the same nappe, though in small amounts.

Non-specific polyaromatic hydrocarbons as alkyl naphthalenes and phenanthrenes are the predominant constituents of the aromatic fractions together with triaromatic steranes (Fig. 7). Among alkylphenanthrenes the methyl derivatives are found in significant concentrations with prevalence of thermodynamically less stable isomers (1- and 9-methyl) over the more stable couple (2- and 3-methyl). Methylphenanthrene Index 1 (MPI-1; Radke and Welte, 1983) was calculated for a limited number of the samples (Table 2). For the Tarcău Nappe rocks MPI-1 falls in the range of 0.33–0.60 (av. 0.49), while for the Vrancea Nappe 0.35–0.58 (av. 0.48). The wide range of the MPI-1 values for each section shows that the isomer distribution may be controlled by not only thermodynamic factors.

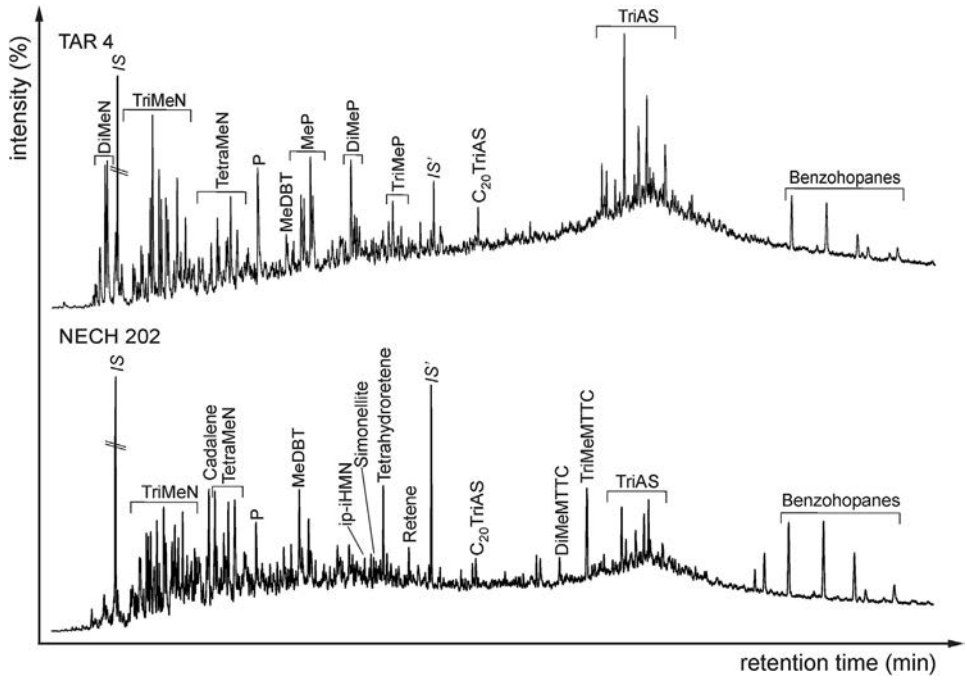

Fig. 7. Distribution of aromatic compounds for representative samples from the Tarcău (TAR 4) and Vrancea (NECH 202) Nappes. Note abundant unspecific polycyclic hydrocarbons expressing advanced aromatisation in the Tarcău Nappe sample and occurrence of chromans and vascular plant biomarkers in the Vrancea Nappe. DiMeN – dimethylnaphtalenes; TriMeN – trimethylnaphtalenes; TetraMeN – tetramethylnaphtalenes; P – phenanthrene; MeP – methylphenanthrenes; DiMeP – dimethylphenanthrenes; TriMP – trimethylphenanthrenes; MeDBT – methyldibenzothiophene; TriAS – triaromatic steranes; IS – internal standard (hexamethylbenzene); IS' – internal standard (2-hexadecylthiophene). TIC chromatograms, column HP-5 MS.

5. Discussion

Determination of organic matter thermal maturity and its hydrocarbon potential as the main goals of the presented study were approached, however, their reliable dissertation needs the knowledge of organic matter source, type and palaeoenvironment context. The type of organic matter is related to its origin and the origin identification allows inferring the composition and scale of hydrocarbon generation during maturation (Tissot and Welte, 1984). Biomarker and Rock Eval data provided insight into entry conditions of hydrocarbon generation leading to a model outlined below.

5.1. Organic matter origin and palaeoenvironmental background

The variability of the organic matter is expressed by the hydrogen index (HI) values, which vary within the sections and between the sub-basins. The investigated organic matter represents a mixture of type II and III kerogen (Table 1; Fig. 5A), i.e. a blend of marine and terrigenous organic matter. The type II endmember is dominating in black siliceous shales and cherts of the Lower Menilite Mb. pointing to the importance of diatom derived silica and organic matter contribution. Higher marine input to the Vrancea vs. Tarcău Nappe rocks is indicated by observable kerogen-point cloud shift towards type II kerogen (Fig. 5A). The HI values for the Vrancea Nappe samples are never as low as for the Tarcău Nappe rocks. Proportional increase of type III kerogen is observed with increasing contribution of turbiditic currents to sediment supply (in samples representing mudstones).

For the Tarcău Nappe section the obtained results on kerogen composition are consistent with the limited number of published data for the same location (log 1, Tărcuța section, Belayouni et al., 2009) revealing occurrence of type II/III kerogen (Fig. 5B). Type I kerogen was identified in the Lower Menilite Mb. rocks in the Tarcău Nappe but exclusively from the section situated about 100 km to the north in Moldovița Village area at banks of the Săcrieș River (log 3 in Belayouni et al., 2009). Such HI differences point to strong axial variability in kerogen origin in the flysch subbasin.

For the Vrancea Nappe section the results for the Lower Menilite Mb. can be compared to very limited number of the data published from the Bistrița tectonic half-window (Amadori et al., 2012). Amadori et al. (2012) reported type II kerogen (HI 470 mg HC/g TOC, 4 wt% TOC) from one chert sample, and type II/III from two others. Our data (Table 1) shows that the kerogen is represented by array of the composition varying between type II and III, though the contribution of type II seems to be higher comparing to the Tărcuța section of the Tarcău Nappe (Fig. 5B). Interestingly, the Bituminous Marl Mb. rocks are rich in type I kerogen (Amadori et al., 2012; Sachsenhofer et al., 2015).

Examination of the plot of the Rock Eval data for the Lower Dysodilic Shale Mb. (Belayouni et al., 2009; Amadori et al., 2012; Sachsenhofer et al., 2015) reveals increasing contribution of type III kerogen upward in the Oligocene sections in the Vrancea Nappe (Fig. 5C). For the Tarcău Nappe the number of the available data is too limited to unequivocally recognise a trend in the kerogen composition.

The variation in kerogen composition can furthermore result from duration of transport and temporary near-surface deposition before burial. In present-day turbidites reaching the Madeira abyssal plain organic matter becomes depleted in hydrogen from ~600 to ~300 mg HC/g TOC. HI lowering occurs due to exposition of organic-rich shelf-deposited sediments to oxic water during transportation and redeposition. In oxidised turbidite sediments further oxidation can reduce the HI to ~50 mg HC/g TOC (Cowie et al., 1995). Thus the continuous cloudy array of the kerogen compositions (Fig. 5) can arise not only from varying proportions of kerogens type II and III but also from the oxidation overprint.

On the molecular level significant contribution of marine organisms is reflected in high relative proportion of *n*-alkanes in the range of *n*-C_{15} to *n*-C_{19} (e.g. Fig. 2S, sample TAR 4) which is usually attributed to algal and cyanobacterial source (Gelpi et al., 1970; Brassell et al., 1980; Tissot and Welte, 1984). Occurrence of intermediate molecular weight *n*-alkanes (*n*-C_{21} to *n*-C_{25}) can be assigned to organic matter derived from aquatic macrophytes (Ficken et al., 2000). In this range an overlap exists with *n*-alkanes derived from biolipids possessing linear carbon skeleton like *n*-alkanes, *n*-alkanols, and *n*-alkanoic acids characteristic for epicuticular waxes of vascular land plants (Tulloch, 1976; Barthlott et al., 1998; Otto et al., 2005) and yielding upon diagenesis molecules in the range of *n*-C_{22} to *n*-C_{32}. However, contribution of the epicuticular leaf waxes to sedimentary and fossilised organic matter is usually recognised based on the predominance of odd-numbered long chain (*n*-C_{27}, *n*-C_{29}, *n*-C_{31}) *n*-alkanes over even-numbered ones (Eglinton and Hamilton, 1967). Examination of *n*-alkane distribution reveals again the high variability in organic matter type changing with lithology in both tectonic units, which comes along with HI variation (Fig. 6). The samples characterised by low HI contain a significant proportion of *n*-alkanes in the range of *n*-C_{25} to *n*-C_{31} showing a slight odd-over-even predominance (Fig. 6, samples TAR 16 and NECH 19A), in opposite to those with high HI and high concentrations of *n*-C_{14} to *n*-C_{19} homologues (Fig. 6, samples TAR 8 and NECH 0D). Occurrence of simonellite, retene and 1,2,3,4-tetrahydroretene exclusively in the rocks form the Vrancea Nappe suggests contribution from conifers (Simoneit, 1977; Alexander et al., 1988; van Aarssen et al., 2000; Otto and Simoneit, 2001) and is probably related to transport from different directions in both sub-basins. The presence of conifer biomarkers in sediments deposited along the eastern coastline suggests conifer vegetation on Perimoldavian Cordillera (forebulge). Such variability is consistent with flysch sedimentation characterised by strong dependence of organic matter type (autochthonous vs. allochthonous) on the proportion of redeposited vs. pelagic sediment. Such phenomenon has been widely recognised, e.g. in the Western Carpathians (Köster et al., 1998b). Variation of organic matter type is, however, not reflected in steroid distribution. Similar concentrations of C_{27} to C_{29} steroids may suggest balanced input from phototrophic land and marine organisms with marine algae marked by the presence of the C_{27} sterane and 24-methylsterane (e.g. Volkman, 1986; Brown and Kenig, 2004). The hopane distribution is not specific with dominance of C_{30} and C_{31} compounds. The highest hopane concentrations are restricted to siliceous facies with diatom-derived silica pointing to their marine origin. This is consistent with their provenance from bacteria dwelling in photic water column, possibly cyanobacteria, as it was revealed by the hopane C isotope composition in the Menilite rocks of the Western Carpathians (Köster et al., 1998b). For the whole Menilite siliceous facies the origin of silica from opaline diatom frustules is clear. The importance of the diatom contribution is not reflected, however, by biomarker record in the studied sections, in contrary to other parts of the Paratethys with HBIs being significant components (ten Haven et al., 1993; Rospondek et al., 1997; Köster et al., 1998b; Sachsenhofer et al., 2015).

Rather oxic conditions during the deposition of organic matter are witnessed by CPI values slightly above 1.0 for the investigated Vrancea Nappe samples. Balanced CPI close to odd-even equilibrium observed in the Tarcău Nappe section (Table 2) could suggest transition from oxic to dysoxic conditions (Bray and Evans, 1961), however, here such values are interpreted as results of higher thermal maturity (see further discussion). Commonly applied Pr/Ph ratio in 90% of the studied samples from both nappes fall in the range of 1.2–3.0 (Table 2) also indicating oxidative normal-marine environment (Didyk et al., 1978; Goossens et al., 1984; Volkman and Maxwell, 1986; ten Haven et al., 1987). This interpretation is supported by hopane distribution (Peters and Moldowan, 1991) with high relative proportions of the αβ-C_{30} hopane and sharply decreasing concentrations of higher homologues (Fig. 4S). On the other hand, lack of bioturbation and domination of small-sized pyrite framboids (below 0.6 μm) reveal anoxia in deeper part of the water column (Wendorff et al., 2016a,b) favouring good preservation of organic matter in sediments (TOC up to 8.6 wt%). Highly anoxic environment during sedimentation of the Menilite facies is often documented throughout the Carpathians (Koltun, 1992; ten Haven et al., 1993; Kruge et al., 1996; Koltun et al., 1998; Curtis et al., 2004; Amadori et al., 2012), sometimes with euxinia reaching photic zone (Köster et al., 1995, 1998b; Kotarba et al., 2007; Sachsenhofer et al., 2015), however, biomarkers (isorenieratene derivatives) indicating euxinia in photic zone (e.g. Koopmans et al., 1996) were detected exclusively in the uppermost part of the Lower Menilite Mb. of the Vrancea Nappe.

5.2. Level of thermal maturity

Source rocks can produce hydrocarbons only under a favourable thermal regime, thus the maturity of organic matter is an important parameter that needs to be assessed in terms of source rock potential (Tissot and Welte, 1984). The maturity assessment for the purpose of this study is based on vitrinite reflectance (R_o) and Rock Eval peak temperature (T_{max}) along with biomarker parameters.

5.2.1. Bulk maturity indicators

5.2.1.1. Vitrinite reflectance. A slightly higher maturity for the rocks from the Tarcău Nappe than those from the Vrancea Nappe section is indicated by R_o in the range of 0.43–0.59% (av. 0.5%) and 0.34–0.43% (av. 0.4%), respectively (Table 1). Considering R_o > 0.5–0.6% as a limit value for the onset of source rocks' catagenesis (Tissot and Welte, 1984), the samples from the Tarcău Nappe section are early mature while those from the Vrancea Nappe section are immature. Increased fluorescence noted in some vitrinite-type grains (Fig. 3) seems to result from bitumen impregnation, which could have suppressed vitrinite reflectance values. It has been shown that large amounts of bitumen can retard the normal progression of R_o with maturation (Hutton et al., 1980; Jiménez et al., 1998). The bitumen was probably generated *in situ* and migrated only at a small distance within the source rocks as inferred from high EOM yields reaching up to 6.8 mg EOM/g rock for the Tarcău Nappe samples and up to 3.9 mg EOM/g rock for the Vrancea Nappe samples.

5.2.1.2. Rock Eval pyrolysis parameters. The T_{max} values that group between 416 and 434 °C (Table 1, Fig. 5A) indicate that the organic matter in both sections is mostly thermally immature, although some samples from the Tarcău Nappe almost reached the onset of oil generation window (~435 °C; Peters and Cassa, 1994). However, in this case a threshold temperature ~430 °C seems more appropriate due to dominance of type II kerogen. The immature nature of the organic matter in the Vrancea Nappe section is generally consistent with the low EOM/TOC and PI values (Peters and Cassa, 1994) (Fig. 8A), as well as with the results reported by Amadori et al. (2012) for rocks from the Vrancea Nappe, i.a. from the Nechit River section. The Tarcău Nappe samples reveals higher averages of PI (av. ~0.27) and EOM/TOC values (av. ~155 mg EOM/g TOC), thus organic matter in this unit can be characterised as early to peak mature (PI ~0.25–0.40 for peak mature; Peters and Cassa, 1994) (Fig. 8A).

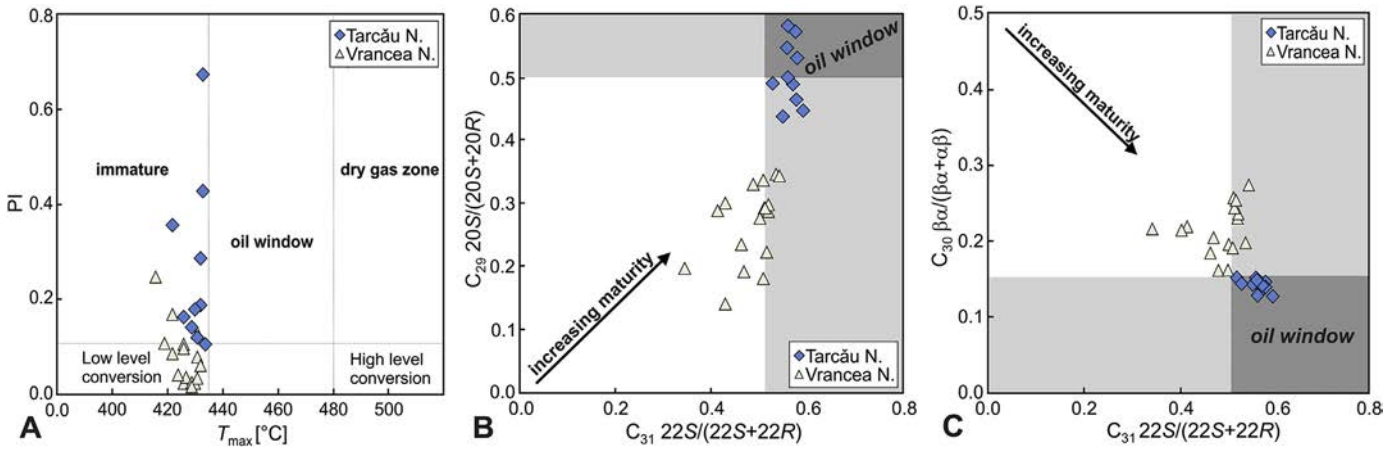

Fig. 8. Cross-plots outlining maturity variation between the Tarcău and Vrancea Nappes. (A) Production index PI=$S_1/(S_2 + S_1)$ vs. T_{max} (according to Espitalié et al., 1977), (B) C_{31} hopane epimer ratio C_{31} 22*S*/(22*S* + 22*R*) vs. C_{29} sterane epimer ratio C_{29} 20*S*/(20*S* + 20*R*), (C) C_{30} hopane structural isomer ratio C_{30} αβ/(αβ + βα) vs. C_{31} hopane epimer ratio C_{31} 22*S*/(22*S* + 22*R*).

5.2.2. Biomarker maturity parameters

Proportions between *n*-alkanes and polycyclic alkanes (steranes and hopanes) can reflect either maturity or biodegradation level. Due to preservation of the whole *n*-alkane homologue series with clear origin-related imprint in both Vrancea and Tarcău Nappe samples, predominance of the hopanes over *n*-alkanes, observed in several samples, is considered as indicative for relatively low maturity range. This phenomenon is clear in the sample NECH 0D, in which sterane and hopane series strongly predominate over *n*-alkanes (Fig. 6). Such pattern becomes less clear for organic matter reaching main stage of catagenesis, because a large portion of *n*-alkanes is generated from cleavage of kerogen.

5.2.2.1. n-Alkane distribution. The CPI values (Bray and Evans, 1961) oscillating around unity suggest thermal maturity reaching catagenesis stage in the Tarcău Nappe. More variable CPI values (0.8–1.5) point to immature to early mature organic matter (Tissot and Welte, 1984) for the Vrancea Nappe. Very similar CPI values have been obtained for the upper part of the Menilite succession (starting from Bituminous Marl Mb.) by Sachsenhofer et al. (2015). *n*-Alkane distribution can be precursor related, hence its interpretation is equivocal and must be supported by other data.

5.2.2.2. Sterane isomerisation. The 20*S*/(20*S* + 20*R*) ratios for C_{29} regular steranes are partly in the range of thermal equilibrium (0.52–0.55; Seifert and Moldowan, 1986) for the samples from the Tarcău Nappe (Table 2), thus suggesting that maturity in the range of the peak of oil window has been reached (Fig. 8B). Lower C_{29} 20*S*/(20*S* + 20*R*) values (~0.28) for the samples from the Vrancea Nappe section indicate thermal immaturity (Table 2, Fig. 8B). The low maturity of these samples is revealed as well by the dominance of steranes possessing ααα-20*R* stereochemistry. The αββ isomers are present but occur in low concentrations, however, their contents clearly increase with advancing organic matter maturation in the Tarcău Nappe samples (Fig. 3S). The Triaromatic Sterane Index TA(I)/TA(I + II) supports this maturity trend despite its high variability (Table 2). Higher average values were obtained for the Tarcău Nappe rocks (av. 8.6%), thus revealing their higher maturity and lower values for the Vrancea Nappe samples (av. 5.0%) resulted from the less advanced organic matter diagenesis.

5.2.2.3. Hopane isomerisation. The 22*S*/(22*S* + 22*R*) ratio calculated for C_{31} homohopanes in the narrow range of 0.52–0.60 for the samples from the Tarcău Nappe section (Table 2; Fig. 8C) corresponds to the early mature source rocks, reaching the oil generation zone, where the 0.57 value marks the transition from early to peak oil generation (Seifert and Moldowan, 1986). This is in accordance with the data obtained for the βα/(βα + αβ) C_{30} hopane ratio (Table 2), close to the value characterising oil window (0.15; Seifert and Moldowan, 1980). Values of the 22*S*/(22*S* + 22*R*) C_{31} ratio ranging from 0.41 to 0.54 and for the C_{30} βα/(βα + αβ) ratio in the range of 0.16–0.27 for the rocks from the Vrancea Nappe indicate rather thermally immature rocks in agreement with the sterane and CPI data (see above). The large spread of the data points reflects kinetic control influencing the hopane isomer distribution in the Vrancea Nappe, but smooth data array in the Tarcău Nappe is in accordance with thermodynamic control (Fig. 8C).

The trisnorhopane Ts/(Ts + Tm) ratios of av. 0.50 and 0.24 for the Tarcău and Vrancea Nappe samples, respectively, also lend support to the above interpretations. However, high variability of this parameter among different lithologies can suggest an influence of organic matter mineral matrix as a factor controlling the ratio (e.g. Moldowan et al., 1986; Kluska et al., 2013). Alternatively, the ratio may be source-related, as it is unclear whether the conversion of Tm to Ts occurs.

In summary, the organic matter of the rocks from the Tarcău Nappe reached higher maturity comparing to the Vrancea Nappe section. Only organic matter of the Tarcău Nappe attained the window of oil generation (Fig. 8A), which is marked by generally dominating thermally stable isomers (Figs. 3S and 4S and Fig. 8B and C), CPI ~1 and higher vitrinite reflectance. The organic matter from the Vrancea Nappe samples is immature to early mature. Such difference in maturity results from location of the Tarcău Nappe succession in a more inner site of the orogen in relation to the Vrancea Nappe, thus it is related to different burial timing and variation in subsequent erosion and exhumation levels. Thermal stress related to thrusting/folding seems to contribute less to the maturation (Polissar et al., 2011). Otherwise lower units should generally show higher maturity. Recent distance between the studied sections is ~15 km, but the presence of the Vrancea succession beneath the Tarcău Nappe was documented in numerous wells as far as 35–40 km westward from its present wedge indicating large distance shortening (Stefanescu et al., 2006). Such trend in maturation is commonly observed in thin skinned fold-thrust orogenic belts, e.g. in the Western Flysch Carpathians (eastern part in Poland) where the Silesian Nappe (av. T_{max} ~450 °C)

overthrusted onto the Skole Unit (av. ~T_{max} 421 °C) has higher maturity, i.a. in the sections studied by Köster et al. (1998a) and Kotarba et al. (2007).

On a local scale, however, no evident stratigraphic trend in the maturity was recognised along the studied sections, which may have resulted from insignificant diagenesis progress yet during incipient folding (as proposed by Bessereau et al., 1997; Köster et al., 1998a; Sachsenhofer et al., 2015). In fact, the available continuous segments of the studied Lower Oligocene sequence are limited, thus potential maturity trends can be masked by other factors, like effects of mineral matrix/lithology (Peters, 1986) or influence by redox conditions (e.g. Szczerba and Rospondek, 2010) during diagenesis/catagenesis.

5.3. Hydrocarbon potential

High contents of organic matter are a prerequisite for a good source rock (Tissot and Welte, 1984), though to eliminate influence of inert carbon, hydrocarbon potential assessment usually takes into consideration EOM content and pyrolysis yields, i.e. Rock Eval S_1 and S_2 data (Peters, 1986).

Good organic richness has been determined in the samples from the Tarcău Nappe as expressed by an average of 1.9 wt% TOC and 155 mg EOM/g TOC (Table 1, Fig. 9), which is consistent with amounts of thermally released hydrocarbons (S_1 ~1.3 mg HC/g rock). In turn, the samples from the Vrancea Nappe have good to sporadically even excellent (with max ~8.6 wt% TOC for the Lower Menilite Mb.) hydrocarbon richness revealed by higher TOC values (av. 3.6 wt%). Slightly less optimistic evaluation was obtained based on the average EOM content of 84 mg EOM/g TOC and S_1 ~0.9 mg HC/g rock, thus suggesting fair to good HC potential for the Vrancea Nappe rocks.

The remaining HC potential is expressed by the Rock Eval S_2 peak area that is related to yields of the hydrocarbons generated from potential cracking of kerogen (Peters, 1986; Dembicki, 2009). The greatest values (up to 44.98 mg HC/g rock) were found in the rocks from the Vrancea Nappe section (Table 1) pointing to their very good HC potential.

Another approach to the petroleum potential can be obtained using the cross-plot of the sum $S_1 + S_2$ vs. TOC (Fig. 9). This approach reveals good HC potential for the Vrancea Nappe, but more variable potential, from fair to good, for the Tarcău Nappe

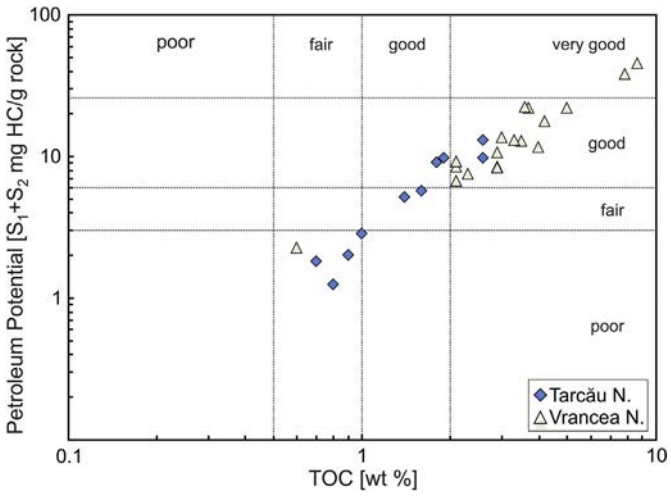

Fig. 9. Petroleum Potential ($S_1 + S_2$) vs. TOC presenting fair to good hydrocarbon potential of the Tarcău Nappe and good to very good potential of the Vrancea Nappe rocks.

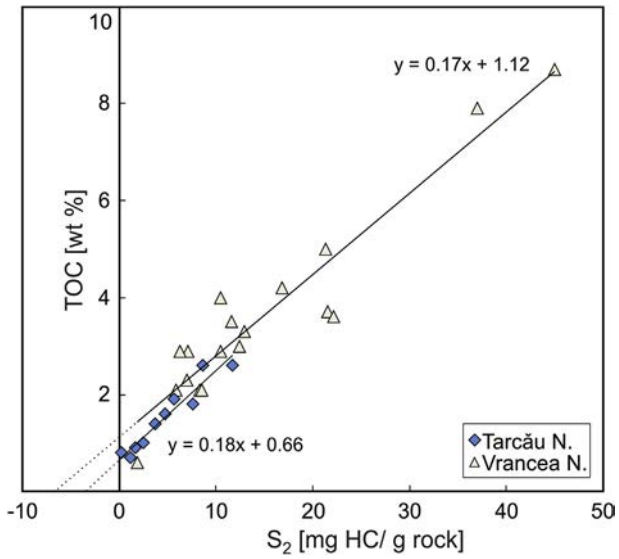

Fig. 10. Plot of TOC vs. S_2 (according to Langford and Blanc-Valleron, 1990; Dahl et al., 2004) revealing the amount of "dead organic carbon" (regression line offset is 0.66 wt% for the Tarcău and 1.12 wt% for the Vrancea Nappe) and allowing reconstruction of "live HI" (for the Tarcău 384 mg HC/g TOC and for the Vrancea 597 mg HC/g TOC).

source rocks.

Comprehensive insight into the original oil and gas potentials in the whole source rock sequences can be gained by applying the method suggested by Dahl et al. (2004). The average HI of the "live organic material" from a source rock section can be calculated when the inert organic component (TOC "inert") is subtracted from the overall TOC. In the studied sections, sedimentary organic matter has a fraction of inert organic material, which does not disproportionate during pyrolysis. This is revealed by the offset from the origin of the regression line in TOC vs. S_2 diagram (Langford and Blanc-Valleron, 1990; Dahl et al., 2004) (Fig. 10). The estimated amounts of the TOC "inert" are 0.66 and 1.12 wt% for the Tarcău and Vrancea Nappes, respectively. The recalculated average HI "live" of ~597 mg HC/g TOC (Dahl et al., 2004) for the Vrancea section is higher compared to the measured HI data cluster located between ~250 and 450 mg HC/g TOC (Fig. 5). The average HI "live" of ~384 mg HC/g TOC for the Tarcău Nappe is as well significantly higher than the average of measured HI. The estimated HI values highlight more oil-prone potential of the studied source rocks. Lower HI values for the rocks from the Tarcău Nappe may be effect of the hydrocarbon release due to more advanced maturity (in accordance with higher S_1).

Summarising, the studied rocks of the Menilite sequence have good petroleum potential, although this assessment is limited to the organic matter-rich facies. Hydrocarbons have been generated to some extent in the Tarcău Nappe due to sufficient maturity in contrary to immature Vrancea Nappe rocks. The hydrocarbon potential has not been exhausted as revealed by still high HI values. In Piatra Neamţ area the rocks of the Menilite facies have been proposed as source rocks for noncommercial hydrocarbon deposits like the Cuejdiu and Moineşti/Comăneşti gas/oil fields (Stefanescu et al., 2006). There, the Vrancea Nappe Oligocene source rocks and oil flows from the associated Kliwa Sandstones have been recorded at a depth of 5500 and 5350 m.

6. Conclusions

Insights into quantity and quality of the organic matter from the Menilite facies of the Lower Oligocene from two closely

neighbouring tectonic units: the Tarcău and Vrancea Nappes of the Romanian Eastern Flysch Carpathians were gained from Rock Eval pyrolysis, vitrinite reflectance and biomarker analysis in order to asses and compare their hydrocarbon potential and organic matter maturity.

The organic matter content varies with lithology reaching peak values in relatively thin set of the siliceous black shales of the Lower Menilite Member. The average TOC is ~1.9 wt % in the Tarcău and 3.7 wt% Vrancea Nappe samples.

The significant variability of the organic matter provenance is indicated by biomarker distributions and HI values, which vary within the sections and between the sub-basins. The phenomenon is common for sedimentary sequences influenced by deposition from turbiditic currents supplying terrigenous organic matter to the central basin zone. Depending on the proportion between pelagic and turbiditic current sediment input, continuous compositional trend between type II and III kerogen end-members is common in both tectonic units, indicating oil-prone and subordinately mixed oil/gas-prone source rocks.

The Rock Eval results and those from biomarkers indicate changeable importance of the organic matter contribution from autochthonous marine algal/planktonic organisms including bacterial and marine eucaryota in relation to land plant biomass. The siliceous facies possess distinctive marine characteristic with higher short-chained *n*-alkane and hopane concentrations accompanied by the highest observed HI. Such lithology and organic matter composition point to importance of diatoms, but from those groups not biosynthesising highly branched isoprenoids.

The depositional environment was oxygen-depleted but with euxinia limited to deeper parts of the water column as revealed by the pyrite framboid size distribution and common lack of bioturbations.

The early/peak mature organic matter (onset of hydrocarbon generation) in the Tarcău Nappe samples is revealed by vitrinite reflectance together with Rock Eval T_{max} and PI, while organic matter from the Vrancea Nappe is immature. The molecular parameters provide a more accurate assessment of organic matter thermal maturity comparing to the pyrolysis Rock Eval and R_o data, offering the best resolution of the thermal maturity variability in the studied sections. An eastward decreasing organic matter maturity trend from the early mature, partly reaching oil generation zone in the inner Tarcău Nappe to immature in the outer Vrancea Nappe is revealed.

The difference in maturity levels between the nappes must result from the position of the Tarcău Nappe in more inner zone of the Carpathian orogen in relation to the Vrancea Nappe located towards foreland. Therefore, it is linked to different burial timing, which is related to variation of subsequent erosion and exhumation levels. Nevertheless, the sampled sections are located in the distance of 15 km from each other along the cross-section perpendicular to the basin axis and consequently for unambiguous evaluation of maturity at a given site, it would be necessary to analyse samples originating from a single well core.

The Vrancea Nappe rocks reveal good to occasionally excellent petroleum potential although they did not attain the hydrocarbon generation stage. In turn, the Tarcău Nappe source rocks have fair to good HC potential and the organic matter is mature and has reached early oil window, as also confirmed by the elevated EOM yields. The generated hydrocarbons have been locally expelled from the Tarcău Nappe source rocks, thus impregnating rock fissures with solid bitumen. In the studied area hydrocarbon prospects are nonetheless low due to deep erosion (in tectonic windows) and insufficient organic matter maturity in the Vrancea Nappe rocks.

Acknowledgements

The authors would like to thank Anna Lewandowska and Robert Loręc for their assistance during the fieldwork and Magdalena Misz-Kennan (University of Silesia) for her help in vitrinite reflectance measurements. Foraminifera identification was performed by Lucyna Bobrek. The anonymous reviewers are gratefully acknowledged for their critical remarks and constructive suggestions. Funding for this research was provided by the Jagiellonian University projects for young scientists (DS/MND/WBiNoZ/ING/13/2014 and DS/MND/WBiNoZ/ING/14/2015).

Appendix A. Supplementary data

Supplementary data related to this article can be found at http://dx.doi.org/10.1016/j.apgeochem.2017.01.009.

References

Alexander, R., Larcher, A.V., Kagi, R.I., Price, P., 1988. The use of plant-derived biomarkers for correlation of oils with source rocks in the Cooper/Eromanga Basin system, Australia. Aust. Pet. Explor. Assoc. J. 28, 310–328.

Amadori, M.L., Belayouni, H., Guerrera, F., Martín-Martín, M., Martín-Rojas, I., Miclăuș, C., Raffaelli, G., 2012. New data on the Vrancea Nappe (Moldavidian basin, outer Carpathian domain, Romania): Paleogeographic and geodynamic reconstructions. Int. J. Earth Sci. 101, 1599–1623.

Barthlott, W., Neinhuis, C., Cutler, D., Ditsch, F., Meusel, I., Theisen, I., Wilhelmi, H., 1998. Classification and terminology of plant epicuticular waxes. Bot. J. Linn. Soc. 126, 237–260.

Bădescu, D., 2005. Evoluția Tectono-stratigrafică a Carpaților Orientali În Decursul Mezozoicului Și Neozoicului. Editura Economică, Bucharest, p. 312.

Bechtel, A., Hámor-Vidó, M., Gratzer, R., Sachsenhofer, R.F., Püttmann, W., 2012. Facies evolution and stratigraphic correlation in the early Oligocene Tard Clay of Hungary as revealed by maceral, biomarker and stable isotope composition. Mar. Pet. Geol. 35, 55–74.

Bechtel, A., Movsumova, U., Strobl, S.A.I., Sachsenhofer, R.F., Soliman, A., Gratzer, R., Püttmann, W., 2013. Organofacies and paleoenvironment of the Oligocene Maikop series of Angeharan (eastern Azerbaijan). Org. Geochem. 56, 51–67.

Bechtel, A., Movsumova, U., Pross, J., Gratzer, R., Coric, S., Sachsenhofer, R.F., 2014. The Oligocene Maikop series of Lahich (eastern Azerbaijan): paleoenvironment and oil–source rock correlation. Org. Geochem. 71, 43–59.

Belayouni, H., di Staso, A., Guerrera, F., Martín-Martín, M., Miclauș, C., Serrano, F., Tramontana, M., 2009. Stratigraphic and geochemical study of the organic-rich black shales in the Tarcău Nappe of the Moldavidian domain (Carpathian chain, Romania). Int. J. Earth Sci. 98, 157–176.

Bessereau, G., Roure, F., Kotarba, M., Kuśmierek, J., Strzetelski, W., 1997. Structure and hydrocarbon habitat of the polish Carpathians. In: Ziegler, P.A., Horvfith, F. (Eds.), Peri-tethys Mémoir 2 – Structure and Prospects of Alpine Basins and Forelands. Mémoires du Muséum National d'Histoire Naturelle, Paris, pp. 343–373.

Brassell, S.C., Comet, P.A., Eglinton, G., Isaacson, P.J., McEvoy, J., Maxwell, J.R., Thompson, I.D., Tibbetts, P.J.C., Volkman, J.K., 1980. The origin and fate of lipids in the Japan Trench. In: Douglas, A.G., Maxwell, J.R. (Eds.), Advances in Organic Geochemistry, 1979. Pergamon Press, Oxford, pp. 375–392.

Bray, E.E., Evans, E.D., 1961. Distribution of *n*-paraffins as a clue to recognition of source beds. Geochim. Cosmochim. Acta 22, 2–15.

Brown, T.C., Kenig, F., 2004. Water column structure during deposition of Middle Devonian-Lower Mississippian black and green/gray shales of the Illinois and Michigan basins: a biomarker approach. Paleogeography, Palaeoclimatology. Palaeoecology 215, 59–85.

Cowie, G.L., Hedges, J.I., Prahl, F.G., De Lange, G.J., 1995. Elemental and major biochemical changes across an oxidation front in a relict turbidite: an oxygen effect. Geochim. Cosmochim. Acta 59, 33–46.

Curtis, J.B., Kotarba, M.J., Lewan, M.D., Więcław, D., 2004. Oil/source rock correlations in the Polish Flysch Carpathians and Mesozoic basement and organic facies of the Oligocene Menilite Shales: insights from hydrous pyrolysis experiments. Org. Geochem. 35, 1573–1596.

Dahl, B., Bojesen-Koefoed, J., Holm, A., Justwan, H., Rasmussen, E., Thomsen, E., 2004. A new approach to interpreting Rock-Eval S_2 and TOC data for kerogen quality assessment. Org. Geochem. 35, 1461–1477.

Dembicki Jr., 2009. Three common source rock evaluation errors made by geologists during prospect of play appraisals. Am. Assoc. Pet. Geol. Bull. 93, 342–356.

Didyk, B.M., Simoneit, B.R.T., Brassell, S.C., Eglinton, G., 1978. Organic geochemical indicators of paleoenvironmental conditions of sedimentation. Nature 272, 216–222.

Eglinton, G., Hamilton, R.J., 1967. Leaf epicuticular waxes. Science 156, 1322–1335.

Espitalié, J., Laporte, J.L., Madec, M., Marquis, F., Le Plat, P., Paulet, J., Boutefeu, A., 1977. Methode rapide de caracterisation des roches meres de leur potential petrolier et de leur degre d'evolution. Rev. l'Institut Français Pétrole 32, 23–41.

Espitalié, J., Madec, M., Tissot, B., 1980. Role of mineral matrix in kerogen pyrolysis: influence on petroleum generation and migration. Am. Assoc. Pet. Geol. Bull. 64, 59–66.
Espitalié, J., Deroo, G., Marquis, F., 1985. La pyrolyse Rock-Eval et ses applications. Première partie. Rev. l'Institut Français Pétrole 40, 563–579.
Ficken, K.J., Li, B., Swain, D.L., Eglinton, G., 2000. An *n*-alkane proxy fort the sedimentary input of submerged/floating freshwater aquatic macrophytes. Org. Geochem. 31, 745–749.
Gelpi, E., Schneider, H., Mann, J., Oró, J., 1970. Hydrocarbons of geochemical significance in microscopic algae. Phytochemistry 9, 603–612.
Goossens, H., de Leeuw, J.W., Schenck, P.A., Brassell, S.C., 1984. Tocopherols as likely precursors of pristane in ancient sediments and crude oils. Nature 312, 440–442.
Guerrera, F., Martín-Martín, M., Martín-Pérez, J.A., Martín-Rojas, I., Miclăuş, C., Serrano, F., 2012. Tectonic control on the sedimentary record of the central Moldavidian basin (Eastern Carpathians, Romania). Geol. Carp. 63, 463–479.
Gürgey, K., 2003. Correlation, alteration, and origin of hydrocarbons in the GCA, Bahar, and Gum Adasi fields, western South Caspian Basin: geochemical and multivariate statistical assessments. Mar. Pet. Geol. 20, 1119–1139.
Haczewski, G., 1989. Poziomy wapieni kokkolitowych w serii menilitowo-krośnienskiej – rozróżnianie, korelacja i geneza. Ann. Soc. Geol. Pol. 59, 435–523.
Hussler, G., Connan, J., Albrecht, P., 1984. Novel families of tetra- and hexacyclic aromatic hopanoids predominant in carbonate rocks and crude oils. Org. Geochem. 6, 39–49.
Hutton, A.C., Kantsler, A.J., Cook, A.C., Mckirdy, D.M., 1980. Organic matter in oil shales. J. Aust. Pet. Explor. Assoc. 20, 44–67.
Jiménez, A., Iglesias, M.J., Laggoun-Defarge, F., Suarez-Ruiz, I., 1998. Study of physical and chemical properties of vitrinite. Inferences on depositional and coalification controls. Chem. Geol. 150, 197–221.
Katz, B.J., 1983. Limitations of Rock-Eval pyrolysis for typing of organic matter. Org. Geochem. 4, 195–199.
Klemme, H.D., Ulmishek, G.F., 1991. Effective petroleum source rocks of the world: stratigraphic distribution and controlling depositional factors. Am. Assoc. Pet. Geol. Bull. 75, 1809–1851.
Kluska, B., Rospondek, M.J., Marynowski, L., Schaeffer, P., 2013. The Werra cyclotheme (Upper Permian, Fore-Sudetic Monocline, Poland): insights into fluctuations of the sedimentary environment from organic geochemical studies. Appl. Geochem. 29, 73–91.
Koltun, Y.U., 1992. Organic matter in Oligocene Menilite formation rocks of the Ukrainian Carpathians: paleoenvironment and geochemical evolution. Org. Geochem. 4, 423–430.
Koltun, Y.U., Espitalié, J., Kotarba, M., Roure, F., Ellouz, N., Kosakowski, P., 1998. Petroleum generation in the Ukrainian external Carpathians and the adjacent foreland. J. Pet. Geol. 21, 265–288.
Kotarba, M.J., Więcław, D., Koltun, Y.V., Marynowski, L., Kuśmierek, J., Dudok, I.V., 2007. Organic geochemical study and genetic correlation of natural gas, oil and Menilite source rocks in the area between San and Stryi rivers (Polish and Ukrainian Carpathians). Org. Geochem. 38, 163–180.
Kotarba, M.J., Koltun, Y.V., 2006. The origin and habitat of hydrocarbons of the Polish and Ukrainian parts of the Carpathian Province. In: Golonka, J., Picha, F.J. (Eds.), The Carpathians and Their Foreland: Geology and Hydrocarbon Resources, vol. 84. American Association of Petroleum Geologists Memoir, pp. 395–442.
Koopmans, M.P., Köster, J., van Kaam-Peters, H.M.E., King, F., Schouten, S., Hartgers, W.A., de Leeuw, J.W., Sinninghe Damsté, J.S., 1996. Diagenetic and catagenetic products of isorenieratene: molecular indicators for photic zone anoxia. Geochim. Cosmochim. Acta 60, 4467–4496.
Köster, J., Rospondek, M., Zubrzycki, A., Kotarba, M., de Leeuw, J.W., Sinninghe Damsté, J.S., 1995. A molecular organic geochemical study of black shales associated with diatomites from the Oligocene Menilite Shales (Flysch Carpathians, SE Poland). In: Grimalt, J.O., Dorronsoro, C. (Eds.), Organic Geochemistry: Developments and Applications to Energy, Climate, Environment and Human History. A.I.G.O.A., September 4–8, 1995 San Sebastian, Spain, pp. 87–89.
Köster, J., Kotarba, M., Lafaruge, E., Kosakowski, P., 1998a. Source rock habitat and hydrocarbon potential of Oligocene Menilite Formation (Flysch Carpathians of Southeast Poland): an organic geochemical and isotope approach. Org. Geochem. 29, 543–558.
Köster, J., Rospondek, M., Schouten, S., Kotarba, M., Zubrzycki, A., Sinninghe Damsté, J.S., 1998b. Biomarker geochemistry of a foreland basin: the Oligocene Menilite Formation in the Flysch Carpathians of southeast Poland. Org. Geochem. 29, 649–669.
Krézsek, C., Bally, A.W., 2006. The Transylvanian Basin (Romania) and its relation to the Carpathian fold and thrust belt: insights in gravitational salt tectonics. Mar. Pet. Geol. 23, 405–442.
Kruge, M.A., Mastalerz, M., Solecki, A., Stankiewicz, B.A., 1996. Organic geochemistry and petrology of oil source rocks, Carpathian Overthrust region, southeastern Poland: implications for petroleum generation. Org. Geochem. 24, 897–912.
Langford, F.F., Blanc-Valleron, M.M., 1990. Interpreting Rock-Eval pyrolysis data using graphs of pyrolyzable hydrocarbons vs. total organic carbon. Am. Assoc. Pet. Geol. Bull. 74, 799–804.
Lichtschlag, A., Felden, J., Wenzhöfer, F., Schubotz, F., Ertefai, T.F., Boetius, A., de Beer, D., 2010. Methane and sulfide fluxes in permanent anoxia: in situ studies at the Dvurechenskii mud volcano (Sorokin Trough, Black Sea). Geochim. Cosmochim. Acta 74, 5002–5018.
Maţenco, L., Krézsek, C., Merte, S., Schmid, S., Sierd Cloetingh, S., Andriessen, P., 2010. Characteristics of collisional orogens with low topographic build-up: an example from the Carpathians. Terra nova 22, 155–165.
Miclăuş, C., Loiacono, F., Puglisi, D., Baciu, D.S., 2009. Eocene-Oligocene sedimentation in the external areas of the Moldavide basin (marginal folds Nappe, Eastern Carpathians, Romania): sedimentological, paleontological and petrographic approaches. Geol. Carp. 60, 397–417.
Moldowan, J.M., Sudararaman, P., Schoell, M., 1986. Sensitivity of biomarker properties to depositional environments and/or source input in the Lower Toarcian of SW Germany. Org. Geochem. 10, 915–926.
Murgeanu, G., Mirăuţă, O., 1968. Geological Map of Romania. In: Scale, 1. Institutul Geologic al României, Bucureşti, Piatra Neamţ, p. 200, 000, sheet 13.
Otto, A., Simoneit, B.R.T., 2001. Chemosystematics and diagenesis of terpenoids in fossil conifer species and sediment from the Eocene Zeitz formation, Saxony, Germany. Geochim. Cosmochim. Acta 65, 505, 3527.
Otto, A., Simoneit, B.R.T., Rember, W.C., 2005. Conifer and angiosperm biomarkers in clay sediments and fossil plants from the Miocene Clarkia Formation, Idaho, USA. Org. Geochem. 36, 907–922.
Peters, K.E., 1986. Guidelines of evaluating petroleum source rock using programmed pyrolysis. Bull. Am. Assoc. Pet. Geol. 70, 318–329.
Peters, K.E., Moldowan, J.M., 1991. Effects of source, thermal maturity, and biodegradation on the distribution and isomerization of homohopanes in petroleum. Org. Geochem. 17, 47–61.
Peters, K.E., Cassa, M.R., 1994. Applied source rock geochemistry. In: Magoon, L.B., Dow, W.G. (Eds.), The Petroleum System: from Source to Trap, vol. 60. American Association of Petroleum Geologists Memoir, pp. 93–120.
Peters, K.E., Walters, C.C., Moldowan, J.M., 2005. The Biomarker Guide. In: Biomarkers and Isotopes in Petroleum Systems and Earth History, vol. 2. Cambridge University Press, Cambridge.
Polissar, P.J., Savage, H.M., Brodsky, E.E., 2011. Extractable organic material in fault zones as a tool to investigate frictional stress. Earth Planet. Sci. Lett. 311, 439–447.
Popescu, B.M., 1995. Romania's petroleum systems and their remaining potential. Pet. Geosci. 1, 337–350.
Popov, S.V., Rögl, F., Rozanov, A.Y., Steininger, F.F., Shcherba, I.G., Kovač, M., 2004. Lithological-paleogeographic Maps of Paratethys–10 MAPS Late Eocene to Pliocene. Courier Forschungsinstitut Senckenberg 250, Frankfurt, p. 46.
Philp, R.P., 1985. Fossil fuel Biomarkers. Applications and Spectra. Elsevier, Amsterdam, p. 294.
Radke, M., Welte, D.H., 1983. The Methylphenanthrene Index (MPI): a maturity parameter based on aromatic hydrocarbons. In: Bjorøy, M., Albrecht, P., Cornford, C. (Eds.), Advances in Organic Geochemistry, 1981. John Wiley and Sons, New York, pp. 504–512.
Radomski, A., Ślączka, A., 1985. Jawornik marls, a deposit of pelitic turbidity currents. In: Proceeding Reports of the XIII-th Congress of Carpatho–Balkan Geological Association, September 5–10, 1985. Polish Geological Institute, Cracow, Cracow, Poland, pp. 172–175.
Rospondek, M.J., Köster, J., Sinninghe Damsté, J.S., 1997. Novel C26 highly branched isoprenoid thiophenes and alkane from the Menilite Formation, Outer Carpathians, southeast Poland. Org. Geochem. 26, 295–304.
Rögl, F., 1999. Mediterranean and Paratethys. Facts and hypotheses of an Oligocene to Miocene paleogeography (short overview). Geol. Carp. 50, 339–349.
Sachsenhofer, R.F., Stummer, B., Georgiev, G., Dellmour, R., Bechtel, A., Gratzer, R., Ćorić, S., 2009. Depositional environment and hydrocarbon source potential of the Oligocene Ruslar Formation (Kamchia depression; western Black sea). Mar. Pet. Geol. 26, 57–84.
Sachsenhofer, R.F., Hentschke, J., Bechtel, A., Ćorić, S., Gratzer, R., Gross, D., Horsfield, B., Rachetti, A., Soliman, A., 2015. Hydrocarbon potential and depositional environments of Oligo-Miocene rocks in the Eastern Carpathians (Vrancea Nappe, Romania). Mar. Pet. Geol. 68, 269–290.
Săndulescu, M., 1984. Geotectonics of Romania. Editura Tehnică, Bucharest, p. 336.
Schaeffer, P., Adam, P., Trendel, J.M., Albrecht, P., Connan, J., 1995. A novel series of benzohopanes widespread in sediments. Org. Geochem. 23, 87–89.
Seifert, W.K., Moldowan, J.M., 1978. Applications of steranes, terpanes and monoaromatics to the maturation, migration and source of crude oils. Geochim. Cosmochim. Acta 42, 77–95.
Seifert, W.K., Moldowan, J.M., 1980. The effect of thermal stress on source-rock quality as measured by hopane stereochemistry. Phys. Chem. Earth 12, 229–237.
Seifert, W.K., Moldowan, J.M., 1986. Use of biological markers in petroleum exploration. In: Johns, R.B. (Ed.), Methods Geochem. Geophys. 24, 261–290.
Simoneit, B.R.T., 1977. Diterpenoid compounds and other lipids in deep sea sediments and their geochemical significance. Geochim. Cosmochim. Acta 41, 463–476.
Sinninghe Damsté, J.S., Kock-Van Dalen, A.C., de Leeuw, J.W., Schenck, P.A., Guoying, S., Brassell, S.C., 1987. The identification of mono-, di- and trimethyl 2-methyl-2-(4,8,12-trimethyltridecyl)chromans and their occurrence in the geosphere. Geochim. Cosmochim. Acta 51, 2393–2400.
Stefanescu, M., Dicea, O., Butac, A., Ciulavued, D., 2006. The geology and hydrocarbon resources of the Eastern and Southern Carpathians on the territory of Romania. In: Golonka, J., Picha, F.J. (Eds.), The Carpathians and Their Foreland: Geology and Hydrocarbon Resources. American Association of Petroleum Geologists, vol. 84, pp. 521–568. Memoir.
Szczerba, M., Rospondek, M.J., 2010. Controls on distributions of methylphenanthrenes in sedimentary rock extracts: critical evaluation of existing

geochemical data from molecular modelling. Org. Geochem. 41, 1297–1311.
Ślączka, A., Kruglow, S., Golonka, J., Oszczypko, N., Popadyuk, I., 2006. The general geology of the Outer Carpathians, Poland, Slovakia and Ukraine. In: Golonka, J., Picha, F.J. (Eds.), The Carpathians and Their Foreland: Geology and Hydrocarbon Resources. American Association of Petroleum Geologists, vol. 84, pp. 221–258. Memoir.
ten Haven, L.H., de Leeuw, J.W., Rullkötter, J., Sinninghe Damsté, J.S., 1987. Restricted utility of the pristane/phytane ratio as a palaeoenvironmental indicator. Nature 330, 641–643.
ten Haven, H.L., Lafargue, E., Kotarba, M., 1993. Oil/oil and oil/source rock correlations in the Carpathian Foredeep and overthrust, south-east Poland. Org. Geochem. 20, 935–959.
Tissot, B.P., Welte, D.H., 1984. Petroleum Formation and Occurrence. Springer-Verlag, p. 699. Berlin, Heidelberg.
Tulloch, A.P., 1976. Chemistry of waxes of higher plants. In: Kolattukudy, P.E. (Ed.), Chemistry and Biochemistry of Natural Waxes. Elsevier, Amsterdam, pp. 235–289.
Uhlig, V., 1907. Über die Tektonik der Karpathen. Sitzungsberichte der Kaiserlichen Academie der Wissenschaften, Mathematisch-Naturwissenschaftliche Klasse, vol. 116, pp. 871–981. Wien.
Volkman, J.K., 1986. A review of sterols of marine and terrigenous organic matter. Org. Geochem. 9, 83–99.
Volkman, J.K., Maxwell, J.R., 1986. Acyclic isoprenoids as biological markers. In: Johns, R.B. (Ed.), Biological Markers in the Sedimentary Record. Elsevier, Amsterdam, p. 42.
van Aarssen, B.G.K., Alexander, R., Kagi, R.I., 2000. Higher plant biomarkers reflect palaeovegetation changes during Jurassic times. Geochim. Cosmochim. Acta 64, 1417–1424.
Wendorff, M., Marynowski, L., Rospondek, M., 2016a. Pyrite framboid diameter distribution in the Lower Oligocene black shales of the Vrancea Nappe as an indicator of changes in redox conditions, Eastern Outer Carpathians, Romania. In: Geophysical Research Abstracts 18, EGU General Assembly, April 17–22, 2016 (Vienna, Austria).
Wendorff, M., Rospondek, M., Marynowski, L., 2016b. The Oligocene black shales depositional environment revealed by pyrite framboid diameter distribution and biomarkers, Tarcău Nappe, Eastern Outer Carpathians, Romania. In: Abstracts of AAPG European Region Annual Conference, May 19–20, 2016 (Bucharest, Romania).

Supporting materials

Age		Tarcău Nappe Tărcuţa Creek Section	Sample no	Vrancea Nappe Nechit River Section	Sample no
MIOCENE	Aquitanian	Vinetişu Fm. (<230 m)		Gura Şoimului Fm.	
		Upper Dysodilic Shale Mb. & Fusaru Fm. (~500 m)		Upper Dysodilic Shale Mb. (~100-110 m)	
OLIGOCENE	Chattian	Lower Dysodilic Shale Mb. (~250 m) ? Jasło Limestone		Lower Dysodilic Shale Mb. & Kliwa Sandst. Fm. (~110-120 m)	
	Rupelian	Bituminous Marl Mb.* (~20-25 m)	TAR 17-22	Bituminous Marl Mb.* (~20-50 m)	NECH 100-103 NECH 212
		Lower Menilite Mb.* (~70-80 m) Tylawa Limestone	TAR 11-16 TAR 10 TAR 1-9	Lower Menilite Mb.* (~20-30 m)	NECH 200-211 NECH 0-25
		Ardeluţa Mb. (~40 m)			
		Podu Secu Mb. (~130 m)		Globigerina Marl Mb. (~20 m) Bisericani Fm. (~140 m)	
EOCENE	Priabonian	Tarcău Sandst. Fm. (>50 m)			

Figure 1S. Lithostratigraphic nomenclature, thickness and sample position in the Tarcău and Vrancea Nappe successions (compilation after Belayouni et al., 2009; Miclăuş et al., 2009; Guerrera et al., 2012; Sachsenhofer et al., 2015). * - the stratigraphic position of the rock units as recently revised by Sachsenhofer et al. (2015).

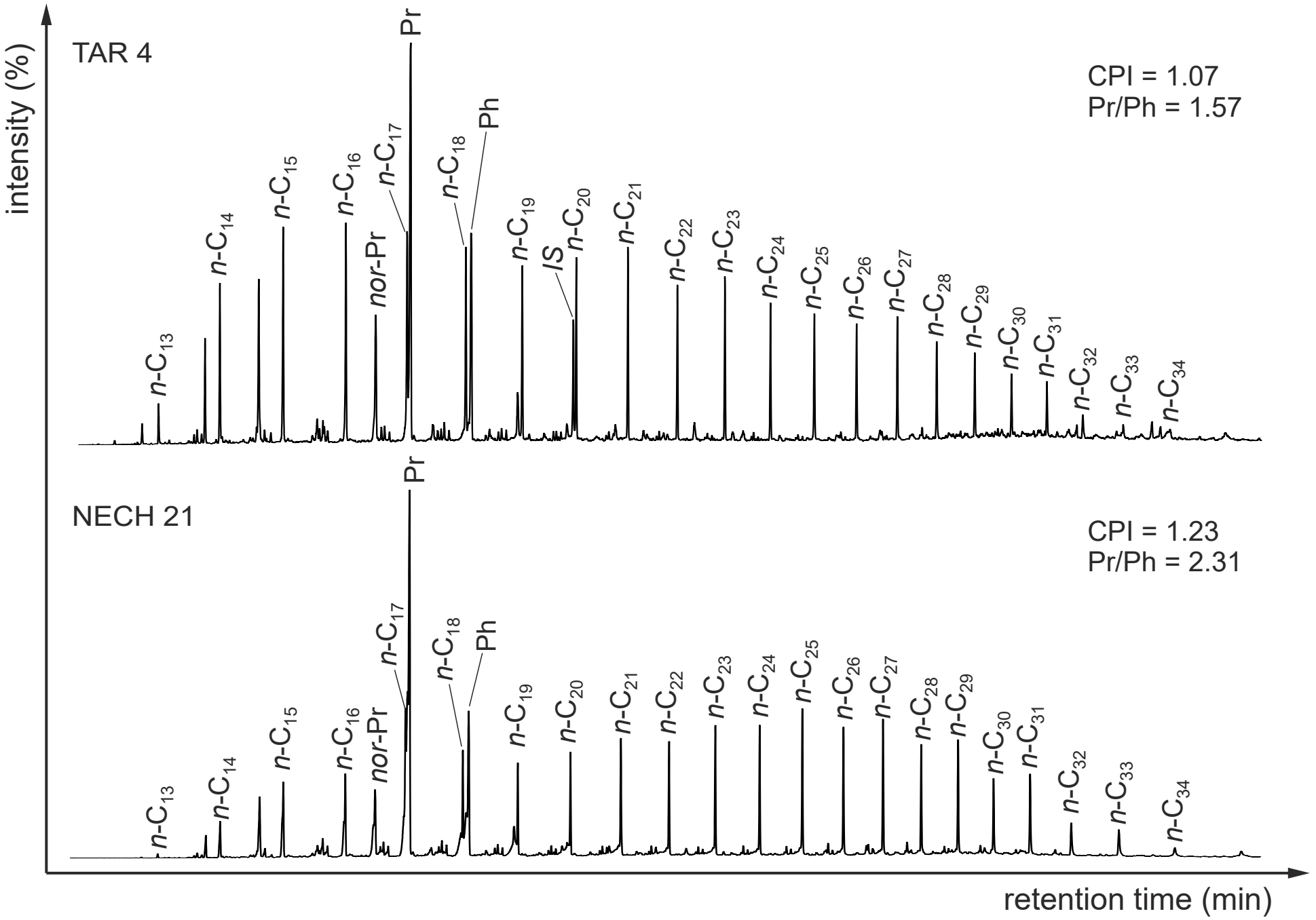

Figure 2S. Distribution of *n*-alkanes and acyclic isoprenoids in the Tarcău (TAR 4) and Vrancea (NECH 21) Nappes (*m/z* 71 mass chromatograms, column HP-5 MS). nor-Pr – *nor*-pristane, Pr – pristane, Ph – phytane, IS – internal standard (*n*-eicos-1-ene).

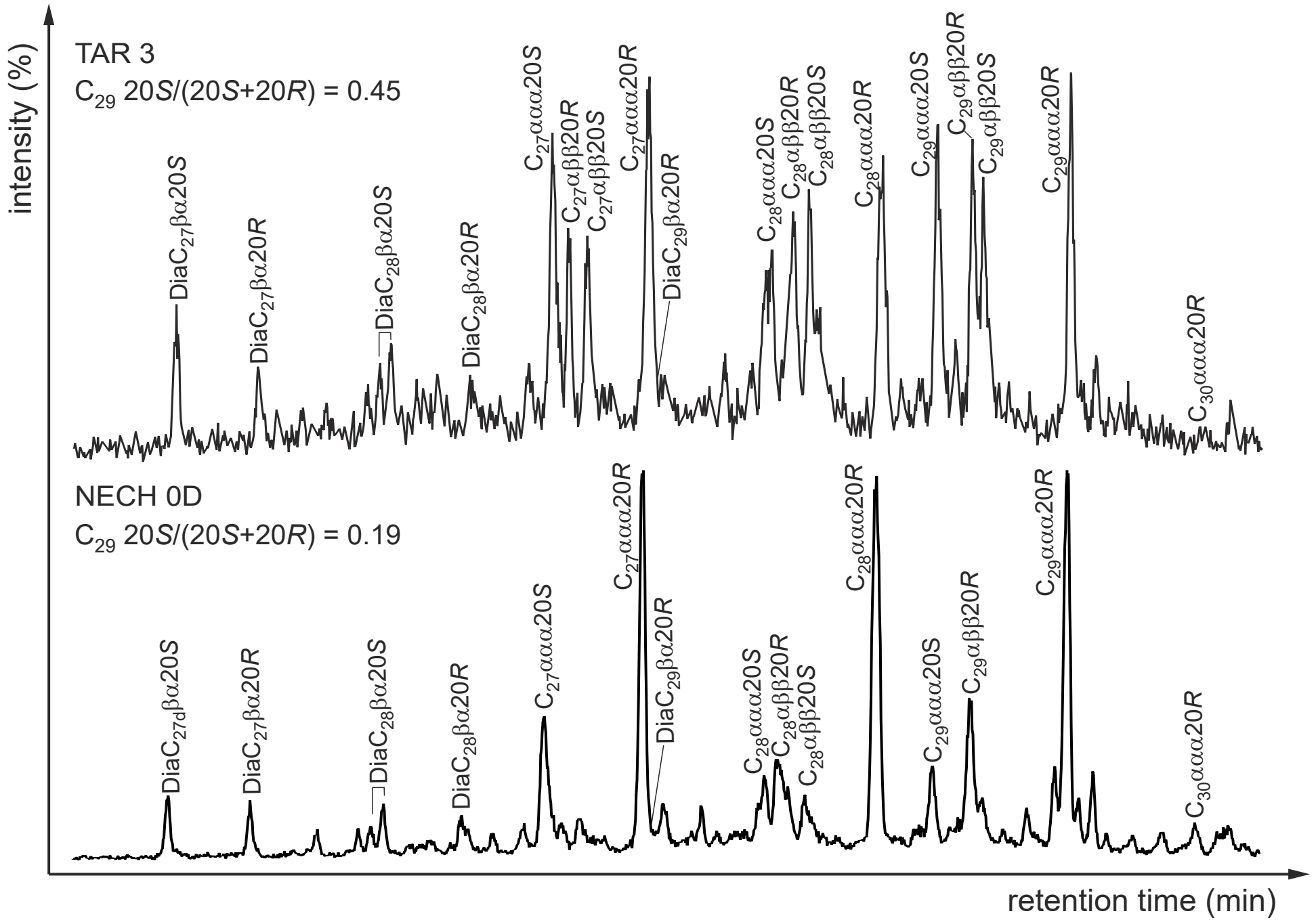

Figure 3S. Variation in the distribution of steranes for representative samples from the Tarcău (TAR 3) and Vrancea (NECH 0D) Nappes (*m/z* 217 mass chromatograms, column HP-5 MS). Note higher concentrations of thermally more stable αββ isomers in the Tarcău Nappe sample.

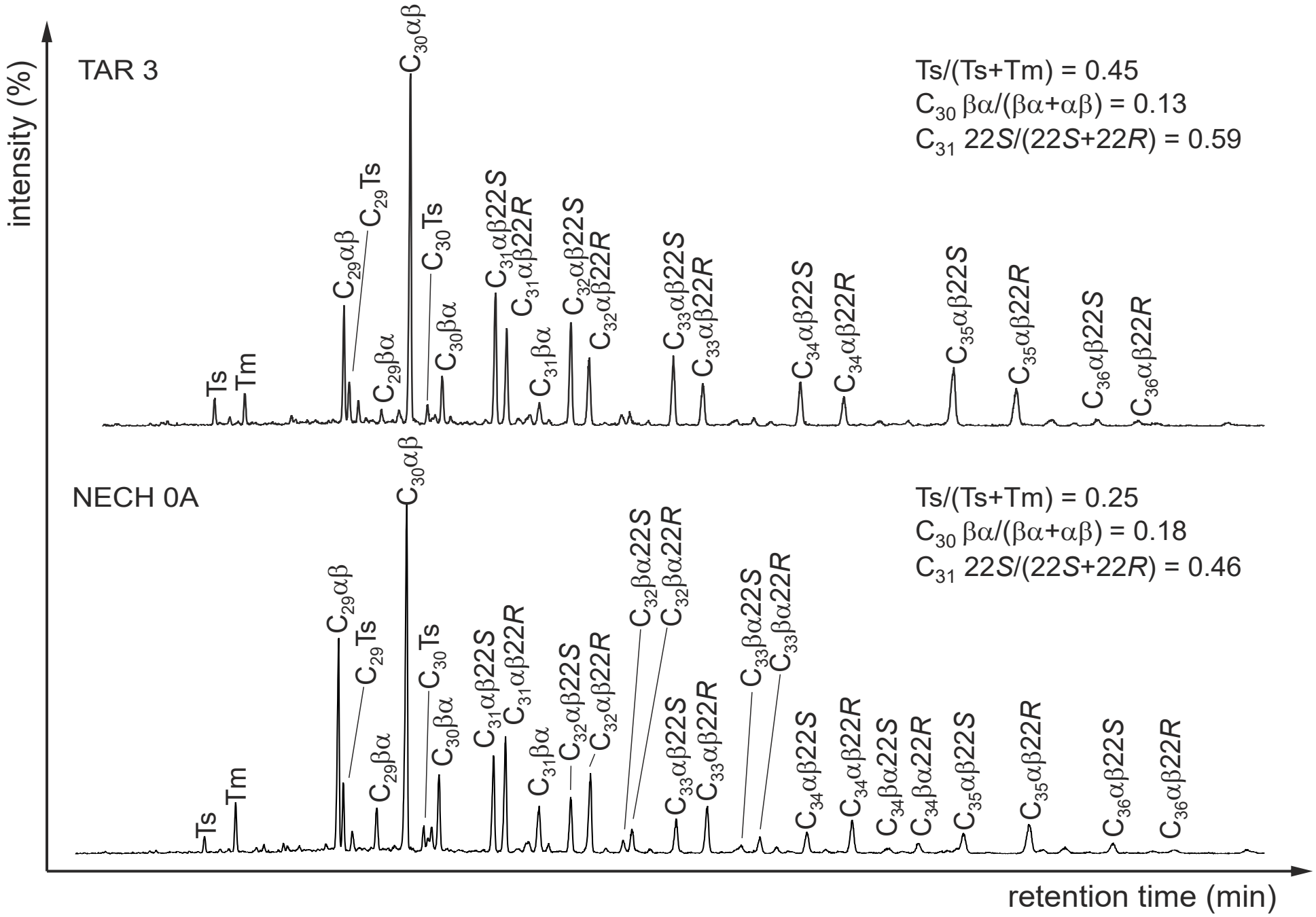

Figure 4S. Distribution of hopanoids for representative samples from the Tarcău (TAR 3) and Vrancea (NECH 0A) Nappes (*m/z* 191 mass chromatograms, column HP-5 MS). Note higher concentrations of thermally more stable *S* epimers in the Tarcău Nappe sample.

Publikacja 2

Wendorff-Belon, M., Rospondek, M., Marynowski, L., 2021. Early Oligocene environment of the central Paratethys revealed by biomarkers and pyrite framboids from the Tarcău and Vrancea nappes (Eastern Outer Carpathians, Romania). Marine and Petroleum Geology 128, 105037.

Marine and Petroleum Geology 128 (2021) 105037

Contents lists available at ScienceDirect

Marine and Petroleum Geology

journal homepage: www.elsevier.com/locate/marpetgeo

Early Oligocene environment of the Central Paratethys revealed by biomarkers and pyrite framboids from the Tarcău and Vrancea Nappes (Eastern Outer Carpathians, Romania)

Małgorzata Wendorff-Belon [a,*], Mariusz Rospondek [a], Leszek Marynowski [b]

[a] Institute of Geological Sciences, Jagiellonian University, ul. Gronostajowa 3a, 30-387, Kraków, Poland
[b] Faculty of Natural Sciences, University of Silesia, ul. Będzińska 60, 41-200, Sosnowiec, Poland

ARTICLE INFO

Keywords:
Early oligocene
Central paratethys
Menilite facies
Biomarkers
Pyrite framboids
Paleoenvironmental conditions
Euxinia

ABSTRACT

The Menilite facies, representing the most prolific hydrocarbon source rocks in the Carpathian fold and thrust belt, has been studied in two outcrop sections of the Vrancea and Tarcău Nappes (Eastern Romania) with the aim of determining the depositional environment during the Early Oligocene in the Vrancea and Tarcău sub-basins of the Central Paratethys. The biomarker composition indicates spatial variability in organic matter sources with mainly algal (particularly diatoms and dinoflagellates) and bacterial contributions in both sub-basins. This is reflected by the occurrence of such biomarkers as triaromatic dinosteroids, C_{25} highly branched isoprenoid thiophenes, marine *n*-alkanes, hopanoids and monomethyl alkanes. Solely in the Vrancea domain, the input of terrigenous organic matter of higher plant origin can be anticipated from the presence of abietane-class biomarkers (conifer-derived) and oleanane (angiosperm-derived). Distinct nutrient availability related to different positions of individual sub-basins (i.e. shallower, temporarily eutrophic Vrancea sub-basin vs. open-marine mesotrophic Tarcău domain) is reflected by different paleoproductivity indicators, such as the total organic carbon content, hydrogen index and 17α-hopanes to steranes ratio.

Water column stratification with bottom water anoxia enhanced by bacterial sulfate reduction stretching into the chemocline, at least intermittently, is expressed by a characteristic tiny pyrite framboid distribution and the lack of bioturbation. However, molecular indicators (Pr/Ph ratio, C_{35} homohopane index) imply fluctuations of redox conditions with the dominance of dysoxic conditions, which may suggest the occasional oxidation of bottom waters linked to local upwelling. Early diagenetic organic matter transformations such as photodegradation taking place in the oxidised upper part of the water column could also have affected the biomarker distributions. The presence of aryl isoprenoids and Me,*i*-Bu-maleimides indicates periods of euxinic conditions within the photic zone only in the Vrancea sub-basin during the deposition of the Lower Menilite Member. This is probably related to freshwater incursions from the adjacent, at least partly emerged forebulge, as suggested by a high MTTC ratio and the occurrence of higher plant-derived organic matter.

1. Introduction

Rock formations rich in organic matter (OM) deposited in ancient marine settings are of great interest due to their importance as potential hydrocarbon source rocks and their crucial role in understanding the processes of organic carbon transformation in biogeochemical cycles. Such important source rocks of large hydrocarbon deposits in the Outer Carpathians and around the Black Sea and Caspian Sea regions formed during the Oligocene/Early Miocene in the Paratethys basin (e.g. Sachsenhofer et al., 2018). This isolated, intracontinental marine realm stretched from the Rhône Basin and Alpine Foreland Basin in the west, to the present-day Caspian Sea and Kura Basin in the east (Fig. 1) (Laskarev, 1924; Popov, 2004). The birth of the Paratethys started around the Eocene/Oligocene boundary (33.9 Ma; Cohen et al., 2013) as a result of the collision of the Eurasian platform and the Alpine tectonic domain (Báldi, 1980). Contemporaneous climate cooling (e.g. Zachos et al., 1996; Galeotti et al., 2016) and the separation of the Paratethys from the Mediterranean and Indo-Pacific realms led to the formation of organic-rich sediments (Popov and Stolyarov, 1996; Schulz et al., 2005). These are represented by the Oligocene Menilite Formation occurring in

* Corresponding author
E-mail address: malgorzata.wendorff@uj.edu.pl (M. Wendorff-Belon).

https://doi.org/10.1016/j.marpetgeo.2021.105037
Received 30 September 2020; Received in revised form 2 February 2021; Accepted 6 March 2021
Available online 17 March 2021

large areas of the Western and Central Paratethys (Fig. 1). In the Eastern Paratethys, equivalent facies are called Maikop Formation and their deposition continued until the Lower Miocene (Bechtel et al., 2013, 2014; Sachsenhofer et al., 2018). The most prolific source rocks accumulated in the Central Paratethys, the present-day Outer Carpathians of Poland, Ukraine and Romania, where the Lower Oligocene part of the Menilite Formation could generate up to 10 t HC/m^2 (Kosakowski, 2013; Sachsenhofer et al., 2018), and locally in the Ukrainian Carpathians up to 15 t HC/m^2 (Rauball et al., 2019). Due to the high petroleum potential of these rocks, they have been intensively studied over the last three decades, especially in the fields of petroleum geology, geochemistry, sedimentology and tectonics (e.g. Koltun, 1992; ten Haven et al., 1993; Lafargue et al., 1994; Kruge et al., 1996; Bessereau et al., 1997; Rospondek et al., 1997; Köster et al., 1998a,b; Kotarba et al., 2007; Miclăuş et al., 2009; Guerrera et al., 2012; Sachsenhofer et al., 2015; Kosakowski et al., 2018; Filipek et al., 2020). These works have demonstrated the strong facial and geochemical heterogeneity of the Menilite rocks, and therefore the complexity of their formation history and related hydrocarbon systems.

The aim of this study is to shed new light on the depositional environment of the Menilite facies of the Central Paratethys using biomarkers combined with pyrite framboid distribution analysis. The research is focused on the environmental changes and sources of OM imprinted in biomarker records from the representative Early Oligocene cross-sections of the Tarcău and Vrancea Nappes in the Eastern Carpathians, Eastern Romania. Previous work by Wendorff et al. (2017), which described the OM maturity and source rock potential of the samples discussed therein, was based on bulk geochemical analysis and preliminary biomarker study. The total organic carbon (TOC) data, hydrogen index (HI) values and selected biomarker indices (pristane/-phytane ratio) were complemented in this study by additional biomarker signatures of past redox, organic productivity and salinity conditions, as well as by pyrite framboid analysis, to obtain a more comprehensive understanding of the Early Oligocene paleoenvironment in the Central Paratethys sub-basins.

To date, organic geochemical studies of the Menilite rocks have concentrated on the Polish and Ukrainian Carpathians, while those in Romania concerned bulk geochemistry (Belayouni et al., 2009; Amadori et al., 2012; Sachsenhofer et al., 2015) and palynofacies analysis (Filipek, 2020). Biomarker analyses were limited to the Oligocene/Early Miocene rocks from the Vrancea Nappe (Sachsenhofer et al., 2015).

2. Geological background

The study area is located within the Romanian Outer Carpathians, representing the eastern segment of the Carpathian fold belt, a large orogenic belt joining the Alps to the west and the Balkanides and Rhodopes to the south. The Carpathians were formed as a result of collision between the African–Arabic and European plates, and the subsequent gradual closure of the Tethys–Paratethys Ocean during the Cretaceous and Miocene convergence events (e.g. Săndulescu, 1984; Froitzheim et al., 2008). The Carpathians are subdivided into two main domains, namely the Inner and Outer Carpathians deformed and thrusted during the Late Jurassic–Late Cretaceous, and the Paleogene–Neogene, respectively (Golonka et al., 2006, and references therein). In Romania, the Inner and Outer Carpathians are known as the Dacides and Moldavides, respectively (Săndulescu, 1988). The Moldavides correspond to a major part of the Eastern Outer Carpathians or to the East Carpathian Flysch Zone. They comprise north-west to south-east oriented and north-east facing allochthonous tectonostratigraphic units (nappes), that are progressively overthrusted over the Neogene Foredeep and underlying platforms (Moldavian, Scythian and Moesian). From west to east, the following nappes are distinguished: Teleajen, Macla, Audia (Internal Moldavides), Tarcău, Vrancea (or Marginal Folds) and the Subcarpathian (or Pericarpathian) Nappes (External Moldavides) (Săndulescu, 1984, 1988). The Tarcău and Vrancea Nappes consist of the Cretaceous to Early Miocene successions of siliciclastic and carbonate turbidites, including pelagic intervals. Their Early Oligocene

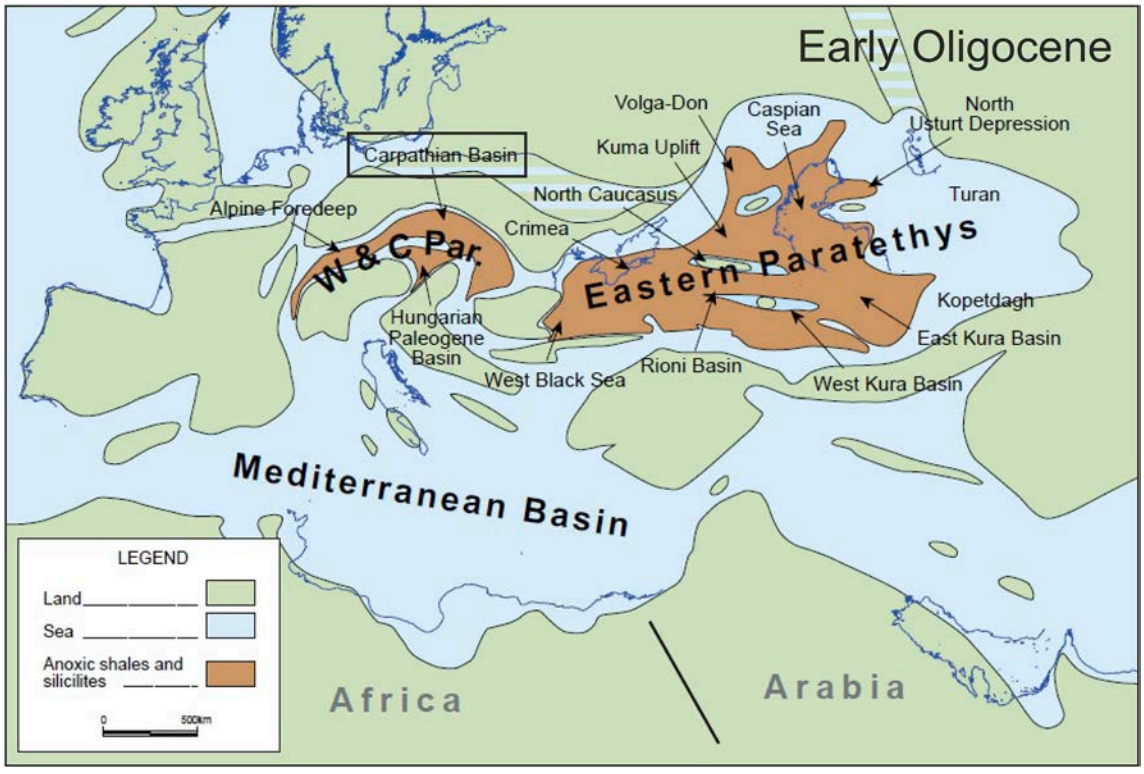

Fig. 1. Paleogeographic map of the Paratethys realm in the Early Oligocene (after Sachsenhofer et al., 2018) with the distribution of organic-rich facies (after Popov, 2004). W & C Par. – Western and Central Paratethys.

deposits comprise the Lower Rupelian sandy turbidites and the Upper Rupelian organic-rich shales of the Lower Menilite Member (Mb.) (NP21-22 zone), and overlying OM-rich marls called the Bituminous Marls Mb. (NP22-23 zone) (in the text, collectively referred to as the Menilite facies). The Late Oligocene (Chattian) sequence consists of coarse-grained sandstones deposited in shelf (Kliwa) and deep-marine (Fusaru and partly Kliwa) settings associated with OM-rich shales of the Lower Dysodilic Shale Mb. Pelagic/hemipelagic deposits that continue up to the Early Miocene (Aquitanian) are represented by the Upper Dysodilic Shale Mb. Unfortunately, the precise age of the Menilite facies remains inconclusive (e.g. Melinte-Dobrinescu and Bustur, 2008; Amadori et al., 2012; Guerrera et al., 2012; Sachsenhofer et al., 2015).

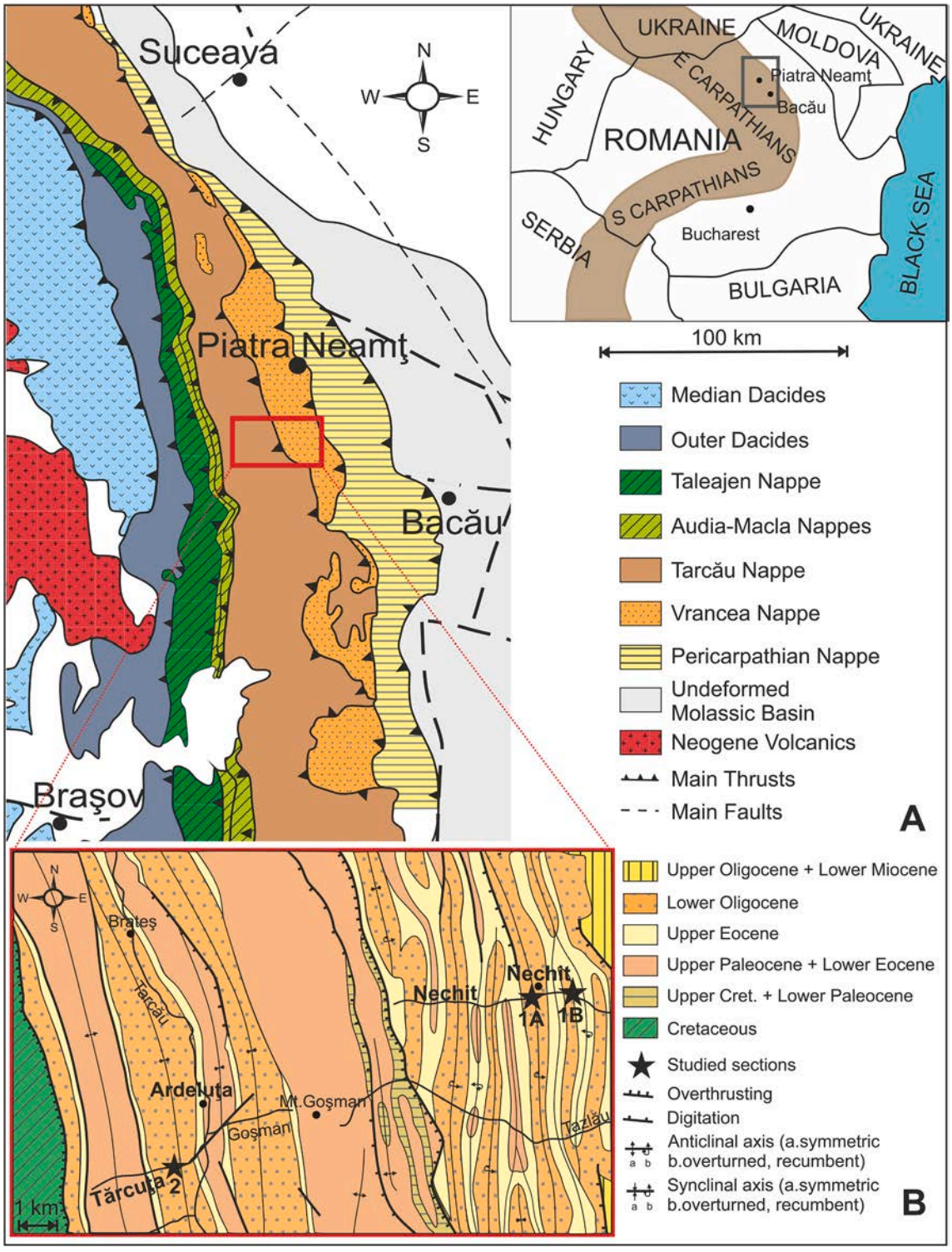

Fig. 2. (A) Geological map of the Eastern Outer Carpathians (after Bădescu, 2005; modified), with the location of study area marked as a red rectangle. (B) Detailed geological map (after Murgeanu and Mirăută, 1968; simplified) of the study area with sampled sites marked as asterisks: 1A and 1B: Nechit sub-sections in the Vrancea Nappe, 2: Tărcuţa section in the Tarcău Nappe. (For interpretation of the references to colour in this figure legend, the reader is referred to the Web version of this article.)

The most recent works are in favour of shifting the age of the Lower Menilite and Bituminous Marls Mbs towards the late Rupelian, or even placing the boundary between the Rupelian and Chattian within these units (Amadori et al., 2012; Guerrera et al., 2012). Taking into consideration the fact that the Bituminous Marls Mb. can be a time equivalent of the Dynow Formation from the Alpine Foreland Basin (Schulz et al., 2002) and the Polish Carpathians (e.g. Miclăuş and Schieber, 2014), this member can be dated as late Rupelian (i.e. for the NP23 zone).

During the Oligocene, the turbiditic deposits of the External Moldavides were accumulated in the Carpathian foredeep (foreland) basin (*sensu* DeCelles and Giles, 1996) (Fig. 1). This basin was internally divided into narrow, parallel sub-basins, from which the Vrancea and Tarcău units developed. Based on the long history of provenance studies (e.g. Zuber, 1902; Grasu et al., 1988; 2002; Oaie et al., 2005), it has been assumed that the siliciclastics were supplied from two main opposite sources. In the east and south, an external (cratonic) area (i.e. the East European/Moesian foreland) supplied coarse material represented by so called "green schists" clasts of the Central Dobrogea type and quartzose sand, permanently identified in the Cretaceous to Late Miocene rocks of the External Moldavides. In the west, an internal (orogenic) alimentation area consisted of the already-stacked units of the Median and Outer Dacides forming the Cretaceous Carpathian accretionary prism (Săndulescu and Micu, 1989). It was probably partially submerged in the northern part of the basin, and therefore connected with the Transylvanian Basin (Krézsek and Bally, 2006). This concept is supported by the paleo-flow directions in the Oligocene turbidites of the Transylvanian Basin. Overall, these indicate a western to south-western provenance with no evidence of sources from the accretionary prism or its backstop in the east (Krézsek and Bally, 2006).

3. Materials and methods

3.1. Samples

Forty samples, displaying high organic carbon content within the total set of sixty-five samples, were selected and analysed for the purpose of this research. The samples, representing the Early Oligocene rocks of the Lower Menilite and Bituminous Marls Mbs were collected during several field excursions between 2013 and 2016 in the Piatra Neamţ area, Eastern Romania, from two sections localised at a distance of ~15 km from each other. The first one is situated in the Nechit area (referred to below as the Nechit section; abbreviation = NECH) of the Vrancea Nappe, and the second one in the Ardeluta area (referred to below as the Tărcuţa section; abbreviation = TAR) of the Tarcău Nappe (Fig. 2).

The Nechit section cropping out along the Nechit River consists of two sub-sections (Fig. 3A and B) localised on the western (Fig. 2B, location 1A) and eastern (Fig. 2B, location 1B) limb of the anticline, with Eocene greenish pelites of the Bisericani Beds and whitish Globigerina Marls in the core. The first sub-section (46°46′13.10"N and 26°24′07.20"E) starts with the Lower Menilite Mb. represented by black shales and greenish pelites (NECH 8–25), and 200 m below continues with finely laminated cherts and siliceous shales (NECH 0–7) alternating with quartz-rich sandstones. The overlaying rocks of the Bituminous Marls Mb. are mainly bituminous marls (NECH 100–103) and grey shales associated with cross-laminated sandstone layers. The samples of the second sub-section (46°46′16.67"N and 26°25′22.47"E) represent cherts and siliceous shales (NECH 199–211) of the Lower Menilite Mb., as well as bluish-grey bedded limestone (NECH 212) of the Bituminous Marls Mb. The lithology of the investigated sections is displayed in Fig. 3. More comprehensive sedimentological and lithofacial characteristic of the Nechit section is provided by Miclăuş et al. (2009) and Filipek (2020).

The samples from the Tărcuţa section (Fig. 3C) were collected along the Tărcuţa Creek (Fig. 2B) and represent silicified black shales, black cherts and subordinately grey shales (TAR 1–15) of the Lower Menilite Mb. Several horizons (at least seven) of the coccolithic, laminated limestone (TAR 10), presumably the Tylawa Limestone, were discerned within distal turbidites of the Lower Menilite Mb. (46°42′39.80"N and 26°11′43.60"E). These characteristic rocks are widely recognised in the Outer Carpathians as the Early Oligocene marker bed (e.g. Haczewski, 1989; Stefănescu et al., 1993; Melinte, 1995; Rusu et al., 1996). The overlaying samples of the Bituminous Marls Mb. are mainly grey shales and bituminous marls (TAR 17–22), and quartzarenites. The biostratigraphy and sedimentology of the Tărcuţa succession were presented by Belayouni et al. (2009) and Guerrera et al. (2012).

3.2. Methods

3.2.1. Extraction, separation and derivatisation

The extraction and fractionation of forty pulverised rock samples (~100 g) comprised the following main steps: Soxhlet extraction in pre-extracted cellulose thimbles with dichloromethane (DCM)/methanol (7.5 : 1 vol) for 48 h, asphaltene precipitation from *n*-hexane/DCM solution (80 : 1 vol), fractionation of an aliquot of the obtained maltenes (~50–100 mg) using a column packed with activated Al_2O_3 (at 150 °C for 2 h) into apolar, aromatic and polar fractions using three bed volumes of *n*-hexane, *n*-hexane/DCM (7 : 3 vol) and DCM/methanol (1 : 1 vol), respectively. Prior to chromatography, internal standards including eicos-1-ene (140 μg), hexadecylthiophene (27.9 μg), hexamethylbenzene (40.2 μg) and 2-phenylindene (39.8 μg) were added to maltenes.

The polar fractions were derivatised with MTBSTFA (*N-tert*-butyldimethylsilyl-*N*-methyl trifluoroacetamide) to obtain tertiary-butyldimethylsilyl maleimide derivatives. Samples were derivatised with reagents dissolved in super-dehydrated DCM and heated at 50 °C for 1 h prior to gas chromatography-mass spectrometry (GC-MS) analysis (Grice et al., 1997).

3.2.2. Gas chromatography-mass spectrometry

GC–MS analyses of all the fractions were carried out on an Agilent 7890A chromatograph equipped with an EPC Cool On-Column Inlet and Agilent 5975C Network mass spectrometer with Triple-Axis Detector at the Faculty of Natural Sciences, Sosnowiec, Poland. Separation was achieved on an HP-5 MS fused silica capillary column (60 m × 0.32 mm, 0.25 μm film thickness) with helium used as the carrier gas at a constant flow of 2.6 ml/min. The GC oven temperature program was set as follows: 40 °C constant for 3 min, 20 °C/min from 40 to 120 °C and 3 °C/min from 120 to 300 °C, followed by an isothermal period of 60 min. The GC column outlet was coupled directly to the ion source of the mass selective detector (MSD). The MS was operated in the electron impact mode with an ionisation energy of 70 eV. An ion source temperature was set at 200 °C and a cycle time of 1 s in the scan range of m/z 50–700. The Wiley Registry of Mass Spectral Data (9th ed.) and an Agilent Technologies MSD ChemStation E.02.01.1177 software, together with published data were used for MS data comparison. Absolute and relative concentrations of individual compounds and compound groups were obtained using peak areas in the total ion current chromatograms in relation to those of internal standards or by the integration of peak areas in appropriate mass chromatograms.

3.2.3. Pyrite framboid diameter analysis

Twenty samples (ten from each section) were used for the pyrite framboid diameter analysis. Pyrite diameters were measured on polished block samples using field emission scanning electron microscopy (FE-SEM; Hitachi S-4700 microscope) in a back-scattered electron (BSE) mode at the Institute of Geological Sciences of the Jagiellonian University, Krakow, Poland. At least 100 pyrite specimens were measured in a given sample. Such statistical parameters as minimum, maximum and mean values, as well as the standard deviation were calculated and presented in Table 2, and as box-and-whisker plots (after Wignall and Newton, 1998) in Fig. 3.

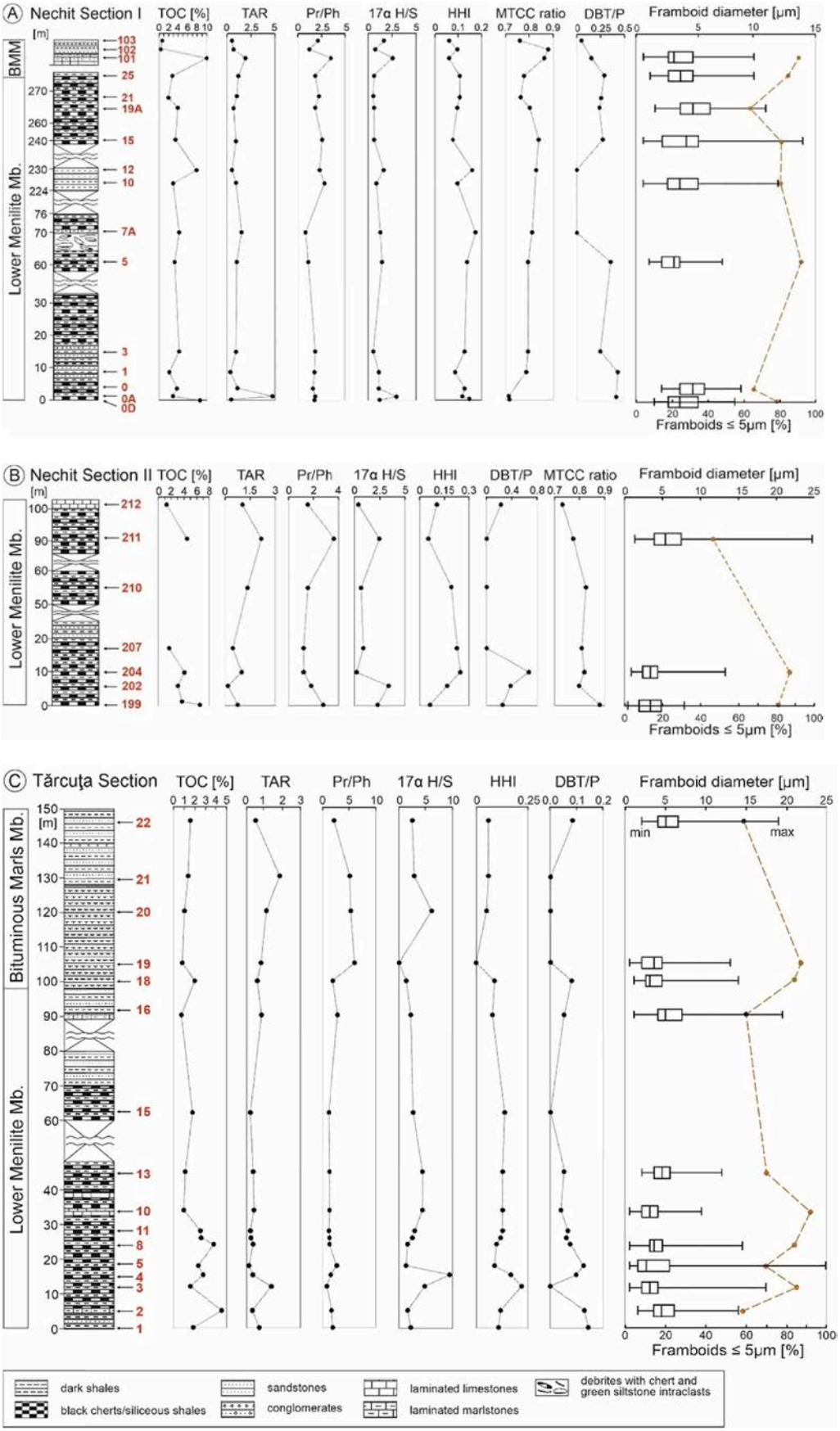

Fig. 3. Lithostratigraphic columns with sample positions and stratigraphic variation of selected biomarker indices and pyrite framboid size distribution statistic data. (A) Nechit Section I, (B) Nechit Section II, (C) Tărcuța section. Percentage of framboids ≤5 µm is represented by a dashed line. Each box extends from the 25th to the 75th percentile, with median values shown as a vertical line, and minimum and maximum values as a horizontal line. TOC and Pr/Ph data adapted from Wendorff et al. (2017). Biomarker parameter abbreviations described in Table 1.

Table 1
Bulk organic data, biomarker parameters and selected biomarker concentrations for the Lower Oligocene samples from the Nechit and Tărcuţa sections. TOC – total organic carbon (wt%); HI – hydrogen index (mg HC/g TOC); TAR – terrigenous vs aquatic *n*-alkanes ratio ($(C_{27}+C_{29}+C_{31})/(C_{15}+C_{17}+C_{19})$); CPI_{25-31} – Carbon Preference Index $(1/2([(C_{25}+C_{27}+C_{29})/(C_{26}+C_{28}+C_{30})]/[(C_{27}+C_{29}+C_{31})]/[(C_{26}+C_{28}+C_{30})])$; Pr/Ph – pristane/phytane ratio; 17α H/S – 17α hopanes to steranes ratio (the sum of 17α C_{29} to C_{33} (22S + R) hopanes versus the sum of regular C_{27} to C_{29} ααα (20S + R) + αββ (20S + R) steranes); C_{35} HHI – C_{35} homohopane index (17α (22S + R) C_{35} homohopane versus the sum of 17α (22S + R) C_{31}-C_{35} homohopanes); MTTC – ratio of trimethylated 2-methyl-2-(trimethyltridecyl)chroman versus the sum of mono, di- and trimethylated 2-methyl-2-(trimethyltrdecyl)chromans; DBT/P – dibenzothiophene/phenanthrene ratio; ∑ Abiet. – concentration of summed abietane derivatives (simonellite, retene and tetrahydroretene) (μg/g TOC); C_{25} HBIT – concentration of C_{25} highly branched isoprenoid thiophene (μg/g TOC); n.d. – not determined. TOC, HI and Pr/Ph data adapted from Wendorff et al. (2017).

Sample	TOC [wt %]	HI [mg HC/g TOC]	TAR	CPI_{25-31}	Pr/Ph	17αH/S	C_{35} HHI	MTTC ratio	DBT/P	∑ Abiet. [μg/g TOC]	C_{25} HBIT [μg/g TOC]
Nechit Section											
Bituminous Marls Mb.											
NECH 103/marly shale	0.78	n.d.	0.43	1.16	2.16	1.74	0.06	0.76	0.07	0.94	0.09
NECH 102/marly shale	0.57	329	0.65	0.78	1.24	0.81	0.10	0.88	n.d.	n.d.	0.44
NECH 101/laminated marl	10.82	n.d.	1.86	1.34	3.55	2.62	0.06	0.87	0.17	27.90	0.28
Lower Menilite Mb.											
NECH 212/limestone (calciturbidite)	1.31	n.d.	1.09	0.45	1.56	0.46	0.11	0.73	0.23	n.d.	n.d.
NECH 211/black siliceous shale	4.54	n.d.	2.18	1.39	3.60	2.51	0.06	0.78	n.d.	27.34	2.10
NECH 210/black siliceous shale	n.d.	n.d.	1.39	1.15	1.61	0.88	0.19	0.84	n.d.	23.76	3.30
NECH 207/black chert	1.73	n.d.	0.49	1.19	1.24	0.97	0.23	0.81	n.d.	1.45	0.58
NECH 204/black siliceous shale	4.15	400	1.02	1.13	1.20	0.26	0.25	0.82	0.39	2.86	0.37
NECH 202/black siliceous shale	3.09	n.d.	0.22	1.14	1.84	3.42	0.17	0.80	0.69	2.67	0.08
NECH 199/black shale	6.54	n.d.	0.77	1.18	2.72	2.30	0.07	0.88	0.26	5.81	0.23
NECH 25/black shale	2.86	247	1.15	1.06	1.89	0.59	0.11	0.78	0.29	9.16	0.36
NECH 21/black marly shale	2.12	275	0.96	1.30	2.31	0.55	0.11	0.76	0.26	8.20	0.30
NECH 19A/black shale	4.01	261	0.66	1.16	1.85	0.58	0.10	0.80	0.25	13.20	0.33
NECH 15/black shale	3.47	333	0.85	1.30	2.63	0.64	0.08	0.84	0.28	6.52	0.57
NECH 12/black siliceous shale	7.90	469	0.47	1.21	2.45	1.63	n.d.	0.83	0.35	15.30	0.27
NECH 10/black marly shale	3.02	411	0.85	1.12	2.86	0.89	0.10	n.d.	n.d.	2.92	0.40
NECH 7A/black shale	3.93	396	1.49	1.03	0.76	1.23	0.17	0.78	n.d.	1.13	0.40
NECH 5/black siliceous shale	3.22	401	0.96	1.13	1.17	1.42	0.14	0.80	0.36	5.13	0.69
NECH 3/black marly shale	4.02	n.d.	0.87	1.32	1.90	0.51	0.13	0.80	0.25	6.13	0.12
NECH 1/black marly shale	2.10	405	0.30	1.20	1.80	1.09	0.09	0.79	0.44	6.53	0.26
NECH 0/black shale	3.70	581	1.01	1.56	1.67	1.13	0.13	n.d.	n.d.	0.32	0.27
NECH 0A/black siliceous shale	n.d.	n.d.	4.73	0.94	1.90	2.96	0.12	0.72	n.d.	13.95	0.28
NECH 0D/black chert	8.62	522	0.33	0.98	1.80	1.18	0.15	0.72	0.42	9.90	0.71
Tărcuţa Section											
Bituminous Marls Mb.											
TAR 22/black shale	1.63	n.d.	0.53	1.02	2.32	2.64	0.06	n.d.	0.09	n.d.	n.d.
TAR 21/black shale	1.41	265	1.92	1.17	5.29	3.03	0.06	n.d.	0.09	n.d.	n.d.
TAR 20/marly grey shale	1.04	247	1.12	1.27	5.88	6.60	0.04	n.d.	0.05	n.d.	n.d.
TAR 19/black shale	0.85	30	0.80	1.21	6.18	n.d.	n.d.	n.d.	n.d.	n.d.	n.d.
TAR 18/marly grey shale	2.00	n.d.	0.62	0.98	2.03	1.75	0.09	n.d.	0.08	n.d.	n.d.
TAR 16/marly grey shale	0.80	165	0.85	1.13	2.95	2.30	0.08	n.d.	0.05	n.d.	n.d.
Lower Menilite Mb.											
TAR 15/black siliceous shale	1.81	422	0.21	1.04	1.22	2.80	0.14	n.d.	n.d.	n.d.	n.d.
TAR 13/marly shale	1.16	n.d.	0.38	1.06	1.33	4.44	0.13	n.d.	0.05	n.d.	n.d.
TAR 11/black shale	2.58	335	0.22	0.98	1.31	4.41	0.13	n.d.	0.07	n.d.	n.d.
TAR 10/laminated limestone	0.98	169	0.43	1.02	1.19	3.08	0.13	n.d.	0.04	n.d.	n.d.
TAR 8/black siliceous shale	2.61	450	0.27	0.91	1.31	2.65	0.12	n.d.	0.06	n.d.	n.d.
TAR 7/black siliceous shale	3.80	n.d.	0.37	0.97	1.30	1.70	0.10	n.d.	0.08	n.d.	n.d.
TAR 5/black chert	2.38	n.d.	0.11	1.18	2.76	1.42	0.09	n.d.	0.13	n.d.	n.d.
TAR 4/black chert	2.65	n.d.	0.39	1.04	1.57	9.48	0.17	n.d.	0.10	n.d.	n.d.
TAR 3/black chert	1.59	269	1.41	0.98	0.80	4.88	0.22	n.d.	n.d.	n.d.	n.d.
TAR 2/laminated grey marl	4.57	n.d.	0.35	0.90	1.67	1.68	0.12	n.d.	0.13	n.d.	n.d.
TAR 1/black shale	1.90	n.d.	0.72	1.00	2.04	2.32	0.11	n.d.	0.15	n.d.	n.d.

3.2.4. Micropaleontological studies

Fourteen sediment samples, weighing approximately 200 g, were processed and examined for foraminiferal/microfossil content. Ten samples were disintegrated by a repeated freeze–thaw method in a saturated solution of Glauber's salt (Na_2SO_4 x $10H_2O$) and four samples were decomposed with the use of liquid nitrogen (LN_2) (Remin et al., 2012). Then, the material was washed through a 63 μm sieve and air dried. The dried residue of each sample was examined for microfossils under a Nikon SMZ1500 stereomicroscope. Microphotographs of a few characteristic forams were made using the Hitachi S-4700 FE-SEM in a secondary electron (SE) mode at the Institute of Geological Sciences of the Jagiellonian University.

4. Results

4.1. Molecular composition

The aim of this study is to characterise paleoenvironmental conditions in the Tarcău and Vrancea sub-basins; therefore, the emphasis is placed on selected biomarker indicators (Fig. 3) related to specific OM producers, primary productivity and redox conditions. General geochemical molecular characterisation of the analysed rock samples

Table 2
Pyrite framboid diameter statistic data from the selected samples from the Nechit and Tărcuţa sections. Min, Max FD – the smallest/largest pyrite framboid diameter; SD – standard deviation; N – number of measurements; %F ≤ 5 μm – percentage of pyrite framboids with diameter equal or lower than 5 μm.

Sample	Min FD [μm]	Max FD [μm]	Mean [μm]	SD	N	% F ≤ 5 μm
Nechit Section						
NECH 211	1.5	28	6.6	4.3	137	46.3
NECH 204	1	13.5	3.7	1.9	134	87.3
NECH 199	0.5	8	3.5	1.7	125	81.6
NECH 101	0.5	9.5	3.4	1.5	113	90.3
NECH 25	1	9.5	3.7	1.6	122	84.4
NECH 19A	1.5	10.5	4.9	1.7	114	62.3
NECH 15	0.5	13.5	3.9	2.2	110	80.9
NECH 10	0.5	11.5	3.8	2.0	130	80.8
NECH 5	1	7	3.1	1.3	124	92.1
NECH 0	2	8.5	4.8	1.5	114	64.9
NECH 0D	1.5	8	3.9	1.6	111	78.4
Tărcuţa Section						
TAR 22	2	19	5.6	2.7	118	58.8
TAR 19	0.5	13	3.5	2.1	100	87
TAR 18	1	14	3.8	2.1	100	84
TAR 16	1	19.5	5.7	3.3	50	60
TAR 13	2	12	4.7	1.7	116	69.8
TAR 10	0.5	9.5	3.1	1.4	130	92.3
TAR 8	0.5	14.5	4.0	2.2	118	83.1
TAR 5	0.5	25	4.2	4.2	137	74.8
TAR 3	0.5	17.5	3.6	2.6	123	84.7
TAR 2	1.5	14	5.0	2.3	114	59.6

was presented in a previous work concerning OM maturity assessment (Wendorff et al., 2017).

4.1.1. Alkanes, pristane and phytane

The terrigenous versus aquatic *n*-alkane ratio (TAR, Bourbonniere and Meyers, 1996), the carbon preference indices ($CPI_{25\text{-}31}$, Bray and Evans, 1961; "modified" after Marzi et al., 1993), and the pristane to phytane ratio (Pr/Ph ratio; Didyk et al., 1978) are presented in Table 1 and Fig. 3. The Nechit section samples show the diversified TAR values falling in the 0.22–4.73 range (Table 1). The TAR values for the Tărcuţa section samples vary in a range from 0.11 to 1.92; nevertheless, most of the samples reveal values lower than 1.

The $CPI_{25\text{-}31}$ is also variable for the Nechit section, ranging from 0.45 to 1.56 (Table 1). The preponderance of long chain odd-carbon-numbered *n*-alkanes over even-numbered homologues is common in this section. The Tărcuţa section samples reveal balanced relative abundances among long chain *n*-alkanes in the Lower Menilite Mb. where the $CPI_{25\text{-}31}$ oscillates ~1.0. Higher $CPI_{25\text{-}31}$ values are observed for the rocks from the Bituminous Marls Mb. (Table 1).

Pristane prevails over phytane in both sections (Fig. 4), with the Pr/Ph ratio varying from 1.17 to 3.60 for the Nechit section, and from 1.19 to 6.18 for the Tărcuţa section. The Pr/Ph ratio <1 was noted only for two samples (NECH 7A and TAR 3; Table 1, Fig. 3C).

Several samples, especially those from the Nechit section, contain monomethyl alkanes with mainly *iso* (2-methyl) and *anteiso* (3-methyl) configurations ranging from C_{14} up to C_{26}, and with a maximum at C_{16} for both isomer series (Fig. 4). The mid-chain branched homologues (from 4- to 7-methyl isomers) occur in relatively low abundances. As with the *n*-alkanes, the monomethyl alkanes show a predominance of low carbon numbers (C_{16}–C_{19}). It should be mentioned that Brocks et al. (2008) described monomethyl alkanes as OM contaminants. However, due to high TOC concentrations, high bitumen yields and the occurrence of monomethyl alkanes in all samples, we suggest their primary character.

4.1.2. Highly branched isoprenoids

Highly branched isoprenoids (HBIs) are represented by the C_{25} HBI alkanes (2,6,10,14-tetramethyl-7-(3-methylpentyl)-pentadecane) and C_{25} HBI thiophenes (2,3-dimethyl-5-[7′-(2′,6′,10′,14′-tetramethyl pentadecyl)]thiophene). The C_{25} HBI thiophenes were found in small concentrations (0.1–2 μg/g TOC) exclusively in the Nechit samples. The highest concentrations were noted in the siliceous shales of the Lower Menilite Mb. (NECH 211, 210; Table 1). The C_{25} HBI alkane co-elutes with the *n*-C_{21} alkane, and apart from the Nechit samples, it occurs in the sample of the Tylawa limestone (TAR 10) from the Tărcuţa section.

4.1.3. Steroids

Steroids are prominent constituents of the apolar and aromatic fractions in the Nechit section, while in some of the Tărcuţa samples these biomarkers are present in small amounts or even absent (TAR 19). Regular steranes occur in the C_{27}–C_{30} range, with various intensities of each sterane member (Fig. 5). The C_{29} sterane predominates over the C_{27} and C_{28} homologues more frequently in the Nechit samples, and consists from 29 to 51% (av. 39%) of the summarised regular sterane relative abundances. For the Tărcuţa section, the C_{27} sterane is more abundant (29–44%, av. 36%). The C_{28} homologue occurs in similar percentages of ~30% throughout both sections. Among the C_{30} steranes, 24-*n*-propylcholestane and C_{30} 4-methylsteranes were detected in low abundances in both sections.

Aromatic steroids are represented by monoaromatic, triaromatic and A-ring methyl triaromatic steranes. The C_{27}–C_{29} A-ring methyl triaromatic (A-ring Me TA) steroids including triaromatic dinosteroids (Fig. 6) were assigned from the *m/z* 245 chromatogram based on their elution times after Ma et al. (2008), Brocks et al. (2016) and Ando et al. (2017). All three isomers (i.e. 2-, 3- and 4-methyl) of each C_{27}, C_{28} and C_{29} A-ring Me TA steroids were identified with generally 3- and 4-Me isomers prevailing over the 2-Me counterparts. The most intense peaks are those identified as 3- and 4-Me TA ergosteroids, probably co-eluting with 3- and 4-Me TA cholesteroids, which enhances their intensities. Seven isomers of TA dinosteroids (D1–D7, Fig. 6) were assigned on the basis of a molecular ion at *m/z* 386 and the retention time (after Ma et al., 2008; Brocks et al., 2016). Those compounds are well separated and their occurrence was observed in considerable abundances in both sections, especially in the chert samples from the Lower Menilite Mb.

4.1.4. Hopanoids and oleanane

Hopanoids were identified as one of the dominant compound groups in the aliphatic fractions, especially in the Tărcuţa section. Their distribution pattern is quite uniformly characterised by the occurrence of C_{27} to C_{35} (occasionally C_{36}) pseudohomologues, with C_{28} hopanes being absent (Fig. 7). The rearranged hopanes are represented by C_{27}, C_{29} and C_{30} neohopanes (18α(H)). The predominant hopanoid is the C_{30} 17α(H),21β(H) hopane in all the samples, while the homohopane distribution differs among the samples, as expressed by the C_{35} homohopane index values (C_{35} HHI; 17α (22S + R) C_{35} homohopane versus the sum of 17α (22S + R) C_{31}-C_{35} homohopanes; Peters et al., 2005). The C_{35} homohopane is more abundant than lower homologues (C_{33}, C_{34}) in cherts of the Lower Menilite Mb., reaching 0.25 in the Nechit section (NECH 207) and 0.22 in the Tărcuţa section (TAR 3). In both sections, the ratio shows a decreasing trend for the Bituminous Marls Mb. (Table 1).

The ratio of 17α-hopanes to steranes (17α H/S; the sum of 17α C_{29} to C_{33} (22S + R) hopanes versus the sum of regular C_{27} to C_{29} ααα (20S + R) + αββ (20S + R) steranes) was determined (Table 1). The hopane preponderance over steranes is clear for the Tărcuţa samples, with the highest value reaching 9.48 (TAR 4 sample). In contrast, many samples from the Nechit section show a preponderance of steranes over hopanes (17α H/S as low as 0.26; Table 1).

Oleanane, a pentacyclic triterpenoid, was tentatively identified in both sections based on its elution time and mass spectrum (e.g. Nytoft et al., 2002). It occurs frequently in the Nechit section (including NECH

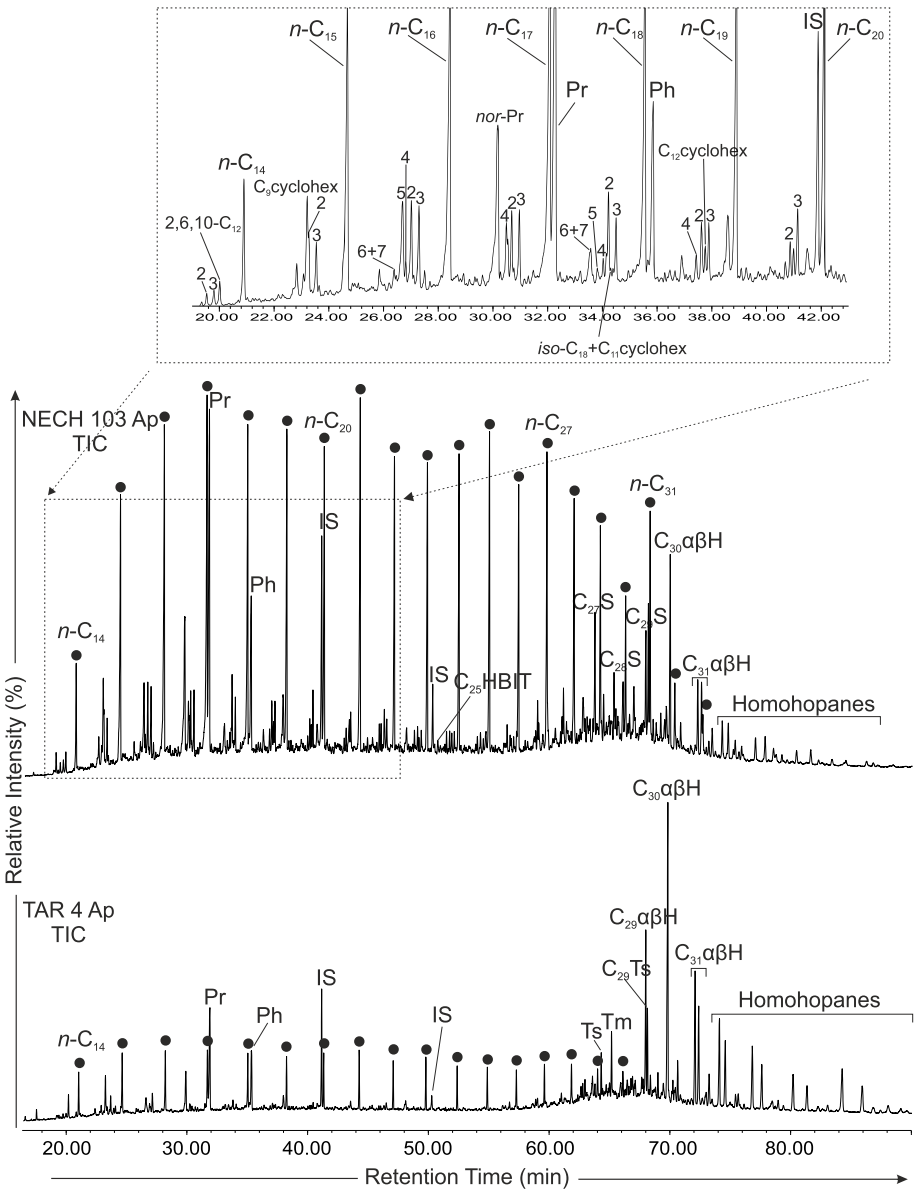

Fig. 4. Total ion current (TIC) chromatograms of aliphatic hydrocarbons from the NECH 103 and TAR 4 samples. Insert depicts the distribution of monomethylated alkanes, with the numbers indicating the position of methyl group. Circles – *n*-alkanes, *nor*-Pr – *nor*-pristane, Pr – pristane, Ph – phytane, H – hopanes, S – steranes, Ts - 18α(H)-22,29,30-trisnorneohopane, Tm – 17α(H)-22,29,30-trisnorhopane, C_{25}HBIT – C_{25} highly branched isoprenoid thiophene, IS – internal standards (described in the Methods).

207 and NECH 103; Fig. 7), except for most of the siliceous rocks of the Lower Menilite Mb. (NECH 199–212). In the Tărcuţa section, oleanane is more abundant in the Bituminous Marls Mb. (see TAR 16 in Fig. 7), while it is absent or present only in trace amounts (see TAR 4 in Fig. 7) in the Lower Menilite Mb.

4.1.5. *Aromatic sesqui- and diterpenoids*

Aromatic terpenoids (sesqui- and diterpenoids) were identified in almost all the samples from the Nechit section, while in the Tărcuţa section these compounds were absent. The most prominent are tetrahydroretene (Fig. 8) or retene, accompanied by simonellite and minor bisnorsimonellite (Philp, 1985; Otto and Simoneit, 2001). Cadalene and 6-*iso*propyl-1-*iso*hexyl-methylnaphtalene (*ip*-*i*HMN) are also present in considerable concentrations, while 2,2,9-trimethyltetrahydropicene (Laflamme and Hites, 1979; Otto and Simoneit, 2001) was identified in only few samples (e.g. NECH 101).

4.1.6. *Aryl isoprenoids*

The analysed samples were examined with the aim of identifying diagenetic products of isorenieratene degradation (Koopmans et al., 1996a). The occurrence of aryl isoprenoids (1-alkyl-2,3, 6-trimethylbenzenes) was noted only in several samples of siliceous shales and cherts from the Lower Menilite Mb. in the Nechit section (Fig. 8). This biomarker group is represented by the homologue chain of monoaryl C_{14} to C_{20} isorenieratene derivatives, and occasionally by diaryl short chain isoprenoids (M^+ 448 and M^+ 434, Fig. 8; identification after Koopmans et al., 1996a). Sample NECH19A shows trace amounts of the intact isorenieratane.

4.1.7. *Dibenzothiophene and phenanthrene*

Dibenzothiophene (DBT) and phenanthrene (P) are present in most of the samples, and the DBT/P ratio was calculated (Table 1). The samples from the Nechit section reveal values in the 0.23–0.69 range. The NECH 103 sample is the only one showing a very low DBT/P ratio, that is, 0.07 (Table 1, Fig. 3A). The ratio is generally lower for the Tărcuţa section and varies from 0.04 to 0.15.

4.1.8. *Chromans*

2-Methyl-2-(4,8,12-trimethyltridecyl)chromans (MTTCs) were found only in the rocks from the Nechit section. 5,7,8-trimethyl-MTTC prevails over mono- and di-methyl derivatives. This is expressed by the MTTC ratio (5,7,8-trimethyl-MTTC/total MTTCs; Sinninghe Damsté

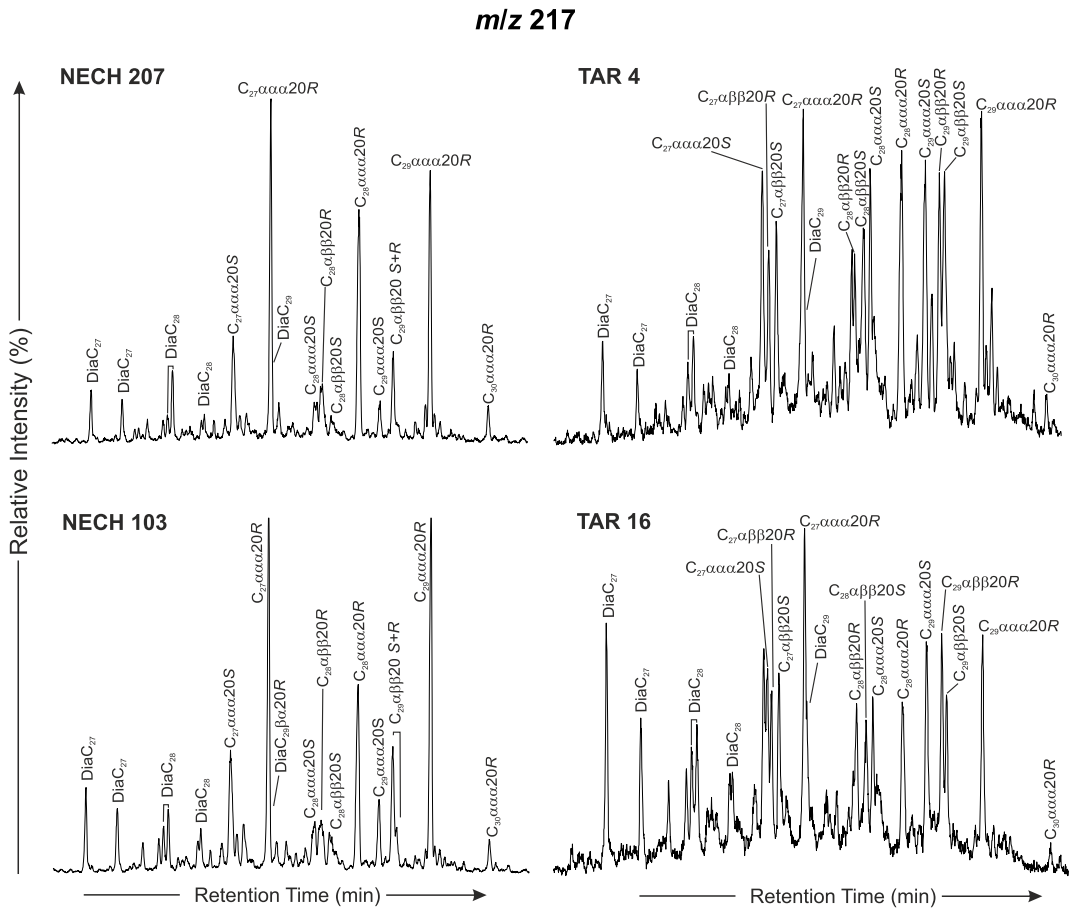

Fig. 5. Regular sterane and diasterane distributions on partial mass chromatograms (*m/z* 217) from representative samples from the Nechit (NECH 103 and 207) and Tărcuţa (TAR 4 and 16) sections. Dia – diasteranes.

et al., 1993) falling in the range of 0.72–0.88, with a mean value of 0.80 (Table 1).

4.1.9. Maleimides

Maleimides (1 *H*-pyrrole-2,5-diones), porphyrin degradation products, were found in all the derivatised polar fractions from both sections. The only maleimide compounds occurring in the Tărcuţa samples are Me,Me and Me,Et (3-ethyl,4-methyl-1*H*-pyrrole-2,5-dione) maleimides. In contrast, rocks from the Nechit section contain a major series of methyl maleimides with *n*-alkyl substituents from C_1 to C_5, except for C_4 (i.e. Me,H, Me,Me, Me,Et, Me,*n*-Pr and Me,*n*-pentyl components) (Fig. 9). Minor constituents are Me,*i*-Pr, Et,Et, Me,*sec*-Bu, Me,*i*-Bu (3-*iso*-butyl-4-methyl-1*H*-pyrrole-2,5-dione) and Me,*neo*-pentyl. The dominance of the Me,Me and Me,Et components is characteristic for all the analysed samples. Prominent compounds marked with asterisks in Fig. 9 were tentatively identified as derivatisation artefacts from maleimides cyclisation.

4.2. Pyrite framboid diameter analysis

Pyrite occurs mostly in a form of singular framboids (Fig. 10). Rather uncommon pyrite lumps, overgrown framboids and macroframboids indicating a diagenetic origin were excluded from the framboid diameter analysis.

Samples from the Nechit section are exceptionally abundant in pyrite framboids. Small framboids ≤5 μm prevail over larger ones, comprising up to 95% of the total volume (Fig. 3A and B). The minimum values of pyrite diameters vary in a narrow range of 0.5–1.5 μm, with the maximum values ranging from 7 to 13.5 μm, and mean sizes from 3.1 to 4.9 μm. Significant differences in the calculated parameters were observed for the NECH 204 sample, characterised by the highest maximum framboid diameter reaching 28 μm, a mean diameter size of 6.6 μm and the lowest percentage (46.3%) of the framboids ≤5 μm (Table 2).

In the samples from the Tărcuţa section, the pyrite framboids are also very common. They have a relatively wide range of diameters from 0.5 to 19 μm, although the mean sizes are low, varying from 3.1 to 5.6 μm (standard deviations: 1.4–4.2 μm). Populations of framboids with diameters smaller than or equal to 5 μm are dominant in all the samples, reaching 92% (Table 2, Fig. 3C).

4.3. Foraminiferal assemblages

The foraminiferal assemblages displayed a small number of specimens. Five samples were barren of microfossils and three samples yielded rare fish teeth and sponge spicules. In most cases, foraminifera are preserved in a form of pyritised steinkerns. The agglutinated foraminifera are represented by a few, long ranging, cosmopolitan taxa such as *Bathysiphon*, *Rhabdammina, Ammodiscus, Saccammina, Glomospira charoides* (Jones et Parker), *Glomospira gordialis* (Jones et Parker), and *Haplophragmoides* sp. This kind of impoverished assemblage was found in the sample NECH 209.

The relatively richest assemblage was recovered from the sample TAR 16 (Fig. 11). It consists of some benthic, less numerous planktic taxa and pyrite infillings of probably agglutinated tubular forms. *Tenuitella munda* (Jenkins), *T. gemma* (Jenkins) and *Subbotina droogeri* (Mjatliuk) are examples of planktic species. *Praeglobobulimina* cf. *pyrula* (d'Orbigny), *Virgulinella chalkophila* (Hagn), *V. karagiensis* Mikhailova,

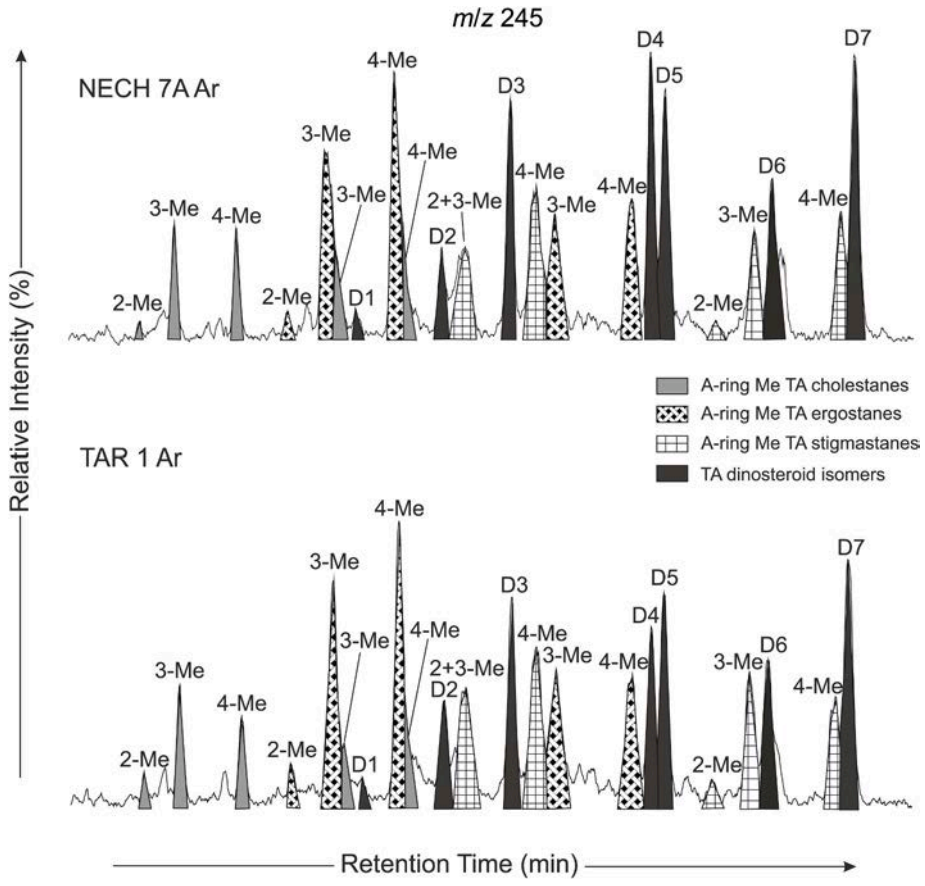

Fig. 6. Distributions of A-ring methyl triaromatic (A-ring Me TA) steranes on mass fragmentograms (*m/z* 245) in representative samples from the Nechit (NECH 7A) and Tărcuţa (TAR 1) sections. D1–D7 – isomers of TA dinosteroids.

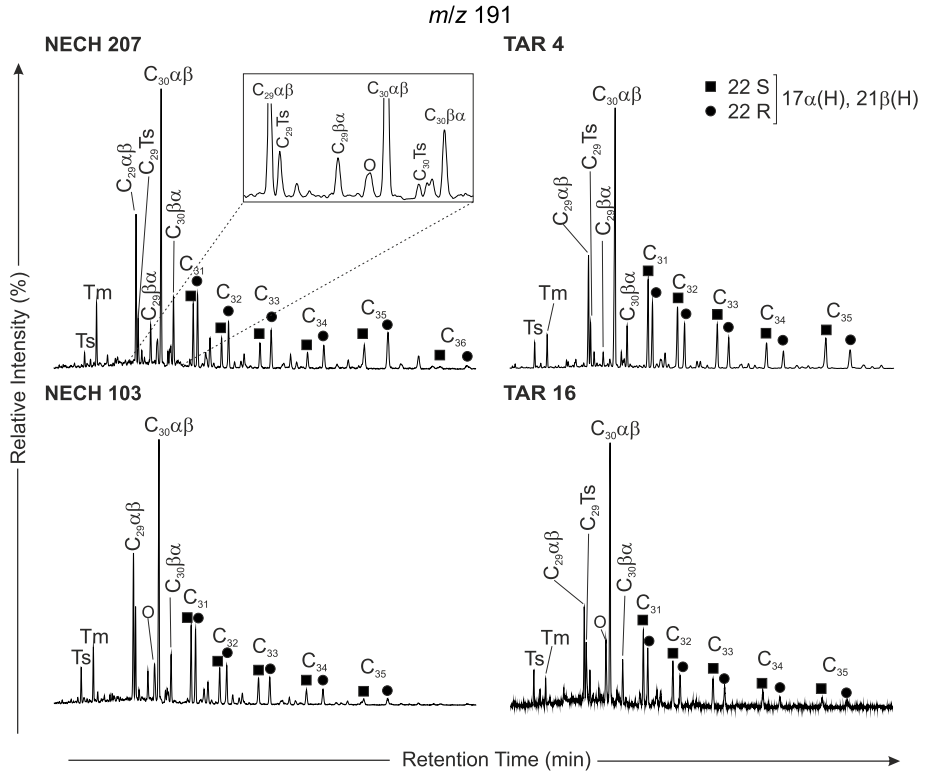

Fig. 7. Partial mass chromatograms of *m/z* 191 showing different distributions of homohopanes among samples in the Nechit (NECH 207 and 103) and Tărcuţa (TAR 4 and 16) sections. Ts – 18α(H)-22,29,30-trisnorneohopane, Tm – 17α(H)-22,29,30-trisnorhopane, C_{29}Ts – 18α(H)-30-norneohopane, O – oleanane.

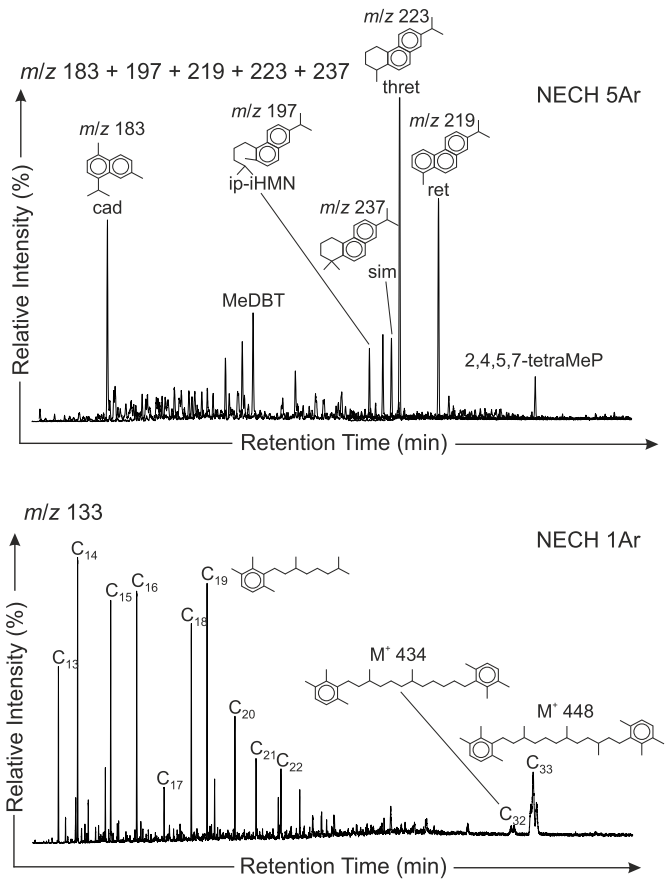

Fig. 8. Summed mass chromatogram for *m/z* 183 + 197 + 219 + 223 + 237 + 252 showing the distributions of aromatic biomarkers in the NECH 5 sample, and partial mass chromatogram for *m/z* 133 presenting aryl isoprenoids in the NECH 19A sample from the Nechit section. Cad – cadalene, MeDBT – methyldibenzothiophene, *ip*-*i*HMN - 6-*iso*propyl-1-*iso*hexyl-methylnaphtalene, sim – simonellite, thret – tetrahydroretene, ret – retene, 2,4,5,7-tetraMeP - 2,4,5,7-tetramethylphenanthrene.

Bulimina tenera Reuss, *Pleurostomella* cf. *acuta* Hantken, *Nonionella liebusi* Hagn and *Chilostomella* cf. *ovoidea* Reuss are the most characteristic of benthic species. The mentioned species commonly occur in the Menilite–Krosno series of the Western Outer Carpathians (e.g. Olszewska, 1982; Bąk, 1999). This assemblage shows some similarities to the assemblage II described by Olszewska (1982) from the upper part of the Menilite Beds in the Skole Nappe, and the lower Krosno Beds in other units in the Polish Outer Carpathians. The biostratigraphic ranges of both planktic and benthic taxa point to the Oligocene age excluding the lowermost Rupelian (Olszewska, 1982; Olszewska et al., 1996; Cicha et al., 1998). This estimation does not contradict the most recent dating of the Lower Menilite and Bituminous Marls Mbs based on calcareous nannofossil assemblages (Belayouni et al., 2009) as not older than the late Rupelian.

5. Discussion

Organic geochemical studies presented for the Nechit and Tărcuţa cross-sections representing the Early Oligocene sedimentation in the Vrancea and Tarcău domains demonstrate differences in biomarker composition between these two settings. Variable biomarker assemblages identified in the rocks from the Nechit section contrast with rather poor molecular composition in the Tărcuţa section. This can result from several factors, including the nature and quantity of terrestrial OM input, as well as the redox state within the water column or sediments in both Paratethys sub-basins. Characteristic origin-related distributions of *n*-alkanes and high proportions of cyclic isoprenoids (hopanes, steranes) versus *n*-alkanes would point to a rather low biodegradation and maturity level. The maturity stage determined for the analysed rocks in the previous research (Wendorff et al., 2017) is well within the biomarker thermodynamic stability window (Peters et al., 2005). The Nechit samples were characterised by av. vitrinite reflectance (R_o) of 0.38% and av. T_{max} ~425 °C, while the Tărcuţa samples showed av. R_o ~0.51% and av. T_{max} ~430 °C. Thus, the absence of thermally less stable biomarkers like MTTCs or aromatised abietane derivatives in the Tărcuţa section can rather be associated with primary OM features than with a higher maturity stage. In the following, these results are discussed in relation to OM sources and 'paleoredox' conditions, which allowed us to create an overall model of sedimentation conditions for the Vrancea and Tarcău sub-basins.

5.1. Organic matter sources

The observed diversity of biomarkers and their distributions through the analysed sections suggests variable input of both autochthonous and allochthonous OM. This variability is evidently controlled by the differing admixtures of pelagic versus redeposited material imprinted in the lithological heterogeneity of the Menilite facies. Biomarkers of organisms from the eukaryotic and prokaryotic domains of life are present, evidenced by the occurrence of steroids and hopanoids. The identification of some specific compounds, such as C_{25} HBIs, TA dinosteroids or abietane derivatives was useful for more detailed OM sources' determination.

5.1.1. Origin of n-alkanes

n-Alkanes are quantitatively the most abundant compound group in the studied Lower Oligocene rocks. *n*-Alkanes in the range of *n*-C_{15} to *n*-C_{19} are usually linked to algal and cyanobacterial sources (Gelpi et al., 1970; Brassell et al., 1980; Jaffé et al., 2001). The occurrence of intermediate molecular weight homologues (*n*-C_{21} to *n*-C_{25}) can be attributed to OM originating from aquatic macrophytes (Ficken et al., 2000), while odd- over even-carbon numbered long chain *n*-alkanes (*n*-C_{27}, *n*-C_{29}, *n*-C_{31}) predominance is usually typical of the contribution of the epicuticular leaf waxes of vascular plants (Eglinton and Hamilton, 1967; Rieley et al., 1991). Based on these general premises, several *n*-alkane indices have been elaborated, including the TAR (Bourbonniere and Meyers, 1996) and $CPI_{25\text{-}31}$ (Bray and Evans, 1961; Marzi et al., 1993) used in this study. TAR is a ratio commonly applied to evaluate the importance of terrigenous OM input in comparison to aquatic contribution. In the Nechit section, variable TAR values suggest differing admixtures of land-derived and marine OM, although common values < 1 point to a prevailing proportion of autochthonous algal and cyanobacterial production in the Vrancea basin during the Early Oligocene. Generally, a prevalence of odd-carbon numbered long chain *n*-alkanes (max. CPI = 1.56) is indicative of the moderate input of OM of terrestrial origin. Most of the studied rocks from the Tărcuţa section exhibit very low TAR values, as low as 0.1, suggesting mainly marine origin of OM. Increasing admixture of land-derived *n*-alkanes in the Bituminous Marls Mb. is indicated by the relatively higher TAR (reaching 1.9) and CPI (up to 1.3) values. However, a possible contribution of microalgae and bacteria to the long chain alkanes (Volkman et al., 1998), together with the fact that land plants are generally more rich in *n*-alkanes than aquatic OM (Peters et al., 2005), can lead to the overestimation of terrigenous OM contribution on the basis of *n*-alkane distribution.

A constant high proportion (av. 30%) of intermediate molecular weight *n*-alkanes relative to the total *n*-alkane abundances in both sections can imply the contribution of aquatic macrophytes to the deposited OM (Ficken et al., 2000).

5.1.2. Algal phytoplankton

In marine realms, the predominant primary producer of OM is eukaryotic algal phytoplankton inhabiting the photic zone. This wide

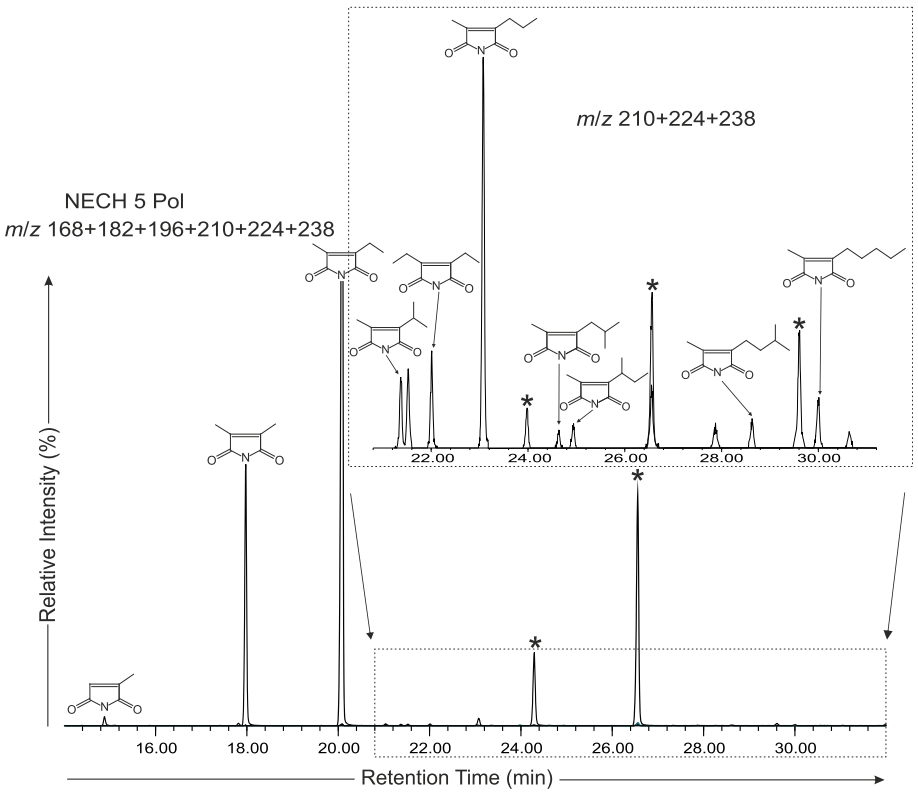

Fig. 9. Maleimides distribution as *tertiary*-butyl-dimethylsilyl derivatives in the NECH 5 sample from the Nechit section. * – possible artefacts from maleimides cyclisation.

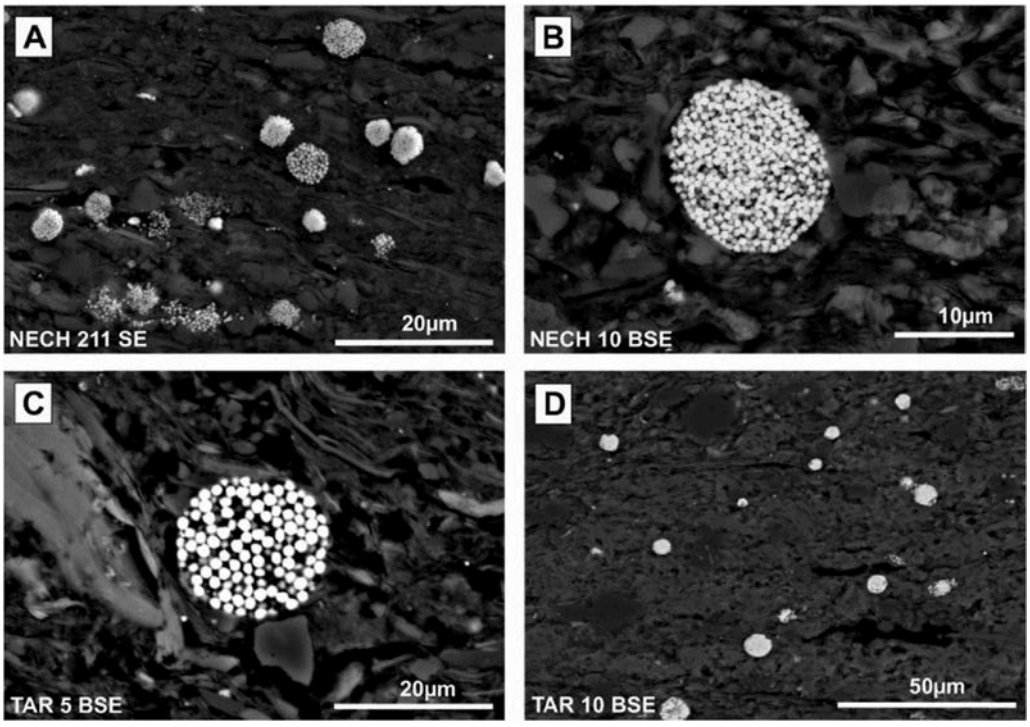

Fig. 10. Back-scattered electron images of pyrite framboids. (A) Abundant pyrite framboids from sample NECH 211. (B) and (C) Framboids with different density of packing of pyrite microcrystals in NECH 10 and TAR 5 samples. (D) Dispersed pyrite framboids in sample TAR 10.

group of organisms synthesises a great diversity of sterols (Volkman, 1986) (i.e. sterane precursors). Generally, the C_{27} sterols are interpreted as deriving from algae, while C_{29} sterols are from land plants (Volkman, 1986). According to such simplified interpretation, the contribution of marine algae is higher in the Tărcuţa section, where C_{27} regular steranes are more abundant. In the Nechit section, land plant-derived OM

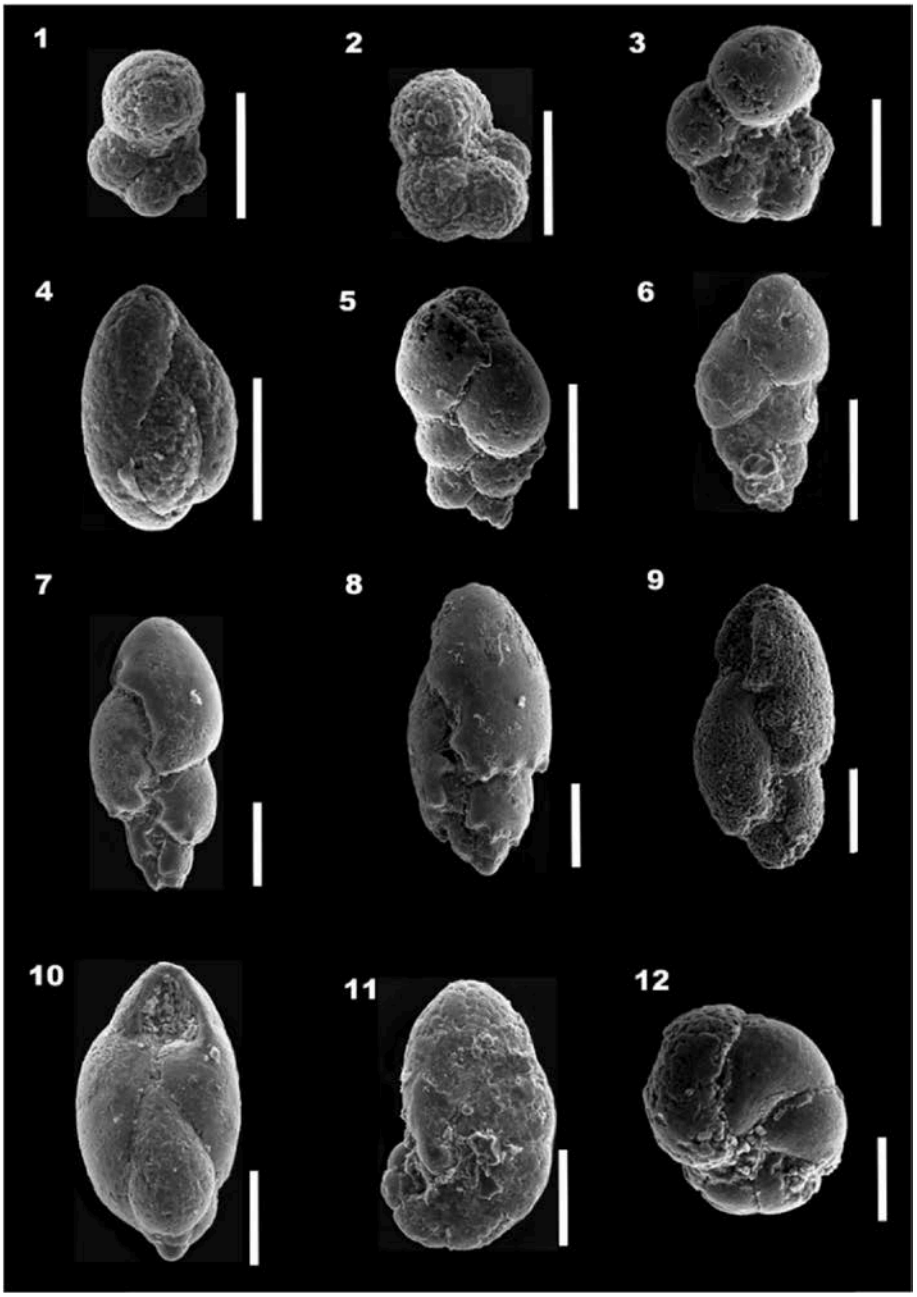

Fig. 11. Examples of planktic (1–3) and benthic (4–12) foraminifera preserved as pyritised steinkerns in sample TAR 16: 1. *Globigerinella* sp., 2. *Tenuitella munda* (Jenkins), 3. *Tenuitella gemma* (Jenkins), 4. *Praeglobobulimina* cf. *pyrula* (d'Orbigny), 5–6. *Fursenkoina* sp., 7. *Virgulinella chalkophila* (Hagn), 8. *Virgulinella karagiensis* Mikhailova, 9. *Virgulinella chalkophila* (Hagn), 10. *Pleurostomella* cf. *acuta* Hantken, 11. *Nonionella liebusi* Hagn, 12. *Nonion* sp. 1–3: scale bar = 50 μm; 4–12: scale bar = 100 μm.

prevails, as inferred from the frequent preponderance of the C_{29} sterane. However, high percentages of C_{29} steranes (35–40%) are not necessarily indicative of land plants, as sometimes interpreted (see Huang and Meinschein, 1979; Jiao et al., 2009). Some algae, such as diatoms and brown or green algae can also be the source of C_{29} sterols, C_{29} sterane precursors (e.g. Volkman et al., 1998, and references cited therein; Kodner et al., 2008). The prominence of the C_{29} sterane member has been observed in many typically marine sedimentary rocks (e.g. Volkman, 2005; Wang et al., 2008).

Significant percentages (av. 30%) of C_{28} steranes in both sections most probably reflect an important contribution from diatoms, as their evolution resulted in a noticeable increase of C_{28} steranes in the Upper Cretaceous and Tertiary oils derived from marine source rocks (Grantham and Wakefield, 1988). Diatom productivity in the Early Oligocene can be confirmed by the permanent occurrence of the C_{25} HBI alkanes and thiophenes across the Nechit section, although in small concentrations (Table 1). These biomarkers are derived from C_{25} HBI alkadienes (Summons et al., 1993; Volkman et al., 1994) commonly associated with marine diatoms of such genera as *Rhizosolenia*, *Haslea*, *Navicula* and *Pleurosigma* (Volkman et al., 1994; Sinninghe Damsté et al., 1999, 2004; Grossi et al., 2004). In the Tărcuţa section, only the Tylawa limestone (TAR 10) contains the C_{25} HBI alkane (co-eluting with C_{21} *n*-alkane). The presence of this biomarker is in accordance with a widely proposed origin of the Tylawa limestone as a result of diatom and coccolithophore blooms in a restricted anoxic basin (Haczewski, 1989). The HBIs have been identified in the Menilite rocks across the Outer Carpathians (Rospondek et al., 1997; Köster et al., 1998b), including the Bituminous Marls Mb. from the Vrancea Nappe (Sachsenhofer et al., 2015). This suggests the widespread occurrence of diatoms in the Central Paratethys in the Early Oligocene. In our case, the low concentrations of HBIs in the Nechit section and their absence in the Tărcuţa section do not reflect the high productivity of diatoms, as indicated by the ubiquitous Lower Oligocene siliceous facies (cherts, siliceous shales – Menilites *s.s.*) with clear origin from diatom opaline frustules (Kaczmarska and Kilarski,

1979; ten Haven et al., 1993; Köster et al., 1998b). This may be due to the presence of diatoms not synthesising HBI precursor compounds in those basins, or their decomposition in the oxygenated part of the water column.

Contributions from dinoflagellates can be implied from the wide occurrence of TA dinosteroids throughout both sections (Fig. 6). These compounds are assumed to derive from dinosterol and structurally related 4,23,24-trimethyl cholesterols, well known from modern marine dinoflagellates (e.g. Kokinos et al., 1998). In general, C_{27}–C_{29} 4-Me TA steroids, detected in the analysed rocks, are also related to dinoflagellates (Curiale, 1987; Robinson et al., 1984; Volkman et al., 1990; Peters et al., 2005), although some haptophytes (Volkman et al., 1990), methanotrophic bacteria (*Methylococcaceae*; Schouten et al., 2000) and higher plants (Menounos et al., 1986) can also synthesise their precursor compounds. Dinoflagellate-derived biomarkers (Rospondek et al., 1997; Köster et al., 1998b) and scarce dinoflagellate cysts (Gedl, 2000; Sachsenhofer et al., 2015; Ţabără, 2017) were noticed in the Menilite shales across the Carpathians, including few shale samples from the Nechit section (Filipek, 2020).

C_{30} sterane (24-*n*-propylcholestane), although detected in small concentrations, is another unambiguous marker of marine microalgae. Its precursor molecules (24-*n*-propyldiene-cholesterol and 24-*n*-propylcholesterol) have at present only been identified in the Pelagophyceae, a small class of marine chromophyte algae (Volkman, 2003; Giner et al., 2009) and in the heterotrophic foraminifer *Allogromia laticollaris* (Grabenstatter et al., 2013).

5.1.3. Prokaryotes

The biological precursors of hopanoids ubiquitous in all the samples are bacteriohopanepolyols identified in bacteria, as well as in some ferns and moss (Ourrison et al., 1979; Rohmer et al., 1992). Relatively high bacterial input expressed by high 17α H/S ratio are apparent for the Tărcuţa section (Fig. 12) and sporadically for the siliceous facies from the Nechit section (e.g. chert sample TAR 4; Table 1). High concentrations of hopanoids together with the presence of diatom-derived C_{25} HBIs in the siliceous samples is suggestive for their marine origin. This is consistent with the hopane provenance from cyanobacteria dwelling in the photic zone, as it was revealed by the hopane carbon isotope ratio in the Menilite rocks of the Polish Outer Carpathians (Köster et al., 1998b). The most elevated 17α H/S ratios correlate with the presence of monomethylated alkanes suggestive of a strong predominance of bacteria over eukaryotic algae (e.g. Ourisson et al., 1979; Brocks et al., 1999). The presence of these compounds can be ascribed to cyanobacterial production, as they have been identified in numerous cyanobacterial cultures (Gelpi et al., 1970; Coates et al., 2014), and in modern cyanobacterial mats (Shiea et al., 1990; Dembitsky et al., 2001), as well as in ancient sediments characterised by a substantial contribution of cyanobacterial OM (Kenig et al., 1995). However, they may derive from other microbial sources (Thiel et al., 1999), and also from thermal maturation (Kissin, 1987). *Iso*- and *anteiso*-alkanes, especially *iso*- and *anteiso*-C_{15} and C_{17} alkanes, are widespread in anoxygenic bacteria (Kaneda, 1991), including sulfate-reducing bacteria (Wakeham et al., 2007), as well as in fungi and marine phytoplankton (Perry et al., 1979). The provenance from sulfate-reducing bacteria in the studied rocks seems plausible, as an intense operation of these prokaryotes during OM sedimentation and diagenesis is suggested (see further discussion).

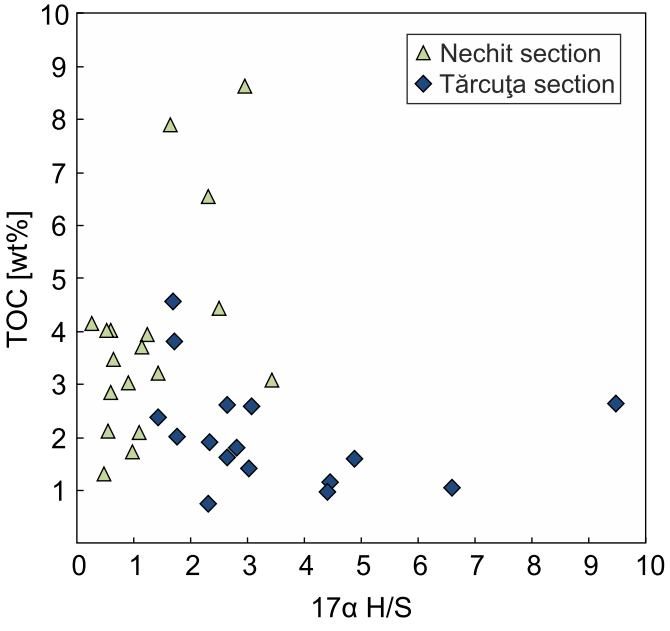

Fig. 12. Crossplot of TOC values (adapted from Wendorff et al., 2017) versus 17α hopanes to steranes ratio (17α H/S) showing higher concentrations of steranes in the Nechit section, and in contrast, the dominance of hopanes in the Tărcuţa section.

5.1.4. Green sulfur bacteria (Chlorobiaceae)

This specific group of phototrophic bacteria involves obligate anaerobes adapted to thrive in the water column when hydrogen sulfide is present (Pfennig, 1978; Hartgers et al., 1993). For anoxygenic photosynthesis, they use specific pigments such as bacteriochlorophylls (*c*, *d*, and *e*) and carotenoids like isorenieratene (Summons and Powell, 1987; Koopmans et al., 1996a). These intact compounds, together with their degradation products (i.e. Me,*i*-Bu maleimides and aryl isoprenoids, respectively), are therefore well-established markers of green sulfur bacteria operating in the euxinic water column (e.g. Grice et al., 1996; Pancost et al., 2002; Naeher et al., 2013; Tulipani et al., 2015a; Smolarek et al., 2017). Aryl isoprenoids, found in ten samples from the Nechit section (Fig. 8), may have additional sources, like renieratene or β-carotene (Grice et al., 1996; Koopmans et al., 1996b). However, their co-occurrence with isorenieratane (only in one sample: NECH 19A), Me, *i*-Bu maleimides (Fig. 9) and tiny pyrite framboids suggests the temporal activity of green sulfur bacteria in the Vrancea basin during the deposition of the Menilite facies. Aryl isoprenoids assigned to *Chlorobiaceae* based on their specific carbon isotope ratio were reported in equivalent rocks from the Polish part of the Outer Carpathians by Köster et al. (1998b), and in the Carpathian oils by Kotarba et al. (2007).

5.1.5. Higher plants

Direct evidence for the contribution of OM derived from higher plants in the Nechit section includes such biomarkers as tetrahydroretene, retene and simonellite (Simoneit, 1985; Alexander et al., 1988; van Aarssen et al., 2000) (Fig. 8). Their biological precursors are abietane class diterpenoids, mainly abietic acid, and also phenolic abietanes and other abietanoic acids, synthesised by conifers as constituents in resins and supportive tissues (Simoneit et al., 1986; Otto and Simoneit, 2001; Stefanova et al., 2002; Hautevelle et al., 2006). Another biomarker of land plant origin is oleanane, detected frequently in small amounts in the Nechit section and in equivalent rocks throughout the Polish and Ukrainian Carpathians (Kruge et al., 1996; Köster et al., 1998b; Kotarba et al., 2007; Rauball et al., 2019). Triterpenoids possessing the oleanane skeleton are produced almost exclusively by angiosperms (flowering plants), except for a lichen and a few ferns (Moldowan et al., 1994, and references therein). A terrigenous source of these compounds is in accordance with the co-occurrence of other biomarkers associated dominantly with higher plants, such as *ip*-*i*HMN (Ellis et al., 1996), cadalene (Simoneit, 1985) and tetrahydropicene (Otto and Simoneit, 2001). However, the increased contribution of higher land plant-derived OM is evident only for two samples (NECH 211 and 101), in which high concentrations of the abietane derivatives correlate with significantly higher CPI, TAR and Pr/Ph values (Table 1) and C_{29} sterane percentages (50% of total regular steranes). In contrast, in the Tărcuţa section (Table 1) the sole compound of land plant origin

identified in small abundances in the Bituminous Marls Mb. is oleanane, indicating a minor contribution from angiosperms. The lack of abietane-derived biomarkers and generally low TAR values point to a negligible input of terrigenous OM into the Tarcău basin in the Early Oligocene.

Vegetation dominated by plants adapted to cold climate conditions such as conifers, as inferred from the constant presence of their biomarkers, seems to be in accordance with a widely recognised cooling event starting at the Eocene/Oligocene boundary and continuing through the Oligocene (Soták, 2010, and references therein).

MTTCs are compounds mainly used as indicators of paleosalinity (e.g. Sinninghe Damsté et al., 1987; Grice et al., 1998; Wang et al., 2011); nevertheless, they can also imply OM primary producers. Although the origin of MTTCs has not been unambiguously established to date, they have been found almost exclusively in rocks post-dating the evolution of vascular plants (Sinninghe Damsté et al., 1987). One of the recent hypotheses for the formation of MTTCs includes the condensation reactions of chlorophyll phytol side chain and higher plant-derived alkylphenols at early stages of diagenesis (Li et al., 1995; Tulipani et al., 2013, 2015b). In the Nechit section, the co-occurrence of MTTCs with distinctive higher plant biomarkers suggests terrestrial sources of these compounds.

5.2. Paleosalinity

The MTTC ratio has been established as a reliable index of paleosalinity above the chemocline (e.g. Sinninghe Damsté et al., 1987, 1993; Schwark and Püttmann, 1990). In combination with the Pr/Ph ratio, it can be used to distinguish normal marine, hyper- and meso-saline conditions (Schwark et al., 1998; Peters et al., 2005, Wang et al., 2011). According to the plot of these two indices (Fig. 13; after Wang et al., 2011), the deposition of the Lower Oligocene rocks in the Vrancea domain took place in meso-saline to even freshwater conditions. The high MTTC ratio, reaching 0.9, obtained for the lowermost part of the Lower Menilite Mb. (NECH 199) and upper part of the Bituminous Marls Mb. (NECH 101 and 102) can be attributed to freshwater incursions (e.g. Tulipani et al., 2015b). Decreasing salinity during the deposition of the Menilite shales from the Nechit section is also suggested by Filipek (2020) through the presence of *Botryococcus* sp., a group of green algae-forming mats in fresh or brackish water environments (Metzger and Largeau, 2006). Moreover, calcareous nannoplankton assemblages characterised by endemic species adapted for unstable salinity conditions together with a species typical for brackish water settings, namely *Braarudosphaera bigelowii* (Gran and Braarud) Deflandre, have been reported in other locations in the Romanian Carpathians (Melinte, 2005). However, the position of the samples on the plot (Fig. 13) can be linked to elevated values of pristane associated with its additional source, besides the side chain of chlorophyll (e.g. tocopherols; see Goossens et al., 1984).

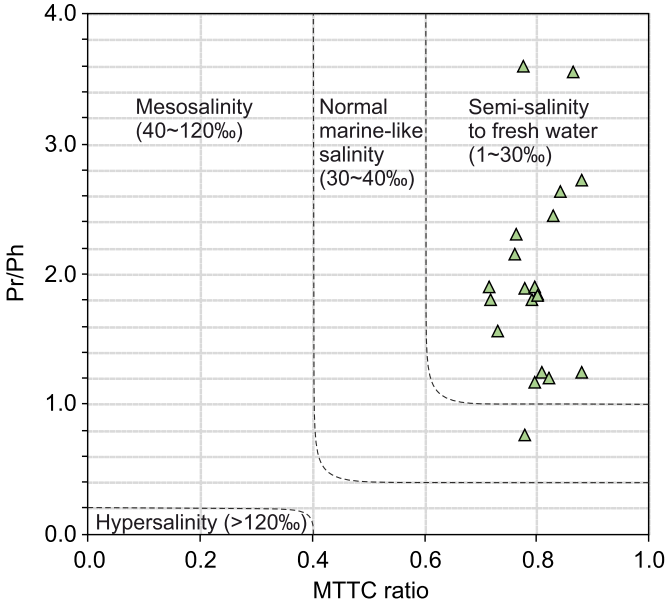

Fig. 13. Crossplot of Pr/Ph versus MTTC ratio for samples from the Nechit section. Boundaries between salinity fields after Wang et al. (2011).

5.3. Redox conditions

Bacterial sulfate reduction leading to the formation of hydrogen sulfide occurs commonly in marine organic-rich sediments. Reactive iron easily reacts with hydrogen sulfide to form iron sulfide. Therefore, concentrations of both reactive iron and hydrogen sulfide are thought to be limiting factors in the production of organic compounds containing sulfur in sediments (e.g. Sinninghe Damsté et al., 1989; Sinninghe Damsté and de Leeuw, 1990). The high abundance of small pyrite framboids (<5 μm) in the analysed samples suggests the availability of both hydrogen sulfide and reactive iron in the water column. Reactive iron was probably supplied by rivers to the system and an excess free sulfur species left after iron sulfide formation could react with organic compounds (van Kaam-Peters et al., 1998; Kok et al., 2000), forming thiophenes for example, such as DBTs or C_{25} HBI thiophenes. The DBT/P ratio reflects the availability of reduced sulfur for incorporation into OM in the depositional/diagenetic environment (Hughes et al., 1995). Relatively low DBT/P ratio values, especially in the Tărcuţa section (Table 1), suggest the importance of sulfur fixation by iron. The absence of C_{25} HBI thiophenes in this section can be linked to the lack of HBI producers or the complete decomposition of HBI precursors, that is, poly-unsaturated C_{25} HBIs (widely occurring in recent sediments; Dunlop and Jefferies, 1985; Rowland and Robson, 1990). The sulfurisation of C_{25} HBI precursors leading to C_{25} HBI thiophene formation contrasts with aromatisation as a main process that has affected other major biomarker groups (mono and triaromatic steranes and benzohopanes). This may reflect different habitats of precursor organisms in the water column (i.e. diatoms vs. most sterol-producing eukaryote and cyanobacteria).

The size distribution of pyrite framboids in both ancient and modern sediments has become a well-established proxy for local redox conditions (Wilkin et al., 1996, 1997; Wignall and Newton, 1998; Bond and Wignall, 2010). It has been concluded that pyrite framboids are able to form via two different mechanisms. They can grow during very early diagenesis within the upper centimetres of sediments under suboxic to anoxic seafloor conditions, where they can reach larger sizes (Wilkin et al., 1996, 1997; Wilkin and Arthur, 2001; Wei et al., 2015). Alternatively, framboids form in the euxinic water column, near the redoxcline, where H_2S and dissolved Fe are present, while O_2 is also available for the nucleation of iron monosulfide precursors (Wilkin and Barnes, 1997; Wignall et al., 2005). Under these circumstances, framboids grow usually up to a maximum of 5–6 μm and subsequently precipitate to become finally buried within the sediment (e.g. Wilkin et al., 1996).

In the studied sections, the conspicuous domination of small pyrite framboids (Fig. 3; Fig. 14), reaching up to 90% of all the framboid populations in cherts and black shales from the Nechit section, suggests widespread anoxic/euxinic conditions at the sediment–water interface, expanding into the water column due to enhanced bacterial sulfate reduction (Wilkin et al., 1996; Bond and Wignall, 2010; Dustira et al., 2013). Oxygen-deficient conditions can also be inferred from the common lack of bioturbations and the morphotype character of benthonic foraminifera identified in the analysed rocks (De Stiger et al., 1998). *Bulimina* and *Chilostomella* are commonly described as "low oxygen taxa", inhabiting dysoxic to even anoxic deep-sea bottom environments, although Rathburn and Corliss (1994) observed that their dominance is typical of environments with a high organic flux, rather than with low

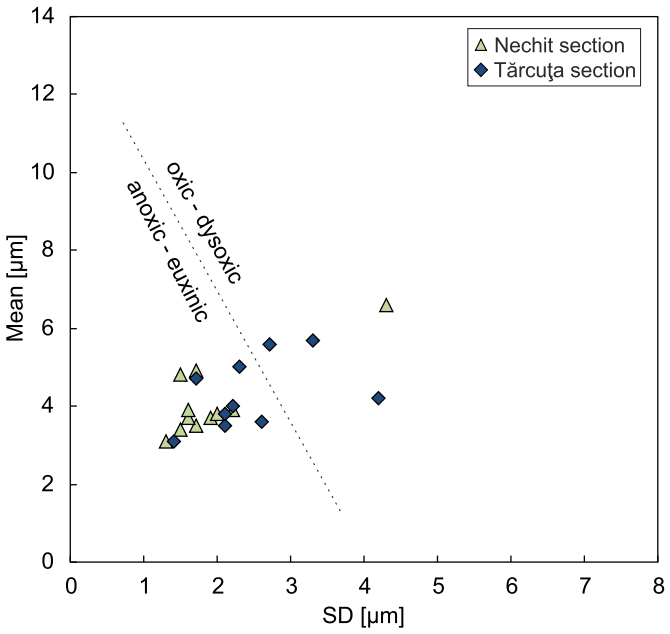

Fig. 14. Plot of the pyrite framboid size distribution statistic data: mean pyrite framboid diameter (Mean) versus standard deviation (SD) indicating prevailing anoxic/euxinic conditions during the deposition of the analysed rocks.

oxygen concentrations.

Interestingly, paleo-redox interpretation based on the pyrite framboid diameter observations differs from that derived from the biomarker record, for example, from the moderate to high Pr/Ph ratio (Table 1, Fig. 3A, B, C), suggesting rather oxidative OM transformation. The Pr/Ph ratio is a frequently used paleo-redox indicator (Didyk et al., 1978) based on the favoured formation of pristane over phytane, during chlorophyll *a* (and bacteriochlorophyll *a* and *b*) decay under oxic conditions (Brooks et al., 1969; Powell and McKirdy, 1973). This ratio can, however, be affected by different OM sources, such as tocopherols (Goossens et al., 1984; Li et al., 1995), unsaturated isoprenoids in zooplankton (Blumer et al., 1963) and higher animals (Blumer and Thomas, 1965), or by the preferential formation of pristane during maturation (Connan, 1974). In our case, the latter factor should not have significantly altered this ratio due to the low OM maturity of the Menilite shale samples (Wendorff et al., 2017). Fluctuations of the redox environment with the preponderance of oxic/suboxic conditions can be concluded, again based on the generally low values of the C_{35} HHI (Table 1). In oxidising environments the C_{35} homohopane undergoes degradation, which finally leads to increased concentrations of C_{31} homohopane (Peters and Moldowan, 1991; Peters et al., 2005). The C_{31} homohopane is indeed the most abundant homohopane homologue in the analysed rocks (Fig. 7), although the C_{35} HHI can also be influenced by different source organisms (e.g. Obermajer et al., 2000), clay content in the sediment or thermal maturity (e.g. Peters and Moldowan, 1991; Peters et al., 2005). Nevertheless, the general trend of more oxygenated conditions in the Bituminous Marls Mb. and oxygen deficiency in the siliceous facies of the Lower Menilite Mb. is apparent in both sections.

Evident discrepancies between biomarker and pyrite framboid records can be related to processes proceeding in different parts of the water column. The early diagenesis of precursors from photoautotrophic organisms are likely to have begun in the upper oxygenated water layer, possibly influenced by photodegradation (Rontani et al., 1991) and thus limiting precursor reactivity towards reduced sulfur. On the contrary, pyrite framboids were mostly formed deeper in the water column near the chemocline.

5.4. Photic zone euxinia

Water masses affected by photic zone euxinia (PZE) provide a supreme environment for green sulfur bacteria (*Chlorobiaceae*) to thrive (Pfennig, 1978; Summons and Powell, 1987; Hartgers et al., 1993). Their intermittent presence in the water column in the Vrancea domain was suggested above, and hence the periodic development of PZE can be inferred. Similarly to this study, temporal PZE has been recognised to occur in the Paratethys basin during the Oligocene, based on the presence of isorenieratene derivatives in the Menilite facies (Köster et al., 1998b; Kotarba et al., 2007; Sachsenhofer et al., 2015).

The lack of biomarkers of green sulfur bacteria in the samples from the Tărcuţa section does not, however, exclude PZE in the Tarcău sub-basin. For instance, the existence of green sulfur bacteria producing different stains lacking the Me,*i*-Bu component cannot be precluded (Grice et al., 1997; Pancost et al., 2002). Alternatively, euxinic conditions in the Tarcău sub-basin could have been present below the photic zone. This scenario can be explained by the lack of isorenieratene derivatives or Me,*i*-Bu maleimides, as well as by the domination of tiny pyrite framboids in most of the samples.

6. Paleoenvironmental implications

Our data imply that the source of OM deposited in the Paratethys sub-basins in the Early Oligocene was mainly of marine origin. Algal productivity is reflected in high steroid concentrations, especially in the Vrancea basin. Significant prokaryotic, mainly cyanobacterial input, is imprinted in the preponderance of hopanoids co-occurring with monomethylated alkanes in the Tarcău sub-basin. Among algal phytoplankton, the most important are biosilicifying organisms represented by diatoms and dinoflagellates, as inferred from the occurrence of C_{25} HBI alkanes and thiophenes, and TA dinosteroids, respectively. The frequent presence of conifer-derived biomarkers (e.g. simonellite, retene) and angiosperm-derived oleanane in the Nechit section suggests a constant admixture of terrigenous OM in the Vrancea domain. Differences in biomarker assemblages between the analysed sections must reflect different primary environmental conditions controlled by bioproductivity, in turn linked to the distinctive positions of the Vrancea and Tarcău sub-basins in the Early Oligocene. According to the 17α H/S ratio (Table 1, Fig. 12), high TOC (av. 3.5 wt%) and HI (av. 385 mg HC/g rock; Wendorff et al., 2017) values, the primary production remained constantly higher in the Vrancea domain compared to the Tarcău sub-basin during the deposition of the Menilite facies. Such an intense bioproductivity imprint and the presence of higher plant biomarkers in this section could be linked to the Vrancea domain's proximity to the land, where nutrient availability would favour the proliferation of marine organisms (Fig. 15). The episodes of freshwater flux are implied here by the high MTTC ratio, indicating decreased salinity conditions, especially during the deposition of the Bituminous Marls Mb. At that time, the combination of salinity-induced stratification and enhanced productivity could have occurred. This was suggested for the Western Paratethys at the end of the Early Oligocene when the Dynow Formation was deposited (NP23; Schulz et al., 2005). This scenario is consistent with rather shallow to moderate water depths, strong terrestrial supply, and high transport energy in the Vrancea basin, as postulated by Miclăuş et al. (2009). These authors based their interpretation on the presence of sandstones with hummocky cross-stratification (also see Filipek, 2020), and the identification of a well-preserved fossilised flat fish in the Bituminous Marls Mb. (Baciu and Chanet, 2002). It has been suggested that during the Early Oligocene, the Vrancea sub-basin was located in the vicinity of an at least partly emerged forebulge with an active deltaic system. This was supported by the mineralogical composition of quartzarenites, indicating detrital input from the Eastern European Platform (Miclăuş et al., 2009) and the occurrence of a polygenic conglomerate with extra-basinal clasts (Amadori et al., 2012). Moreover, the dinoflagellate cysts' assemblages with co-occurring *Deflandrea*

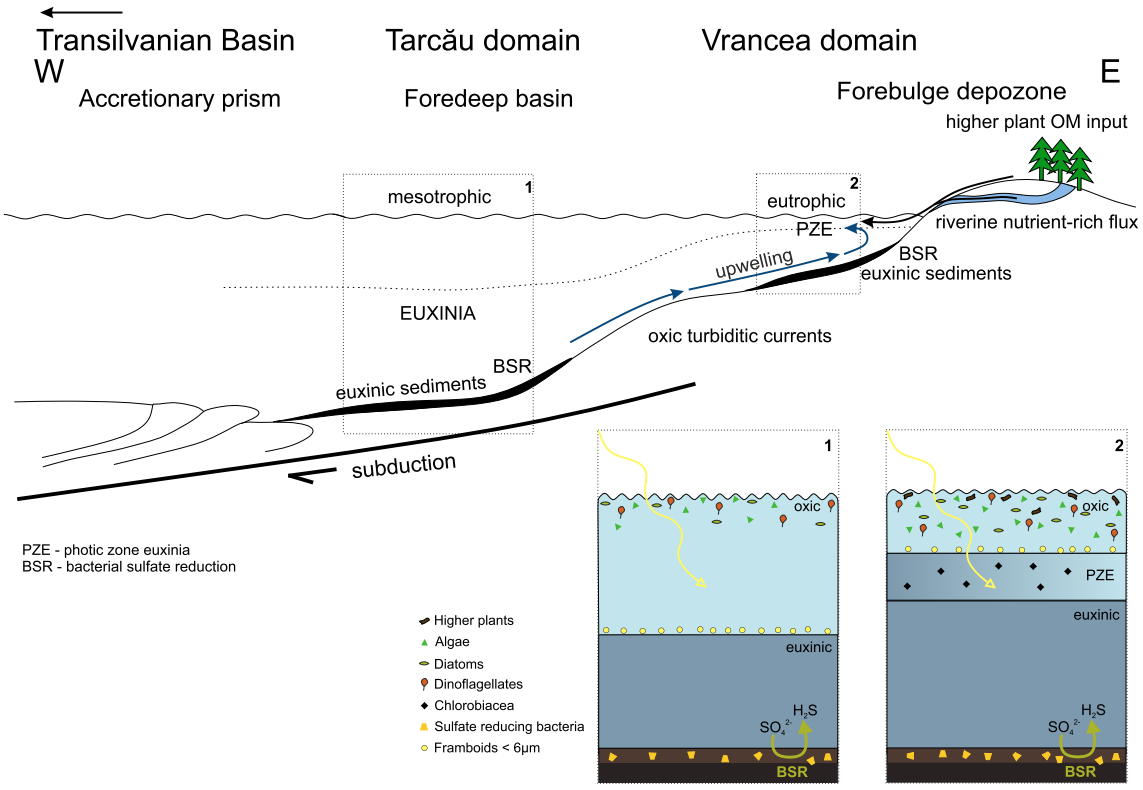

Fig. 15. Schematic model of the depositional conditions in the Nechit and Tarcău sub-basins. (1) and (2) are simplified models of the water column stratification and OM producers in both sub-basins.

spp. and *Wetzeliella* spp. identified by Sachsenhofer et al. (2015) in the Bituminous Marls Mb. may point to a nutrient-rich near-shore setting, if we exclude their transport into deeper water environments (Sachsenhofer et al., 2015). Similarly, Filipek (2020) implied near-shore conditions in the Vrancea sub-basin, based on the presence of cuticle fragments and algae tolerant of low-salinity conditions in the Menilite shales from the Vrancea Nappe. In contrast, Amadori et al. (2012) assumed a (hemi-) pelagic depositional environment for the Bituminous Marls Mb., similarly to Miclăuş and Schieber (2014), suggesting relatively deep water conditions with strong bottom current activity.

In contrast, the Tărcuţa section is characterised by high 17α H/S ratio, low TAR values, the absence of higher plant biomarkers (except for oleanane) and, in general, lower TOC (av. 1.9 wt%) and HI (av. 270 mg HC/g rock; Wendorff et al., 2017) values. The Tarcău sub-basin may thus represent a mesotrophic open-marine environment during the Early Oligocene (Fig. 15). In such a setting, a limitation in the productivity of sterol synthesising organisms would be related to restriction in the nutrient supply at the open sea. The deep water conditions in the Tarcău domain were also proposed by Ţabără (2017) who suggested, based on palynological studies, that the Lower Menilite and Bituminous Marls Mbs were deposited in the distal suboxic–anoxic basin. Similarly, a (hemi-) pelagic environment was proposed by Amadori et al. (2012) for the Bituminous Marls Mb.

Despite the differences in the productivity characterising both sub-basins, it is tempting to conclude that the net ecosystem production in the Early Oligocene was very high, as it is supported by remarkably abundant pyrite and generally high TOC content in the analysed Menilite facies. Primary organic production is represented by the total sedimentary organic carbon plus sedimentary pyrite, with the latter resulting from the transformation of OM to reduced sulfur (Schlesinger and Bernhardt, 2013).

High preservation potential during OM deposition was probably an effect of the water column stratification in the isolated basin, with the bottom water anoxia extending higher towards the chemocline, as indicated by the tiny pyrite framboids populations in both sections. However, our biomarker data imply fluctuations of redox conditions with a prevalence of dysoxic environment. This may suggest the occasional oxidation of bottom waters linked to upwellings, although less distinct than those during the late Rupelian and Chattian (Kotlarczyk and Uchman, 2012). Upwelling as a main process causing anoxia and high bioproductivity in the Central Paratethys in the Early Oligocene has been postulated by some authors (e.g. Vetö, 1987; Koltun, 1992; Soták, 2010). However, Kotlarczyk and Uchman (2012) demonstrated that in the Skole Basin, considered as a prolongation of the Tarcău sub-basin, upwelling anoxia developed in the late Rupelian and Chattian (NP24–NP25), that is, after the deposition of the Bituminous Marls Mb. Nevertheless, we cannot exclude that the less common local upwelling was present during the deposition of the Menilite facies in the studied part of the Paratethys. In the case of the Vrancea sub-basin, presumably located in the marginal part of the Central Paratethys, the local coastal upwelling combined with terrigenous nutrient supply and an elevated productivity seems possible. The phenomenon of coastal upwelling is commonly observed in modern shelf environments (e.g. Peru offshore), and has also been reported from ancient basins (e.g. Permian Phosphoria Formation; Maughan, 1993). In addition to upwelling, another possibility for recurring oxygenation for such restricted sub-basins might be periodic saline inflow events at depth, as in the recent Baltic Sea (e.g. Mohrholz et al., 2006, 2015). For instance, in the Gotland Deep the occasional replenishing of anoxic bottom waters with more saline, oxygen-rich North Sea water occurs over timescales of decades (Franck et al., 1987; Mohrholz et al., 2015).

Interestingly, euxinic conditions could have periodically reached the photic zone in the Vrancea sub-basin during the deposition of the Lower Menilite Mb., as supported by the occurrence of aryl isoprenoids and Me, *i*-Bu maleimides. The PZE could have been triggered by a nutrient-rich freshwater flux into the isolated basin, enhancing primary production and finally eutrophication. Individualisation of the sub-basins favouring the accumulation and preservation of OM can be clearly linked to the

widely recognised Paratethys isolation starting at the Eocene/Oligocene boundary (Báldi, 1980; Rögl, 1998; Popov et al., 2010). The model of a topographically restricted semi-isolated basin affected by tectonic activity causing variable sea-floor morphology has been suggested for the Oligocene Carpathian foredeep basin (e.g. Miclăuş et al., 2009; Jankowski and Probulski, 2011; Guerrera et al., 2012). In such a setting, the development of smaller domains (e.g. the Vrancea and Tarcău sub-basins) differing in terms of productivity, salinity, water column structure and so forth seems plausible. To test this model, however, more integrated case studies along the basin axis should be undertaken.

7. Conclusions

New molecular data from the Early Oligocene cross-sections from the Vrancea and Tarcău Nappes enabled a detailed reconstruction of the sedimentary conditions over this time period in the Vrancea and Tarcău sub-basins of the Central Paratethys. Well preserved biomarker assemblages indicate OM contribution from mainly marine algal-bacterial communities, while minor and varying terrigenous admixture characterises exclusively the Vrancea domain. The remarkable differences in molecular composition of the Menilite facies between the analysed sections reflect some primary environmental conditions controlled by productivity, in turn related to the nutrient availability in the Vrancea and Tarcău sub-basins. Variations in paleoproductivity and terrigenous OM input imprinted in the biomarker signatures and bulk geochemical data (TOC, HI) imply distinct positions of both sub-basins within the Central Paratethys. The Vrancea sub-basin would therefore represent a temporarily eutrophic, shallower setting, where extensive algal biomass accumulations were likely caused by eutrophication triggered by a nutrient-rich riverine input. In the Tarcău basin mesotrophic, open marine conditions with limited nutrient-availability developed.

Reduced sulfur sequestration proceeded mainly via pyrite formation in the water column, supported by highly abundant pyrite framboids in the studied rocks. The sulfur incorporation into OM affected diatom-derived HBI precursors (forming C_{25} HBI thiophenes) probably already in the water column, whereas DBT and its alkyl homologues formed during late diagenesis.

The isolation of the Paratethys, starting at the Eocene/Oligocene boundary, was associated with persistent water column euxinia, as is revealed by the dominating populations of small pyrite framboids. On the other hand, the suboxic/oxic conditions suggested by some molecular redox markers (Pr/Ph, HHI) probably reflect the early diagenesis of algal precursor molecules in oxygenated surface waters (e.g. by photodegradation). Intermittent PZE was limited to the Vrancea sub-basin and was probably linked to the freshwater incursions and upwelling of nutrient-rich water masses. In the open marine Tarcău basin, euxinia persistently occurred deeper below the photic zone.

Declaration of competing interest

The authors declare that they have no known competing financial interests or personal relationships that could have appeared to influence the work reported in this paper.

Acknowledgements

The authors are grateful to Anna Lewandowska and Robert Loręc for their help during the field campaign, and to Lucyna Bobrek for the foraminifera preparation. Ewa Malata is kindly acknowledged for the foraminifera assignment, and especially for her constructive comments on the manuscript. The careful reviews by Volker Thiel, James McEvoy and one anonymous journal reviewer have greatly improved the paper. Financial support was provided by the Jagiellonian University (Projects For Young Scientists No. DS/MND/WBiNoZ/ING/13/2014 and DS/MND/WBiNoZ/ING/14/2015).

Appendix A. Supplementary data

Supplementary data to this article can be found online at https://doi.org/10.1016/j.marpetgeo.2021.105037.

CRediT author statement

Małgorzata Wendorff-Belon: Conceptualization, Investigation, Writing – original draft, Visualization. Mariusz Rospondek: Conceptualization, Writing – original draft, Supervision. Leszek Marynowski: Writing – review & editing, Supervision, Resources.

References

Alexander, R., Larcher, A.V., Kagi, R.I., Price, P., 1988. The use of plant-derived biomarkers for correlation of oils with source rocks in the Cooper/Eromanga Basin system, Australia. APEA J. 28, 310–328.
Amadori, M.L., Belayouni, H., Guerrera, F., Martín-Martín, M., Martín-Rojas, I., Miclăuş, C., Raffaelli, G., 2012. New data on the Vrancea nappe (moldavidian basin, outer carpathian domain, Romania): paleogeographic and geodynamic reconstructions. Int. J. Earth Sci. 101, 1599–1623.
Ando, T., Sawada, K., Okano, K., Takashima, R., Nishi, H., 2017. Marine primary producer community during the mid-Cretaceous oceanic anoxic events (OAEs) 1a, 1b and 1d in the Vocontian Basin (SE France) evaluated from triaromatic steroids in sediments. Org. Geochem. 106, 13–24.
Baciu, D.S., Chanet, B., 2002. Les Poissons plats fossiles (Teleostei: pleuronectiformes) de l'Oligocene de Piatra Neamţ (Roumanie). ORYCTOS 4, 17–38.
Báldi, T., 1980. The early history of the Paratethys. Földt. Közl. Bulletin of the Hungarian Geological Society 110, 456–472.
Bechtel, A., Movsumova, U., Strobl, S.A.I., Sachsenhofer, R.F., Soliman, A., Gratzer, R., Püttmann, W., 2013. Organofacies and paleoenvironment of the Oligocene Maikop series of angeharan (eastern Azerbaijan). Org. Geochem. 56, 51–67.
Bechtel, A., Movsumova, U., Pross, J., Gratzer, R., Coric, S., Sachsenhofer, R.F., 2014. The Oligocene Maikop series of Lahich (eastern Azerbaijan): paleoenvironment and oil–source rock correlation. Org. Geochem. 71, 43–59.
Belayouni, H., di Staso, A., Guerrera, F., Martín-Martín, M., Miclauş, C., Serrano, F., Tramontana, M., 2009. Stratigraphic and geochemical study of the organic-rich black shales in the Tarcău nappe of the moldavidian domain (carpathian chain, Romania). Int. J. Earth Sci. 98, 157–176.
Bessereau, G., Roure, F., Kotarba, M., Kuśmierek, J., Strzetelski, W., 1997. Structure and hydrocarbon habitat of the polish Carpathians. In: Ziegler, P.A., Horvfith, F. (Eds.), Peri-Tethys Mémoir 2 – Structure and Prospects of Alpine Basins and Forelands. Mémoires du Muséum National d'Histoire Naturelle, Paris, pp. 343–373.
Blumer, M., Thomas, D.W., 1965. Zamene," Isomeric C_{19} monoolefins from marine zooplankton, fishes, and mammals. Science 148, 370–371.
Blumer, M., Mullin, M.M., Thomas, D.W., 1963. Pristane in zooplankton. Science 140, 974.
Bond, D.P.G., Wignall, P.B., 2010. Pyrite framboid study of marine Permian–Triassic boundary sections: a complex anoxic event and its relationship to contemporaneous mass extinction. Geol. Soc. Am. Bull. 122, 1265–1279.
Bourbonniere, R.A., Meyers, P.A., 1996. Sedimentary geolipid records of historical changes in the watersheds and productivities of Lakes Ontario and Erie. Limnol. Oceanogr. 41, 352–359.
Brassell, S.C., Comet, P.A., Eglinton, G., Isaacson, P.J., McEvoy, J., Maxwell, J.R., Thompson, I.D., Tibbetts, P.J.C., Volkman, J.K., 1980. The origin and fate of lipids in the Japan Trench. In: Douglas, A.G., Maxwell, J.R. (Eds.), Advances in Organic Geochemistry, 1979. Pergamon Press, Oxford, pp. 375–392.
Bray, E.E., Evans, E.D., 1961. Distribution of *n*-paraffins as a clue to recognition of source beds. Geochem. Cosmochim. Acta 22, 2–15.
Brocks, J.J., Grosjean, E., Logan, G.A., 2008. Assessing biomarker syngeneity using branched alkanes with quaternary carbon (BAQCs) and other plastic contaminants. Geochem. Cosmochim. Acta 72, 871–888.
Brocks, J.J., Jarrett, A.J.M., Sirantoine, E., Kenig, F., Moczydłowska, M., Porter, S., Hope, J., 2016. Early sponges and toxic protists: possible sources of cryostane, an age diagnostic biomarker antedating Sturtian Snowball Earth. Geobiology 14, 129–149.
Brooks, J.D., Gould, K., Smith, J.W., 1969. Isoprenoid hydrocarbons in coal and petroleum. Nature 222, 257–259.
Bădescu, D., 2005. Evoluţia Tectono-Stratigrafică a Carpaţilor Orientali În Decursul Mezozoicului Şi Neozoicului. Editura Economică, Bucharest, p. 312.
Bąk, K., 1999. Late Oligocene foraminifera from the Krosno beds in the san valley section (Bieszczady mountains); silesian unit, polish outer Carpathians. Ann. Soc. Geol. Pol. 69, 195–217.
Cicha, I., Rögl, F., Rupp, Ch, Ctyroka, J., 1998. Oligocene – Miocene foraminifera of the Central Paratethys. Abhandlungen der Senckenbergischen Naturforschenden Gesellschaft, vol. 549. Verlag Waldemara Kramer, Frankfurt a M, p. 325.
Coates, R.C., Podell, S., Korobeynikov, A., Lapidus, A., Pevzner, P., Sherman, D.H., Allen, E.E., Gerwick, L., William, H., Gerwick, W.H., 2014. Characterization of cyanobacterial hydrocarbon composition and distribution of biosynthetic pathways. PloS One 9 (1), e85140. https://doi.org/10.1371/journal.pone.0085140.
Cohen, K.M., Finney, S.C., Gibbard, P.L., Fan, J.-X., 2013. The ICS international chronostratigraphic chart. Episodes 36, 199–204.

Connan, J., 1974. Diagenese naturelle et diagenèse artificielle de la matière organique à éléments végétaux dominants. In: Tissot, B., Bienner, F. (Eds.), Advances in Organic Geochemistry, 1973. Editions Technic, Paris, pp. 73–95.
Curiale, J.A., 1987. Steroidal hydrocarbons of the kishenehn formation, northwest Montana. Org. Geochem. 11, 233–244.
De Stiger, H.C., Jorissen, F.J., Van der Zwaan, G.J., 1998. Bathymetric distribution and micohabitat partitioning of life (Rose Bengal stained) benthic foraminifera along a shelf to deep sea transect in the southern Adriatic Sea. J. Foraminifer. Res. 28, 40–65.
DeCelles, P.G., Giles, K.A., 1996. Foreland basin systems. Basin Res. 8, 105–123.
Dembitsky, V.M., Dor, I., Shkrob, I., Aki, M., 2001. Branched alkanes and other apolar compounds produced by the cyanobacterium Microcoleus vaginatus from the Negev Desert. Russ. J. Bioorg. Chem. 27, 110–119.
Didyk, B.M., Simoneit, B.R.T., Brassell, S.C., Eglinton, G., 1978. Organic geochemical indicators of paleoenvironmental conditions of sedimentation. Nature 272, 216–222.
Dunlop, R.W., Jefferies, P.R., 1985. Hydrocarbons of the hypersaline basins of shark Bay, western Australia. Org. Geochem. 8, 216–222.
Dustira, A.M., Wignall, P.B., Joachimski, M., Blomeier, D., Hartkopf-Fröder, C., Bond, D. P.G., 2013. Gradual onset of anoxia across the permian–triassic boundary in svalbard, Norway. Palaeogeogr. Palaeoclimatol. Palaeoecol. 374, 303–313.
Eglinton, G., Hamilton, R.J., 1967. Leaf epicuticular waxes. Science 156, 1322–1335.
Ellis, L., Singh, R.K., Alexander, R., Kagi, R.I., 1996. Formation of isohexyl alkylaromatic hydrocarbons from aromatization-rearrangement of terpenoids in the sedimentary environment—a new class of biomarker. Geochem. Cosmochim. Acta 60, 4747–4763.
Ficken, K.J., Li, B., Swain, D.L., Eglinton, G., 2000. An n-alkane proxy fort the sedimentary input of submerged/floating freshwater aquatic macrophytes. Org. Geochem. 31, 745–749.
Filipek, A., 2020. Palynofacies analysis, sedimentology and hydrocarbon potential of the menilite beds (Oligocene) in the slovakian and Romanian outer Carpathians. Geol. Q. 64, 589–610. https://doi.org/10.7306/gq.1541.
Franck, H., Matthäus, W., Sammler, R., 1987. Major inflows of saline water into the Baltic Sea during the present century. Gerlands Beiträge zur Geophysik 96, 517–531.
Froitzheim, N., Plašienka, D., Schuster, R., 2008. Alpine tectonics of the Alps and western Carpathians. In: McCann, T. (Ed.), The Geology of Central Europe. Volume 2. Mesozoic and Cenozoic. Geological Society, London, pp. 1141–1232.
Galeotti, S., DeConto, R., Naish, T., Stocchi, P., Florindo, F., Pagani, M., Barrett, P., Bohaty, S.M., Lanci, L., Pollard, D., Sandroni, S., Talarico, F.M., Zachos, J.C., 2016. Antarctic ice sheet variability across the Eocene-Oligocene boundary climate transition. Science 352, 76–80.
Gedl, P., 2000. Biostratigraphy and palaeoenvironment of the Podhale Palaeogene (Inner Carpathians, Poland) in the light of palynological studies. Part II. Summary and systematic descriptions. Stud. Geol. Pol. 117, 155–303.
Gelpi, E., Schneider, H., Mann, J., Oró, J., 1970. Hydrocarbons of geochemical significance in microscopic algae. Phytochemistry 9, 603–612.
Giner, J.-L., Zhao, H., Boyer, G.L., Satchwell, M.F., Andersen, R.A., 2009. Sterol chemotaxonomy of marine Pelagophyte algae. Chem. Biodivers. 6, 1111–1130.
Golonka, J., Gahagan, L., Krobicki, M., Marko, F., Oszczypko, N., Ślączka, A., 2006. Plate tectonic evolution and paleogeography of the circum Carpathian region. Am. Assoc. Pet. Geol. Mem. 84, 395–442.
Goossens, H., de Leeuw, J.W., Schenck, P.A., Brassell, S.C., 1984. Tocopherols as likely precursors of pristane in ancient sediments and crude oils. Nature 312, 440–442.
Grabenstatter, J., Méhay, S., McIntyre-Wressnig, A., Giner, J.-L., Edgcomb, V.P., Beaudoin, D.J., Bernhard, J.M., Summons, R.E., 2013. Identification of 24-*n*-propylidenecholesterol in a member of the foraminifera. Org. Geochem. 63, 145–151.
Grantham, P.J., Wakefield, L.L., 1988. Variations in the sterane carbon number distribution of marine source rocks derived crude oils through geological time. Org. Geochem. 12, 61–74.
Grasu, C., Catană, C., Grinea, D., 1988. Carpathian flysch: petrography and economic evaluations. Editura Tehnica, Bucureşti 1–208 (in Romanian).
Grasu, C., Miclăuş, C., Brânzilă, M., Boboş, I., 2002. The Sarmatian from the foreland basin systems of the Eastern Carpathians. Editura Tehnica, Bucureşti 1–407 (in Romanian).
Grice, K., Gibbson, R., Atkinson, J.E., Schwark, L., Eckardt, C.B., Maxwell, J.R., 1996. Maleimides (1H-pyrrole-2,5-diones) as molecular indicators of anoxygenic photosynthesis in ancient water column. Geochem. Cosmochim. Acta 60, 3913–3924.
Grice, K., Schaeffer, P., Schwark, L., Maxwell, J.R., 1997. Changes in palaeoenvironmental conditions during deposition of the Permian Kupferschiefer (Lower Rhine Basin, N.W. Germany) from variations in isotopic compositions of biomarker components. Org. Geochem. 26, 677–690.
Grice, K., Schouten, S., Nissenbaum, A., Charrach, J., Sinninghe Damsté, J.S., 1998. A remarkable paradox: sulfurised freshwater algal (*Botryococcus braunii*) lipids in an ancient hypersaline euxinic ecosystem. Org. Geochem. 28, 195–216. https://doi.org/10.1016/S0146-6380(97)00127-7.
Guerrera, F., Martín-Martín, M., Martín-Pérez, J.A., Martín-Rojas, I., Miclăuş, C., Serrano, F., 2012. Tectonic control on the sedimentary record of the central moldavidian basin (eastern Carpathians, Romania). Geol. Carpathica 63, 463–479.
Haczewski, G., 1989. Poziomy wapieni kokkolitowych w serii menilitowo-krośnieńskiej - rozróżnianie, korelacja i geneza. Ann. Soc. Geol. Pol. 59, 435–523 (in Polish).
Hartgers, W.A., Koopmans, M.P., Sinninghe Damsté, J.S., de Leeuw, J.W., 1993. Sedimentary evidence for a diaromatic carotenoid with an unprecedented aromatic substitution pattern. J. Chem. Soc. D Chem. Commun. 23, 1715–1716.
Hautevelle, Y., Michels, R., Malartre, F., Trouiller, A., 2006. Vascular plant biomarkers as proxies for palaeoflora and palaeoclimatic changes at the Dogger/Malm transition of the Paris Basin (France). Org. Geochem. 37, 610–625.
Huang, W.-Y., Meinschein, W.G., 1979. Sterols as ecological indicators. Geochem. Cosmochim. Acta 43, 739–745.
Hughes, W.B., Holba, A.G., Dzou, L.I.P., 1995. The ratios of dibenzothiophene to phenanthrene and pristane to phytane as indicators of depositional environment and lithology of petroleum source rocks. Geochem. Cosmochim. Acta 59, 3581–3598.
Jaffé, R., Mead, R., Hernandez, M., Peralba, M., DiGuida, O., 2001. Origin and transport of sedimentary organic matter in two subtropical estuaries: a comparative, biomarker-based study. Org. Geochem. 32, 507–526. https://doi.org/10.1016/S0146-6380(00)00192-3.
Jankowski, L., Probulski, J., 2011. Tectonic and basinal evolution of the Outer Carpathians based on example of geological structure of the Grabownica, Strachocina and Łodyna hydrocarbon deposits (in Polish with English summary). Geologia 37, 555–583.
Kaczmarska, I., Kilarski, W., 1979. The structure of Melosira sulcate (Ehr.) Kütz. var. sulcata frustules from Lower Oligocene diatomites from Futoma (Carpathians, Poland). Ann. Soc. Geol. Pol. 49, 185–194.
Kaneda, T., 1991. Iso-fatty and anteiso-fatty acids in bacteria – biosynthesis, function, and taxonomic significance. Microbiol. Rev. 55, 288–302.
Kenig, F., Sinninghe Damsté, J.S., Kock-van Dalen, A.C., Rijpstra, W.I.C., Huc, A.Y., de Leeuw, J.W., 1995. Occurrence and origin of mono-, di-, and tri-methylalkanes in modern and Holocene cyanobacterial mats from Abu Dhabi, United Arab Emirates. Geochem. Cosmochim. Acta 59, 2999–3015.
Kissin, Y.V., 1987. Catagenesis and composition of petroleum: origin of *n*-alkanes and *iso*alkanes in petroleum crudes. Geochem. Cosmochim. Acta 51, 2445–2457.
Kok, M.D., Rijpstra, Irene C., Robertson, L., Volkman, J.K., Sinninghe Damsté, J.S., 2000. Early steroid sulfurisation in surface sediments of a permanently stratified lake (Ace Lake, Antarctica). Geochem. Cosmochim. Acta 64, 1425–1436.
Kokinos, J.P., Eglinton, T.I., Goñi, M.A., Boon, J.J., Martoglio, P.A., Anderson, D.M., 1998. Characterization of a highly resistant biomacromolecular material in the cell wall of a marine dinoflagellate resting cyst. Org. Geochem. 28, 265–288.
Koltun, Y.V., 1992. Organic matter in Oligocene Menilite Formation rocks of the Ukrainian Carpathians: palaeoenvironment and geochemical evolution. Org. Geochem. 18, 423–430.
Koopmans, M.P., Köster, J., van Kaam-Peters, H.M.E., King, F., Schouten, S., Hartgers, W. A., de Leeuw, J.W., Sinninghe Damsté, J.S., 1996a. Diagenetic and catagenetic products of isorenieratene: molecular indicators for photic zone anoxia. Geochem. Cosmochim. Acta 60, 4467–4496.
Koopmans, M.P., Schouten, S., Kohnen, M.E.L., Sinninghe Damsté, J.S., 1996b. Restricted utility of aryl isoprenoids as indicators for photic zone anoxia. Geochem. Cosmochim. Acta 60, 4873–4876.
Kosakowski, P., 2013. 1D mod el ling of hydrocar bon generation and expulsion from Oligocene Menilite source rocks in the San and Stryi rivers region (Polish and Ukrainian Carpathians). Geol. Q. 57, 307–324.
Kosakowski, P., Koltun, Y., Machowski, G., Poprawa, P., Papiernik, B., 2018. The geochemical characteristics of the Oligocene – lower Miocene Menilite Formation in the polish and Ukrainian outer Carpathians: a review. J. Petrol. Geol. 41, 319–336.
Köster, J., Kotarba, M., Lafargue, E., Kosakowski, P., 1998a. Source rock habitat and hydrocarbon potential of Oligocene Menilite Formation (Flysch Carpathians, Southeast Poland): an organic geochemical and isotope approach. Org. Geochem. 29, 543–558.
Köster, J., Rospondek, M., Schouten, S., Kotarba, M., Zubrzycki, A., Sinninghe Damsté, J. S., 1998b. Biomarker geochemistry of a Foreland Basin: the Oligocene Menilite Formation in the flysch Carpathians of southeast Poland. Org. Geochem. 29, 649–669.
Kotarba, M.J., Więcław, D., Koltun, Y.V., Marynowski, L., Kuśmierek, J., Dudok, I.V., 2007. Organic geochemical study and genetic correlation of natural gas, oil and Menilite source rocks in the area between San and Stryi rivers (Polish and Ukrainian Carpathians). Org. Geochem. 38, 1431–1456.
Kotlarczyk, J., Uchman, A., 2012. Integrated ichnology and ichthyology of the Oligocene Menilite Formation, Skole and subsilesian nappes, polish Carpathians: a proxy to oxygenation history. Palaeogeography, Palaeoclimatology, Palaeoecology 331– 332, 104–118.
Krézsek, C., Bally, A.W., 2006. The Transylvanian Basin (Romania) and its relation to the Carpathian fold and thrust belt: insights in gravitational salt tectonics. Mar. Petrol. Geol. 23, 405–442.
Kruge, M.A., Mastalerz, M., Solecki, A., Stankiewicz, B.A., 1996. Organic geochemistry and petrology of oil source rocks, Carpathian Overthrust region, southeastern Poland: implications for petroleum generation. Org. Geochem. 24, 897–912.
Lafargue, E., Ellouz, N., Roure, F., 1994. Thrust-controlled exploration plays in the outer Carpathians and their foreland (Poland, Ukraine and Romania). First Break 12, 69–79.
Laflamme, R.E., Hites, R.A., 1979. Tetra- and pentacyclic, naturally-occurring, aromatic hydrocarbons in recent sediments. Geochem. Cosmochim. Acta 43, 1687–1691.
Laskarev, V., 1924. Sur les equivalents du Sarmatien superieur en Serbie. In: Vujević, P. (Ed.), Receuil de traveaux offert à M. Jovan Cvijic par ses amis et collaborateurs. Drzhavna Shtamparija, Beograd, pp. 73–85.
Li, M., Larter, S.R., Taylor, P., Jones, D.M., Bowler, B., Bjoroy, M., 1995. Biomarkers or not biomarkers? A new hypothesis for the origin of pristane involving derivation from methyltrimethyltridecylchromans (MTTCs) formed during diagenesis from chlorophyll and alkylphenols. Org. Geochem. 23, 159–167.
Ma, A., Zhang, S., Zhang, D., 2008. Ruthenium ion-catalyzed oxidation of asphaltenes of heavy oils in Lunnan and Tahe oilfields in Tarim Basin, NW China. Org. Geochem. 39, 1502–1511.

Marzi, R., Torkelson, B.E., Olson, R.K., 1993. A revised carbon preference index. Org. Geochem. 20, 1303–1306.
Maughan, E.K., 1993. Phosphoria Formation (permian) and its resource significance in the western interior, USA. In: Presented at the CSPG Pangeo: Global Environment and Resources Conference, Calgary, August 15-19.
Melinte, M., 1995. Changes in nannofossil assemblages during the oligocene–lower Miocene interval in the east Carpathians and transylvania. Rom. J. Stratigr. 76, 171–172.
Melinte, M.C., 2005. Oligocene palaeoenvironmental changes in the Romanian Carpathians, revealed by calcareous nannofossils. Stud. Geol. Pol. 124, 341–352.
Melinte-Dobrinescu, M., Brustur, T., 2008. Oligocene – lower Miocene events in Romania. Acta Palaeontologica Romaniae 6, 203–215.
Menounos, P., Staphylakis, K., Gegiou, D., 1986. The sterols of *Nigella sativa* seed oil. Phytochemistry 25, 761–763.
Metzger, P., Largeau, C., 2006. *Botryococcus braunii*: a rich source for hydrocarbons and related ether lipids. Appl. Microbiol. Biotechnol. 66, 486–496.
Micläuş, C., Schieber, J., 2014. A hierarchy of current-produced bedforms in a source rock from the Eastern Carpathians points to predominant bedload deposition of an organic-rich mudstone. In: AAPG Annual Convention and Exhibition. Houston, Texas, April 6–9, 2014. Search and Discovery Article #51006(2014).
Micläuş, C., Loiacono, F., Puglisi, D., Baciu, D.S., 2009. Eocene-oligocene sedimentation in the external areas of the moldavide basin (marginal folds nappe, eastern Carpathians, Romania): sedimentological, paleontological and petrographic approaches. Geol. Carpathica 60, 397–417.
Mohrholz, V., Mohrholz Dutz, J., Gerd Kraus, G., 2006. The impact of exceptionally warm summer inflow events on the environmental conditions in the Bornholm Basin. J. Mar. Syst. 60, 285–301. https://doi.org/10.1016/j.jmarsys.2005.10.002.
Mohrholz, V., Naumann, M., Nausch, G., Krüger, S., Gräwe, U., 2015. Fresh oxygen for the Baltic Sea – an exceptional saline inflow after a decade of stagnation. J. Mar. Syst. 148, 152–166. https://doi.org/10.1016/j.jmarsys.2015.03.005.
Moldowan, J.M., Dahl, J., Huizinga, B.J., Fago, F.J., Hickey, L.J., Peakman, T.M., Taylor, D.W., 1994. The molecular fossil record of oleanane and its relation to angiosperms. Science 265, 768–771.
Murgeanu, G., Mirăută, O., 1968. Geological Map of Romania, Scale 1:200 000, Sheet 13 Piatra Neamţ. Institutul Geologic al României, Bucureşti.
Naeher, S., Schaeffer, P., Adam, P., Schubert, C.J., 2013. Maleimides in recent sediments — using chlorophyll degradation products for palaeoenvironmental reconstructions. Geochem. Cosmochim. Acta 119, 248–263.
Nytoft, H.P., Bojesen-Koefoed, J.A., Christiansen, F.G., Fowler, M.G., 2002. Oleanane or lupane? Reappraisal of the presence of oleanane in Cretaceous–Tertiary oils and sediments. Org. Geochem. 33, 1225–1240.
Oaie, Gh, Seghedi, A., Rădan, S., Vaida, M., 2005. Sedimentology and source area composition for the Neoproterozoic-Eocambrian turbidites from East Moesia. Geol. Belg. 8, 78–105.
Obermajer, M., Fowler, M.G., Snowdon, L.R., Macqueen, R.G., 2000. Compositional variability of crude oils and source kerogen in the Silurian carbonate-evaporite sequences of the eastern Michigan Basin, Ontario, Canada. Bull. Can. Petrol. Geol. 48, 307–322.
Olszewska, B., 1982. Some remarks on biostratigraphy of the menilite-krosno series in the polish outer Carpathians. (In polish, English summary). Kwart. Geol. 26, 137–145.
Olszewska, B., Odrzywolska-Bieńkowa, E., Giel, M.D., Pożaryska, K., Szczechura, J., 1996. Atlas skamieniałości przewodnich i charakterystycznych; Rząd Foraminiferida. (In Polish). In: Malinowska, L., Piwocki, M. (Eds.), Budowa Geologiczna Polski, Tom 3, Kenozoik, Paleogen. Polska Agencja Ekologiczna, Warszawa, pp. 45–215.
Otto, A., Simoneit, B.R.T., 2001. Chemosystematics and diagenesis of terpenoids in fossil conifer species and sediment from the Eocene Zeitz formation, Saxony, Germany. Geochem. Cosmochim. Acta 65, 505–3527.
Ourisson, G., Albrecht, P., Rohmer, M., 1979. The hopanoids: palaeochemistry and biochemistry of a group of natural products. Pure Appl. Chem. 51, 709–729.
Pancost, R.D., Crawford, N., Maxwell, J.R., 2002. Molecular evidence for basin-scale photic zone euxinia in the Permian Zechstein Sea. Chem. Geol. 188, 217–227.
Perry, G.J., Volkman, J.K., Johns, R.B., Bavor Jr., H.J., 1979. Fatty acids of bacterial origin in contemporary marine sediments. Geochem. Cosmochim. Acta 43, 1715–1725.
Peters, K.E., Moldowan, J.M., 1991. Effects of source, thermal maturity, and biodegradation on the distribution and isomerization of homohopanes in petroleum. Org. Geochem. 17, 47–61.
Peters, K.E., Walters, C.C., Moldowan, J.M., 2005. The Biomarker Guide: Interpreting Molecular Fossils in Petroleum and Ancient Sediments. Prentice-Hall, New Jersey.
Pfennig, N., 1978. General physiology and ecology of photosynthetic bacteria. In: Clayton, R.K., Sistrom, W.R. (Eds.), Photosynthetic Bacteria. Plenum, New York, pp. 3–16.
Philp, R.P., 1985. Fossil Fuel Biomarkers. Applications and Spectra. Elsevier, Amsterdam, p. 294.
Popov, S.V., Stolyarov, A.S., 1996. Paleogeography and anoxic environments of the oligocene–early Miocene Paratethys. Isr. J. Earth Sci. 45, 161–167.
Popov, S.V., Rögl, F., Rozanov, A.Y., Steininger, F.F., Shcherba, I.G., Kovač, M., 2004. Lithological-paleogeographic Maps of Paratethys–10 MAPS Late Eocene to Pliocene, vol. 250. Courier Forschungsinstitut Senckenberg, Frankfurt, p. 46.
Popov, S.V., Antipov, M.P., Zastrozhnov, A.S., Kurina, E.E., Pinchuk, T.N., 2010. Sea-level fluctuations on the northern shelf of the eastern Paratethys in the oligocene-neogene. Stratigr. Geol. Correl. 18, 200–224.
Powell, T.G., McKirdy, D.M., 1973. Relationship between ratio of pristane to phytane, crude oil composition and geological environment in Australia. Nature 243, 37–39.
Rathburn, A.E., Corliss, B.H., 1994. The ecology of living (stained) deep-sea benthic foraminifera from the Sulu Sea. Paleoecology 9, 87–150.
Rauball, J.F., Sachsenhofer, R.F., Bechtel, A., Coric, S., Gratzer, R., 2019. The oligocene–miocene Menilite Formation in the Ukrainian Carpathians: a world-class source rock. J. Petrol. Geol. 42, 393–416.
Remin, Z., Dubicka, Z., Kozłowska, A., Kuchta, B., 2012. A new method of rock disintegration and foraminiferal extraction with the use of liquid nitrogen [LN2]. Do conventional methods lead to biased paleoecological and paleoenviromental interpretations? Mar. Micropaleontol. 86–87, 11–14.
Rieley, G., Collier, R.J., Jones, D.M., Eglinton, G., Eakin, P.A., Fallick, A.E., 1991. Sources of sedimentary lipids deduced from stable carbon-isotope analyses of individual compounds. Nature 352, 425–427.
Robinson, N., Eglinton, G., Brassell, S., Cranwell, P.A., 1984. Dinoflagellate origin for sedimentary 4α-methylsteroids and 5α(H)-stanols. Nature 308, 419–422.
Rögl, F., 1998. Palaeogeographic consideration for mediterranean and Paratethys seaways (Oligocene to Miocene). Annalen des Naturhistorischen Museum in Wien 99A, 279–310.
Rohmer, M., Bisseret, P., Neunlist, S., 1992. The hopanoids, prokaryotic triterpenoids and precursors of ubiquitous molecular fossils. In: Moldowan, J.M., Albrecht, P., Philp, R.P. (Eds.), Biological Markers in Sediments and Petroleum. Prentice-Hall, Englewood Cliffs, NJ, pp. 1–17.
Rontani, J.F., Baillet, G., Aubert, C., 1991. Production of acyclic isoprenoid compounds during the photodegradation of chlorophyll a in sea water. J. Photochem. Photobiol. Chem. 59, 369–377.
Rospondek, M.J., Köster, J., Sinninghe Damsté, J.S., 1997. Novel C26 highly branched isoprenoid thiophenes and alkane from the Menilite Formation, Outer Carpathians, southeast Poland. Org. Geochem. 26, 295–304.
Rowland, S.J., Robson, J.N., 1990. The widespread occurrence of highly branched acyclic C_{20}, C_{25} and C_{30} hydrocarbons in recent sediments and biota – a review. Mar. Environ. Res. 30, 191–216.
Rusu, A., Popescu, G., Melinte, M., 1996. Oligocene–Miocene transition and main geological events in Romania. Excursion Guide of IGCP Project No. 326. Rom. J. Stratigr. 76, 3–47.
Sachsenhofer, R.F., Hentschke, J., Bechtel, A., Ćorić, S., Gratzer, R., Gross, D., Horsfield, B., Rachetti, A., Soliman, A., 2015. Hydrocarbon potential and depositional environments of oligo-miocene rocks in the eastern Carpathians (Vrancea nappe, Romania). Mar. Petrol. Geol. 68, 269–290.
Sachsenhofer, R.F., Popov, S.V., Ćorić, S., Mayer, J., Misch, D., Morton, M.T., Pupp, M., Rauball, J., Tari, G., 2018. Paratethyan petroleum source rocks: an overview. J. Petrol. Geol. 41, 219–246.
Schlesinger, W.H., Bernhardt, E.S., 2013. Biogeochemistry: an Analysis of Global Change, third ed. Elsevier, p. 688.
Schouten, S., Bowman, J.P., Rijpstra, W.I.C., Sinninghe Damsté, J.S., 2000. Sterols in a psychrophilic methanotroph, *Methylosphaera hansonii*. FEMS (Fed. Eur. Microbiol. Soc.) Microbiol. Lett. 186, 193–195.
Schulz, H.-M., Sachsenhofer, R.F., Bechtel, A., Polesny, H., Wagner, L., 2002. The origin of hydrocarbon source rocks in the Austrian Molasse Basin (Eocene-Oligocene transition). Mar. Petrol. Geol. 19, 683–709.
Schulz, H.-M., Bechtel, A., Sachsenhofer, R.F., 2005. The birth of the Paratethys during the early Oligocene: from Tethys to an ancient Black Sea analogue? Global Planet. Change 49, 163–176.
Schwark, L., Püttmann, W., 1990. Aromatic hydrocarbon composition of the permian kupferschiefer in the lower rhine basin, NW Germany. Org. Geochem. 16, 749–761.
Schwark, L., Vliex, M., Schaeffer, P., 1998. Geochemical characterization of malm zeta laminated carbonates from the franconian alb, SW-Germany (II). Org. Geochem. 29, 1921–1952.
Shiea, J., Brassell, S.C., Ward, D.M., 1990. Midchain branched monomethyl and dimethyl alkanes in hot-spring cyanobacterial mats – a direct biogenic source for branched alkanes in ancient sediments. Org. Geochem. 15, 223–231.
Simoneit, B.R.T., 1985. Cyclic terpenoids in the geosphere. In: Johns, R.B. (Ed.), Methods in Geochemistry and Geophysics, vol. 25. Elsevier, pp. 43–99.
Simoneit, B.R.T., Grimalt, J.O., Wang, T.G., Cox, R., Hatcher, P.G., Nissenbaum, A., 1986. Cyclic terpenoids of contemporary resinous plant detritus and of fossil woods, ambers and coals. Org. Geochem. 10, 877–889.
Sinninghe Damsté, J.S., de Leeuw, J.W., 1990. Analysis, structure and geochemical significance of organically-bound sulphur in the geosphere: state of the art and future research. In: Durand, B., Behar, F. (Eds.), Advances in Organic Geochemistry 1989, vol. 16. Organic Geochemistry, pp. 1077–1101.
Sinninghe Damsté, J.S., Kock-Van Dalen, A.C., De Leeuw, J.W., Schenck, P.A., Guoying, S., Brassell, S.C., 1987. The identification of mono-, di- and trimethyl 2-methyl-2-(4,8,12-trimethyltridecyl)chromans and their occurrence in the geosphere. Geochem. Cosmochim. Acta 51, 2393–2400.
Sinninghe Damsté, J.S., Rijpstra, W.I.C., Kock-van Dalen, A.C., de Leeuw, J.W., Schenck, P.A., 1989. Quenching of labile functionalised lipids by inorganic sulphur species: evidence for the formation of sedimentary organic sulphur compounds at the early stages of diagenesis. Geochem. Cosmochim. Acta 53, 1343–1355.
Sinninghe Damsté, J.S., Keely, B.J., Betts, S.E., Baas, M., Maxwell, J.R., de Leeuw, J.W., 1993. Variations in abundances and distributions of isoprenoid chromans and long-chain alkylbenzenes in sediments of the Mulhouse Basin: a molecular sedimentary record of palaeosalinity. Org. Geochem. 20, 1201–1215.
Smolarek, J., Marynowski, L., Trela, W., Kujawski, P., Simoneit, B.R.T., 2017. Redox conditions and marine microbial community changes during the end-Ordovician mass extinction event. Global Planet. Change 149, 105–122.
Soták, J., 2010. Paleoenvironmental changes across the eocene-oligocene boundary: insights from the central-carpathian Paleogene basin. Geol. Carpathica 61, 393—418. https://doi.org/10.2478/v10096-010-0024-1.

Stefănescu, M., Popescu, I., Ivan, V., Melinte, M., Stănescu, V., 1993. Aspects of the possibilities of the lithological correlation of oligocene–lower Miocene deposits of the Buzău valley. Rom. J. Stratigr. 75, 83–91.
Stefanova, M., Oros, D.R., Otto, A., Simoneit, B.R.T., 2002. Polar aromatic biomarkers in the Miocene Maritza-East lignite, Bulgaria. Org. Geochem. 33, 1079–1091.
Summons, R.E., Powell, T.G., 1987. Identification of aryl isoprenoids in source rocks and crude oils: biological markers for the green sulphur bacteria. Geochem. Cosmochim. Acta 51, 557–566.
Summons, R.E., Barrow, R.A., Capton, R.J., Hope, J.M., 1993. The structure of a new C_{25} isoprenoid alkene biomarker from diatomaceous microbial communities. Aust. J. Chem. 46, 407–413.
Săndulescu, M., 1984. Geotectonica romaniei, 1–336. Editura Tehnică, Bucureşti.
Săndulescu, M., 1988. Cenozoic tectonic history of the Carpathians. In: Royden, L.H., Horvath, F. (Eds.), The Pannonian Basin: A Study in Basin Evolution, vol. 45. AAPG Memoir, pp. 17–25.
Săndulescu, M., Micu, M., 1989. Oligocene paleogeography of the east Carpathians. In: Ghergari, L., et al. (Eds.), The Oligocene from the Transylvanian Basin, pp. 79–86. Cluj-Napoca.
ten Haven, H.L., Lafargue, E., Kotarba, M., 1993. Oil/oil and oil/source rock correlations in the Carpathian Foredeep and overthrust, south-east Poland. Org. Geochem. 20, 935–959.
Thiel, V., Jenisch, A., Worheide, G., Lowenberg, A., Reitner, J., Michaelis, W., 1999. Mid-chain branched alkanoic acids from "living fossil" demosponges: a link to ancient sedimentary lipids? Org. Geochem. 30, 1–14.
Tulipani, S., Grice, K., Greenwood, P., Schwark, L., 2013. A pyrolysis and stable isotopic approach to investigate the origin of methyltrimethyltridecylchromans (MTTCs). Org. Geochem. 61, 1–5.
Tulipani, S., Grice, K., Greenwood, P.F., Haines, P.W., Sauer, P.E., Schimmelmann, A., Summons, R.E., Foster, C.B., Böttcher, M.E., Playton, T., Schwark, L., 2015a. Changes of palaeoenvironmental conditions recorded in Late Devonian reef systems from the Canning Basin, Western Australia: a biomarker and stable isotope approach. Gondwana Res. 28, 1500–1515.
Tulipani, S., Grice, K., Greenwood, P.F., Schwark, L., Böttcher, M.E., Summons, R.E., Foster, C.B., 2015b. Molecular proxies as indicators of freshwater incursion-driven salinity stratification. Chem. Geol. 409, 61–68.
van Aarssen, B.G.K., Alexander, R., Kagi, R.I., 2000. Higher plant biomarkers reflect palaeovegetation changes during Jurassic times. Geochem. Cosmochim. Acta 64, 1417–1424.
Vetö, I., 1987. An Oligocene sink for organic carbon: upwelling in the Paratethys? Palaeogeogr. Palaeoclimatol. Palaeoecol. 60, 143–153.
Volkman, J.K., 1986. A review of sterols of marine and terrigenous organic matter. Org. Geochem. 9, 83–99.
Volkman, J.K., 2003. Sterols in microorganisms. Appl. Microbiol. Biotechnol. 60, 495–506.
Volkman, J., 2005. Sterols and other triterpenoids: source specificity and evolution of biosynthetic pathways. Org. Geochem. 36, 139–159.
Volkman, J.K., Kearney, P., Jeffrey, S.W., 1990. A new source of 4-methyl sterols and 5a (H)-stanols in sediments: prymnesiophyte microalgae of the genus *Pavlova*. Org. Geochem. 15, 489–497.
Volkman, J.K., Barrett, S.M., Dunstan, G.A., 1994. C_{25} and C_{30} highly branched isoprenoid in laboratory cultures of two marine diatoms. Org. Geochem. 21, 407–414.
Volkman, J.K., Barrett, S.M., Blackburn, S.I., Mansour, M.P., Sikes, E.L., Gelin, F., 1998. Microalgae biomarkers: a review of recent research developments. Org. Geochem. 29, 1163–1179.
Wakeham, S.G., Amann, R., Freeman, K.H., Hopmans, E.C., Jorgensen, B.B., Putnam, I.F., Schouten, S., Sinninghe Damsté, J.S., Talbot, H.M., Woebken, D., 2007. Microbial ecology of the stratified water column of the Black Sea as revealed by a comprehensive biomarker study. Org. Geochem. 39, 2070–2097.
Wang, T.-G., He, F., Wang, Ch, Zhang, W., Wang, J., 2008. Oil filling history of the Ordovician oil reservoir in the major part of the Tahe Oilfield, Tarim Basin, NW China. Org. Geochem. 39, 1637–1646.
Wang, L., Song, Z., Yin, Q., George, S.M., 2011. Paleosalinity significance of occurrence and distribution of methyltrimethyltridecyl chromans in the upper Cretaceous Nenjiang Formation, Songliao Basin, China. Org. Geochem. 42, 1411–1419.
Wei, H., Algeo, T.J., Yu, H., Wang, J., Guo, C., Shi, G., 2015. Episodic euxinia in the Changhsingian (late Permian) of South China: evidence from framboidal pyrite and geochemical data. Sediment. Geol. 319, 78–97.
Wendorff, M., Rospondek, M., Kluska, B., Marynowski, L., 2017. Organic matter maturity and hydrocarbon potential of the lower Oligocene menilite facies in the eastern flysch Carpathians (Tarcău and Vrancea nappes), Romania. Appl. Geochem. 78, 295–310.
Wignall, P.B., 2005. The link between large igneous province eruptions and mass extinctions. Elements 1, 293–297.
Wignall, P.B., Newton, R., 1998. Pyrite framboid diameter as a measure of oxygendeficiency in ancient mudrocks. Am. J. Sci. 298, 537–552.
Wilkin, R.T., Arthur, M.A., 2001. Variations in pyrite texture, sulfur isotope composition, and iron systematics in the Black Sea: evidence for Late Pleistocene to Holocene excursions of the O_2-H_2S redox transition. Geochem. Cosmochim. Acta 65, 1399–1416.
Wilkin, R.T., Barnes, H.L., 1997. Formation processes of framboidal pyrite. Geochem. Cosmochim. Acta 61, 323–339.
Wilkin, R.T., Barnes, H.L., Brantley, S.L., 1996. The size distribution of framboidal pyrite in modern sediments: an indicator of redox conditions. Geochem. Cosmochim. Acta 60, 3897–3912.
Wilkin, R.T., Arthur, M.A., Dean, W.E., 1997. History of water-column anoxia in the Black Sea indicated by pyrite framboid size distributions. Earth Planet Sci. Lett. 148, 517–525.
Zachos, J.C., Quinn, T.M., Salamy, K.A., 1996. High-resolution (104 years) deep-sea foraminiferal stable isotope records of the Eocene-Oligocene climate transition. Paleoceanography 11, 251–266.
Zuber, R., 1902. Neue karpathenstudien. Jahrbuch der Kaiserlich Königlichen Geologischen Reichsanstalt 52, 245–258.
Ţabără, D., 2017. Dinoflagellate cysts stratigraphy and palynofacies of Oligocene sequences in the northern eastern Carpathians. Acta Palaeontologica Romaniae 13, 49–63.

Publikacja 3

Wendorff-Belon, M., Loręc, R., Wierzbicki, A., Rospondek, M., Marynowski, L., 2025. Oligocene environmental changes in the Central Paratethys: geochemical and palynofacial record from the north-western Transylvanian Basin (Romania). Palaeogeography, Palaeoclimatology, Palaeoecology 676, 113124.

Palaeogeography, Palaeoclimatology, Palaeoecology 676 (2025) 113124

Contents lists available at ScienceDirect

Palaeogeography, Palaeoclimatology, Palaeoecology

journal homepage: www.elsevier.com/locate/palaeo

Oligocene environmental changes in the Central Paratethys: Geochemical and palynofacial record from the north-western Transylvanian Basin (Romania)

Małgorzata Wendorff-Belon [a,*], Robert Loręc [b], Adam Wierzbicki [b], Mariusz Rospondek [b], Leszek Marynowski [c]

[a] Oil and Gas Institute-National Research Institute, ul. Lubicz 25a, 31-503 Kraków, Poland
[b] Institute of Geological Sciences, Jagiellonian University, ul. Gronostajowa 3a, 30-387 Kraków, Poland
[c] Faculty of Natural Sciences, University of Silesia, ul. Będzińska 60, 41-200 Sosnowiec, Poland

ARTICLE INFO

Editor: Rebecca L. Totten

Keywords:
Biomarkers
Palynofacies
Rock-Eval
euxinia
Oligocene
Transylvanian Basin
Paratethys

ABSTRACT

The Oligocene succession exposed at Fântânele village in the north-western Transylvanian Basin (Romania), composed of the Ileanda and Vima formations, was deposited in a semi-closed Central Paratethys domain. Foraminiferal associations and lithology revealed the Late Rupelian (NP 24) and Late Rupelian-Chattian (NP 24/25) ages for these formations.

The analysed organic matter, particularly abundant in the black shales of the Ileanda Formation, is of low thermal maturity (T_{max} ~ 420 °C, R_o ~ 0.4 %). Thus, it has not reached the hydrocarbon generation stage. The Ileanda Formation contains mainly Type II kerogen, reflecting a period of increased marine phytoplankton production driven primarily by diatoms (high C_{28} steranes and HBIs) and dinoflagellates (4-methyldiasterenes and dinoflagellate cysts), with bacteria playing a lesser role. The Vima Formation shows a more significant influence of terrestrial inputs, evidenced by Type II/III and III kerogen, a high share of phytoclasts, and substantial amounts of angiosperm- and conifer-derived biomarkers.

High primary bioproductivity combined with basin deepening in the Rupelian resulted in water column stratification and subsequent enhanced organic matter preservation imprinted by high TOC, hydrogen index values, and steranes/hopanes ratios in the Ileanda Formation. Low Pr/Ph ratio (mostly <1), higher contents of aryl isoprenoids, the occurrence of sulfurised highly branched isoprenoids, and a high proportion (86–96 %) of tiny pyrite framboids point to permanent anoxia/euxinia in the sea floor expanding higher, at least intermittently, into the photic zone. At the Late Rupelian/Chattian transition, the depositional setting changed to an outer shelf characterised by normal-marine conditions with oxygen-deficient bottom water. Later in the Chattian, shorter episodes of anoxia/euxinia related to freshwater incursions and subsequent salinity stratification are evidenced by pronounced input of higher plant-derived organic matter recorded in the uppermost part of the Vima Formation.

The findings highlight the role of regional tectonic activity in the Transylvanian Basin and its implications for understanding the hydrocarbon potential of similar basins in the region.

1. Introduction

The Transylvanian Basin (TB) is a major sedimentary basin and one of south-eastern Europe's most important hydrocarbon provinces (e.g., Ionescu, 1994). In the Oligocene, it was a part of the marginal Paratethys domain (Laskarev, 1924; Rögl, 1998), called an anoxic giant (Palcu and Krijgsman, 2023). This large marginal sea stretched from the Rhone Basin in the west to the Tarim Basin in the east (Fig. 1A). It consisted of a tectonically active region with minor, shorter-lived basins called Western Paratethys (western Alpine foreland basin) and Central Paratethys (e.g., Popov et al., 2004; Kováč et al., 2016), and a tectonically stable region around the Black Sea – Caspian Sea basins forming the Eastern Paratethys (Popov et al., 2019). Recurring isolation of the Paratethys from the global ocean and internal changes in marine gateways

* Corresponding author.
E-mail address: wendorff-belon@inig.pl (M. Wendorff-Belon).

https://doi.org/10.1016/j.palaeo.2025.113124
Received 13 January 2025; Received in revised form 2 July 2025; Accepted 5 July 2025
Available online 11 July 2025

configuration in the Oligocene, as well as concurrent climate cooling continuing from the terminal Eocene (Zachos et al., 2001), favoured the development of brackish episodes, with endemic fauna represented by, e.g., mollusks (e.g., Baldi, 1986; Popov et al., 1993; Popov and Studencka, 2015) and calcareous nannoflora (e.g., Melinte, 2005). Organic-rich rocks were, in turn, extensively deposited in the entire Paratethys, providing the source for large hydrocarbon deposits (e.g., Rögl, 1999; Popov et al., 2008). These specific rocks are represented by the Oligocene Menilite Formation (Fm.) in the Outer Carpathians, the Tard Clay Fm. in the Pannonian Basin, and the less prominent Ileanda Fm. in the TB, as well as the Oligocene-Miocene Maikop Fm. in the Black Sea and Caspian Sea region. Their lithofacial and geochemical heterogeneity, as well as diachronous sedimentation, result in a very complex and site-specific depositional history. Nonetheless, these rocks provide a detailed archive of the paleoenvironmental changes in the Oligocene/-Miocene Paratethys basin governed by the complex interplay of local and global tectonic activity and eustatic and climatic fluctuations.

Despite the widespread interest of researchers in many Paratethys' basins, e.g., the Carpathian (e.g., Golonka et al., 2006 and references therein) or the Pannonian basins (e.g., Bechtel et al., 2012; Ozsvárt et al., 2016), there is a limited number of studies concerning the TB in the wider context of the Paratethys paleogeographic and paleoenvironmental evolution in the Oligocene (Melinte-Dobrinescu and Brustur, 2008; Székely and Filipescu, 2016; Kallanxhi et al., 2018; Bojanowski et al., 2018). Moreover, two hydrocarbon (HC) plays have been distinguished in the TB so far: the Paleogene one with minor oil occurrences and a few possible source rock formations, and the Neogene one with Miocene-Pliocene source rocks for almost all discovered gas deposits (Stefanescu et al., 2006). The Oligocene sediments with organic-rich black shales of the Ileanda Formation may represent potential source rocks for the Paleogene HC system.

Our study presents data from comprehensive organic petrographic (palynofacies analysis, vitrinite reflectance), molecular (biomarkers), and bulk geochemical (Rock-Eval pyrolysis, elemental C, S) analyses of the Oligocene (Upper Rupelian-Chattian) succession outcropping in the Fântânele village in NW TB, Romania. Our principal aim was to recognise environmental conditions and sources of organic matter (OM) captured during this specific time of the Paratethys evolution. Moreover, we have also determined the OM maturity and HC potential of the Oligocene succession from the Fântânele section. Despite their possible HC potential, the Oligocene rocks from the Fântânele section have been scarcely investigated (Popescu, 1995; De Broucker et al., 1998), and, as far as we know, no molecular approach has been presented to the public.

2. Geological setting and sampled section

The TB is a sedimentary basin located in the south-eastern part of the larger alpine Carpathian-Pannonian orogenic system. This system developed at the western margin of the Eurasian Plate involving at least two smaller lithospheric blocks, the Tisza–Dacia and the ALCAPA blocks (Balla, 1987 Csontos, 1995) (Fig. 2). In its present configuration the TB has a sub-circular form and is surrounded by the Carpathians in the east and south, by the Apuseni Mountains in the west, and the Preluca–Țicău metamorphic massifs to the north (Fig. 2). From the tectonic point of view, it has an upper plate position with respect to the Carpathian subduction system. It developed on top of the Middle Cretaceous basement nappes (internal Carpathians). The TB comprises tectonosedimentary megasequences extending from the Upper Cretaceous to the Upper Miocene (Krézsek and Bally, 2006). The Oligocene, mainly siliciclastic sediments, belong to the Paleogene megasequence deposited during one of the sag stages of the Carpathian orogen evolution (Krézsek and Bally, 2006). In general, the deepening of the basin from SW

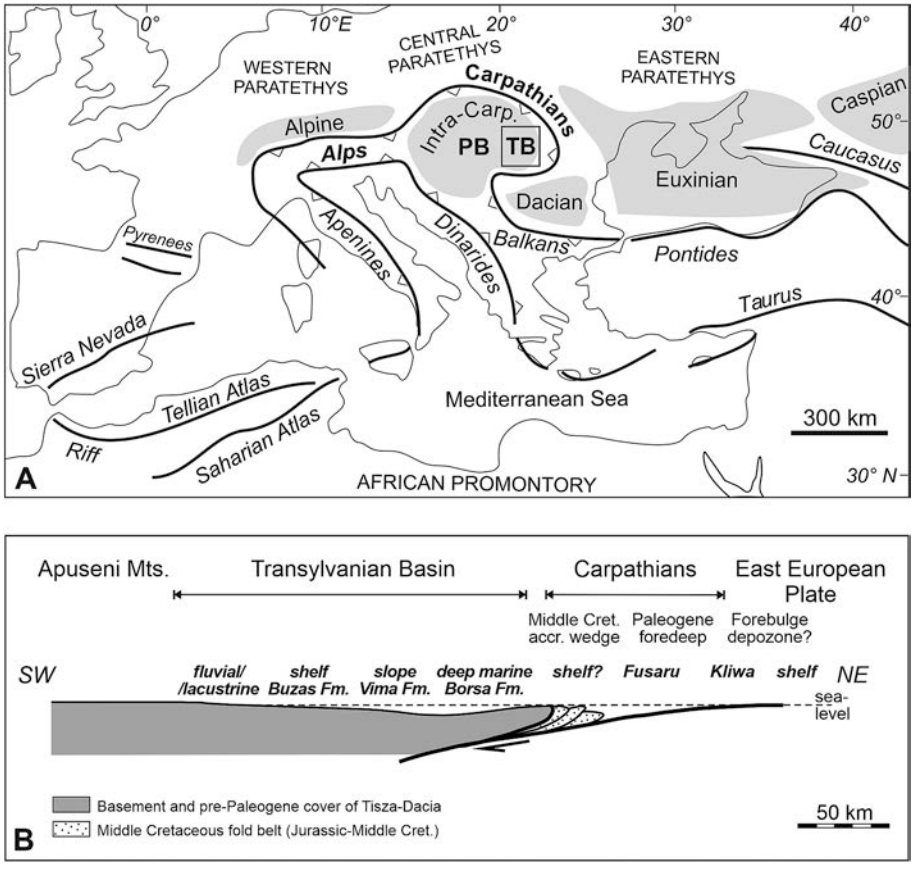

Fig. 1. (A) Overview of the Paratethys basin systems with the Transylvanian Basin (TB) and the Pannonian Basin (PB) belonging to the Central Paratethys, (B) Reconstructed Oligocene paleogeography on the regional cross-section of the TB and the Carpathians foredeep (after Krézsek and Bally, 2006).

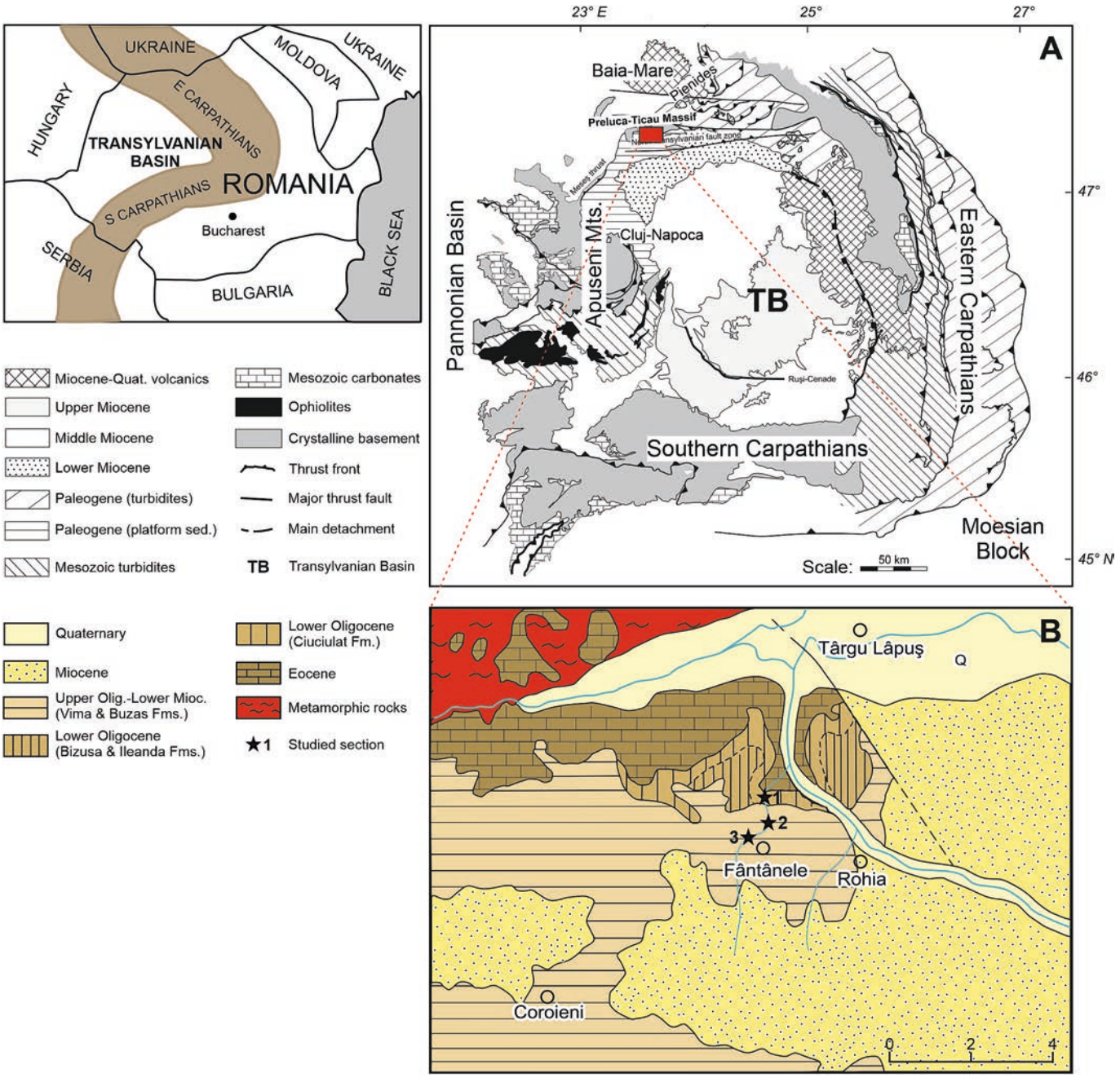

Fig. 2. (A) Geological map of the Transylvanian Basin and surroundings with the location of the study area marked as a red rectangle (modified after Krézsek and Bally, 2006). (B) Detailed geological map of the investigated area with sampled sections marked as asterisks (after Giuşcă and Rădulescu, 1967). (For interpretation of the references to colour in this figure legend, the reader is referred to the web version of this article.)

towards NE is reflected by the laterally changing lithofacial record. In the Early Oligocene (Rupelian), most of the southern part of the basin was exposed, while the inner and outer shelf environments dominated the central part of the basin. Towards the north, a deeper marine slope with outer and middle fan settings prevailed (e.g., Dicea et al., 1980). The Upper Rupelian–Chattian (Upper Oligocene) sequence, locally onlapping the Lower Rupelian unconformity, consists of lowstand and transgressive depositional settings with widespread anoxic sequences (Ileanda, Valea Carelor, and Dâncu-Tamasa Fms). At that time, a major regional drowning event occurred, creating a new east-west trending basin, resulting in the strongly transgressive character of the Upper Rupelian (De Broucker et al., 1998; Ciulavu et al., 2000). The Chattian is mainly siliciclastic and overall progradational with widespread continental environments characterised by a clastic input from the northwest (De Broucker et al., 1998; Popescu, 2021). This trend was linked to the basement uplift and tilting, and subsequent deposition of continental to shallow marine sandstone wedge (Buzaş Fm.; Fig. 1B), passing laterally to the outer shelf (Vima Fm.).

The study area is located in the NW TB within the Preluca area, named after the adjacent crystalline massif. In this part of the basin, the Oligocene-Lower Miocene marine succession is continuous and available for studies in a few locations, including Fântânele village (referred to below as the Fântânele section). The Rupelian/Chattian boundary was determined in the monotonous Vima Fm. based on calcareous nannofossils (Kallanxhi et al., 2018) and foraminiferal assemblages (Székely and Filipescu, 2015). The Oligocene/Miocene transition (Chattian/Aquitanian; NP25/NN1 Calcareous Nannoplankton Zone of Martini, 1971) is placed in the higher part of the Vima Fm. (Mészáros

et al., 1979; Rusu et al., 1996; Melinte-Dobrinescu and Brustur, 2008). Within the Fântânele section, the occurrence of two finely laminated isochronous coccolith limestone horizons, namely the Tylawa and Jasło limestones, was previously reported by Melinte-Dobrinescu and Brustur (2008) and Bojanowski et al. (2018). These limestone horizons display well-documented marker beds throughout the Outer Carpathians (e.g., Koszarski and Żytko, 1959; Haczewski, 1989; Melinte, 2005; Ciurej and Haczewski, 2012), the TB (Melinte-Dobrinescu and Brustur, 2008; Bojanowski et al., 2018) and even the Caucasus (Nagymarosy and Voronina, 1992). The Tylawa Limestone was deposited in the Early Oligocene (NP23 zone; Krhovský, 1981), whereas the Jasło horizon represents the Rupelian-Chattian transition (NP24 zone; Krhovský, 1981; Bąk, 2005; Švábenická et al., 2007).

3. Material and methods

3.1. Studied section and samples

The Fântânele section (Fig. 2B) is located along the Fântânele Creek in the village of the same name, southeast of Baia Mare (Fig. 2A), and it consists of three small outcrops. In total, 34 samples (F1-F34) were collected at 1–2 m intervals, depending on the heterogeneity of the outcropping rocks. The first outcrop (GPS: 47°24′58.3"N, 23°49′39.7″E), about 18 m thick, is represented by black, laminated shales (samples F1–F11) of the Ileanda Fm. with characteristic intercalation of a finely laminated Tylawa Limestone (F7). The lithology changes into grey marly mudstones (F12-F14) representing the Vima Fm. The second one (47°24′50.4"N, 23°49′35.1″E), outcropping about 200 m distance up the creek, consists of light and dark grey marly and silty mudstones

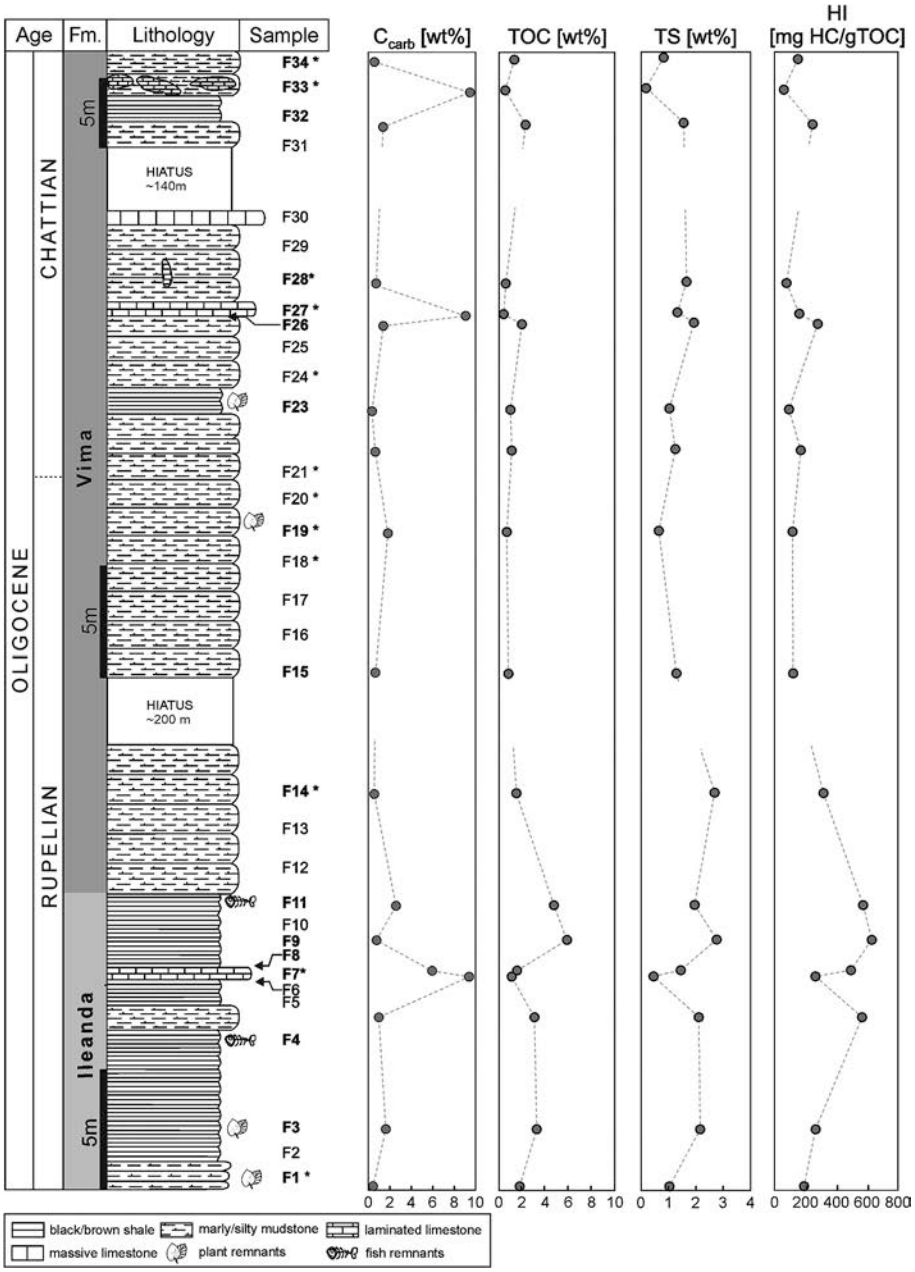

Fig. 3. Simplified lithostratigraphic column of the Fântânele section with sample positions and logs of selected parameters determined by elemental analysis and Rock-Eval pyrolysis. C_{carb} – carbonate carbon [wt%]; TOC – total organic carbon [wt%]; TS – total sulfur [wt%]; HI – hydrogen index [mg HC/g TOC]. Samples signed with an asterisk were processed for foraminiferal study; those marked in bold were used for palynofacial and geochemical analyses.

(F15–F30) of the Vima Fm. It is about 25 m thick with an intercalation of a finely laminated Jasło Limestone (F27), orange on weathered surfaces. Here, a thin intercalation of black shales occurs (F23) and a distinct massive limestone/dolostone layer (F30). The third outcrop (GPS: 47°24′42.6"N, 23°49′36.9″E), separated by a hiatus of about 140 m, is approx. 7.5 m thick and composed of mudstones (F31, F34), dark grey shales (F32), and a horizon of grey, nodular limestone/dolostone (F33). The composite lithostratigraphic profile with sample positions is presented in Fig. 3. The Rupelian/Chattian boundary was approximately determined based on the foraminiferal assemblage studies. The lithology determined during the fieldwork was confirmed using X-ray diffraction.

3.2. Methods

3.2.1. Pyrite framboids analysis

For pyrite framboid distribution analysis, the polished chips of thirteen samples (out of 34) were examined using a scanning electron microscope (FE-SEM; Hitachi S-4700 microscope, Jagiellonian University, Kraków) set in backscatter mode. At least 100 pyrite framboid diameters were measured per sample, and the size-frequency distribution was used to calculate mean and maximum framboid diameters and the standard deviation (SD), as well as the proportion of framboids with diameters smaller than 5 μm.

3.2.2. Vitrinite reflectance measurements

The same set of polished block samples was used for vitrinite reflectance (R_o) measurements with an AXIOPLAN II microscope (University of Silesia, Sosnowiec) using 546 nm light and immersion oil of refractive index 1.546 at a total magnification of 500. The standards used had R_o values of 0.898 %.

3.2.3. Palynofacial analysis

For the palynofacies analysis, thirteen samples were processed using a non-oxidative preparation procedure (Jagiellonian University, Kraków). About 40–50 g of cleaned and crushed material was treated with HCl (35–38 % vol.) and HF (40 % vol.) to remove carbonate and silicate phases, respectively. Samples were then carefully rinsed with deionised water several times and sieved (10 μm mesh). A heavy liquid (sodium polytungstate; 2.05 g/cm^3) with centrifugation separation was used to concentrate sedimentary organic matter (SOM) components. The received organic residuum was rinsed and sieved through a 10 μm mesh sieve. The obtained material was placed on slides using a mixture of glycerine and gelatine as a mounting medium. Microscopic observations were conducted using a Nikon Eclipse Ni polarizing microscope, coupled with a Prior Lumen 200 UV illumination system and a Prior Proscan III stage and controller, all equipped with a Nikon DS. Fi 1C camera, Nikon Digital Sight DS-U3 Camera Control Unit. An average of 1000 SOM components was counted per slide and grouped into twelve categories of palynofacies (see classification after Tyson, 1993, 1995; McArthur et al., 2016; Emmings et al., 2019; Filipek, 2020).

3.2.4. Foraminiferal assemblages analysis

Twelve samples were selected and processed for foraminiferal analysis (see Fig. 3). Each sample of about 300 g dry weight was disintegrated by a repeated freeze-thaw method, using a saturated solution of sodium sulfate ($Na_2SO_4 \times 10H_2O$) and then washed through a 63 μm mesh sieve and dried out. Residues were sieved into a few fractions (>0.063 mm), and each fraction was picked separately in a conventional manner. The samples were not quantitatively analysed. In those poor in foraminifera, the whole residue was checked, while in the others, a sufficient number of foraminifera was picked to determine their composition and biostratigraphy. Three samples were barren of any microfossils. All foraminiferal taxa identified in other samples are listed in Appendix A.

3.2.5. Elemental analysis

Eighteen samples were subjected to elemental analyses for total carbon and total sulfur (TS) content using a ThermoScientific Flash 2000 CHNS/O analyser (Oil and Gas Institute, Kraków). Total organic carbon (TOC) was measured with the same instrument on samples pre-treated with 10 % HCl at 50 °C until total carbonate decomposition. Total inorganic carbon (C_{carb}) was calculated by the difference.

3.2.6. Pyrolysis Rock-Eval

Rock-Eval pyrolysis was performed for the same samples using the Delsi Rock-Eval II Analyser following standard methods described by Espitalié et al. (1985) and Peters (1986). The S_2 (mg HC/g rock) peak was used to calculate the hydrogen index (HI = S_2 x 100/TOC [mg HC/g TOC]). The temperature at which S_2 reaches its maximum (T_{max}) was applied as a maturity parameter (Espitalié and Bordenave, 1993).

3.2.7. Extraction and chromatographic separation

For biomarker composition, the same set of samples as for the Rock-Eval pyrolysis was used. To minimise the influence of weathering on geochemical results, the outer rims of the rock samples were cut off before milling. The interior parts were washed in acetone, dried, and pulverised. About 100 g of each sample was extracted with a dichloromethane/methanol mixture (DCM:MeOH, 7.5:1 vol.) using an accelerated solvent extractor Dionex ASE 350. Activated copper mesh was used for elemental sulfur removal. Obtained extracts were dried close to dryness in a rotary evaporator, and then asphaltenes were precipitated from an *n*-hexane solution by centrifugation. The *n*-hexane-soluble fractions (maltenes) were separated into aliphatic, aromatic, and polar fractions on a column packed with activated alumina (2 h at 150 °C) using solvents with increasing polarity. The aliphatic and aromatic fractions relevant to this study were eluted in three bed volumes of *n*-hexane and *n*-hexane/DMC (7:3 vol.), respectively. The polar fractions were eluted in DCM/MeOH (1:1 vol.). *n*-Eicos-1-ene (140 μg), 2-hexadecylthiophene (29.7 μg), and hexamethylbenzene (40.2 μg) were added to maltenes as internal standards prior to column chromatography.

3.2.8. Gas chromatography-mass spectrometry

The hydrocarbon fractions were analysed by an Agilent Technologies 7890 A gas chromatograph equipped with a 60 m HP-5MS fused silica capillary column (60 m × 0.32 mm, 0.25 μm film thickness) interfaced to an Agilent 5975C Network mass spectrometer 71 with a Triple-Axis Detector (University of Silesia, Sosnowiec). The oven temperature was programmed with a 40 °C constant for 3 min, then the temperature increased to 120 °C at 20 °C/min and from 120° to 300 °C at 3 °C/min, followed by an isothermal period of 60 min. Helium was used as a carrier gas. The mass spectrometer was operated in the electron impact mode and with a cycle time of 1 s in the scan range of *m/z* 50–700. Individual compounds were identified based on retention time in the total ion current chromatogram and comparison of the mass spectra with published data. Although the internal standards were added, absolute concentrations of different compounds or compound groups have given unsatisfactory results. The main reason was the significant difference in TOC contents associated with facial/lithological variations, generating significant errors when calculating the concentrations of individual samples. Instead, many indices were compared to trimethylated 2-methyl-2-(trimethyltridecyl)chroman, the common and usually dominant compound in all samples.

4. Results

4.1. Biostratigraphy

The analysed section consists of three intervals, i.e., the shaly organic-rich lowest part of the section corresponding to the Ileanda Fm., the monotonous muddy organic-lean middle part of the section corresponding to the lower interval of the Vima Fm., and the muddy/marly

uppermost part of the section corresponding to the upper interval of the Vima Fm. (Fig. 3). These apparent lithofacial variations reflect paleoenvironmental changes, further discussed in the work.

Ileanda Fm. is of Upper Rupelian age (upper part of NP23 zone), as can be deduced from the occurrence of the Tylawa Limestone interval (sample F7) and confirmed by the presence of the Rupelian foraminiferal assemblages above it (samples F14, F18, F19). The same age assignment for this interval, based on calcareous nannoplankton, was presented by Melinte-Dobrinescu and Brustur (2008). The boundary between the Rupelian and Chattian can be roughly situated within the monotonous marly mudstones of the Vima Fm. (F20-F21). In sample F20, the planktonic species *Bella rohiensis* (Popescu et Brotea) was noted (Appendix A), which, according to Spezzaferri et al. (2018), should be considered as *Quiltyella clavacella* (Rögl). Its stratigraphic range begins in the uppermost Rupelian (O4 Zone) and lasts until the Lower Miocene. Sample F21 yielded relatively most numerous planktonic foraminifera with such species as *Globigerinella megaperta* Rögl known from the Upper Rupelian (O3 Zone) till Lower Chattian (O5 Zone), *G. navazuelensis* (Molina) whose stratigraphic range is the uppermost Rupelian (O4 Zone) to Lower Miocene Zone M2 (Spezzaferri et al., 2018) and *Paragloborotalia opima* (Bolli) known from Upper Rupelian (O2 Zone) and displaying the highest occurrence at the O5/O6 zonal boundary (Leckie et al., 2018). Thus, the co-occurrence of the abovementioned species points to the uppermost Rupelian-lowermost Chattian age for this part of the Vima Fm. Slightly upper in the section, the presence of the Jasło Limestone (Lower Chattian, NP24 zone; Melinte-Dobrinescu and Brustur, 2008) would be consistent with the assumed Chattian age. The uppermost part of the Vima Fm. in the Fântânele section, based on our foraminiferal data, can be roughly estimated for the Chattian age, while Kallanxhi et al. (2014, 2018) point more precisely to the lower part of the NP25 zone.

4.2. Pyrite framboid diameter distribution

Statistical data of the pyrite framboid analyses are presented in Table 1. Pyrite framboids are very common in all the samples, especially in the shales of the Ileanda Fm., where the framboids <5 μm consist of 86 to 96 % of the framboid populations. Framboid diameters in the Vima Fm. samples are more diversified, with populations of tiny framboids (<5 μm) consisting of 13 to 95 % (Table 1).

4.3. Vitrinite reflectance

The measured R_o values vary from 0.37 % to 0.49 % (Table 2). The Ileanda Fm. reveals a mean R_o of 0.43 % and a mean SD of 0.17 %, whereas the Vima Fm. reveals 0.43 % and 0.15 %, respectively.

Table 1
Pyrite framboid diameter statistical data from the Fântânele section samples. Min, Max FD – the smallest/largest pyrite framboid diameter; SD – standard deviation; N – number of measurements; %F < 5 μm – the percentage of pyrite framboids with diameters lower than 5 μm.

Sample	MinFD [μm]	MaxFD [μm]	Mean [μm]	SD	N	% < 5 μm
Vima Formation						
F34	1.4	32.2	5.6	3.5	106	48
F32	1.0	10.0	3.4	1.3	134	95
F28	2.8	39.2	7.8	3.8	100	13
F26	1.0	14.0	3.5	2.0	165	88
F22	1.0	47.0	5.9	5.1	156	60
F19	2.4	53.4	8.0	5.5	122	21
F15	1.9	41.9	7.9	5.8	107	21
Ileanda Formation						
F11	1.3	12.0	3.3	1.4	118	96
F9	1.0	8.5	3.2	1.3	126	93
F8	0.5	6.5	3.0	1.3	152	95
F7	1.1	10.0	3.7	1.7	100	86
F4	0.5	10.5	3.3	1.7	142	91
F3	1.5	10.7	3.5	1.5	112	88

4.4. Palynofacies composition

In general, the preservation state of palynofacies components is diverse, from perfectly preserved to crushed and deformed. The relative abundances of each palynofacial group are reported in Table 3. Samples from the Ileanda Fm. are characterised by a high abundance of amorphous organic matter (AOM), revealing mainly granular structure with patchy fluorescence and numerous pyrites present, as well as yellowish to brownish colour in transmitted light (Fig. 4). The less abundant type of AOM is brown, homogenous, and often structureless. In a few samples, UV analysis revealed the presence of palynomorphs hosted within the AOM (e.g., sample F11; Fig. 4). The second most prominent components are those from the phytoclasts group, i.e., cuticle and translucent wood fragments. Pollens and spores were identified in notable abundances in F3, F4, and F11 samples (Table 3). In the lowest part of the section, dinoflagellate cysts in different preservation states were also identified (up to 4.6 %).

In the Vima Fm. AOM is still the most prominent group, represented mainly by heterogeneous and secondarily by opaque fragments (Table 3, Fig. 4). Phytoclasts (cuticles, translucent wood) gain importance and consist of up to 39.9 % (sample F34, Fig. 4F) of SOM. Samples from the uppermost part of the section are characterised by a higher abundance of well-preserved pollens (e.g., sample F26 in Fig. 4). Dinoflagellate cysts occur throughout the Vima Fm. in abundances around 2.2–4.7 %. Additionally, the rare presence of reworked freshwater algae, e.g., *Botryococcus* sp., was demonstrated by relatively weak fluorescence.

4.5. Elemental analysis and Rock-Eval data

The TOC, C_{carb}, TS and HI profiles are shown in Fig. 3. The results for the analysed samples are presented in Table 2. The siliceous dark shales of the Ileanda Fm. are OM- and sulfur-rich with low to moderate C_{carb} content (Table 2). Light grey and dark grey mudstones from the Vima Fm. contain av. 1.1 wt% TOC, 1.2 wt% TS and mostly less than 1 wt% of carbonates (Table 2). The three layers of carbonate-rich rocks (the Tylawa, Jasło, and nodular limestones/dolostones layers) exhibiting $C_{carb} \sim 10$ wt% are OM- and sulfur lean (Table 2).

HI data are highly variable, ranging from 60 to 630 mg HC/g TOC (Table 2, Fig. 3), while T_{max} values are generally around 420 °C. The highest values obtained for organic-lean samples (TOC < 1 wt%) should be treated with caution, as the mineral matrix error can affect the T_{max} results (Katz, 1983).

4.6. Biomarker composition

4.6.1. *n*-Alkanes and acyclic isoprenoids

n-Alkanes are prominent constituents of all the aliphatic fractions (Fig. 5) with carbon chain length typically from C_{13}-C_{14} to C_{33}, sporadically up to C_{35}. The predominance of the odd-numbered members is reflected by the carbon preference index (CPI; modified after Bray and Evans, 1961) in the range $CPI_{15–22}$ and $CPI_{23–32}$ values >1 for most of the samples (Table 2). Highly variable values among the samples were obtained for the terrestrial-to-aquatic ratio (TAR; Bourbonniere and Meyers, 1996) (Table 4).

The acyclic isoprenoids pristane (I; structures in Appendix A) and phytane (II) occur in all samples as the most abundant constituents of aliphatic fractions. The pristane to phytane ratio (Pr/Ph; Didyk et al., 1978) ranges from 0.5 to 6.9, with an increasing trend upward in the section (Table 4).

4.6.2. Highly branched isoprenoids (HBIs)

HBIs occurred commonly throughout the section and were identified by comparison of their mass spectra with those available in Sinninghe Damsté et al. (1989), Rospondek et al. (1997), and Kohnen et al. (1990).

Table 2
Selected elemental, pyrolysis Rock-Eval and biomarker maturity parameters throughout the Fântânele section showing very low thermal maturity. TOC = total organic carbon; TS = total sulfur; C_{carb} = carbonate carbon; HI = hydrogen index, T_{max} = temperature of maximum HC yield; C_{31}H S/(S + R) = C_{31} homohopane 22S/(22S + 22R) epimer ratio; C_{29}St S/(S + R) = C_{29} ααα sterane 20S/(20S + 20R) epimer ratio; CPI = carbon preference index calculated according to $\Sigma C_{odd}/\Sigma C_{even}$ over the range of C_{15} to C_{22} and C_{23} to C_{32}, respectively. n.a. = not analysed; n.d. = not determined.

Sample	TOC [wt%]	TS [wt%]	C_{carb} [wt%]	HI [mg HC/g rock]	T_{max} [°C]	C_{31}H S/(S + R)	C_{29}St S/(S + R)	$CPI_{15–22}$	$CPI_{23–32}$	R_o [%]
Vima Formation										
F34	1.32	0.83	0.57	151	430	0.10	n.d.	1.24	2.58	n.a.
F33	0.55	0.19	9.48	60	414	n.d.	0.13	1.81	1.37	n.a.
F32	2.30	1.56	1.38	246	421	0.14	0.09	1.42	2.06	0.40
F28	0.58	1.66	0.72	78	421	0.13	n.d.	1.21	2.06	n.a.
F27	0.40	1.33	9.07	160	422	0.21	0.09	1.15	1.12	n.a.
F26	1.98	1.94	1.40	280	419	0.13	n.d.	1.74	3.16	0.41
F23	0.99	1.04	0.35	94	427	0.13	n.d.	0.81	2.43	n.a.
F22	1.10	1.26	0.66	170	424	0.36	n.d.	1.21	2.40	0.49
F19	0.67	0.66	1.83	117	427	0.11	n.d.	1.83	2.37	n.d.
F15	0.81	1.30	0.65	121	427	0.11	n.d.	2.12	2.50	n.d.
F14	1.51	2.69	0.55	317	423	0.39	n.d.	1.16	2.43	n.a.
Ileanda Formation										
F11	4.75	1.96	2.57	573	413	0.31	0.05	1.50	1.87	0.46
F9	5.88	2.76	0.77	629	414	0.26	0.08	1.48	1.43	0.37
F8	1.56	1.46	5.94	494	419	0.22	0.06	1.48	1.14	n.d.
F7	1.10	0.46	9.39	265	420	0.24	0.06	1.46	0.94	n.d.
F4	3.07	2.11	0.97	567	413	0.24	0.06	1.66	1.29	0.46
F3	3.25	2.16	1.64	266	417	0.28	0.07	1.48	1.17	n.a.
F1	1.78	1.04	0.44	191	419	0.26	0.06	1.02	2.44	n.a.

The C_{25} HBI alkanes (M^+ 238) are present in almost all samples; however, co-eluting with C_{21} *n*-alkane. Especially abundant are HBIs in sulfurised forms, i.e. C_{25} HBI thiophenes (HBIT). They occur as two isomers possessing structures III and IV (Fig. 6). Their mass spectra are characterised by a molecular ion M^+ 378 and fragment ions at *m/z* 125 and *m/z* 237, respectively. Additionally, in several samples, C_{30} HBIT (M^+ 448) as two isomers (V; *m/z* 125) and (VI; *m/z* 391) were also identified. An exceptional HBI distribution was noted in sample F7, representing the Tylawa Limestone (see also Bojanowski et al., 2018) from the Ileanda Fm. Apart from C_{25} and C_{30} HBIT, it contained C_{25} (VII) and C_{30} HBI thiolanes (VIII), eluting shortly after the corresponding C_{25} and C_{30} HBIT (Fig. 6). These compounds were identified using key ion at *m/z* 115 and by comparison with mass spectra presented in Kohnen et al. (1990).

The relative abundance of C_{25} HBIT (III) to the nearest *n*-C_{23} alkane (C_{25}HBIT/*n*-C_{23}) is highest in the uppermost part of the section (Table 4).

4.6.3. Steroids

All the samples reveal complex distributions of saturated, unsaturated, and aromatised steroids with various relative abundances of each sterane group strongly dependent on the lithology. The Ileanda Fm. sedimentary rocks are the most abundant in regular and monoaromatic steranes, recognised on *m/z* 217 and *m/z* 253 mass chromatograms, respectively. The marly mudstones of the Vima Fm. contain mostly rearranged sterenes, i.e. diaster-13(17)-enes (IX) (diasterenes) and subordinate 4-methyldiaster-13(17)-enes (X) (4-methyldiasterenes), identified on *m/z* 257 and *m/z* 271 mass chromatograms, respectively. Regular steranes occur in the C_{26}-C_{30} range, represented by 20R isomers in ααα configuration and less prominent αββ configurations (Fig. 5). The C_{27}-C_{29} steranes are the most abundant with various relative intensities of each sterane member. The C_{29}αααR regular sterane shows predominance over the C_{27}αααR sterane as expressed by the C_{29}αααR/C_{27}αααR ratio (C_{29}/C_{27} sterane) for the samples from the lowermost Ileanda Fm. and most samples from the Vima Fm. (Table 4).

The diasterenes and 4-methyldiasterenes occur in the C_{26}-C_{29} and C_{28}-C_{30} ranges (Fig. 5), respectively. Their distributions are dominated by the 20S and 20R 10α(H)-isomers (e.g., Brassell, 1984; Volkman et al., 2015). An additional minor series of diasterenes assigned as the corresponding 10β(H)-isomers were identified based on nearly identical mass spectra and expected retention times (Peakman et al., 1989; Volkman et al., 2015).

4.6.4. Hopanoids and oleanenes

Generally, samples contain small amounts of hopanoids throughout the section. This compound group is represented by hopanes, hop-17(21)-enes (XI), neohop-13(18)-enes (XII) and benzohopanes. Among hopanes, C_{30} 17α,21β(H) hopane is the dominant constituent; however, ββ and βα configurations were also noted. Homohopanes occur in a few samples in the full range (C_{31}-C_{35}), while the most common range covers homologues with C_{31}-C_{33} carbon atoms. These compounds were present as both αβ and ββ epimers (Fig. 7), with the most abundant 22R 17α,21β(H)-homohopane (Fig. 7). A notable predominance of the 22R over the 22S epimers is expressed by very low values of the C_{31} homohopane 22S/(S + R) epimer ratio (0.1–0.3; Table 2). Norhopanes, 17α(H)-trisnorhopane and trisnorneohopane, as well as 17β,21α (H)-30-norhopane, are also present. All aliphatic fractions contain unsaturated hopanoids, including the most prominent in many samples, C_{29} norneohop-13(18)-ene, followed by C_{30} neohop-13(18)-ene and less abundant C_{30} hop-17(21)-ene. The C_{31}–C_{34} benzohopanes (Hussler et al., 1984) were identified, especially in black shales from the Ileanda Fm.

The ratio of steranes to 17α-hopanes (ΣS/ΣH; the sum of regular C_{27} to C_{29} ααα (20S + R) + αββ (20S + R) steranes versus the sum of 17α C_{29} to C_{33} (22S + R) hopanes) was calculated (e.g., Brocks et al., 1999; Tulipani et al., 2015) and generally, the predominance of steranes over hopanes is conspicuous (Table 4). The highest values were obtained for the samples F7–F11 of the Ileanda Fm., reaching up to 16.5 (Table 4).

The oleanane-class hydrocarbons are comprised of monounsaturated 18α(H)olean-12-ene (XXI) and olean-13(18)-ene (XXII), present in almost all samples (e.g. Fig. 7). The ratio of the sum of oleanenes (18α(H)olean-12-ene and olean-13(18)-ene) to C_{30} αβ hopane (O/[O + H]) is very low for the Ileanda Fm. samples (av. 0.1) and sharply increases at the Rupelian/Chattian transition marked by the values up to 1.0 for the Vima Fm. (Table 4).

4.6.5. Aromatic biomarkers

Aromatic fractions are dominated by 5,7,8-trimethyl-2-methyl-2-(4,8,12-trimethyltridecyl) chromans (XIII) (triMe-MTTCs). Mono- and dimethyl MTTCs are also present, but in significantly lower concentrations, as expressed by the MTTCI (triMe-MTTC/total MTTCs index; Sinninghe Damsté et al., 1987, 1993) (Table 4).

All samples were examined to identify isorenieratane (XIV) and most

Table 3
Relative abundances of different palynofacial groups recognised in the selected Oligocene samples from the Fântânele section [%].

Sample	Structured								Unstructured			
	Palynomorphs group			Other microplankton		Phytoclasts group			Amorphous group			
	Sporomorphs		Marine phytoplankton			Macrophyte plant debris			Amorphous Organic Matter AOM			Higher plant secretions
	Saccate pollen grains	Non-saccate pollens and spores	Dinoflagellate cysts	Colonial freshwater algae (e.g., *Botryococcus* sp.)	Other (e.g., acritarchs, foraminiferal tests, fungal spores, remains)	Cuticule	Translucent wood	Opaque wood	Opaque/ dark AOM	Homogeneous/ translucent AOM	Heterogeneous/ translucent AOM	Resin
Vima Formation												
F34	2.3	5.0	2.7	0.3	5.0	30.2	8.4	1.3	5.5	2.1	36.9	0.2
F32	2.7	5.0	4.7	1.9	3.3	19.1	7.5	0.6	3.5	1.8	49.3	0.5
F28	0.5	1.6	2.7	2.8	7.3	26.3	4.7	1.4	13.2	2.1	36.7	0.7
F26	5.2	3.9	2.2	0.9	5.9	14.1	7.7	1.8	6.7	4.2	47.1	0.3
F22	1.8	3.4	3.8	0.6	3.0	22.0	13.3	2.0	8.9	6.1	34.7	0.5
F19	0.6	2.1	2.7	4.8	2.6	24.9	6.0	1.3	6.0	1.2	47.7	0.2
F15	1.2	4.8	2.5	0.9	5.2	18.3	10.0	0.8	7.6	3.1	45.5	0.2
Ileanda Formation												
F11	0.8	6.3	1.0	0.0	1.6	6.2	1.3	0.0	2.1	2.5	78.0	0.1
F9	0.4	2.9	1.8	1.0	1.6	8.7	6.0	0.3	3.3	6.4	67.4	0.3
F8	0.5	3.9	0.8	0.0	1.6	8.7	2.9	0.1	2.7	2.0	76.7	0.0
F7	0.5	2.1	2.0	0.0	1.0	13.9	4.0	0.6	4.7	10.7	60.4	0.1
F4	0.4	5.2	3.5	0.2	1.6	9.6	4.4	0.3	4.3	2.7	67.6	0.4
F3	1.1	6.5	4.6	0.8	2.1	12.5	3.1	0.3	2.9	1.4	64.8	0.0

of its derivatives by the *m/z* 133 and *m/z* 237 key fragment ions after Koopmans et al. (1996). Intact isorenieratane was noted in small amounts in only three shale samples from the Ileanda Fm. Plenty of mono- and diaryl isoprenoids with additional aromatic rings were identified throughout the profile (Fig. 8). The ratio of the sum of all isorenieratane derivatives (including isorenieratane itself) versus triMe-MTTC (ARI/triMTTC, Table 4) attains two peak values, first in the lower part of the profile within the black shales of the Ileanda Fm. and second at the top of the Vima Fm.

Higher plant biomarkers are widely represented throughout the section by aromatic sesqui- and diterpenoids, as well as by triterpenoids in aromatised forms.

Cadalene (XV), retene (XX), simonellite (XVIII) and tetrahydroretene (XIX) occur in all samples. In the Vima Fm., 14-methyl-16,17-bisnorabieta-8,11,13-triene (XVI) and dehydroabietane (XVII) were also identified.

The monoaromatic 27,28-bisnoroleana-13,15,17-triene (XXIII) and des-A-oleanane (XXVI) (e.g., Jacob et al., 2005), as well as diaromatic des-A-24,27-dinoroleana-5,7,9,11,13-pentaene (XXVII), appear in three samples of the uppermost part of the Vima Fm. In the same samples, ursane- and lupane-class biomarkers are represented by monoaromatic 27,28-bisnorursana-13,15,17-triene (XXIV) and 27,28-bisnorlupana-13,15,17-triene (XXV).

5. Discussion

5.1. Organic matter maturity and hydrocarbon potential

The analysed rocks show low thermal maturity, evident in R_o values all <0.5 %, as well as in all the presented molecular indicators (Table 3). High abundances of hopane and sterane isomers in their biological configuration in relation to the more thermally stable geological isomers are expressed, e.g., in very low C_{31} homohopane 22S/(22S + 22R) epimer ratio (Seifert and Moldowan, 1980) and C_{29} ααα sterane 20S/(20S + 20R) epimer ratio (Seifert and Moldowan, 1986). Highly variable modified CPI values ($CPI_{15–22}$ and $CPI_{23–32}$) are also characteristic of very low thermal OM alteration. However, parameters based on *n*-alkane distributions can be affected by both maturity and source, especially in deposits with complex marine and terrigenous composition (e.g., Peters et al., 2005). The ubiquitous presence of diasterenes and 4-methyldiasterenes (Fig. 5) is consistent with the low maturity of the Oligocene rocks since these compounds are early-stage diagenetic products of sterols and 4-methylsterols precursors (de Leeuw et al., 1989; Peters et al., 2005). Steranes, final diagenetic products (Mackenzie et al., 1982; Macquaker et al., 1986; van Kaam-Peters et al., 1998), are less prominent than methyldiasterenes in the Vima Fm., which can be related instead to source, i.e., more intense dinoflagellate production in the latest Rupelian and Chattian. Similarly, the high abundance of neohop-13(18)-enes and hop-17(21)-enes is typical for immature clay-rich rocks (e.g., Sinninghe Damsté et al., 1995; Köster et al., 1998; Volkman et al., 2015). Neohop-13(18)-enes are formed during degradation and subsequent rearrangement of a C_{30} hopanoid precursor (e.g., diploptene) induced in the presence of clay minerals (Ensminger, 1977). The occurrence of rearranged hopenes and sterenes would point to diagenetic transformations of original lipids, occurring probably to some extent after OM burial. However, it can be difficult to separate the effects of clay-catalysed reactions during deposition from those of partial oxidation in suboxic depositional environments, as described in many clay-rich source rocks (Moldowan et al., 1991).

Generally, low Rock-Eval T_{max} values (av. 422 °C, Fig. 9A) support the immature character of the OM in most of the analysed samples. Higher T_{max} values, reaching 430 °C (for the F32 sample), although still relating to immature OM (e.g., Peters and Cassa, 1994), are questionable as they are inconsistent with other maturity parameters. It has been demonstrated that mineral matrix can influence the Rock-Eval indices, particularly in OM-lean and carbonate-containing rocks (e.g., Katz,

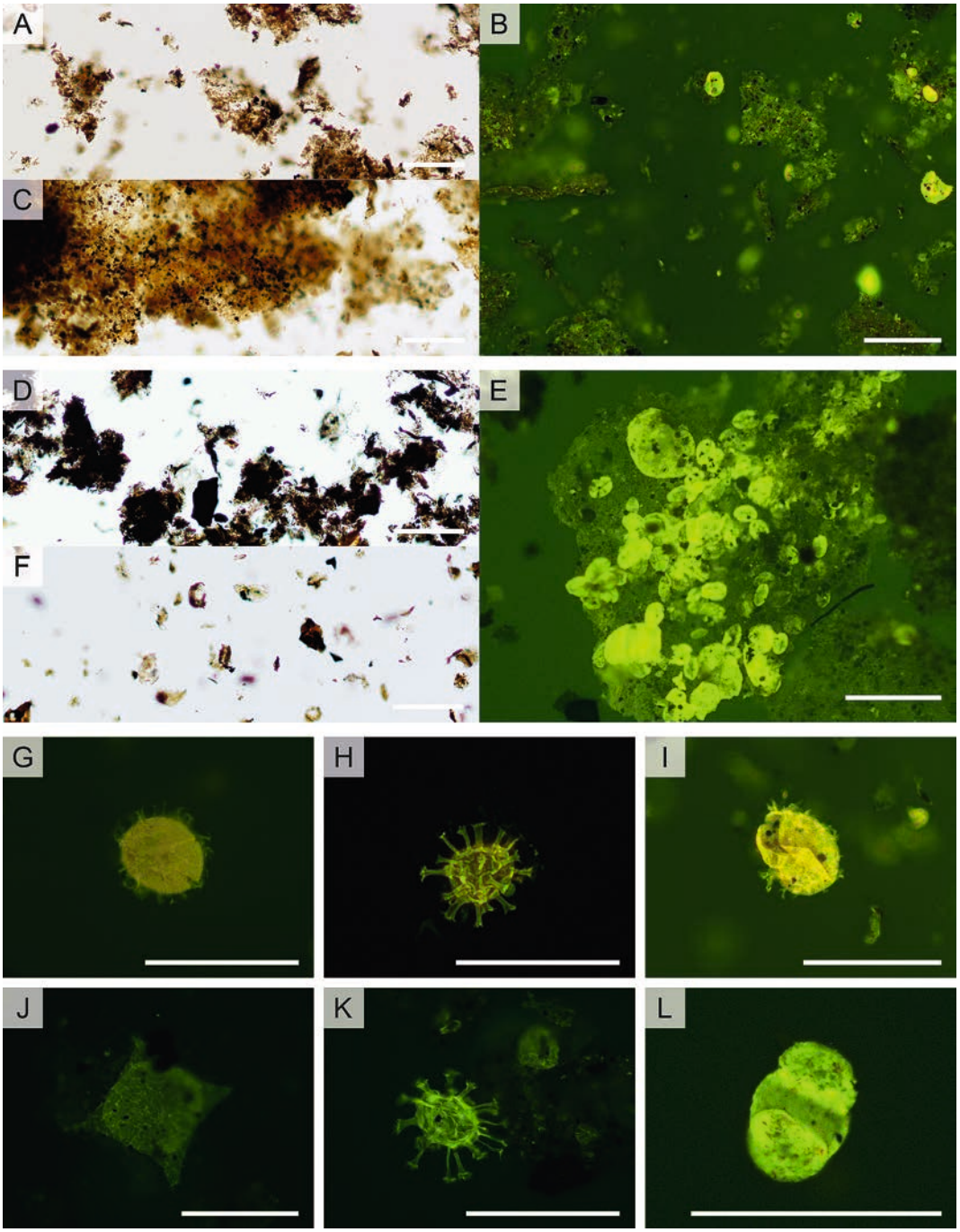

Fig. 4. Palynofacies, phytoclasts, palynomorphs, and sporomorphs from the selected samples. (A) dominating heterogeneous yellowish to brownish AOM, sample F7; (B) mainly AOM with minor numerous palynomorphs with different degree of preservation, sample F9; (C) heterogeneous yellowish to brownish AOM with high pyrite concentrations, sample F11; (D) mainly dark AOM and black/opaque phytoclasts, sample F15; (E) concentration of palynomorphs, mostly pollen grains and spores with intense fluorescence, sample F26; (F) numerous palynomorphs i.e., saccate pollens, dinocysts, spores, with phytoclasts (mainly cuticle elements), sample F34; (G – L) palynomorphs components characterised by different fluorescence and preservation state; (G) dinoflagellate cyst, sample F34; (H) dinoflagellate cyst, sample F3; (I) dinoflagellate cyst, sample F9; (J) dinoflagellate cyst, sample F4; (K) dinoflagellate cyst, sample F26; (L) bisaccate pollen grain, sample F26. Scale white bar - 50 μm (same for all pictures).

1983; Cowie et al., 1999). This can be the case with several samples from the Vima Fm. (see low TOC and high C_{carb} content in Table 2 and Fig. 3).

Mostly very good to good organic richness characterises dark shales of the Ileanda Fm., as revealed in the averaged TOC content of 3 wt% (Peters and Cassa, 1994). In the Vima Fm., the TOC content is significantly lower (av. 1.1 wt%), except for two dark shale intercalations with TOC ~2 wt%. The increase of TOC values correlates with HC content, expressed by the sum of Rock-Eval peak S_1 and S_2 values. This points to the syngenetic nature of HCs in organic-rich rocks, further confirmed by the low S_1 and high S_2 combined with medium to high TOC. Samples from the Ileanda Fm. reveal excellent to good petroleum potential (samples F9, F11) as approached using the plot of TOC vs $S_1 + S_2$ (Fig. 9B). In contrast, rocks of the Vima Fm., with two exceptions of shale layers, exhibit fair to poor HC potential.

Our data lead to the same conclusions as presented in Popescu (1995) and Stefanescu et al. (2006), that despite very good quality and

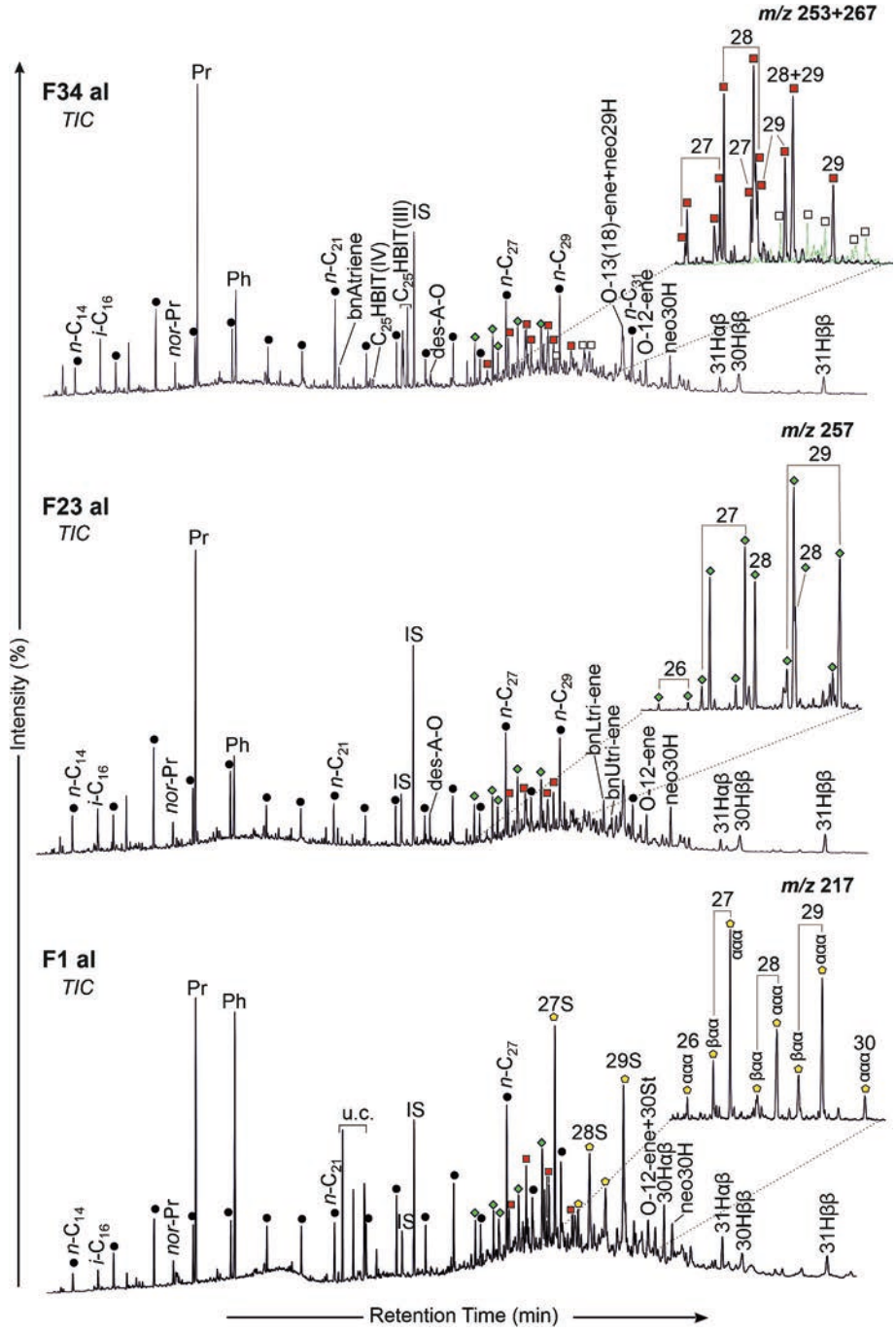

Fig. 5. Total ion chromatograms showing representative aliphatic fractions of the samples from the Ileanda Fm. (F1) and Vima Fm. (F23 and F34). Inserts depict extracted ion chromatograms of: *m/z* 253 + 267 – distribution of monoaromatic steranes (red squares) and their methyl derivatives (white squares); *m/z* 257 – distribution of C_{26}–C_{29} diaster-13(17)-enes (not all isomers of the C_{28} diaster-13(17)-enes could be identified due to coelutions with more abundant C_{27} and C_{29} isomers); *m/z* 217 – distribution of C_{26}–C_{30} regular steranes. Black circles – *n*-alkanes, nor-Pr – nor-pristane, Pr – pristane, Ph – phytane, H – hopanes, S – steranes, bnAtri-ene – 14-methyl-16,17-bisnorabieta-8,11,13-triene, C_{25}HBIT (III) and (IV) – isomers of C_{25} highly branched isoprenoid thiophene, desA-O – des-A-oleanane; O-13-ene + neo29H – olean-13(18)-ene + C_{29} norneohop-13(18)-ene, O-12-ene – 18α(H) olean-12-ene, bnLtri-ene – monoaromatic 27,28-bisnorlupana-13,15,17-triene, bnUtri-ene – monoaromatic 27,28-bisnorursana-13,15,17-triene, IS – internal standard (2-hexadecylthiophene), u.c. – unknown compounds. (For interpretation of the references to colour in this figure legend, the reader is referred to the web version of this article.)

quantity of OM, the black shales of the Ileanda Fm. in the NW TB are immature, and their HC potential has never been realised. Similar Rock-Eval T_{max} values ~420 °C for the outcrop rocks of the Ileanda Fm. were reported by Popescu (1995), whereas De Broucker et al. (1998) reported R_o of 0.55 % from the subsurface data for the same rock formation and showed that the Ileanda Fm. was immature across its whole depositional area. These OM-rich facies have never achieved burial depths corresponding to the onset of the HC generation stage in this area. Gröger et al. (2008), based on the zircon fission track study, excluded a significant increase in heat flow from the Paleogene to Early Miocene burial load in the northern Transylvania region. In the Late Miocene, the area became a sedimentary wedge after a short subaerial exposure, erosion, and substantial tilting linked to the Upper Miocene SW push of Tisza-Dacia (de Leeuw et al., 2013). The region to the south became the

Table 4
Biomarker indices indicative of OM sources: TAR – terrigenous vs aquatic *n*-alkanes ratio ([C_{27} + C_{29} + C_{31}]/[C_{15} + C_{17} + C_{19}]); ∑S/∑H – hopanes to steranes ratio (the sum of 17α C_{29} to C_{33} (22S + R) hopanes vs the sum of regular C_{27} to C_{29} ααα (20S + R) + αββ (20S + R) steranes); C_{29}/C_{27} – ratio of C_{27} ααα20R sterane to C_{29} ααα20R; C_{25}HBIT/*n*-C_{23} – ratio of relative abundance of C_{25} HBIT to *n*-C_{23} alkane; Ab/TriMTTC – ratio of summed abietane derivatives (simonellite, retene, tetrahydroretene, 14-methyl-16,17-bisnorabieta-8,11,13-triene, dehydroabietane) vs trimethylated 2-methyl-2-(trimethyltridecyl)chroman; O/(O + H) – ratio of summed oleananes (18α(H) olean-12-ene, olean-13(18)-ene) vs C_{30}αβ sterane; paleosalinity: MTTCI - ratio of trimethylated 2-methyl-2-(trimethyltridecyl)chroman vs the sum of mono, di- and trimethylated 2-methyl-2-(trimethyltrdecyl)chromans; redox conditions: Pr/Ph – pristane/phytane ratio; Ari/triMTTC – ratio of summed isorenieratane and its derivatives vs. trimethylated 2-methyl-2-(trimethyltridecyl)chroman; n.d. – not determined.

Sample	TAR	∑S/∑H	C_{29}/C_{27}	C_{25}HBIT/ *n*-C_{23}	Ab/ triMTTC	O/(H + O)	MTTCI	Pr/Ph	Ari/ triMTTC
Vima Formation									
F34	1.96	9.61	1.05	4.23	0.10	0.95	0.91	3.77	0.18
F33	5.25	5.70	1.09	8.22	0.88	0.50	0.85	1.41	0.22
F32	1.15	4.93	0.64	3.53	0.29	0.74	0.84	0.74	2.00
F28	3.78	3.85	1.15	3.02	0.09	0.97	0.81	3.34	0.14
F27	0.55	4.09	1.11	2.30	0.40	0.70	0.77	0.53	0.65
F26	1.51	10.50	0.71	4.33	1.76	0.86	0.87	0.98	0.19
F23	1.98	4.03	1.44	0.33	0.75	0.98	0.92	3.98	0.03
F22	2.65	4.25	1.20	0.00	0.06	0.68	0.87	2.38	0.00
F19	0.58	4.91	1.08	1.46	0.36	0.64	0.85	6.92	0.10
F15	3.28	9.05	1.12	1.31	0.04	0.80	0.82	5.45	0.10
F14	0.53	4.52	0.77	0.29	0.05	1.00	0.83	2.05	0.05
Ileanda Formation									
F11	1.61	13.58	0.92	1.98	0.11	0.01	0.94	0.63	0.34
F9	1.09	15.21	0.58	1.20	0.12	n.d.	0.86	0.54	0.09
F8	0.82	16.54	0.87	0.75	0.00	0.00	0.76	0.79	0.08
F7	0.62	11.08	0.71	2.33	0.05	0.24	0.88	0.88	0.28
F4	0.65	5.72	0.61	0.00	0.03	0.19	0.87	0.63	1.19
F3	0.40	5.42	1.14	1.86	0.00	0.05	0.83	0.48	0.04
F1	1.79	1.24	1.09	0.00	0.01	0.28	0.87	1.13	0.00

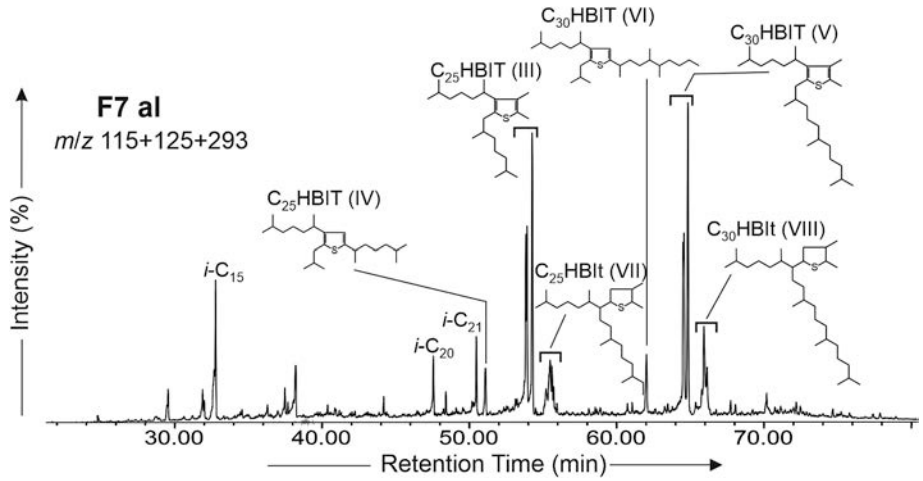

Fig. 6. Summed mass chromatogram for *m/z* 115 + 125 + 293 showing the distribution of highly branched isoprenoid thiophenes (HBIT) and thiolanes (HBIt) in the Tylawa limestone sample (F7 sample) of the Ileanda Fm.

northern margin of the future Middle-Upper Miocene Megasequence of the Neo-TB, the main gas province of Romania.

5.2. Organic matter sources

The diversified palynofacial and biomarker assemblages can infer a wide representation of primary OM producers. Fluctuating through the analysed Oligocene sequence, differing proportions of autochthonous versus allochthonous OM change from the Rupelian marine-dominated Ileanda Fm. to the Latest Rupelian/Chattian Vima Fm., significantly affected by the terrestrial input.

5.2.1. Fluctuations of marine vs terrigenous OM inputs

A rough estimation of the OM sources can be inferred from the Rock-Eval pyrolysis results. High HI values in the dark, laminated, relatively thin interval (F3–F11) of the Ileanda Fm. suggest the prevalence of Type II (marine) kerogen of algal/microbial origin (Fig. 9A; Espitalié et al., 1984). This is consistent with the conspicuous occurrence of "flaky" AOM with granular texture and patchy fluorescence (up to 80 %) (Table 3). Such an AOM type is interpreted as a bacterial degradation product of marine phytoplankton (Pacton et al., 2011; Ţabără et al., 2015). The lowermost Ileanda Fm. and samples representing dark shale intercalations in the Vima Fm. fall in the mixed kerogen Type II/III field on the pseudo-Van Krevelen diagram (Fig. 9A), revealing the importance of marine and terrestrial OM input. In contrast, most rocks from the Vima Fm. reveal low HI values, pointing to a higher contribution of humic material from land plants, as expressed by the domination of Type III kerogen (Fig. 9A). However, in these samples still, an essential input of marine OM is evident, e.g., high abundance of 'marine type' AOM (~40 %), dinoflagellate cysts and some marine algae-specific biomarkers (discussed later on). Predominating Type III kerogen in the Vima Fm. samples can also arise from partial oxidation during transport and redeposition of the organic remains, resulting in decreased HI values (Cowie et al., 1995) and overestimation of the 'terrestrial' kerogen

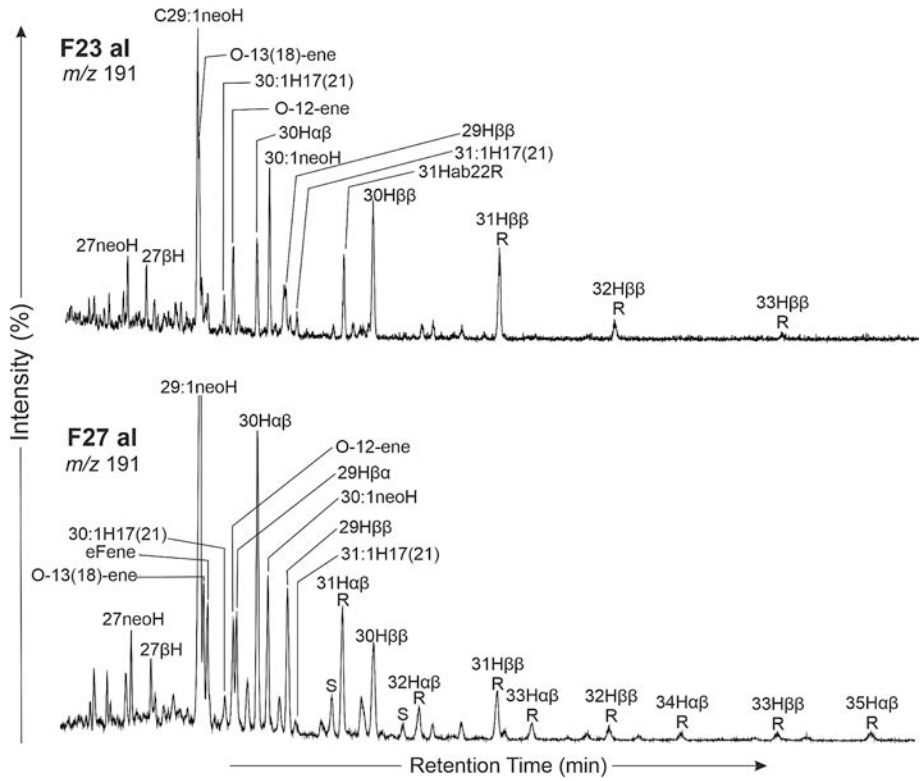

Fig. 7. Distribution of hopanoids and other pentacyclic triterpenoids on mass fragmentograms (*m/z* 191) in samples F23 and F27 from the Vima Fm. 29:1neoH - C_{29} neohop-13(18)-ene; 30:1neoH – C_{30} neohop-13(18)-ene; 30:1H17(21) – C_{30} hop-17(21)-ene; C31:1H17(21) – C_{31} hop-17(21)-ene; hopane isomers are shown as αβ, βα or ββ; for example the C_{31}17β(H),21β(H)-homohopane is shown as 31Hββ; O-13(18)-ene – olean-13(18)-ene; O-12-ene – 18α(H) olean-12-ene; eF-ene – 21-epi-fern-9(11)-ene.

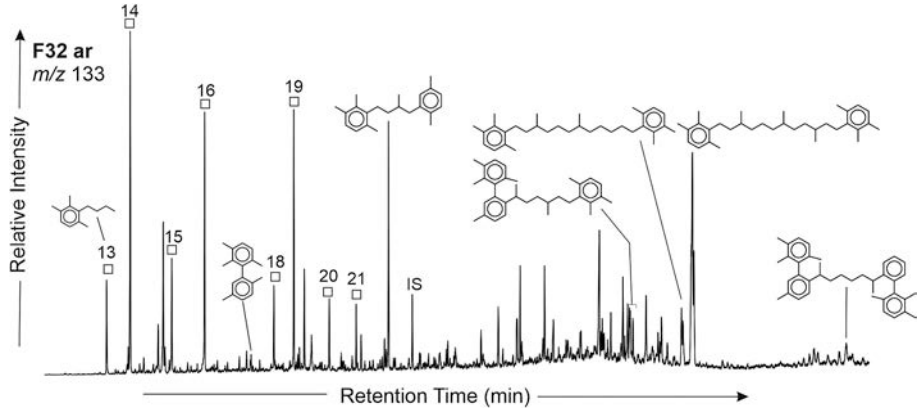

Fig. 8. Partial mass chromatogram for *m/z* 133 presenting aryl isoprenoids in the F32 sample from the Vima Fm. Rectangles with numbers represent monoaryl isoprenoids with respective carbon numbers in the molecule, IS – internal standard.

proportion. In our case, the reworking proxies, including the physical deterioration of sporomorphs and dinoflagellate cysts due to transport processes during redeposition or the growth of pyrite crystals within (e.g., Traverse, 2007; Filipek, 2020; Gedl et al., 2023), along with weaker or barren UV fluorescence intensity linked to the exposure to oxygen or microbial decay (e.g., Waterhouse, 1998; Hoyle et al., 2018), are more frequently observed in samples from the Ileanda Fm. (Fig. 4). In contrast, palynomorphs in the Vima Fm. display more uniform yellow fluorescence and significantly better preservation conditions.

The TAR (Bourbonniere and Meyers, 1996) ratio, based on *n*-alkanes distribution and commonly applied to evaluate the importance of terrigenous OM input compared to aquatic contribution, is mostly <1 for the shaly Ileanda Fm. interval (Fig. 10). Such values point to the predominance of autochthonous OM produced most probably by marine algae or cyanobacteria (Brassell et al., 1980; Jaffé et al., 2001). Despite higher relative concentrations of short-chain *n*-alkanes over long-chain homologues, the odd-carbon-numbered homologues significantly predominate (especially *n*-C_{27} and *n*-C_{29}, see Fig. 10), indicating important higher plant input. The C_{27}, C_{29}, and C_{31} *n*-alkanes in rocks and oils are associated with higher plant epicuticular leaf waxes (Eglinton and Hamilton, 1967). This is emphasised by the $CPI_{23–32}$ values higher than 1 for almost all samples and in the Vima Fm. reaching up to 3 (Table 4). An additional source of long-chain *n*-alkanes can be algae, including *Botryococcus* (Lichtfouse et al., 1994), but given their scarcity among palynomorphs in the lowermost Ileanda Fm. and the Vima Fm. samples (Table 2), they can be excluded as a considerable primary source of these

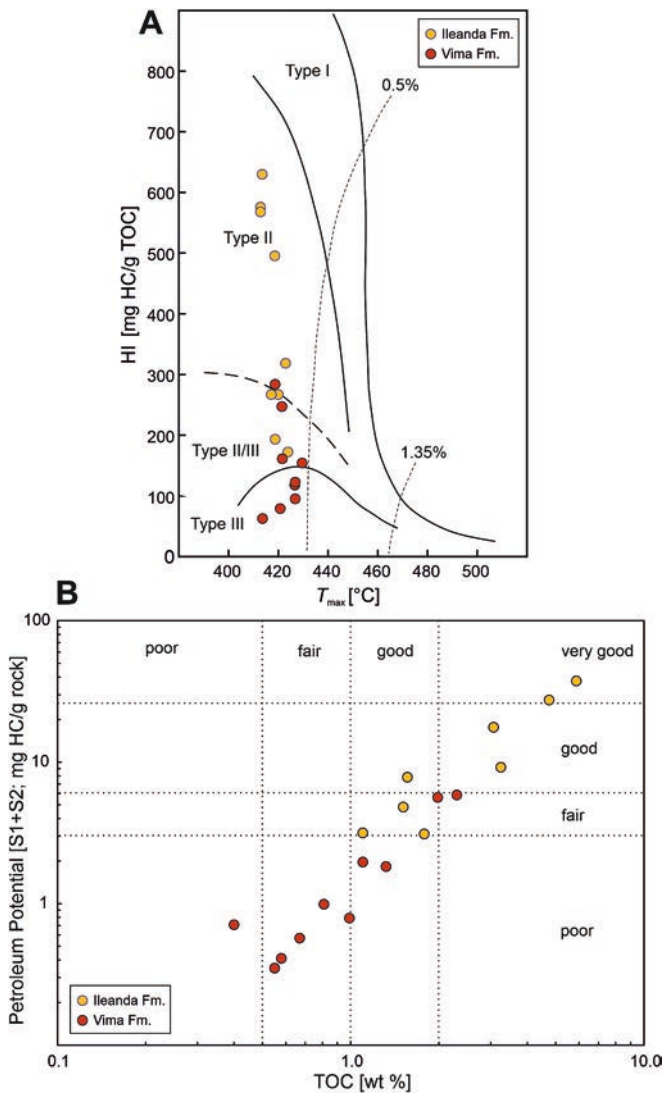

Fig. 9. (A) Plot of hydrogen index (HI) vs. T_{max} (according to Espitalié et al., 1985) outlining kerogen types for the analysed samples; (B) Petroleum Potential ($S_1 + S_2$) vs. TOC showing linear dependence of TOC and HC content, as well as different potentials for each formation.

n-alkanes. A relatively weak fluorescence and signs of reworking would likely point to their redeposition from deltaic environments to the deeper parts of the basin.

In some cases, the C_{29}/C_{27} ratio can indicate the relative inputs of higher plants relative to algae based on the dominance of C_{29} steroids in the former (e.g., Huang and Meinschein, 1979). However, there are also some potential algal contributors of C_{29} steranes, including freshwater green microalgae like *Botryococcus* (Metzger et al., 1990; Kodner et al., 2008), some diatoms as *Haslea ostrearia* (Volkman, 1986), eustigmatophytes (Volkman et al., 1999) and haptophytes (Volkman et al., 1997). In our case, diatoms seem to be the only additional source of C_{29} sterane worth considering, as the occurrence of HBIs, well-established diatom-derived biomarkers, further evidences their significant input. Nevertheless, for most Ileanda Fm., the C_{29}/C_{27} sterane ratio is typically <1, characteristic of marine environments (Grantham and Wakefield, 1988) and consistent with other source-dependent parameters. On the contrary, for most of the Vima Fm. samples, higher C_{29}/C_{27} sterane ratios correlate with other unambiguous higher plant imprints as opaque wood and cuticle fragments, as well as rich assemblages of higher plant-specific biomarkers (Table 4).

An increased supply of the land-derived OM in the Vima Fm. is well reflected by the increasing Ab/triMTTC ratio (Fig. 10). Diterpenoids of the abietane type, as dehydroabietane, simonellite, tetrahydroretene, and retene, are widely proposed diagenetic products of abietic acid, a major component of the conifer resins (e.g., Simoneit, 1977; Alexander et al., 1992; Ellis et al., 1996). However, other abietane-type molecules, such as ferruginol or taxodone produced by Recent *Taxodium* species, can be a source of simonellite and retene (Otto et al., 1997). The latter has also been identified in pyrolysates of algal and bacterial OM (Wen et al., 2000). Notably, the highest values of the Ab/triMTTC ratio for the F26 sample can be linked to the occurrence of numerous aggregates of bisaccate pollen grains generally attributed to conifers (Traverse, 1988). Pronounced peaks of the abietane-derived biomarkers in the upper part of the Vima Fm. correlating with high C_{25}HBIT/*n*-C_{23} ratio and low Pr/Ph ratio values can be related to an intense terrestrial OM supply, enhancing algal blooms and consequent eutrophication-induced oxygen deficit in the water column. Similarly, an increased input of the angiosperm-derived OM in the Chattian is revealed by the O/(O + H) ratio (Fig. 10), pointing to the higher relative contribution of oleanane-type biomarkers, attributed to angiosperm vegetation (e.g., Otto and Simoneit, 2001; Peters et al., 2005, and references therein) vs C_{30} αβ hopane, produced by bacteria. Taylor et al. (2006) confirmed the presence of 18α(H)-oleanane in non-angiosperm seed plant fossils (Cretaceous Bennettitales and the Permian Gigantopteridales), although, given the Oligocene age of the analysed rocks, the angiosperm origin seems plausible. A complex assemblage of compounds possessing oleanane-, ursane-, and lupane-type structures in the Vima Fm. (F23, F28 and F34), together with the prominent shift in abundances of cuticle and woody tissue fragments (Table 3), point unambiguously to an intense transport of higher plant debris to the NW TB in the Chattian, further related to changes in depositional setting.

5.2.2. *Primary marine OM producers*

More specific marine phytoplankton contributors are represented by diatoms, which can be inferred from the common presence of C_{25} and C_{30} HBIs in sulfurised forms (thiophenes, thiolanes). The C_{25} HBI alkenes, C_{25} HBI thiophenes and thiolanes precursor compounds, are synthesised by different widespread diatoms of *Pleurosigma*, *Haslea*, *Rhizosolenia*, and *Navicula* genera (e.g., Volkman et al., 1994; Belt et al., 2001; Massé, 2002), as well as by recently reported *Pseudosolenia calcar-avis* (Kaiser et al., 2016). These diatoms were important OM producers during the deposition of the analysed Oligocene sequence, with the most intense peak in the uppermost interval of the Vima Fm. corresponding to the middle Chattian (lower part of NP25 zone) as evidenced by the highest C_{25}HBIT/*n*-C_{23} ratio (Fig. 10). Interestingly, compounds possessing C_{30} HBI structure were noted exclusively in the shaly interval of the Ileanda Fm. (F3-F11). C_{30} HBI homologues have been related to some *Rhizosolenia* species (Massé, 2002). Likely, these diatoms contributed significantly as a planktonic source of HBIs, especially given their abundance and widespread occurrence (Simonsen, 1974; Hayward, 1993; Shipe et al., 1999).

Dinoflagellates were active primarily at the beginning of the Ileanda Fm. sedimentation and through the Chattian, when Vima Fm. was deposited, as evidenced by the common occurrence of 4-methyldiasteranes. These early diagenetic products of some 4-methylsterols are generally linked to dinoflagellates (e.g., Curiale, 1987; Robinson et al., 1984; Volkman et al., 1998). Although some haptophytes (Volkman et al., 1990), methanotrophic bacteria (Schouten et al., 2000), and higher plants (Menounos et al., 1986) cannot be excluded as their primary source. Nevertheless, the co-occurrence of 4-methyldiasterenes and dinoflagellate cysts and vice versa, the lack of these compounds, and no evidence of dinoflagellates in palynofacial assemblages are in favour of such interpretation.

Another marine phytoplankton biomarker is C_{30} sterane 24-*n*-propylcholestane, which is quite prominent in most of the extracts, except for the lower interval of the Vima Fm. (samples F15-F23). Precursor compounds have been identified to date only in Pelagophyceae, a small

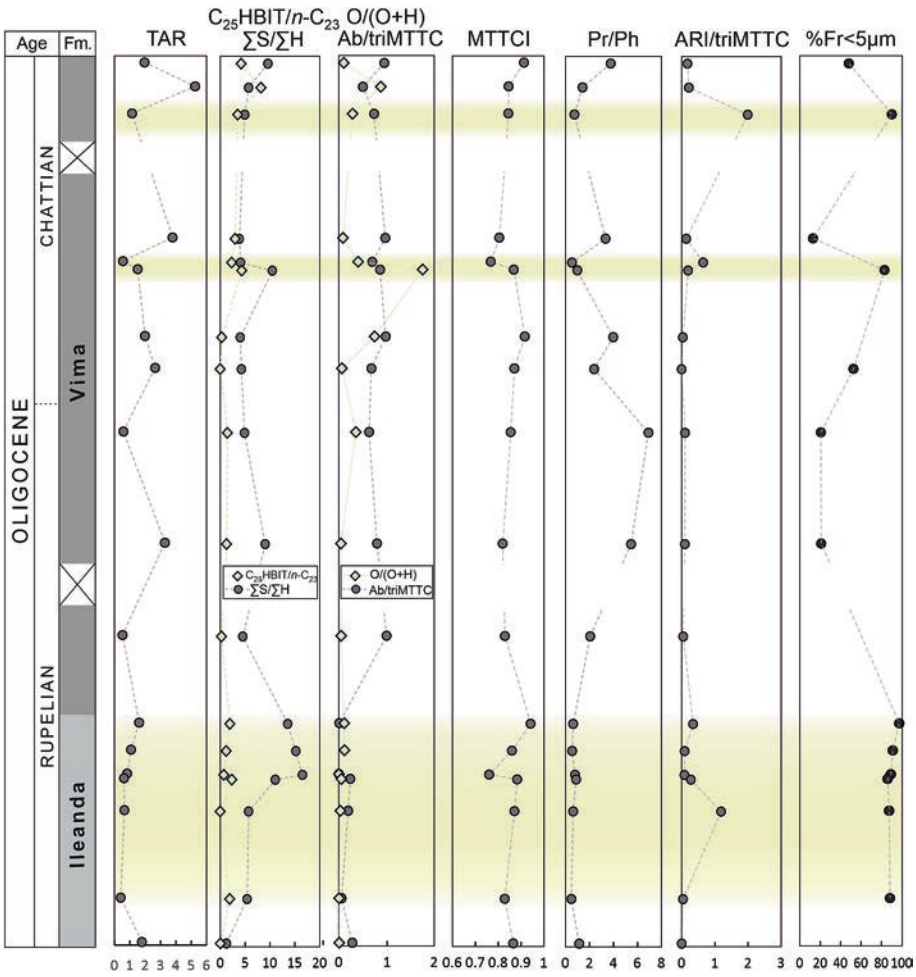

Fig. 10. Logs of selected molecular parameters indicative of OM sources, paleosalinity, and redox conditions; %Fr < 5 µm – percentage share of pyrite framboids <5 µm. Abbreviations of biomarker parameters are described in Table 4. Anoxic episodes are highlighted in grey-yellow. (For interpretation of the references to colour in this figure legend, the reader is referred to the web version of this article.)

class of marine algae (Volkman, 2003; Giner et al., 2009), and in a culture of the heterotrophic foraminifer *Allogromia laticollaris* (Grabenstatter et al., 2013). Occurrence of this compound in the Ileanda Fm. samples and in the upper interval of the Vima Fm. would indicate again more intense marine algal production in the corresponding Late Rupelian and Late Chattian time intervals.

Prokaryotes were another group of organisms contributing to the deposited OM as indicated by hopanoids (e.g., Ourisson et al., 1979) in all the extracts. However, they played a minor role in OM production, as evidenced by the elevated ΣS/ΣH ratio (Table 4; Fig. 10) attributed to significantly higher algal versus bacterial productivity. The ratio reaches its peak (11–16.5) in the laminated shales and the Tylawa Limestone sample of the Ileanda Fm. The deposition of this finely laminated limestone horizon is commonly interpreted as an effect of the extensive phytoplankton blooms (coccoliths, diatoms) linked to salinity drop and basin isolation from the global ocean (e.g., Melinte-Dobrinescu and Brustur, 2008; Ciurej and Haczewski, 2012; Bojanowski et al., 2018).

High concentrations of neohop-13(18)-enes, the most prominent hopanoids in many samples (Fig. 7), can be linked to direct origin from certain bacteria, as, e.g. purple non-sulfur bacterium *Rhodomicrobium vannielii* (Howard et al., 1984) or *Zymonas mobilis* (Douka et al., 2001). However, these compounds are subordinate to other hopanoids in these bacteria. Neohop-13(18)-enes and hop-17(21)-enes are often related to bacteria utilising methane as a carbon source based on their light $\delta^{13}C$ composition (e.g., Freeman et al., 1990; Burhan et al., 2002; Aichner et al., 2010), as it was reported, e.g., in the immature Oligocene Menilite shales from the Polish Outer Carpathians by Köster et al. (1998). Nonetheless, taking into consideration the co-occurrence of these hopenes with other rearranged biomarkers, such as diasterenes and 4-methyldiasterenes, their origin seems to be related instead to clay-catalysed early diagenetic transformations of a C_{30} hopanoid precursor like diploptene or diplopterol (Rohmer et al., 1984) or some bacteriohopanepolyols (Sinninghe Damsté et al., 1995). This is consistent with the presence of both C_{30} hopanes, most probably derived from some C_{30} hopanoid precursors and homohopanes, diagenetic products of bacteriohopanepolyols.

5.3. Paleosalinity

The positive correlation (Fig. 11A) of TOC and TS regarding salinity indicates normal marine depositional conditions (Berner and Raiswell, 1984). MTTCI, a parameter of salinity conditions above the chemocline (Sinninghe Damsté et al., 1993), compared to the Pr/Ph ratio, points to normal marine salinity conditions for the Upper Rupelian Ileanda Fm. Most of the samples from the Vima Fm. fall in the field of decreased salinity (Fig. 11B) with two exceptions of the shaly intervals deposited presumably in normal-marine salinity conditions above the chemocline. Such a transition of normal-marine regime in the Late Rupelian to decreased salinity conditions in the Early Chattian was inferred from the studies of calcareous nannoplankton associations in the Fântânele section by Kallanxhi et al. (2018). Salinity fluctuations in the upper part of the water column were probably controlled by an intense riverine

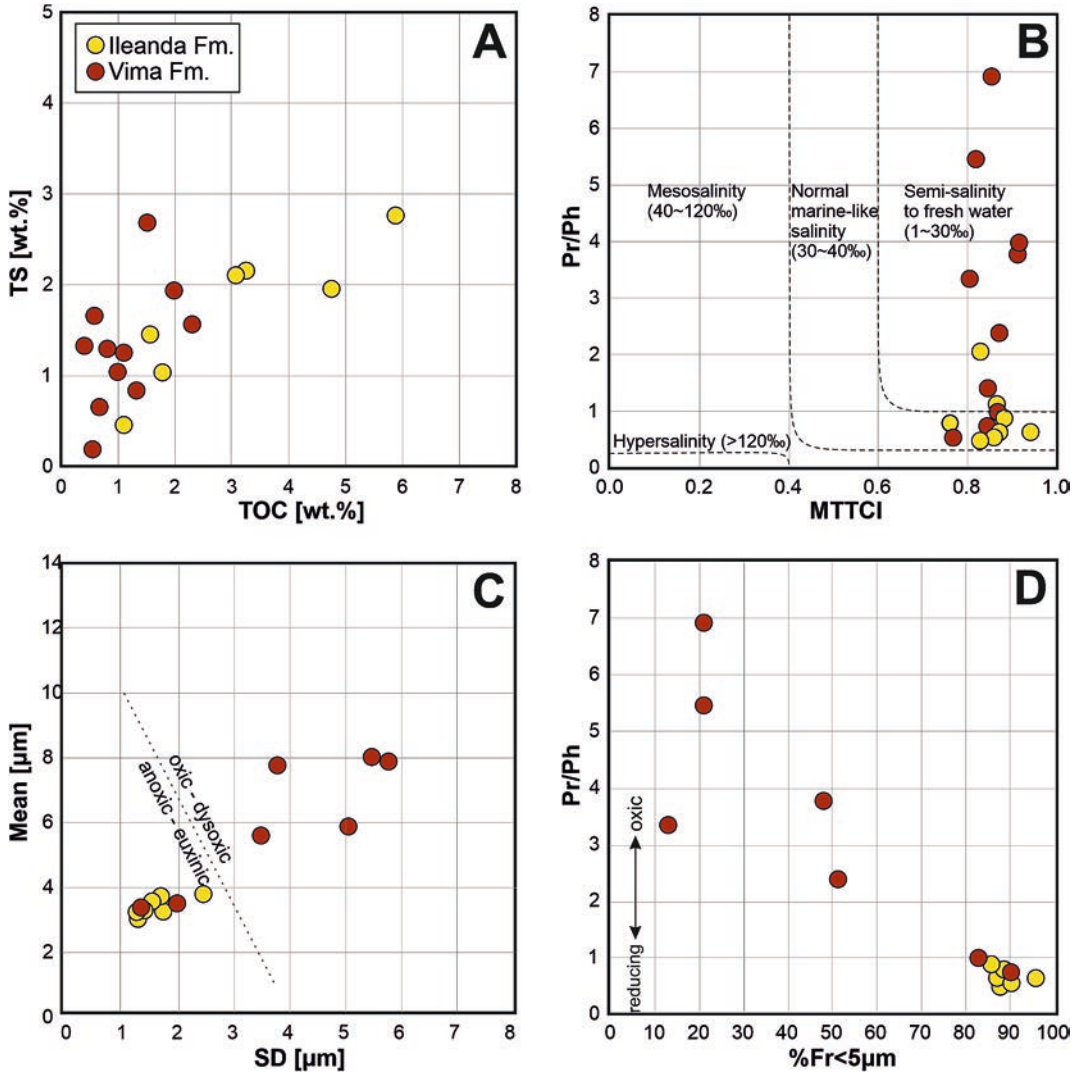

Fig. 11. (A) Total sulfur (TS) versus total organic carbon (TOC) variation diagram (after Wignall, 1994); (B) Crossplot of the pristane to phytane ratio (Pr/Ph) versus methyltrimethyltridecylchroman index (MTTCI) (boundaries of the salinity fields after Wang et al., 2011); (C) Plot of the pyrite framboid size distribution statistic data: mean pyrite framboid diameter (Mean) versus standard deviation (SD), and (D) Pr/Ph versus tiny pyrite framboids share (%Fr < 5 µm) - indicating anoxic/euxinic conditions for the Ileanda Fm. and more oxic for the Vima Fm.

inflow, as demonstrated by the increasing contribution of terrigenous-derived OM in the Chattian. This is evident in shifts towards higher abundances of phytoclasts and higher plant-related biomarkers (e.g., abietane derivatives and oleanenes) in this time interval (Fig. 10). Inferred intense riverine inflow supplying nutrients to the basin could have resulted in episodes of high algal productivity and related enhanced OM accumulations episodically in the Chattian. Relatively high TOC contents, increased C_{25}HBIT/*n*-C_{23} ratio, and elevated $\sum$S/$\sum$H observed for two shaly intervals of the Vima Fm. would reflect such a scenario well. The Tylawa Limestone sample (F7) represents some specific salinity conditions among other Ileanda Fm samples as it shows exceptionally low TS and MTTCI ~0.88. Its formation was recently attributed by Bojanowski et al. (2018) to extremely low-salinity events related to fresh-water incursions and sulfate depletion during periods of perfect isolation of Paratethys from the ocean, based on the high $\delta^{34}S$ and low $\delta^{18}O$ values as well as by ^{87}Sr enrichment.

5.4. Redox conditions on the seafloor and in the water column

High TOC and HI values characterising a relatively thin shaly interval of the Ileanda Fm. (sample F9-F11) can be attributed to anoxic conditions in the Late Rupelian, favouring the preservation of hydrogen-rich, oil-prone OM in marine environments (Calvert, 1987; Peters and Simoneit, 1982). Two shaly intervals of the Vima Fm. can potentially point to some anoxic episodes in the Chattian, as revealed by the elevated OM preservation (TOC ~2 % and HI ~260 mg HC/g TOC). An excess of sulfur in comparison to TOC values (intercept of the regression line at 1 for the Ileanda Fm. and at 0.75 for the Vima Fm.; see Fig. 11A) would point to anoxic/euxinic conditions beneath the sediment/water interface with the H_2S derived via the microbial sulfate reduction (MSR), causing an additional amount of iron to react with reduced sulfur forming pyrite (e.g., Berner, 1984). The latter is commonly observed in all the analysed samples. Two carbonate-rich samples, the Tylawa Limestone (sample F7) and a nodular limestone (sample F34), are sulfur-depleted, which can be linked to the iron limitation that may occur in carbonate-rich sediments such as limestones and cherts (Berner, 1984). However, Bojanowski et al. (2018) pointed to the opposite: a sulfate limitation caused by significant input of sulfate-impoverished fresh water to a probably closed system based on the ^{34}S-enriched pyrite and the absence of foraminifera. This would stand in contradiction to the presence of HBI thiophenes and thiolanes identified in the Tylawa Limestone, related to an intense MSR, exhaustion of iron available for

pyrite formation, and subsequent incorporation of reduced sulfur species into functionalised organic compounds. An alternative explanation of such sulfur impoverishment can be an effect of oxidation of iron sulfide minerals on the regularly ventilated seafloor due to upwelling events and thermohaline circulation, which does not exclude the presence of an anoxic/euxinic zone in the upper part of the water column (e.g., Marynowski et al., 2011).

The presence of abundant H_2S leads to iron limitation for pyrite formation and incorporation of reduced sulfur species into OM at the earliest stages of diagenesis under specific depositional conditions like anoxic and stratified water column, as it has been reported e.g. modern Black Sea sediments (Wakeham et al., 2007) or for recent sediments of Lake Cisó (Hartgers et al., 1997) and Lake Cadagno (Del Don et al., 2001). In our case, high amounts of sulfurised HBI compounds constantly occurring in the section reflect the significance of the sulfur incorporation into algal-derived OM upon early diagenesis (Sinninghe Damsté et al., 1989) or even in the water column (Hebting et al., 2006). Sulfur incorporation occurred probably intramolecularly, leading to the formation of C_{25} and C_{30} HBI thiophenes and thiolanes, present in the free HC fraction (contrary to the sulfur-bound fraction, which was not the subject of this study). Therefore, anoxia/euxinia presumably developed at the sediment–water interface, at least temporarily reaching into the water column. The most prominent HBI compound in our samples is C_{25}HBI thiophene, which is not uncommon, as this compound has been reported from a vast variety of recent environments as the Black Sea (Kohnen et al., 1990), the Caspian Sea (Belt et al., 1994) or the Peru upwelling region (Volkman et al., 1983), as well as from ancient sedimentary settings as the Oligocene Menilite shales (Köster et al., 1998; Wendorff-Belon et al., 2021). Precursor compounds, especially mono- and di-unsaturated C_{25} HBIs, reveal excellent preservation potential thanks to their low reactivity towards photooxidation (Rontani et al., 2011) and autoxidation (Rontani et al., 2014). Moreover, double bonds in their structure make them prone to natural sulfurisation by reaction with inorganic sulfur species (Rowland and Robson, 1990; Sinninghe Damsté and de Leeuw, 1990). Interestingly, the C_{25} and C_{30} HBI thiolanes, early diagenetic intermediates in the formation of the HBI thiophenes (Kohnen et al., 1990), occur exclusively in the dark shales and Tylawa Limestone sample of the Ileanda Fm. This would point to strictly euxinic conditions at the sea floor and in the water column at the deposition time and early diagenesis in the corresponding Late Rupelian, enabling the preservation of these compounds.

Complementary insight into redox conditions can be withdrawn from the analysis of pyrite framboid size distribution, widely applied for local redox reconstructions (e.g., Marynowski et al., 2011; Gallego-Torres et al., 2015; Smolarek et al., 2017). The prevalence of tiny pyrite framboids <5 μm in size (Fig. 10) and generally very low mean framboid diameters (2–4 μm) characterising samples from the Ileanda Fm. and two shaly intervals of the Vima Fm. (Fig. 11C) suggest widespread or prevailing anoxic/euxinic conditions at the sediment/water interface and even expanding into the water column in the Late Rupelian and episodically in the Chattian. It has been demonstrated that the small mean diameters (3–5 μm) with very limited size ranges are usually indicative of euxinic conditions (Wilkin et al., 1996; Wignall and Newton, 1998; Bond and Wignall, 2010; Dustira et al., 2013). In contrast, larger mean diameters and more various sizes of pyrite framboids reaching up to 50 μm for the lower part of the Vima Fm. are indicative of oxygen availability (Fig. 11C) in the water column and better seafloor ventilation (see for comparison Marynowski et al., 2011). Pyrite framboids can reach larger sizes by growing during very early diagenesis within the upper centimetres of sediments under suboxic to anoxic seafloor conditions (Wilkin et al., 1996, 1997; Wilkin and Arthur, 2001; Wei et al., 2015). However, in the upper part of the Vima Fm, the co-occurrence of numerous <5 μm diameter framboids with larger ones in the same populations may suggest episodes of euxinia in the water column with overlying oxygenated waters (e.g., Algeo et al., 2011).

Likewise, the Pr/Ph ratio shows a constant pattern of low values (< 1) for the Ileanda Fm. and shaly intervals of the Vima Fm., thus confirming prevailing anoxic conditions in the Rupelian and intermittently in the Chattian. A transition to a well-mixed, oxygenated water column in the Rupelian/Chattian is evidenced in a higher Pr/Ph ratio (up to 7), especially in the lower part of the Vima Fm. (Fig. 11B). This frequently used paleoredox indicator (e.g., Didyk et al., 1978; Peters et al., 2005) can be affected, however, by other factors, such as OM source, salinity, or preferential release of pristane upon cracking of kerogen (Connan, 1974). In this case, it seems to represent a reliable indicator for anoxia as other parameters, including isorenieratane derivatives or size distribution of pyrite framboids (Fig. 11C, D), support it.

5.5. *Evidence of photic zone euxinia*

Photic zone euxinia (PZE), the phenomenon observed on a large scale in the modern Black Sea and throughout the Earth's history (Grice et al., 1996; Meyer and Kump, 2008; Lyons et al., 2009; Naeher et al., 2013) is an oxygen-depleted state in which free, toxic H_2S is enriched in the water column and penetrates up into the photic zone. Such conditions form a perfect habitat for photosynthetic sulfur bacteria, such as Chlorobiaceae, using specific stains, including carotenoid isorenieratene (Summons and Powell, 1987; Grice et al., 1996; Koopmans et al., 1996; Brocks and Summons, 2003). Therefore, isorenieratene and its diagenetic derivatives as isorenieratane as well as mono- and diaryl- isoprenoids, have been used as diagnostic proxies for PZE in aquatic environments (e.g., Grice et al., 1996; Koopmans et al., 1996; Brocks and Summons, 2003; Schwark and Frimmel, 2004; Naeher et al., 2013). Monoaryl isoprenoids may have additional sources, such as renieratene or β-carotene (e.g., Grice et al., 1996; Koopmans et al., 1996). However, their co-occurrence with isorenieratane suggests at least temporary activity of Chlorobiaceae during the deposition of the Ileanda Fm. This in turn, indicates that in the Rupelian, the base of the photic zone remained more or less persistently anoxic and, in fact, euxinic. Low Pr/Ph ratio (0.5–0.7), the presence of sulfurised HBIs, and the permanent predominance of tiny pyrite framboids (86–96 %) would support such interpretation.

In the lower part of the Vima Fm., a constant occurrence of aryl isoprenoids can suggest some episodes of the weak PZE in the corresponding Late Rupelian/Early Chattian. Prominent peaks of high Ari/triMTTC ratio correlating with the increased share of tiny pyrite framboids and low Pr/Ph ratio for the shaly intervals in the uppermost Vima Fm. (Fig. 10) once again indicates strongly oxygen-deficient conditions with presumably euxinia expanding into the photic zone.

It seems likely that the primary forcing enabling PZE formation during deposition of the Ileanda Fm. and episodically Vima Fm. was twofold. In the first case, the controlling factor could have been basin morphology, i.e., deepening of the NW TB creating estuarine circulation patterns, subsequently leading to regional trapping of nutrients (e.g., Meyer and Kump, 2008). In general more distal and deeper environment for the shales of the Ileanda Fm., defined as distal anoxic/suboxic basin to shelf, can be inferred from the palynofacial assemblages ternary plot (Fig. 12). However episodes of decreased salinity related to an intense continental freshwater inflow causing deposition of the Tylawa Limestone presumably took place in the corresponding Late Rupelian (upper part of the NP23 zone). Similarly, the mechanism of basin individualisation, facilitating OM accumulation through enhanced preservation and partly low sedimentation rates, has been identified as a key factor in the development of PZE during the deposition of the Menilite Shales (Köster et al., 1998). Intermittently in the Chattian, the PZE could have been controlled, by contrast, by the enhanced terrigenous runoff supporting high primary productivity and density stratification leading to oxygenated surface waters overlying deep sulfidic and anoxic waters. Such salinity stratification tends to favour PZE because distinct sources of saline and freshwaters may lead to reduced mixing (e.g., Meyer and Kump, 2008). The transition from distal basin to distal dysoxic/anoxic shelf setting and related shortening of the distance to the shore upward

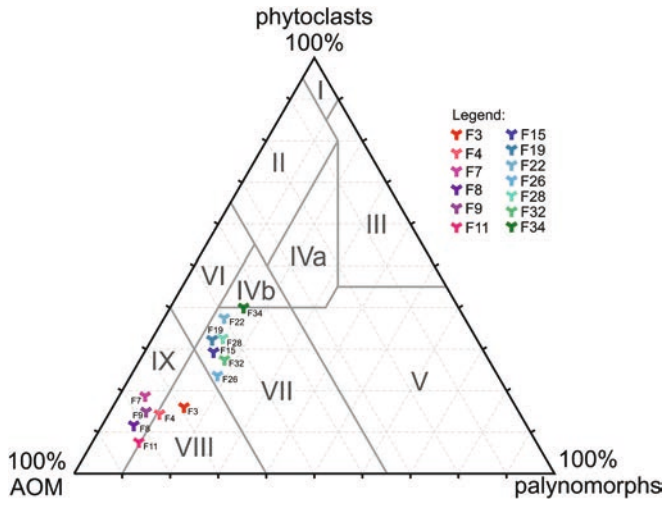

Fig. 12. Amorphous organic matter (AOM)-palynomorphs-phytoclasts ternary plot (after Tyson, 1989) distinguishing changes in depositional environments of the Ileanda and Vima Formations. Palynofacies fields: I – highly proximal shelf or basin, II – marginal dysoxic-anoxic basin, III – heterolithic oxic shelf ("proximal shelf"), IV – shelf to basin transition, V – mud-dominated oxic shelf ("distal shelf"), VI – proximal suboxic-anoxic shelf, VII – distal dysoxic-anoxic "shelf", VIII – distal dysoxic-anoxic shelf, IX – distal suboxic-anoxic basin.

in the section is well documented by the increased phytoclast abundance in the samples from the Vima Fm. (Fig. 12) as well as by well-preserved palynomorphs in the same samples. It cannot be excluded that during the deposition of the uppermost part of the Fântânele section, an overlapping thermal stratification existed, as was pointed out by Székely and Filipescu (2016) and Kallanxhi et al. (2018). These authors have attributed changes in the calcareous nannoplankton and foraminiferal assemblages, from those adapted to open-marine temperate to cooler conditions in the Rupelian, into assemblages preferring near-shore warmer regimes in the Chattian, to the so-called Late Oligocene Warming and the corresponding reduction of Antarctic ice volume (e.g., Zachos et al., 2001).

5.6. Paleoenvironmental implications

In the Early Oligocene time (near the NP22/NP23 zones boundary), the marine connection with the Mediterranean through the North Alpine Foreland Basin closed (van der Boon et al., 2018). Closure resulted in the first endemism within the Paratethys (Baldi, 1984). The core of the Oligocene anoxia was located in the Carpathian basins, where severe restrictions alternating with phases of upwelling led to long-lasting fluctuating anoxia (Kotlarczyk and Uchman, 2012; Rauball et al., 2019; Wendorff-Belon et al., 2021). In contrast, the TB was affected by shorter-lasting oxygen-deficient episodes, as it is reflected by a relatively thin interval of typical black shales of the menilite/maikopian-type deposits characterised by dark, finely laminated shales, sometimes called "paper shales" of the Ileanda Fm. Its conspicuous geochemical features expressed in high TOC, elevated HI, and specific molecular composition (very high $\sum S/\sum H$, low Pr/Ph, presence of HBI thiophenes and thiolanes) all point to specific environmental conditions. The enhanced preservation of organic carbon was most likely caused by more frequent or longer-lasting events of photic zone euxinia (Fig. 13), as revealed by the presence of isorenieratane derivatives and the domination of small-sized pyrite framboid populations. The widespread identification of isorenieratane and its derivatives in the Menilite shales across the Outer Carpathians (Köster et al., 1998; Sachsenhofer et al., 2015; Wendorff-Belon et al., 2021; Zakrzewski et al., 2024) highlights the basin-wide euxinic conditions that influenced the Central Paratethys during the Rupelian time.

The presence of the Tylawa Limestone marks a significant basin isolation event in the Rupelian (NP 23 zone), enabling the development of decreased-salinity conditions in the surface waters and intense algal primary production. Blooms of endemic nanofossil taxa as *Reticulofenstra ornata,* together with *Braarudosphaera bigelowii* adapted to low-salinity and cooler surface waters, identified in the Tylawa Limestone by Melinte-Dobrinescu and Brustur (2008), as well as specific isotopic composition (Bojanowski et al., 2018), would be in favour of such interpretation. Dark shales of the Ileanda Fm. represent basinal facies, characterised by conspicuous domination of AOM in the palynofacial assemblages (Fig. 12). In the Early Oligocene drowning of the shallow marine carbonate platform and subsequent deepening and formation of the euxinic deeper basin in the northern part of the TB resulted most probably from the N-S extensional stress field, documented by *E*-W trending small-scale normal faults in the Oligocene marls cropping out in the southern part of the TB (Huismans et al., 1997). Such basin deepening would generally fit the global eustatic curve by Haq et al. (1987), exhibiting a relative sea-level highstand period through the Rupelian (e.g., Hardenbol et al., 1998).

Open-marine and normal-salinity conditions with probably well-mixed water column (high Pr/Ph ratio, large framboids, no isorenieratane) and some anoxia in the bottom waters (small-sized framboids population, scarce aryl isoprenoids and HBI thiophenes) occurred at the Rupelian/Chattian transition (NP 24 zone) corresponding to the lower part of the Vima Fm. Such conditions are also indicated by the foraminiferal assemblages (F20, F21; Appendix A). Open marine conditions might have prevailed in the Paratethys from the mid-Oligocene to Burdigalian times, as was pointed out by Rögl (1999). This would be supported by the presence of the Jaslo Limestone (Lower Chattian) in the Vima Fm. interpreted as an effect of the cosmopolitan nannofossil blooms (Melinte-Dobrinescu and Brustur, 2008), most probably related to the restoration of the communication between the Paratethys and the Mediterranean through the Slovenian Corridor and Upper Rhine Graben with the North Sea (Baldi, 1984; Kováč et al., 2016).

The upper part of the Vima Fm. (presumably the lower part of NP25 zone) records change from the open marine to the shallower environment affected by an intense delivery of terrigenous OM from the adjacent hinterland, imprinted in the elevated abundances of phytoclasts and higher plant-derived biomarkers. This resulted in some episodes of eutrophication and development of salinity- and thermally-induced stratification, and subsequent PZE recorded in the shaly intervals of the upper part of the Vima Fm. (Fig. 13). Such a scenario can be explained by the Late Oligocene/Early Miocene NW-SE contraction event, affecting especially the northern and north-western part of the TB, governed chiefly by the thrusting of the Pienides (Krézsek and Bally, 2006 and references therein). The regional tectonic activity probably coincided with the Late Oligocene Warming Event (Zachos et al., 2001), as was recorded in the nannoflora (Melinte-Dobrinescu and Brustur, 2008; Kallanxhi et al., 2018) and foraminiferal assemblages (Székely and Filipescu, 2016) adapted to slightly warmer surface waters. The latter authors linked their observations with increased influences from the Mediterranean Sea and Indian Ocean and simultaneously weakening inflow of colder waters due to the closure of the Upper Rhine Graben in the Late Oligocene (Martini, 1990; Gebhardt, 2003). Similarly, Rusu (1996), based on mollusc fauna in the neighbouring Buzaș Formation from the TB, pointed to a boreal influence during the NP24 interval and a warmer climate in the upper NP25 interval.

The carbonate/terrigenous material dilution of OM is visible in lithology and a conspicuous terrestrial influence in the Vima Fm. Some evidence suggests that the detrital mineral component may dilute organic carbon at very high sedimentation rates (> 500 cm/1000 years) despite good preservation conditions (Ibach, 1982; Hedges and Keil, 1995). Therefore, it can be hypothesized that the local tectonics is more explicit in the case of the NW TB than in the neighbouring Carpathian Basin, where sedimentation of black anoxic/dysoxic shales (dysodylic shales) continues up to the earliest Burdigalian (e.g., Miclăuș et al.,

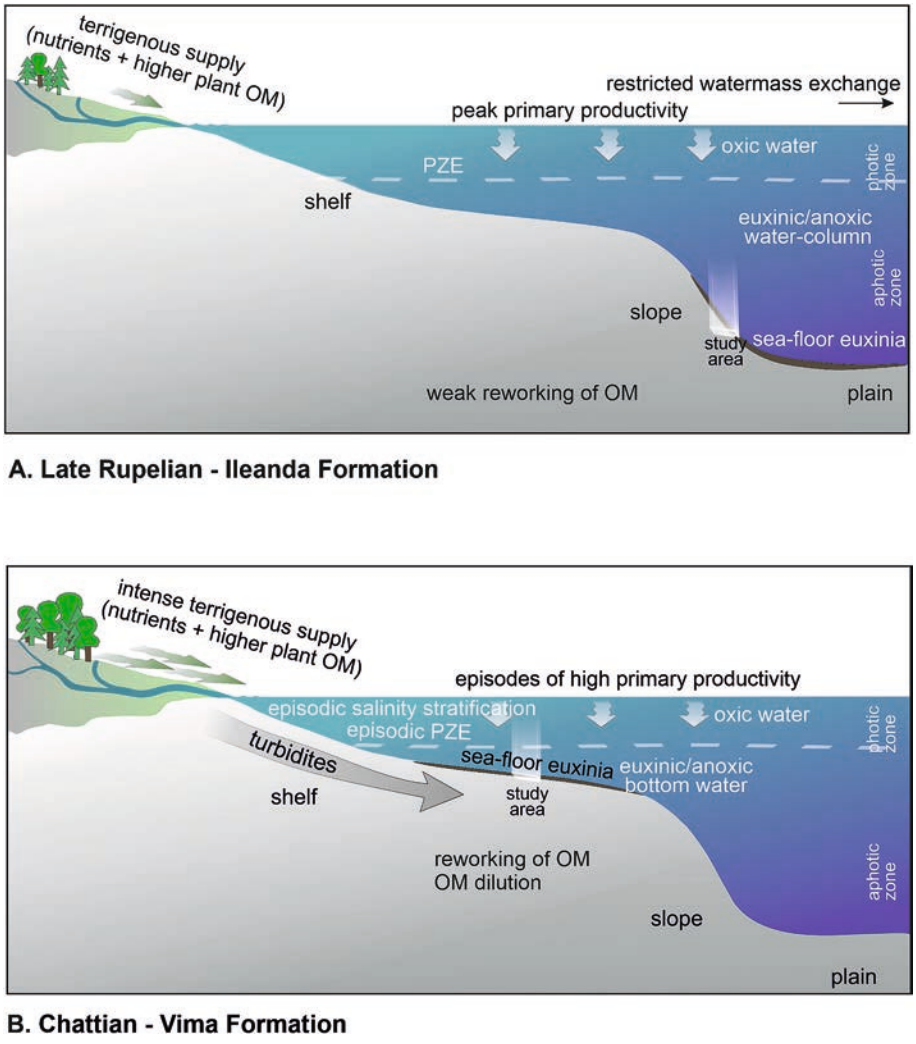

Fig. 13. Sketches showing factors controlling the depositional environment of the Ileanda (A) and Vima (B) Fms. Refer to the text for explanations. OM – organic matter, PZE – photic zone euxinia.

2009; Sachsenhofer et al., 2018).

6. Conclusions

Novel organic geochemical and petrological data from the Fântânele section of the NW TB, representing the Oligocene (Upper Rupelian-Chattian) sedimentation in the semi-restricted Central Paratethys domain, revealed exceptionally well-preserved, complex biomarker and maceral assemblages. Such a preservation state is related to very low thermal maturity, as indicated by the vitrinite reflectance, pyrolysis Rock-Eval, and molecular maturity parameters. Additionally, the largely unaltered biomarker distributions, including unsaturated diasterenes and hopenes, support the immature character of the analysed OM. Laminated black shales of the Ileanda Fm. reveals very good hydrocarbon potential, whereas lithofacially heterogeneous turbiditic Vima Fm. is poor mainly in TOC, except for two shaly intervals with good HC potential. The analysed OM-rich rocks did not attain the oil generation stage due to the insufficient burial heating in the Paleogene-Early Miocene, followed by the subaerial exposure, erosion, and tilting of the NW part of the TB in the Late Miocene.

Changes in palynofacies composition and biomarker distribution document fluctuations of the OM sources and related paleoenvironmental conditions across the Late Rupelian-Chattian time interval. Upper Rupelian black shales of the Ileanda Fm. would represent the period of enhanced marine phytoplankton production (high $\sum S/\sum H$, low C_{29}/C_{27} sterane), with a dominant role of diatoms (high C_{28} sterane, HBIs) and dinoflagellates (4-methyldiasterenes, dinoflagellate cysts) and minor contribution of Prokaryotes (hopanoids). Increasing contribution of the higher plant-derived OM upward in the section, evident in a complex assemblage of mainly angiosperm biomarkers together with the prominent shift in abundances of cuticle and woody tissue fragments, point to an intense transport of higher plant debris to the NW TB in the Chattian. The occurrence of aryl isoprenoids and isorenieratane throughout the section reflects the activity of phototrophic anaerobes during periods of enhanced water column stratification, especially in the Late Rupelian and episodically in the Chattian.

The shales of the Ileanda Fm. were deposited in a stagnant deeper-basin setting with established strictly anoxic bottom water conditions ($Pr/Ph < 1$, constant occurrence of HBI thiophenes), expanding higher into the water column, as revealed by dominant tiny pyrite framboid populations. PZE developed at least intermittently, as evidenced by the presence of isorenieratane and its derivatives. Such conditions triggered the flourishing of primary productivity and consequently enhanced OM accumulations (high TOC and HI) in the corresponding Late Rupelian. Moderate MTTCI and TOC/S would point to normal marine conditions above the chemocline. The Tylawa Limestone horizon presumably represents an episode of salinity drop in a restricted basin leading to eutrophication and oxygen-deficient conditions, enabling, in turn, preservation of redox-sensitive HBI thiolanes and mainly algal-derived proliferous OM.

In contrast, the Upper Rupelian/Chattian sediments represented by the lower portion of the Vima Fm. were laid down under more oxic/dysoxic conditions and a largely well-mixed water column (high Pr/Ph, mixed populations of large and tiny pyrite framboids). Later in the Chattian, the transition to a shallower environment affected by an intense delivery of terrigenous OM from the adjacent hinterland (phytoclasts and higher plant-derived biomarkers) resulted in some episodes of eutrophication (diatom and dinoflagellate blooms) and development of salinity-induced stratification, as well as shorter episodes of PZE recorded in the shaly intervals of the uppermost Vima Fm.

Such particular paleoenvironmental history of the NW TB is most possibly related to the regional tectonic activity, i.e., the basin extension in the Rupelian and presumably episodic isolation of the Paratethys from the global ocean enabling the development of relatively to other Central Paratethys sub-basins short episode of stagnant, stratified deeper-basin conditions. A transition into a contractional regime in the Chattian related to the thrusting of the Pienides was responsible for an active turbiditic sedimentation of the Vima Fm. characterised by the high input of terrigenous OM.

CRediT authorship contribution statement

Małgorzata Wendorff-Belon: Writing – original draft, Visualization, Resources, Investigation, Formal analysis, Conceptualization. **Robert Loręc:** Writing – original draft, Investigation, Conceptualization. **Adam Wierzbicki:** Writing – original draft, Visualization, Investigation. **Mariusz Rospondek:** Conceptualization. **Leszek Marynowski:** Writing – review & editing, Supervision, Conceptualization.

Declaration of competing interest

The authors declare the following financial interests/personal relationships which may be considered as potential competing interests: (Malgorzata Wendorff-Belon reports financial support was provided by Jagiellonian University in Kraków. If there are other authors, they declare that they have no known competing financial interests or personal relationships that could have appeared to influence the work reported in this paper.)

Acknowledgments

Ewa Malata and Lucyna Bobrek are kindly acknowledged for the foraminifera identification, age assignment, and constructive comments on the manuscript of this paper. We thank Magdalena Misz-Kennan for her technical support with vitrinite reflectance measurements, Arkadiusz Krzątała for his assistance with pyrite framboid measurements and Agnieszka Wciślak-Oleszycka for performing elemental analyses. Two anonymous reviewers are thanked for their constructive reviews. The Jagiellonian University partly provided financial support (Project for Young Scientists No·N23/MNW/000044).

Appendix A. Supplementary data

Supplementary data to this article can be found online at https://doi.org/10.1016/j.palaeo.2025.113124.

Data availability

Data will be made available on request.

References

Aichner, B., Wilkes, H., Herzschuh, U., Mischke, S., Zhang, C.J., 2010. Biomarker and compound-specific $\delta^{13}C$ evidence for changing environmental conditions and carbon limitation at Lake Koucha, eastern Tibetan Plateau. J. Paleolimnol. 43, 873–899.

Alexander, R., Larcher, A.V., Kagi, R.I., Price, P.L., 1992. An oil-source correlation study using age-specific plant-derived aromatic biomarkers. In: Moldowan, J.M., Albrecht, P., Philp, R.P. (Eds.), Biological Markers Sediments and Petroleum. Prentice-Hall, Englewood Cliffs, NJ, pp. 201–221.

Algeo, T.J., Kuwahara, K., Sano, H., Bates, S., Lyons, T., Elswick, E., Hinnov, L., Ellwood, B., Moser, J., Maynard, J.B., 2011. Spatial variation in sediment fluxes, redox conditions, and productivity in the Permian–Triassic Panthalassic Ocean. Palaeogeogr. Palaeoclimatol. Palaeoecol. 308, 65–83. https://doi.org/10.1016/j.palaeo.2010.07.007.

Bąk, K., 2005. Foraminiferal biostratigraphy of the Egerian Flysch sediments in the Silesian Nappe, Outer Carpathians, polish part of the Bieszczady Mountains. Ann. Soc. Geol. Pol. 75, 71–93.

Baldi, T., 1984. The terminal Eocene and Early Oligocene events in Hungary and the separation of an anoxic, cold Paratethys. Eclogae Geol. Helv. 77, 1–27.

Baldi, T., 1986. Mid-Tertiary stratigraphy and palaeogeographic evolution of Hungary. Akadémiai Kiadó, Budapest, 1–20.Balla, Z., 1987. Tertiary paleomagnetic data for the Carpatho-Pannonian region in the light of Miocene rotation kinematics. Tectonophysics 139, 67–98.

Balla, Z., 1987. Tertiary paleomagnetic data for the Carpatho-Pannonian region in the light of Miocene rotation kinematics. Tectonophysics 139, 67–98.

Bechtel, A., Hámor-Vidó, M., Gratzer, R., Sachsenhofer, R.F., Püttmann, W., 2012. Facies evolution and stratigraphic correlation in the early Oligocene Tard Clay of Hungary as revealed by maceral, biomarker and stable isotope composition. Mar. Pet. Geol. 35, 55–74.

Belt, S.T., Allard, W.G., Masse, G., Robert, J.-M., Rowland, S.J., 2001. Structural characterisation of C_{30} highly branched isoprenoid alkenes (Rhizenes) in the marine diatom *Rhizosolenia setigera*. Tetrahedron Lett. 42, 5583–5585.

Belt, S.T., Cooke, D.A., Hird, S.J., Rowland, S., 1994. Structural determination of a highly branched C25 sedimentary isoprenoid biomarker by NMR spectroscopy and mass spectrometry. J. Chem. Soc., Chem. Commun. 18, 2077–2078.

Berner, R.A., 1984. Sedimentary Pyrite Formation: an Update. Geochim. Cosmochim. Acta 48, 605–615. https://doi.org/10.1016/0016-7037(84)90089-9.

Berner, R.A., Raiswell, R., 1984. C/S method for distinguishing freshwater from marine sedimentary rocks. Geology 12, 365–368.

Bojanowski, M.J., Ciurej, A., Haczewski, G., Jokubauskas, P., Schouten, S., Tyszka, J., Bijl, P.K., 2018. The Central Paratethys during Oligocene as an ancient counterpart of the present-day Black Sea: Unique records from the coccolith limestones. Mar. Geol. 403, 301–328. https://doi.org/10.1016/j.margeo.2018.06.011.

Bond, D.P.G., Wignall, P.B., 2010. Pyrite framboid study of marine Permian–Triassic boundary sections: a complex anoxic event and its relationship to contemporaneous mass extinction. Geol. Soc. Am. Bull. 122, 1265–1279.

van der Boon, A., Beniest, A., Ciurej, A., Gaździcka, E., Grothe, A., Sachsenhofer, R.F., Langereis, C.G., Krijgsman, W., 2018. The Eocene-Oligocene transition in the North Alpine Foreland Basin and subsequent closure of a Paratethys gateway. Global and Planetary Change 162, 101–119. https://doi.org/10.1016/j.gloplacha.2017.12.009.

Bourbonniere, R.A., Meyers, P.A., 1996. Sedimentary geolipid records of historical changes in the watersheds and productivities of Lakes Ontario and Erie. Limnol. Oceanogr. 41, 352–359.

Brassell, S.C., 1984. Aliphatic hydrocarbons of a cretaceous black shale and its adjacent green claystone from the southern Angola Basin, Deep Sea Drilling Project Leg 75. In: Hay, W.W., Sibuet, J.-C., Shipboard Party (Eds.), Initial Reports of the Deep-Sea Drilling Project, Part 2, vol. 75. US Government Printing Office, Washington, pp. 1019–1030.

Brassell, S.C., Comet, P.A., Eglinton, G., Isaacson, P.J., McEvoy, J., Maxwell, J.R., Thomson, I.D., Tibbetts, P.J.C., Volkman, J.K., 1980. Preliminary lipid analyses of Sections 440A-7-6, 440B-3-5, 440B-8-4, 440B-68-2, and 436–11-4: Legs 56 and 57, Deep Sea Drilling Project. In: Scientific Party, Initial Reports of the Deep Sea Drilling Project, 56/57 (Eds.), Initial Reports of the Deep Sea Drilling Project (U.S. Govt. Printing Office), 56–57, pp. 1367–1390. https://doi.org/10.2973/dsdp.proc.5657.170.1980.

Bray, E.E., Evans, E.D., 1961. Distribution of *n*-paraffins as a clue to recognition of source beds. Geochim. Cosmochim. Acta 22, 2–15.

Brocks, J.J., Summons, R.E., 2003. Sedimentary hydrocarbons, biomarkers for early life. In: Holland, H.D., Turekian, K. (Eds.), Treatise in Geochemistry. Elsevier, Oxford, pp. 65–115.

Brocks, J.J., Logan, G.A., Buick, R., Summons, R.E., 1999. Archean molecular fossils and the early rise of eukaryotes. Science 285, 1033–1036.

Burhan, R.Y.P., Trendel, J.M., Adam, P., Wehrung, P., Albrecht, P., Nissenbaum, A., 2002. Fossil bacterial ecosystem at methane seeps: origin of organic matter from Be'eri sulfur deposit, Israel. Geochim. Cosmochim. Acta 66, 4085–4101.

Calvert, S.E., 1987. Oceanographic controls on the accumulation of organic matter in marine sediments. In: Brooks, J., Fleet, A.J. (Eds.), Marine Petroleum Source Rocks, pp. 137–151. Blackwell, London.

Ciulavu, D., Dinu, C., Szakács, A., Dordea, D., 2000. Neogene kinematics of the Transylvanian Basin, Romania. AAPG Bull. 84, 1589–1615.

Ciurej, A., Haczewski, G., 2012. The Tylawa Limestones – a regional marker horizon in the lower Oligocene of the Paratethys: diagnostic characteristics from the type area. Geol. Q. 56, 833–844. https://doi.org/10.7306/gq.1058.

Connan, J., 1974. Diagenèse naturelle et diagenèse artificielle de la matière organique à éléments végétaux dominants. In: Tissot, B., Bienner, F. (Eds.), Advances in Organic Geochemistry, 1973. Editions Technic, Paris, pp. 73–95.

Cowie, G.L., Hedges, J.I., Prahl, F.G., De Lange, G.J., 1995. Elemental and major biochemical changes across an oxidation front in a relict turbidite: an oxygen effect. Geochim. Cosmochim. Acta 59, 33–46.

Cowie, G.L., Calvert, S.E., Pedersen, T.F., Schulz, H., von Rad, U., 1999. Organic content and preservational controls in surficial shelf and slope sediments from the Arabian Sea (Pakistan margin). Mar. Geol. 161, 23–38. https://doi.org/10.1016/S0025-3227(99)00053-5.

Csontos, L., 1995. Tertiary tectonic evolution of the Intracarpathian area: a review. Acta Vulcanol. 7, 1–13.
Curiale, J.A., 1987. Steroidal hydrocarbons of the Kishenehn Formation, Northwest Montana. Org. Geochem. 11, 233–244.
De Broucker, G., Mellin, A., Duindam, P., 1998. Tectono-Stratigraphic evolution of the Transylvanian Basin, pre-salt sequence, Romania. In: Dinu, C., Mocanu, V. (Eds.), Geological and Hydrocarbon Potential of the Romanian Areas, Bucharest Geosciences Forum, vol. 1, pp. 36–70.
Del Don, C., Hanselmann, K.W., Peduzzi, R., Bachofen, R., 2001. The meromictic alpine Lake Cadagno: Orographical and biogeochemical description. Aquat. Sci. 63, 70–90.
Dicea, O., Duțescu, P., Antonescu, F., Mitrea, G., Botez, R., Donos, I., Lungu, V., Moroşanu, I., 1980. Contribution to the knowledge of Maramureş Transcarpathian Zone stratigraphy (in Romanian). Darea de Seamă Institute Geology of Geoff 65, 21–85.
Didyk, B.M., Simoneit, B.R.T., Brassell, S.C., Eglinton, G., 1978. Organic geochemical indicators of paleoenvironmental conditions of sedimentation. Nature 272, 216–222.
Douka, E., Koukkou, A.I., Drainas, C., Grosdemange-Billiard, C., Rohmer, M., 2001. Structural diversity of the triterpenic hydrocarbons from the bacterium *Zymomonas mobilis*: the signature of defective squalene cyclization by the squalene/hopene cyclase. FEMS Microbiol. Lett. 199, 247–251.
Dustira, A.M., Wignall, P.B., Joachimski, M., Blomeier, D., Hartkopf-Fröder, C., Bond, D. P.G., 2013. Gradual onset of anoxia across the Permian–Triassic boundary in Svalbard, Norway. Palaeogeogr. Palaeoclimatol. Palaeoecol. 374, 303–313.
Eglinton, G., Hamilton, R.J., 1967. Leaf epicuticular waxes. Science 156, 1322–1335.
Ellis, L., Singh, R.K., Alexander, R., Kagi, R.I., 1996. Formation of isohexyl alkylaromatic hydrocarbons from aromatisation-rearrangement of terpenoids in the sedimentary environment: a new class of biomarker. Geochim. Cosmochim. Acta 60, 4747–4763.
Emmings, J.F., Hennissen, J.A.I., Stephenson, M.H., Poulton, S.W., Vane, Ch.V., Davies, S.J., Leng, M.J., Lamb, A., Moss-Hayes, V., 2019. Controls on amorphous organic matter type and sulphurization in a Mississippian black shale. Rev. Palaeobot. Palynol. 268, 1–18.
Ensminger, A., 1977. Evolution de Composés Polycyclic Sédimentaires. Université Louis Pasteur, Strasbourg, Thèse de Doctorat des Sciences.
Espitalié, J., Bordenave, M.L., 1993. Screening techniques for source rocks evaluation; tools for source rocks routine analysis; Rock-Eval pyrolysis. In: Bordenave, M.L. (Ed.), Applied Petroleum Geochemistry. Technip, Paris, pp. 237–261.
Espitalié, J., Senga Makadi, K., Trichet, J., 1984. Role of the mineral matrix during kerogen pyrolysis. Org. Geochem. 6, 365–382. https://doi.org/10.1016/0146-6380(84)90059-7.
Espitalié, J., Deroo, G., Marquis, F., 1985. La pyrolyse Rock-Eval et ses applications. Première partie. Revue de l'Institut Français Pétrole 40, 563–579.
Filipek, A., 2020. Palynofacies analysis, sedimentology and hydrocarbon potential of the Menilite Beds (Oligocene) in the Slovakian and Romanian Outer Carpathians. Geol. Q. 64, 589–610.
Freeman, K.H., Hayes, J.M., Trendel, J.M., Albrecht, P., 1990. Evidence from carbon isotope measurements for diverse origins of sedimentary hydrocarbons. Nature 343, 254–256.
Gallego-Torres, D., Reolid, M., Nieto-Moreno, V., Martínez-Casado, F.J., 2015. Pyrite framboid size distribution as a record for relative variations in sedimentation rate: an example on the Toarcian Oceanic Anoxic Event in Southiberian Palaeomargin. Sediment. Geol. 330, 59–73. https://doi.org/10.1016/j.sedgeo.2015.09.013.
Gebhardt, H., 2003. Palaeobiogeography of Late Oligocene to Early Miocene Central European Ostracoda and Foraminifera: progressive isolation of the Mainz Basin, northern Upper Rhine Graben and Hanau Basin/Wetterau. Palaeogeogr. Palaeoclimatol. Palaeoecol. 201, 343–354.
Gedl, P., Śmist, P., Worobiec, E., 2023. Palynology of the deep structures of the Carpathian Foredeep (3,950–5,467 m) at the front of Carpathian overthrust, the NS-1 Borehole, SE Poland. Ann. Soc. Geol. Pol. 93, 423–445.
Giner, J.-L., Zhao, H., Boyer, G.L., Satchwell, M.F., Andersen, R.A., 2009. Sterol chemotaxonomy of marine Pelagophyte algae. Chem. Biodivers. 6, 1111–1130.
Giuşcă, D., Rădulescu, D., 1967. Harta geologică a României 1:200 000, foaia 3 Baia Mare, L-34-VI, M-34-XXXVI. Comitetul de Stat al Geologiei, Institutul Geologic.
Golonka, J., Gahagan, L., Krobicki, M., Marko, F., Oszczypko, N., Ślączka, A., 2006. Plate tectonic evolution and paleogeography of the Circum-Carpathian region. AAPG Mem. 84, 395–442.
Grabenstatter, J., Méhay, S., McIntyre-Wressnig, A., Giner, J.-L., Edgcomb, V.P., Beaudoin, D.J., Bernhard, J.M., Summons, R.E., 2013. Identification of 24-*n*-propylidenecholesterol in a member of the Foraminifera. Org. Geochem. 63, 145–151.
Grantham, P.J., Wakefield, L.L., 1988. Variations in the sterane carbon number distribution of marine source rocks derived crude oils through geological time. Org. Geochem. 12, 61–74.
Grice, K., Gibbson, R., Atkinson, J.E., Schwark, L., Eckardt, C.B., Maxwell, J.R., 1996. Maleimides (1H-pyrrole-2,5-diones) as molecular indicators of anoxygenic photosynthesis in ancient water column. Geochim. Cosmochim. Acta 60, 3913–3924.
Gröger, H.R., Fügenschuh, B., Tischler, M., Schmid, S.M., Foeken, J.P.T., 2008. Tertiary cooling and exhumation history in the Maramureş area (internal eastern Carpathians, northern Romania): thermochronology and structural data. Geol. Soc. Lond. Spec. Publ. 298, 169–195. https://doi.org/10.1144/sp298.9 0305-8719/08/$15.00.
Haczewski, G., 1989. Poziomy wapieni kokkolitowych w serii menilitowo-krośnienskiej – rozróżnianie, korelacja i geneza. Ann. Soc. Geol. Pol. 59, 435–523 (in Polish with English Summary).
Haq, B.U., Hardenbol, J., Vail, P.R., 1987. The chronology of fluctuating sea level since the Triassic. Science 235, 1156–1167.
Hardenbol, J., Jaquin, T., Vail, P.R. (Eds.), 1998. Mesozoic and Cenozoic Sequence Stratigraphy of European basins. SEPM Spec. Publ. 60, 1–786.
Hartgers, W.A., Lòpez, J.F., Sinninghe Damsté, J.S., Christine Reiss, C., Maxwell, J.R., Grimalt, J.O., 1997. Sulfur-binding in recent environments: II. Speciation of sulfur and iron and implications for the occurrence of organo-sulfur compounds. Geochimica et Cosmochimica Acta 61, 4769–4788. https://doi.org/10.1016/S0016-7037(97)00279-2.
Hayward, T.L., 1993. Oceanography - the rise and fall of *Rhizosolenia*. Nature 363, 675–676.
Hebting, Y., Schaeffer, P., Behrens, A., Adam, P., Schmitt, G., Schneckenburger, P., Bernasconi, S.M., Albrecht, P., 2006. Biomarker evidence for a major preservation pathway of sedimentary organic carbon. Science 312, 1627–1631.
Hedges, J.I., Keil, R.G., 1995. Sedimentary organic matter preservation: an assessment and speculative synthesis. Marine Chemistry 49, 81–115.
Howard, D.L., Simoneit, B.R.T., Chapman, D.J., 1984. Triterpenoids from lipids of *Rhodomicrobium vanniellii*. Arch. Microbiol. 137, 200–204.
Hoyle, T.M., Leroy, S., López-Merino, L., Richards, K., 2018. Using fluorescence microscopy to discern in situ from reworked palynomorphs in dynamic depositional environments — an example from sediments of the late Miocene to early Pleistocene Caspian Sea. Rev. Palaeobot. Palynol. 256, 32–49. https://doi.org/10.1016/j.revpalbo.2018.05.005.
Huang, W.-Y., Meinschein, W.G., 1979. Sterols as ecological indicators. Geochim. Cosmochim. Acta 43, 739–745.
Huismans, R.S., Bertotti, G., Ciulavu, D., Sanders, C.A.E., Cloetingh, S., Dinu, C., 1997. Structural evolution of the Transylvanian Basin (Romania): a sedimentary basin in the bend of the Carpathians. Tectonophysics 272, 249–268.
Hussler, G., Connan, J., Albrecht, P., 1984. Novel families of tetra- and hexacyclic aromatic hopanoids predominant in carbonate rocks and crude oils. Org. Geochem. 6, 39–49.
Ibach, L.E.J., 1982. Relationship between sedimentation rate and total organic carbon content in ancient marine sediments. Am. Assoc. Pet. Geol. Bull. 66, 170–188.
Ionescu, N., 1994. Exploration history and hydrocarbon perspectives in Romania. In: Popescu, B.M. (Ed.), Hydrocarbons of Eastern-Central Europe. Springer, Berlin, pp. 217–248.
Jacob, J., Disnar, J.R., Boussafir, M., Sifeddine, A., Albuquerque, A.L.S., Turcq, B., 2005. Pentacyclic triterpene methyl ethers in recent lacustrine sediments (Lake Caçó, Brazil). Org. Geochem. 36, 449–461.
Jaffé, R., Mead, R., Hernandez, M., Peralba, M., DiGuida, O., 2001. Origin and transport of sedimentary organic matter in two subtropical estuaries: a comparative, biomarker-based study. Org. Geochem. 32, 507–526. https://doi.org/10.1016/S0146-6380(00)00192-3.
van Kaam-Peters, H.M.E., Köster, J., van der Gaast, S.J., Dekker, M., de Leeuw, J.W., Sinninghe Damsté, J.S., 1998. The effect of clay minerals on diasterane/sterane ratios. Geochim. Cosmochim. Acta 62, 2923–2929.
Kaiser, J., Belt, S.T., Tomczak, M., Brown, T.A., Wasmund, N., Arz, H.W., 2016. C25 highly branched isoprenoid alkenes in the Baltic Sea produced by the marine planktonic diatom *Pseudosolenia calcar-avis*. Org. Geochem. 93 (2016), 51–58. https://doi.org/10.1016/j.orggeochem.2016.01.002.
Kallanxhi, M.-E., Bälc, R., Coric, S., Szekely, S.-F., Filipescu, S., 2014. Paleoecology and biostratigraphy of the Oligocene from the NW Transylvanian Basin (Romania) based on calcareous nannofossils. In: Proceedings of XX Congress of the Carpathian-Balkan Geological Association, Tirana, Albania, 24–26 September 2014, pp. 54–56.
Kallanxhi, M.-E., Bälc, R., Ćorić, S., Székely, S.-F., Filipescu, S., 2018. The Rupelian–Chattian transition in the north-western Transylvanian Basin (Romania) revealed by calcareous nannofossils: implications for biostratigraphy and palaeoenvironmental reconstruction. Geol. Carpath. 69, 264–282. https://doi.org/10.1515/geoca-2018-0016.
Katz, B.J., 1983. Limitations of Rock-Eval pyrolysis for typing of organic matter. Org. Geochem. 4, 195–199.
Kodner, R.B., Pearson, A., Summons, R.E., Knoll, A.H., 2008. Sterols in red and green algae: quantification, phylogeny, and relevance for the interpretation of geologic steranes. Geobiology 6, 411–420.
Kohnen, M.E.L., Sinninghe Damsté, J.S., Kock-Van Dalen, A.C., ten Haven, H.L., Rullkötter, J., de Leeuw, J.W., 1990. Origin and diagenetic transformations of C_{25} and C_{30} highly branched isoprenoid Sulphur compounds: further evidence for the formation of organically bound Sulphur during early diagenesis. Geochim. Cosmochim. Acta 54, 3053–3063.
Koopmans, M.P., Köster, J., van Kaam-Peters, H.M.E., King, F., Schouten, S., Hartgers, W. A., de Leeuw, J.W., Sinninghe Damsté, J.S., 1996. Diagenetic and catagenetic products of isorenieratene: Molecular indicators for photic zone anoxia. Geochim. Cosmochim. Acta 60, 4467–4496.
Köster, J., Rospondek, M., Schouten, S., Kotarba, M., Zubrzycki, A., Sinninghe Damsté, J. S., 1998. Biomarker geochemistry of a foreland basin: the Oligocene Menilite Formation in the Flysch Carpathians of Southeast Poland. Org. Geochem. 29, 649–669.
Koszarski, L., Żytko, K., 1959. Remarks on development and stratigraphical of the Jasło Shales in the Menilitc and Krosno Series of the Middle Carpathians (in polish with English summary). Geol. Q. 3, 996–1015.
Kotlarczyk, J., Uchman, A., 2012. Integrated ichnology and ichthyology of the Oligocene Menilite Formation, Skole and Subsilesian nappes, Polish Carpathians: a proxy to oxygenation history. Palaeogeogr. Palaeoclimatol. Palaeoecol. 331–332, 104–118.
Kováč, M., Plašienka, D., Soták, J., Vojtko, R., Oszczypko, N., Less, G., Vlasta, Ć., Fügenschuhe, B., Králiková, S., 2016. Paleogene palaeogeography and basin evolution of the Western Carpathians, Northern Pannonian domain and adjoining areas. Global and Planetary Change 140, 9–27.

Krézsek, C., Bally, A.W., 2006. The Transylvanian Basin (Romania) and its relation to the Carpathian Fold and Thrust Belt: Insights in gravitational salt tectonics. Mar. Pet. Geol. 23, 405–442.
Krhovský, J., 1981. Microbiostratigraphic correlations in the Outer Flysch units of the southern Moravia and influence of the eustacy on their paleogeographical development. Zemni Plyn a Nafta 26, 665–688 (in Czech, summary in English).
Laskarev, V., 1924. Sur les equivalents du Sarmatien superieur en Serbie. In: Vujević, P. (Ed.), Receuil de traveaux offert à M. Jovan Cvijic par ses amis et collaborateurs, Drzhavna Shtamparija, Beograd, pp. 73–85.
Taxonomy, biostratigraphy, and phylogeny of Oligocene and early Miocene *Paragloborotalia* and *Parasubbotina*. In: Leckie, R.M., Wade, B.S., Pearson, P.N., Fraass, A.J., King, D.J., Olsson, R.K., Premoli Silva, I., Spezzaferri, S., Berggren, W.A. (Eds.), 2018. Atlas of Oligocene Planktonic Foraminifera, Cushman Foundation of Foraminiferal Research, Special Publication. In: Wade, B.S., Olsson, R.K., Pearson, P. N., Huber, B.T., Berggren, W.A. (Eds.), 2018, vol. 46, pp. 125–178.
de Leeuw, A., Filipescu, S., Mațenco, L., Krijgsman, W., Kuiper, C., Stoica, M., 2013. Paleomagnetic and chronostratigraphic constraints on the Middle to late Miocene evolution of the Transylvanian Basin (Romania): Implications for the central Paratethys stratigraphy and emplacement of the Tisza-Dacia plate. Glob. Planet. Chang. 103, 82–98. https://doi.org/10.1016/j.gloplacha.2012.04.008.
de Leeuw, J.W., Cox, H.C., van Graas, G., van de Meer, F.W., Peakman, T.M., Baas, J.M. A., van de Graaf, B., 1989. Limited double-bond isomerization and selective hydrogenation of sterenes during early diagenesis. Geochim. Cosmochim. Acta 53, 903–909.
Lichtfouse, E., Derenne, S., Mariotti, A., Largeau, C., 1994. Possible algal origin of long chain odd *n*-alkanes in immature sediments as revealed by distributions and carbon isotope ratios. Org. Geochem. 22, 1023–1027. https://doi.org/10.1016/0146-6380(94)90035-3.
Lyons, T.W., Anbar, A.D., Severmann, S., Scott, C., Gill, B.C., 2009. Tracking euxinia in the ancient ocean: a multiproxy perspective and Proterozoic case study. Annu. Rev. Earth Planet. Sci. 37, 507–534.
Mackenzie, A.S., Brassell, S.C., Eglinton, G., Maxwell, J.R., 1982. Chemical fossils – the geological fate of steroids. Science 217, 491–504.
Macquaker, J.H.S., Farrimond, P., Brassell, S.C., 1986. Biological markers in the Rhaetian black shales of South West Britain. Org. Geochem. 10, 93–100.
Martini, E., 1971. Standard Tertiary and Quaternary calcareous nannoplankton zonations. In: Farinacci, A. (Ed.), Proceedings of the II. Planktonic Conference, Rome, 1970, 2. Editura Tecnoscienza, pp. 739–785.
Martini, E., 1990. The Rhine graben system, a connection between northern and southern seas in the European Tertiary. Veröff. Übersee-Mus. Bremen A 10, 83–98.
Marynowski, L., Rakociński, M., Borcuch, E., Kremer, B., Schubert, B.A., Jahren, A.H., 2011. Molecular and petrographic indicators of redox conditions and bacterial communities after the F/F mass extinction (Kowala, Holy Cross Mountains, Poland). Palaeogeogr. Palaeoclimatol. Palaeoecol. 306, 1–14. https://doi.org/10.1016/j.palaeo.2011.03.018.
Massé, G.G., 2002. Highly branched isoprenoid alkenes from diatoms: a biosynthetic and life cycle investigation. PhD Thesis. University of Plymouth, 192 pp.
McArthur, A.D., Kneller, B.C., Souza, P.A., Kuchle, J., 2016. Characterization of deep-marine channel-levee complex architecture with palynofacies: an outcrop example from the Rosario Formation, Baja California, Mexico. Mar. Pet. Geol. 73, 157–173.
Melinte, M.C., 2005. Oligocene palaeoenvironmental changes in the Romanian Carpathians, revealed by calcareous nannofossils. Studia Geologica Polonica 124, 341–352.
Melinte-Dobrinescu, M., Brustur, T., 2008. Oligocene – lower Miocene events in Romania. Acta Palaeontologica Romaniae 6, 203–215.
Menounos, P., Staphylakis, K., Gegiou, D., 1986. The sterols of *Nigella sativa* seed oil. Phytochemistry 25, 761–763.
Mészáros, N., Gheța, N., Ianoliu, C., 1979. Nannoplankton zones in the Paleogene deposits of the Transylvanian basin. Studii şi Comunicări 23, 73–80.
Metzger, P., Allard, B., Casadevall, E., Berkaloff, C., Cout, A., 1990. Structure and chemistry of a new race of *Botryococcus braunii* (Chlorophyceae) that produces lycopadiene, a tetraterpenoid hydrocarbon. J. Phycol. 26, 258–266.
Meyer, K.M., Kump, L.R., 2008. Oceanic euxinia in Earth history: causes and consequences. Annu. Rev. Earth Planet. Sci. 36, 251–288.
Miclăuş, C., Loiacono, F., Puglisi, D., Baciu, D.S., 2009. Eocene-Oligocene sedimentation in the external areas of the Moldavide Basin (marginal Folds Nappe, Eastern Carpathians, Romania): Sedimentological, paleontological and petrographic approaches. Geol. Carpath. 60, 397–417.
Moldowan, J.M., Fago, F.J., Carlson, R.M.K., Young, D.C., Van Duyne, G., Clardy, J., Schoell, M., Pillinger, C.T., Watt, D.S., 1991. Rearranged hopanes in sediments and petroleum. Geochim. Cosmochim. Acta 55, 3333–3353.
Naeher, S., Schaeffer, P., Adam, P., Schubert, C.J., 2013. Maleimides in recent sediments — using chlorophyll degradation products for palaeoenvironmental reconstructions. Geochim. Cosmochim. Acta 119, 248–263.
Nagymarosy, A., Voronina, A., 1992. Calcareous nannoplankton from the lower Maikopian Beds (early Oligocene, Union of Independent States). Knihovnicka Zemnyho Plynu a Nafty 14b, 189–221.Otto, a., Simoneit, B.R.T., 2001. Chemosystematics and diagenesis of terpenoids in fossil conifer species and sediment from the Eocene Zeitz Formation, Saxony, Germany. Geochim. Cosmochim. Acta 65, 3505–3527.
Otto, A., Simoneit, B.R.T., 2001. Chemosystematics and diagenesis of terpenoids in fossil conifer species and sediment from the Eocene Zeitz formation, Saxony, Germany. Geochem. Cosmochim. Acta 65, 505–3527.
Otto, A., Walther, H., Püttmann, W., 1997. Sesqui- and diterpenoid biomarkers preserved in *Taxodium*-rich Oligocene oxbow lake clays, Weisselster basin, Germany. Org. Geochem. 26, 105–115.
Ourisson, G., Albrecht, P., Rohmer, M., 1979. The hopanoids: palaeochemistry and biochemistry of a group of natural products. Pure Appl. Chem. 51, 709–729.
Ozsvárt, P., Kocsis, L., Nyerges, A., Győri, O., Pálfy, J., 2016. The Eocene-Oligocene climate transition in the Central Paratethys. Palaeogeogr. Palaeoclimatol. Palaeoecol. 459, 471–487. https://doi.org/10.1016/j.palaeo.2016.07.034.
Pacton, M., Gorin, G.E., Vasconcelos, C., 2011. Amorphous organic matter — experimental data on formation and the role of microbes. Rev. Palaeobot. Palynol. 166, 253–267.
Palcu, D.V., Krijgsman, W., 2023. The dire straits of Paratethys: gateways to the anoxic giant of Eurasia. Geol. Soc. Lond. Spec. Publ. 523, 111–139. https://doi.org/10.1144/sp523-2021-73.
Peakman, T.M., ten Haven, H.L., Rechka, J.R., de Leeuw, J.W., Maxwell, J.R., 1989. Occurrence of (20R)- and (20S)-$\Delta^{8(14)}$ and Δ^{14} 5α(H)-sterenes and the origin of 5α(H),14β(H),17β(H)-steranes in an immature sediment. Geochim. Cosmochim. Acta 53, 2001–2009.
Peters, K.E., 1986. Guidelines of evaluating petroleum source rock using programmed pyrolysis. AAPG Bull. 70, 318–329.
Peters, K.E., Cassa, M.R., 1994. Applied source rock geochemistry. In: Magoon, L.B., Dow, W.G. (Eds.), The Petroleum System: From Source to Trap, vol. 60. American Association of Petroleum Geologists Memoir, pp. 93–120.
Peters, K.E., Simoneit, B.R.T., 1982. Rock-Eval pyrolysis of Quaternary sediments from Leg 64, Sites 479 and 480, Gulf of California. Initial Rep. Deep Sea Drill. Proj. 64, 925–931.
Peters, K.E., Walters, C.C., Moldowan, J.M., 2005. The Biomarker Guide, vol. 2: Biomarkers and isotopes in petroleum systems and Earth history. Cambridge University Press, Cambridge.
Popescu, B.M., 1995. Romania's petroleum systems and their remaining potential. Pet. Geosci. 1, 337–350.
Popescu, B.M., 2021. Transcarpathian petroleum province in Romania. Geo-Eco-Marina 27, 5–35. https://doi.org/10.5281/zenodo.5801082.
Popov, S., Akhmet'ev, M.A., Zaporozhets, N.I., Voronina, A.A., Stolyarov, A.S., 1993. Evolution of the Eastern Paratethys in the late Eocene-early Miocene. Stratigr. Geol. Correl. 6, 572–600.
Popov, S.V., Studencka, B., 2015. Brackish-water Solenovian mollusks from the lower Oligocene of the Polish Carpathians. Paleontol. J. 49, 342–355. https://doi.org/10.1134/S0031030115040140.
Popov, S.V., Rögl, F., Rozanov, A.Y., Steininger, F.F., Shcherba, I.G., Kovac, M., 2004. Lithological-paleogeographic maps of Paratethys. CFS Courier Forschungsinstitut Senckenberg 1–46.
Popov, S.V., Sychevskaya, E.K., Akhmet'ev, M.A., Zaporozhets, N.I., Golovina, L.A., 2008. Stratigraphy of the Maikop Group and Pteropoda Beds in northern Azerbaijan. Stratigr. Geol. Correl. 16, 664–677.
Popov, S.V., Rostovtseva, Y.V., Pinchuk, T.N., Patina, I.S., Goncharova, I.A., 2019. Oligocene to Neogene paleogeography and depositional environments of the Euxinian part of Paratethys in Crimean – Caucasian junction. Mar. Pet. Geol. 103, 163–175. https://doi.org/10.1016/j.marpetgeo.2019.02.019.
Rauball, J.F., Sachsenhofer, R.F., Bechtel, A., Coric, S., Gratzer, R., 2019. The Oligocene–Miocene Menilite Formation in the Ukrainian Carpathians: a world-class source rock. J. Pet. Geol. 42, 393–415. https://doi.org/10.1111/jpg.12743.
Robinson, N., Eglinton, G., Brassell, S., Cranwell, P.A., 1984. Dinoflagellate origin for sedimentary 4α-methylsteroids and 5α(H)-stanols. Nature 308, 419–422.
Rögl, F., 1998. Palaeogeographic consideration for Mediterranean and Paratethys seaways (Oligocene to Miocene). Ann. Naturhist. Mus. Wien 99A, 279–310.
Rögl, F., 1999. Mediterranean and Paratethys. Facts and hypotheses of an Oligocene to Miocene paleogeography (short overview). Geol. Carpath. 50, 339–349.
Rohmer, M., Bouvier-Navé, P., Ourisson, G., 1984. Distribution of hopanoid triterpenes in prokaryotes. J. Gen. Microbiol. 130, 1137–1150.
Rontani, J.-F., Belt, S.T., Vaultier, F., Brown, T.A., 2011. Visible light induced photo-oxidation of highly branched isoprenoid (HBI) alkenes: a significant dependence on the number and nature of the double bonds. Org. Geochem. 42, 812–822.
Rontani, J.-F., Belt, S.T., Vaultier, F., Brown, T.A., Masse, G., 2014. Autoxidative and Photooxidative Reactivity of Highly Branched Isoprenoid (HBI) Alkenes. Lipids 49, 481–494. https://doi.org/10.1007/s11745-014-3891-x.
Rospondek, M.J., Köster, J., Sinninghe Damsté, J.S., 1997. Novel C_{26} highly branched isoprenoid thiophenes and alkane from the Menilite Formation, Outer Carpathians, Southeast Poland. Org. Geochem. 26, 295–304.
Rowland, S.J., Robson, J.N., 1990. The widespread occurrence of highly branched acyclic C_{20}, C_{25} and C_{30} hydrocarbons in recent sediments and biota – a review. Mar. Environ. Res. 30, 191–216.
Rusu, A., 1996. Changes in marine molluscan assemblages from the upper Oligocene–lower Miocene in NW Transylvania. Oligocene–Miocene transition and main geological events in Romania, 28 August–2 September 1996. B. Material of Symposium. Rom. J. Paleo. 76 (Suppl. 1), 58–62.
Rusu, A., Popescu, G., Melinte, M., 1996. Oligocene–Miocene transition and main geological events in Romania. Excursion Guide of IGCP Project No.326. Rom. J. Stratigr. 76 (1), 3–47.
Sachsenhofer, R.F., Hentschke, J., Bechtel, A., Coric, S., Gratzer, R., Gross, D., Horsfield, B., Rachetti, A., Soliman, A., 2015. Hydrocarbon potential and depositional environments of oligo-miocene rocks in the eastern Carpathians (Vrancea nappe, Romania). Mar. Pet. Geol. 68, 269–290.
Sachsenhofer, R.F., Popov, S.V., Ćorić, S., Mayer J., J., Misch, D., Morton, M.T., Pupp, M., Rauball, J., Tari, G., 2018. Paratethyan petroleum source rocks: an overview. J. Pet. Geol. 41, 219–246.
Schouten, S., Bowman, J.P., Rijpstra, W.I.C., Sinninghe Damsté, J.S., 2000. Sterols in a psychrophilic methanotroph, *Methylosphaera hansonii*. FEMS Microbiol. Lett. 186, 193–195.

Schwark, L., Frimmel, A., 2004. Chemostratigraphy of the Posidonia Black Shale, SW-Germany: II. Assessment of extent and persistence of photic-zone anoxia using aryl isoprenoid distributions. Chem. Geol. 206, 231–248.
Seifert, W.K., Moldowan, J.M., 1980. The effect of thermal stress on source-rock quality as measured by hopane stereochemistry. Phys. Chem. Earth 12, 229–237.
Seifert, W.K., Moldowan, J.M., 1986. Use of biological markers in petroleum exploration. In: Johns, R.B. (Ed.), Methods in Geochemistry and Geophysics, 24, pp. 261–290.
Shipe, R.F., Brzezinski, M.A., Pilskaln, C., Villareal, T.A., 1999. *Rhizosolenia* mats: an overlooked source of silica production in the open sea. Limnol. Oceanogr. 44, 1282–1292.
Simoneit, B.R.T., 1977. Diterpenoid compounds and other lipids in deep-sea sediments and their geochemical significance. Geochim. Cosmochim. Acta 41, 463–476.
Simonsen, R., 1974. The Diatom Plankton of the Indian Ocean Expedition of R.V. "Meteor". Forschungsergebnisse. In: Reihe D, 19. Gebruder Borntraegier, Berlin, pp. 1–66.
Sinninghe Damsté, J.S., de Leeuw, J.W., 1990. Analysis, structure and geochemical significance of organically-bound sulphur in the geosphere: state of the art and future research. In: Durand, B., Behar, F. (Eds.), Advances in Organic Geochemistry 1989, Organic Geochemistry, 16, pp. 1077–1101.
Sinninghe Damsté, J.S., Kock-Van Dalen, A.C., De Leeuw, J.W., Schenck, P.A., Guoying, S., Brassell, S.C., 1987. The identification of mono-, di- and trimethyl 2-methyl-2-(4,8,12-trimethyltridecyl)chromans and their occurrence in the geosphere. Geochim. Cosmochim. Acta 51, 2393–2400.
Sinninghe Damsté, J.S., van Koert, E.R., Kock-van Dalen, A.C., de Leeuw, J.W., Schneck, P.A., 1989. Characterisation of highly branched isoprenoid thiophenes occurring in sediments and immature crude oils. Org. Geochem. 14, 555–567.
Sinninghe Damsté, J.S., Hartgers, W.A., Baas, M., de Leeuw, J.W., 1993. Characterization of high-molecular-weight organic matter in marls of the Salt IV Formation of Mulhouse Basin. Org. Geochem. 20, 1237–1252.
Sinninghe Damsté, J.S., van Duin, A.C.T., Hollander, D., Kohnen, M.E.L., de Leeuw, J.W., 1995. Early diagenesis of bacteriohopanepolyol derivatives – formation of fossil homohopanoids. Geochim. Cosmochim. Acta 59, 5141–5157.
Smolarek, J., Marynowski, L., Trela, W., Kujawski, P., Simoneit, B.R.T., 2017. Redox conditions and marine microbial community changes during the end-Ordovician mass extinction event. Glob. Planet. Chang. 149, 105–122.
Spezzaferri, S., Coxall, H.K., Olsson, R.K., Hemleben, Ch., 2018. Taxonomy, biostratigraphy, and phylogeny of Oligocene *Globigerina*, *Globigerinella*, and *Quiltyella*. In: Wade, B.S., Olsson, R.K., Pearson, P.N., Huber, B.T., Berggren, W.A. (Eds.), Atlas of Oligocene Planktonic Foraminifera, Cushman Foundation of Foraminiferal Research, Special Publication, 46, pp. 179–214.
Stefanescu, M., Dicea, O., Butac, A., Ciulavu, D., 2006. Hydrocarbon geology of the Romanian Carpathians, their foreland, and the Transylvanian Basin. In: Golonka, J., Picha, F.J. (Eds.), The Carphathians and their Foreland: Geology and Hydrocarbon Resources: AAPG Memoir, vol. 84, pp. 521–567.
Summons, R.E., Powell, T.G., 1987. Identification of aryl isoprenoids in source rocks and crude oils: biological markers for the green Sulphur bacteria. Geochim. Cosmochim. Acta 51, 557–566.
Švábenická, L., Bubík, M., Stráník, Z., 2007. Biostratigraphy and paleoenvironmental changes on the transition from the Menilite to Krosno lithofacies (Western Carpathians, Czech Republic). Geol. Carpath. 58, 237–262.
Székely, S.-F., Filipescu, S., 2015. Taxonomic record of the Oligocene benthic foraminifera from the Vima Formation (Transylvanian Basin, Romania). Acta Palaeontologica Romaniei 11, 25–62.
Székely, S.-F., Filipescu, S., 2016. Biostratigraphy and paleoenvironments of the late Oligocene in the north-western Transylvanian Basin revealed by the foraminifera assemblages. Palaeogeogr. Palaeoclimatol. Palaeoecol. 449, 484–509.
Ţabără, D., Pacton, M., Makou, M., Chirila, G., 2015. Palynofacies and geochemical analysis of Oligo-Miocene bituminous rocks from the Moldavidian Domain (Eastern Carpathians, Romania): implications for petroleum exploration. Revue Paleobot. Palynol. 216, 101–122.
Taylor, D.W., Li, H., Dahl, J., Fago, F.J., Zinniker, D., Moldowan, J.M., 2006. Biogeochemical evidence for the presence of the angiosperm molecular fossil oleanane in Paleozoic and Mesozoic non-angiospermous fossils. Paleobiology 32, 179–190. https://doi.org/10.1666/0094-8373(2006)32[179:BEFTPO]2.0.CO;2.
Traverse, A., 1988. Paleopalynology. Allen and Unwin Inc., Winchester, Masso, 1890. U. S.A., 565 p.
Traverse, A., 2007. Paleopalynology, 2nd ed. Springer, Netherlands, Dordrecht. 816p.
Tulipani, S., Grice, K., Greenwood, P.F., Haines, P.W., Sauer, P.E., Schimmelmann, A., Summons, R.E., Foster, C.B., Böttcher, M.E., Playton, T., Schwark, L., 2015. Changes of palaeoenvironmental conditions recorded in late Devonian reef systems from the Canning Basin, Western Australia: a biomarker and stable isotope approach. Gondwana Res. 28, 1500–1515.
Tyson, R.V., 1989. Late Jurassic palynofacies trends, Piper and Kimmeridge Clay formations, UK onshore and Northern North Sea. In: Batten, D.J., Keen, M.C. (Eds.), North West European Micropalaentology and Palinology, British Micropaleontological Society Series. Ellis Horwood, Chichester, pp. 135–172.
Tyson, R.V., 1993. Palynofacies analysis. In: Jenkins, D.J. (Ed.), Applied Micropaleontology. Kluwer Academic Publishers, Dordrecht, pp. 152–191.
Tyson, R.V., 1995. Sedimentary Organic Matter: Organic Facies and Palynofacies. Chapman and Hall, Torquay, Devon.
Volkman, J.K., 1986. A review of sterols of marine and terrigenous organic matter. Org. Geochem. 9, 83–99.
Volkman, J.K., 2003. Sterols in microorganisms. Appl. Microbiol. Biotechnol. 60, 495–506.
Volkman, J.K., Farrington, J., Gagosian, R., Wakeham, S., 1983. Lipid composition of coastal marine sediments from the Peru upwelling region. Adv. Org. Geochem. 1981, 228–240.
Volkman, J.K., Kearney, P., Jeffrey, S.W., 1990. A new source of 4-methyl sterols and 5a (H)-stanols in sediments: prymnesiophyte microalgae of the genus *Pavlova*. Org. Geochem. 15, 489–497.
Volkman, J.K., Barrett, S.M., Dunstan, G.A., 1994. C_{25} and C_{30} highly branched isoprenoid in laboratory cultures of two marine diatoms. Org. Geochem. 21, 407–414.
Volkman, J.K., Farmer, C.L., Barrett, S.M., Sikes, E.L., 1997. Unusual dihydroxy sterols as chemotaxonomic markers for microalgae from the order Pavlovales (Haptophyceae). J. Phycol. 33, 1016–1023.
Volkman, J.K., Barrett, S.M., Blackburn, S.I., Mansour, M.P., Sikes, E.L., Gelin, F., 1998. Microalgae biomarkers: a review of recent research developments. Org. Geochem. 29, 1163–1179.
Volkman, J.K., Barrett, S.M., Blackburn, S.I., 1999. Eustigmatophyte microalgae are potential sources of C29 sterols, C22–C28 n-alcohols and C28–C32 n-alkyl diols in freshwater environments. Org. Geochem. 30, 307–318.
Volkman, J.K., Zhang, Z., Xie, X., Qin, J., Borjigin, T., 2015. Biomarker evidence for *Botryococcus* and a methane cycle in the Eocene Huadian oil shale, NE China. Org. Geochem. 78, 121–134. https://doi.org/10.1016/j.orggeochem.2014.11.002.
Wakeham, S.G., Amann, R., Freeman, K.H., Hopmans, E.C., Jorgensen, B.B., Putnam, I.F., Schouten, S., Sinninghe Damste, J.S., Talbot, H.M., Woebken, D., 2007. Microbial ecology of the stratified water column of the Black Sea as revealed by a comprehensive biomarker study. Org. Geochem. 39, 2070–2097.
Wang, L., Song, Z., Yin, Q., George, S.M., 2011. Paleosalinity significance of occurrence and distribution of methyltrimethyltridecyl chromans in the upper cretaceous Nenjiang Formation, Songliao Basin, China. Org. Geochem. 42, 1411–1419.
Waterhouse, H.K., 1998. Palynological fluorescence in hinterland reconstruction of a cyclic shallowing-up sequence, Pliocene, Papua New Guinea. Palaeogeogr. Palaeoclimatol. Palaeoecol. 139, 59–82.
Wei, H., Algeo, T.J., Yu, H., Wang, J., Guo, C., Shi, G., 2015. Episodic euxinia in the Changhsingian (late Permian) of South China: evidence from framboidal pyrite and geochemical data. Sediment. Geol. 319, 78–97.
Wen, Z., Ruiyong, W., Radke, M., 2000. Retene in pyrolysates of algal and bacterial organic matter. Org. Geochem. 31, 757–762.
Wendorff-Belon, M., Rospondek, M., Marynowski, L., 2021. Early Oligocene environment of the Central Paratethys revealed by biomarkers and pyrite framboids from the Tarcau and Vrancea nappes (Eastern Outer Carpathians, Romania). Mar. Pet. Geol. 128, 105037.
Wignall, P.B., Newton, R., 1998. Pyrite framboid diameter as a measure of oxygen deficiency in ancient mudrocks. Am. J. Sci. 298, 537–552.
Wilkin, R.T., Arthur, M.A., 2001. Variations in pyrite texture, sulfur isotope composition, and iron systematics in the Black Sea: evidence for late Pleistocene to Holocene excursions of the O_2-H_2S redox transition. Geochim. Cosmochim. Acta 65, 1399–1416.
Wilkin, R.T., Barnes, H.L., Brantley, S.L., 1996. The size distribution of framboidal pyrite in modern sediments: an indicator of redox conditions. Geochim. Cosmochim. Acta 60, 3897–3912.
Wilkin, R.T., Arthur, M.A., Dean, W.E., 1997. History of water-column anoxia in the Black Sea indicated by pyrite framboid size distributions. Earth Planet. Sci. Lett. 148, 517–525.
Zachos, J., Pagani, M., Sloan, L., Thomas, E., Billups, K., 2001. Trends, rhythms, and aberrations in global climate 65 Ma to present. Science 292, 686–693.
Zakrzewski, A., Waliczek, M., Machowski, G., Ząbek, G., Konon, A., Więcław, D., 2024. When an explosion of life leads to death – hypoxic zones in the Menilite Shales from the Silesian Unit (Polish Outer Carpathians). Mar. Pet. Geol. 168, 107024. https://doi.org/10.1016/j.marpetgeo.2024.107024.

Supplementary data

Distribution of determined taxa of Foraminifera
(in alphabetical order within suborders)

	Suggested age	Rupelian				R/Ch		Chattian		
	Foraminifera	**Samples**								
	Suborder Textulariina	**F7**	**F14**	**F18**	**F19**	**F20**	**F21**	**F24**	**F28**	**F34**
Agglutinated	*Ammobaculites agglutinans* (d'Orbigny)									**x**
	Ammobaculites sp.		**x**			**x**				
	Ammodiscus sp.					**x**				
	Bathysiphon sp.								**x**	
	Cyclammina spp.									**x**
	Dendrophrya sp.		**x**							
	Glomospira gordialis (Jones & Parker)								**x**	
	Glomospira sp.					**x**				
	Haplophragmoides carinatus Cushman & Renz					**x**		**C**		**x**
	Haplophragmoides suborbicularis (Grzybowski)					**x**				**x**
	Haplophragmoides spp.				**x**					
	Haplophragmoides sp.							**x**	**x**	
	Hyperammina elongata Brady								**x**	
	Karreriella chilostoma (Reuss)								**x**	
	Karreriella gaudryinoides (Fornasini)					**x**			**x**	
	Karreriella hantkeniana Cushman								**x**	
	Karreriella spp.				**x**					
	Martinotiella communis (d'Orbigny)								**x**	
	Nothia sp.								**x**	
	Recurvoides sp.				**x**					
	Recurvoides spp.								**x**	
	Reophax pilulifer Brady					**x**			**x**	
	Reophax sp.									**x**
	Reticulophragmium acutidorsatum (Hantken)		**x**						**x**	**C**
	Reticulophragmium rotundidorsatum (Hantken)								**x**	
	Reticulophragmium sp.		**x**							
	Spirorutilus carinatus (d'Orbigny)			**x**	**x**	**x**	**x**		**C**	
	Tritaxia szaboi (Hantken)						**x**			
	Trochamminoides sp.		**x**							
	Valvulina flexilis Cushman & Renz								**x**	
	Valvulina sp.								**x**	
	Vulvulina haeringensis (Gümbel)								**x**	
	Vulvulina spinosa Cushman				**x**				**x**	
	Suborder Miliolina									
	Cyclophorina sp.			**x**						
	Quinqueloculina sp.			**x**						
	Sigmoilinita tenuis (Czjzek)			**x**						
	Sigmoilina tenuissima (Reuss)			**x**				**x**		
	Spiroloculina sp.			**x**						
	Miliolidea indet.			**x**						
	Suborder Lagenina									
	Amphicoryna crassa (Hantken)				**x**			**x**		
	Amphicoryna spinicosta (d'Orbigny)			**x**				**x**		
	Astacolus crepidulus (Fichtel & Moll)				**x**					
	Astacolus sp.			**x**						

Dentalina sp.			x						
Dentalinoides approximata (Reuss)			x						
Glandulina dimorpha Bornemann					x				
Guttulina sp.				x	x	x			
Hemirobulina recta (Hantken)			x						
Lagena striata (d'Orbigny)						x			
Lagena sp.			x						
Lenticulina arcuatostriata (Hantken)					x	x		x	
Lenticulina cultratus (Montfort)								x	
Lenticulina inornata (d'Orbigny)				x			x	x	
Lenticulina limbosa (Reuss)				x	x		x		
Lenticulina vortex (Fichtel & Moll)				x	x			x	
Lenticulina spp.								x	x
Marginulina hirsuta d'Orbigny						x			
Nodosaria sp.								x	
Plectofrondicularia striata (Hantken)	x								
Ramulina globulifera Brady								x	
Saracenaria senni (Hadberg)			x						
Vaginulinopsis cumulicostatus (Gümbel)			x			x			
Suborder Rotaliina									
Angulogerina globosa (Stolz)			x						
Angulogerina gracilis (Reuss)							x		
Asterorotalia sp.							x		
Bolivina beyrichi Reuss				x			x		
Bolivina dilatata Reuss					x		x		
Bolivina dilatata hyalina Hofmann							x		
Bolivina fastigia Cushman			x	x	x				
Bolivina semistriata semistriata Hantken					x		x		
Bolivina sp.					x				
Bolivina spp.							A		
Brizalina sp.		x							
Bulimina alsatica Cushman & Parker			x	x		x	A		
Bulimina coprolithoides Andreae			x				C		
Bulimina elongata d'Orbigny							x		
Bulimina schischkinskayae Samoylova					x		A		x
Bulimina sp.									x
Caucasina oligocenica Khalilov			x				x		
Charltonia budensis (Hantken)				x					
Chilostomella cylindroides Reuss			x		x				
Cibicides amphisyliensis (Andreae)	x		x	x	x				
Cibicides sp.	x	x							
Cibicidoides lopjanicus (Mjatliuk)								x	
Cibicidoides pachyderma (Rzehak)					x				
Cibicidoides ungerianus ungerianus (d'Orbigny)					x		x		
Cibicidoides ungerianus filicosta (Hagn)			C	x	x	x			
Cibicidoides sp.								x	
Cribroparella pteromphalia (Gümbel)				x					
Eponides repandus var. *oligocenicus* Cush.& Ellisor					x				
Fursenkoina acuta (d'Orbigny)						x	x		
Fursenkoina schreibersiana (Czjzek)					x				

Calcareous Benthonic

	Fursenkoina sp.				x					
	Globocassidulina globosa (Hantken)					x				
	Globocassidulina subglobosa (Brady)			C			x	x		x
	Gyroidina sp.				x		x			
	Gyroidinoides sp.									x
	Heterolepa eocaena (Gümbel)			A						
	Heterolepa praecincta (Karrer)			A	C	x				
	Heterolepa sp.			x						
	Heterolepa spp.				c		x			
	Lobatula lobatula (Walker et Jacob)			x						
	Neoeponides schreibersi (d'Orbigny)						x			
	Nonion commun e (d'Orbigny)			x				x		
	Nonion sp.									x
	Oridorsalis umbonatus (Reuss)				x					
	Planulina compressa (Hantken)					x				
	Pleurostomella incrassata Hantken			x						
	Praeglobobulimina pupoides (d'Orbigny)				x				x	
	Praeglobobulimina pyrula (d'Orbigny)					x			x	
	Pullenia bulloides (d'Orbigny)						x			
	Pullenia quinqueloba (Reuss)				x					
	Quadromorphina petrolei (Andreae)					x				
	Siphonodosaria sp.				x					
	Sphaeroidina bulloides d'Orbigny				x		x			
	Stilostomella adolphina (d'Orbigny)					x				
	Stilostomella sp.						x			
	Uvigerina bulbacea Galloway et Heminway			x						
	Uvigerina continuosa Lamb						x			
	Uvigerina gracilis var. *oligocaenica* (Andreae)						x			
	Uvigerina moravia Boeresma						x			
	Uvigerina popescui Rogl						A			
	Uvigerina vicksburgensis Cushman & Ellisor			x			x		x	
	Uvigerina sp.				x			x		
	Uvigerina spp.					x	C		x	
	Vaginulinopsis cumulicostatus (Gumbel)						x			
	Suborder Globigerinina									
Planktonic	*Bella rohiensis* (Popescu et Brotea)					x				
	Catapsydrax unicavus Bolli, Loeblich & Tappan				x		x			
	Catapsydrax sp.						x			
	Globigerina officinalis Subbotina			x	x			x		
	Globigerina praebulloides Blow				x			x		
	Globigerina sp.							x		
	Globigerina spp.		x			x	x			
	Globigerinella megaperta Rögl						x			
	Globigerinella navazuelensis (Molina)						x			
	Globigerinella sp.					x				
	Paragloborotalia opima (Bolli)						x			
	Paragloborotalia sp.									
	Paragloborotalia spp.				x					
	Tenuitiella munda (Jenkins)			x						
	Tenuitellinata angustiumbilicata (Bolli)			x	x		x	x		

Other fossils	Ostracods			**x**						
	Fish teeth	**x**	**x**			**x**	**x**	**x**		**x**
	Pyritized moulds of gastropods			**x**		**x**			**x**	
	Plant detritus		**x**							**x**
		F7	**F14**	**F18**	**F19**	**F20**	**F21**	**F24**	**F28**	**F34**

Explanantions: A - abundant; C - common; x - present

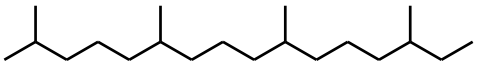

I. Pristane

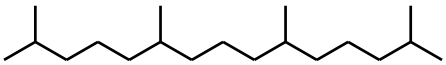

II. Phytane

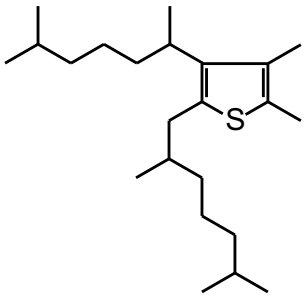

III. C25 HBI thiophene

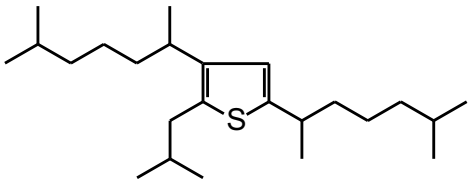

IV. C25 HBI thiophene

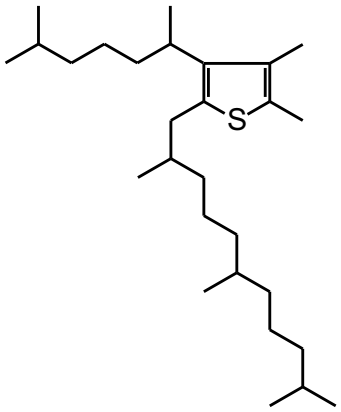

V. C30 HBI thiophene

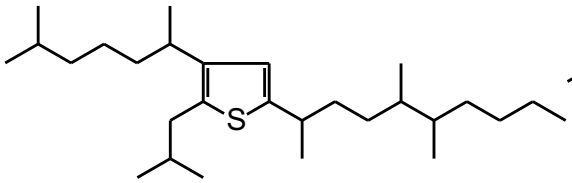

VI C30 HBI thiophene

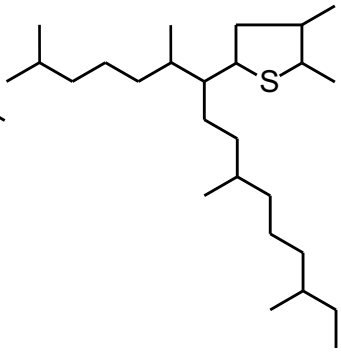

VII. C25 HBI thiolane

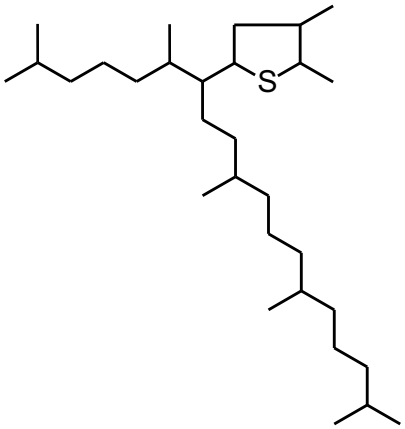

VIII. C30 HBI thiolane

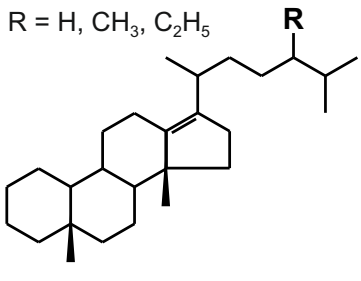

IX. Diaster-13(17)-enes

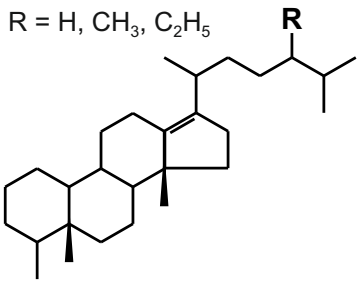

X. 4-Methyldiaster--13(17)-enes

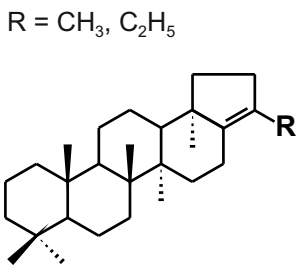

XI. Hop-17(21)-enes

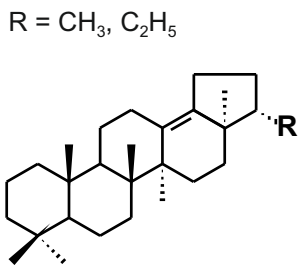

XII. Neohop-13(18)--enes

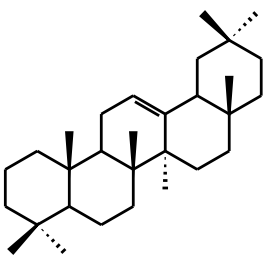

XIII. 18α(H) Olean--12-ene

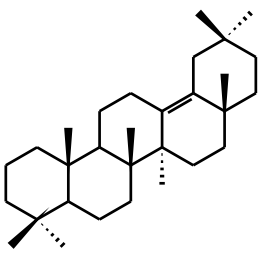

XIV. Olean-13(18)--ene

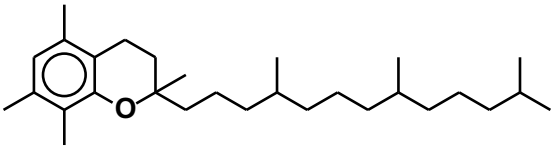

XV. 5,7,8-Trimethyl-2-methyl-trimethyltridecyl chromane

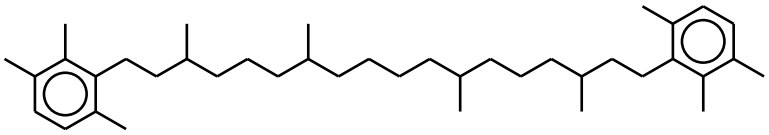

XVI. Isorenieratane

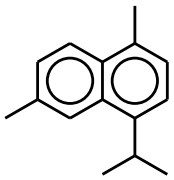

XVII. Cadalene

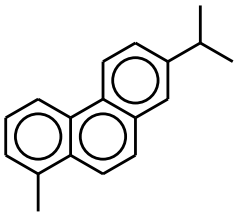

XVIII. Retene

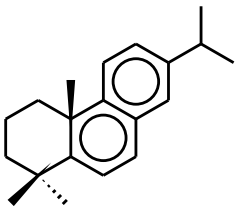

XIX. Simonellite

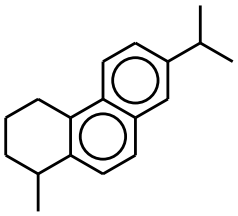

XX. Tetrahydroretene

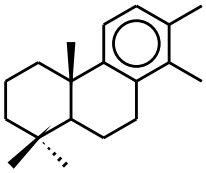

XXI. 14-Methyl-16,17-bisnorabieta-8,11,13-triene

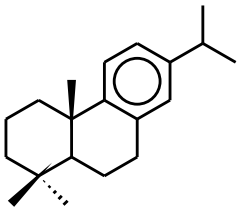

XXII. Dehydroabietane

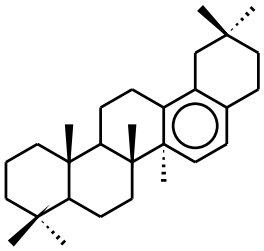

XXIII. 27,28-Bisnor-oleana-13,15,17-triene

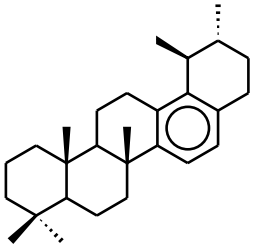

XXIV. 27,28-Bisnor-ursana-13,15,17-triene

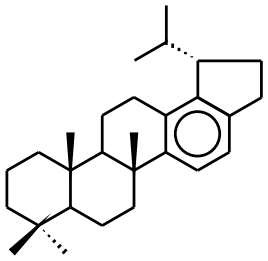

XXV. 27,28-Bisnor-lupana-13,15,17-triene

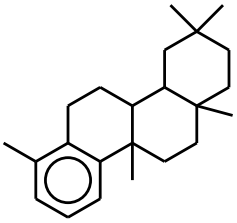

XXVI. Des-A--oleanane

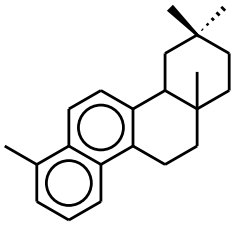

XXVII. Des-A-24,27-dinor-oleana-5,7,9,11,13-pentaene